Investigating the Role of Androgen Receptor Signalling in Oestrogen Receptor Positive Breast Cancer

Emine Cil

A thesis submitted for the degree of Doctor of Philosophy in
Cell and Molecular Biology

School of Life Sciences
University of Essex

October 2021

Impact of COVID-19

This PhD project has been impacted by the COVID-19 pandemic that started in March 2020. As a result of the outbreak, our laboratories were shut for 4 months in accordance with the government guidelines. Further, due to health and safety restrictions, researchers were only allowed to work in the laboratories part-time after the facilities reopened. As a result of reduced delivery times and companies not being able to manufacture products in high demand, there were also delays and issues with the delivery of consumables. Collectively, these issues significantly impacted the progression of my PhD.

Statement of Originality

Unless otherwise stated, I clarify that this thesis is the result of my own work and that this work has not been previously used for the award of any degree. All previously published data and sources are acknowledged accordingly in the thesis.

Acknowledgements

Firstly, I would like to thank and express my sincere gratitude to my PhD supervisor Dr Greg Brooke for his continuous support, his encouragement, his patience, his endless help, and his guidance throughout my PhD research, from beginning to end. Despite all the challenges, including a pandemic, this PhD was one of the best decisions I have ever made, and I could not think of a better supervisor.

Secondly, I would like to thank my fellow lab members of the Molecular Oncology Lab who I have worked with, Fionnuala McKenna, Angela Pine, Ana Maria Isac, Ryan Cronin, and Aygun Azadova for their friendship and support. My PhD friends: Maria Magliulo and Michela Lever, thank you for all the coffees and chats.

I would like to thank Dr Metodi Metodiev, Dr Antonio Marco, Dr Andrea Mohr, and Dr Ralf Zwacka, for their help and guidance with the research. I would like to thank Dr Louise Beard for her help and support. I would like to thank University of Essex for being my home for the last 3 years. Thank you to Emma Revill, our graduate administrator, for always being there to talk to and to help us.

Lastly, I would like to thank my family for their continuous love and support in every step of my life. Without you, I could not have made it this far.

Abstract

Breast cancer (BrCa) is the most common cancer in the UK. The majority of BrCa cases are oestrogen receptor α (ERα) positive, and sensitive to endocrine therapies (antioestrogens and aromatase inhibitors). Endocrine therapies for ERα-positive disease are effective initially, but often fail and the disease progresses to the endocrine resistant stage, for which few therapeutic options exist. The androgen receptor (AR) is the most commonly expressed steroid receptor in BrCa, occurring in up to 90% of cases. AR expression in early disease is associated with positive prognostic outcomes in ERα-positive disease. However, AR expression has also been associated with endocrine resistance. These different roles of AR could be because of the changes in the crosstalk between AR and ERα at different stages of the disease, and these changes might have important implications in endocrine resistance. Hence, this study aimed to understand the role of AR in ERα-positive disease and how this crosstalk is affected by antioestrogen treatments.

Crosstalk studies between the two steroid receptors in ERα-positive cell lines (MCF7, T47D) demonstrated that AR-ERα crosstalk is inhibitory, and that antioestrogens can reverse the inhibitory effect of ERα upon AR target gene expression. This increase in AR activity appears to be as a result of enhanced AR expression and DNA binding. Importantly, the AR was also found to reverse the inhibitory effect of the antioestrogen fulvestrant on BrCa proliferation. RNA-Seq analysis showed that the AR induces pathways linked to cellular proliferation, and becomes transcriptionally more active when ERα is inhibited by fulvestrant. Analysis of the transcriptional activity of AR mutants, identified in BrCa patients, showed that some mutations affect the transcriptional activity of the AR, and AR-ERα crosstalk. The data demonstrates that the role of the AR in BrCa is complex and that targeting both receptors may have a more clinically favourable outcome, and reduce therapy resistance in patients.

Abbreviations

1º: Primary
17β-HSD: 17β-Hydroxysteroid Dehydrogenase
2º: Secondary
A: Androstenedione
Ab: Antibody
AF1: Activation Function 1
AF2: Activation Function 2
AI: Aromatase Inhibitor
AIS: Androgen Insensitivity Syndrome
Akt: Protein Kinase B
APS: Ammonium persulphate
AR: Androgen Receptor
ARA70: Androgen Receptor Associated coregulator 70
ARE: Androgen response element
ARR19: Androgen receptor corepressor, 19 kDa
AR-v: Androgen receptor splice variant
BBS: (BES)-buffered saline
BES: N,N-Bis(2-hydroxyethyl)-2-aminoethanesulphonic acid
BIC: Bicalutamide
BL1: Basal like 1
BL2: Basal like 2
BMI: Body Mass Index
BrCa: Breast cancer
BRCA1: Breast Cancer 1, Early Onset
BRCA2: Breast Cancer 2, Early Onset
BRDU: Bromodeoxyuridine
BSA: Bovine serum albumin
C1orf116: *Chromosome 1 open reading frame 116*
$CaCl_2$: Calcium chloride
CAIS: Complete Androgen Insensitivity Syndrome
CDC: Centres for Disease Control and Prevention
CDK: Cyclin Dependent Kinase

cDNA: Complementary DNA

CHEK2: Checkpoint Kinase 2

ChIP: Chromatin Immunoprecipitation

ChIP-Seq: Chromatin Immunoprecipitation sequencing

CREB1: Cyclic-AMP Responsive Element Binding Protein 1

CRUK: Cancer Research UK

CTC: Circulating tumour cell

C-Terminal: Carboxyl-Terminal

CO_2: Carbon dioxide

CXCL12: *C-X-C Motif Chemokine Ligand 12*

CYP3A4: Cytochrome P450 3A4

C1orf116: Chromosome 1 open reading frame 116

DBD: DNA Binding Domain

D-Box: Distal box region

DC: Detergent compatible

DCIS: Ductal Carcinoma *in situ*

ddH_2O: Double distilled water

DHEA: Dehydroepiandrosterone

DHT: Dihydrotestosterone

DMEM: Dulbecco's Modified Eagle's Medium

DMSO: Dimethyl sulfoxide

DNA: Deoxyribonucleic acid

dNTP: Deoxyribonucleotide

E1: Oestrone

E2: 17-β-Oestradiol

E3: Oestriol

E. coli: *Escherichia coli*

EDTA: Ethylenediaminetetraacetic acid

EGFR: Epidermal Growth Factor Receptor

ENZA: Enzalutamide

ERα: Oestrogen Receptor alpha

ERβ: Oestrogen Receptor beta

ErbB2: Erythroblastosis Oncogene B2

ERE: Oestrogen Response Element

ERK: Extracellular signal regulated kinase

ESR1: *Oestrogen Receptor 1*

ESR2: *Oestrogen Receptor 2*

EtOH: Ethanol

EV: Empty Vector

F: Forward

FBN1: *Fibrillin 1*

FCS: Foetal calf serum

FDA: Food and Drug Administration

FGFR: Fibroblast Growth Factor Receptor

FOX: Forkhead Box

FOXA1: Forkhead Box A1

FSH: Follicle Stimulating Hormone

FULV: Fulvestrant

GATA3: GATA binding protein 3

GEO: Gene Expression Omnibus

GFP: Green Fluorescent Protein

GnRH: Gonadotropin Releasing Hormone

GR: Glucocorticoid receptor

GREB1: *Gene Regulated in Breast Cancer 1*

HDAC4: Histone deacetylase 4

HER2: Human Epidermal Growth Factor Receptor 2

HRE: Hormone response element

HSP90: Heat-shock protein 90

IGFR: Insulin like Growth Factor Receptor

IgG: Immunoglobulin G

IHC: Immunohistochemistry

IM: Immunomodulatory

Jak: Janus Kinase

KCl: Potassium chloride

kDa: Kilodalton

KCNK5: *Potassium Two Pore Domain channel subfamily K Member 5*

ki67: Marker of Proliferation ki-67

L19: RPL19 ribosomal protein

LAR: Luminal androgen receptor

LB: Luria Broth

LBD: Ligand Binding Domain

LCIS: Lobular Carcinoma *in situ*

LH: Luteinizing Hormone

LHRH: Luteinising Hormone Releasing Hormone

lncRNA: Long noncoding RNA

MAPK: Mitogen-activated protein kinase

Me: Mesenchymal

MeOH: Methanol

$MgCl_2$: Magnesium chloride

mRNA: Messenger RNA

MIB: Mibolerone

miRNA: microRNA

MMPED2: *Metallophosphoesterase-Domain-Containing Protein 2*

MPA: Medroxyprogesterone acetate

MR: Mineralocorticoid receptor

MRI: Magnetic Resonance Imaging

MSL: Mesenchymal stem like

MYB: *MYB Proto-Oncogene, Transcription Factor*

mTOR: mammalian target of rapamycin

NaCl: Sodium chloride

NaOH: Sodium hydroxide

NCoR: Nuclear receptor corepressor 1

NDRG1: *N-myc Downstream-Regulated Gene 1*

NGS: Next Generation Sequencing

NR: Nuclear receptor

NST: Invasive carcinomas

N-Terminal: Amino-Terminal

NTD: N-Terminal Domain

Oncogenic miRNA: oncomiR

PAIS: Partial Androgen Insensitivity Syndrome

P-box: Proximal box region

PBS: Phosphate Buffered Saline

PCR: Polymerase Chain Reaction

PCOS: Polycystic Ovarian Syndrome

PFA: Paraformaldehyde

PGR: *Progesterone Receptor*

PIC: Protease inhibitor cocktail

PI3K: Phosphatidylinositol-4,5-Bisphosphate 3-Kinase

PIK3CA: Phosphatidylinositol-4,5-Bisphosphate 3-Kinase Catalytic Subunit Alpha

PK: Protein Kinase

PR: Progesterone receptor

PrCa: Prostate Cancer

PSCA: Prostate Stem Cell Antigen

PTEN: Phosphatase and Tensin Homolog

PVDF: Polyvinylidene difluoride

qPCR: Real-Time quantitative PCR

R: Reverse

RIN: RNA integrity number

RIPA: Radioimmunoprecipitation assay

RNA: Ribonucleic acid

RNA-Seq: RNA-Sequencing

RPMI: Roswell Park Memorial Institute

Rpm: Revolutions per minute

rRNA: ribosomal RNA

RPL19: Ribosomal Protein L19

RT: Room temperature

SARM: Selective Androgen Receptor Modulator

SDS: Sodium dodecyl sulphate

SDS-PAGE: Sodium dodecyl sulphate polyacrylamide gel electrophoresis

SEC14L2: *SEC14 like Lipid binding 2*

sFCS: double charcoal stripped foetal calf serum

SHP: Short Heterodimer Protein

SERD: Selective Oestrogen Receptor alpha Downregulator

SERM: Selective Oestrogen Receptor alpha Modulator

siRNA: small interfering RNA

SOX9: SRY-box-9

SOC: Super optimal broth with catabolite repression

SRC: Steroid receptor coactivator

SUMO: Small ubiquitination like modifier

T: Testosterone

TAE: Tris-Acetate-EDTA

TAM: Tamoxifen

TAU: Transactivation unit

TBE: Tris-Borate-EDTA

TBS: Tris-buffered saline

TCGA: The Cancer Genome Atlas

TE: Tris-EDTA

TEMED: Tetramethyl ethylenediamine

TF: Transcription Factor

TFF1: *Trefoil Factor 1*

TP53: *Tumour Protein 53*

TNBC: Triple Negative Breast Cancer

TRAM1: Thyroid Hormone Receptor Activator 1

Tris-HCl: Tris-Hydrochloric Acid

tsmiR: Tumour suppressor miRNA

UCSC: University of California, Santa Cruz

WT: wild-type

ZBTB16: *Zinc Finger And BTB Domain Containing 16*

Table of Contents

List of Tables

List of Figures

Chapter 1
Introduction

Introduction

1.1 The Structure, Function and Development of the Normal Breast

In humans, the breasts or mammary glands are organs which produce the milk that provides nutrition and immunological protection for offspring (Kumar et al., 2013). The main structure of the mammary gland (Figure 1-1) consists of specialised epithelium (ducts and lobules) surrounded by the stroma (Rezaei et al., 2016). The lobular luminal cells produce milk whereas the myoepithelial cells, which have myofilaments and are able to contract, play an important role in milk ejection from the luminal cells (Rezaei et al., 2016). The stroma contains vascular endothelial cells and immune cells, fibrous and adipose tissue (Macias and Hinck, 2012; Rezaei et al., 2016).

Although the development of the mammary gland begins during embryogenesis, the major changes and development of the breast occur during the reproductive years (Macias and Hinck, 2012). With the onset of puberty, the mammary tissue is exposed to rising oestrogen and progesterone levels within the monthly female sexual cycle, resulting in stimulation of the ductal system and development of the lobule-alveolar system (Arendt and Kuperwasser, 2015). Growth hormone, prolactin and adrenal glucocorticoids also have an important role in the development of the mammary gland, specifically the ductal system (Hall, 2011b). As the levels of ovarian steroids increase and decrease during the menstrual periods, in addition to the endometrial cell proliferation and regression, the epithelial cells of the breast also cycle (Ramakrishnan et al., 2002). The capacity of the mammary gland to repeatedly go through this proliferation and regression process can be explained by the presence of stem cells in the mammary gland (Böcker et al., 2002; Macias and Hinck, 2012; Yang et al., 2017).

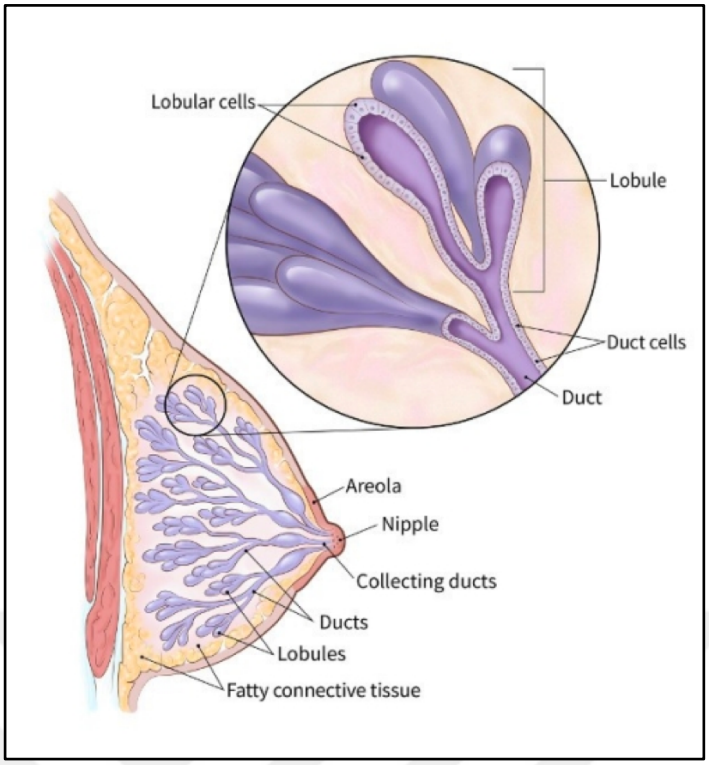

Figure 1-1 The general structure of the human mammary gland

Figure is taken from (American Cancer Society, 2019)

Gene expression analysis of normal breast tissue has demonstrated that the gland contains two distinct types of epithelial cells, which are basal (myoepithelial) and luminal (Perou et al., 2000). Different compartments of the mammary gland have different cell types, for instance the lobules have only terminally differentiated, functional lactating cells whereas the ducts host a proliferative region containing a significant number of progenitor cells (Böcker et al., 2002). Both luminal and myoepithelial cells originate from a type of progenitor cell in the terminal duct of the mammary gland (Böcker et al., 2002; Arendt and Kuperwasser, 2015). Precursor stem cells have the ability, through intermediary cells which coexpress the progenitor cell marker with the glandular or myoepithelial cell markers, to differentiate to myoepithelial or glandular cells (Böcker et al., 2002). It has been suggested that these progenitor cells contribute to remodelling of the mammary gland after lactation (Böcker et al., 2002).

1.2 Gonadotropin Hormone Pathway

Reproductive tissues like breast, endometrium and prostate develop and grow in response to hormones. The hypothalamus produces gonadotropin releasing hormone (GnRH) and in response to GnRH, the pituitary gland releases the gonadotropins into the bloodstream (Figure 1-2) (Hall, 2011b). Luteinising Hormone (LH) and Follicle Stimulating Hormone (FSH) stimulate the gonads to produce the sex steroids. The elevation of sex steroid level in blood inhibits the hypothalamus release of GnRH via a negative feedback loop, therefore inhibiting the production of gonadotropins from the pituitary gland (Hall, 2011b).

This pathway can be disrupted at 3 different steps: gonadotropin release, steroidogenesis, and steroid hormone receptors. GnRH agonists, such as goserelin, facilitate the production of androgens and oestrogens. This increase of sex steroids in the bloodstream then causes the inhibition of gonadotropins via the negative feedback loop, resulting in downregulation of androgen and oestrogen production (Garner, 1994). Steroidogenesis can be disrupted by drugs that inhibit the steroidogenesis conversion enzymes (for example, 17β-Hydroxysteroid dehydrogenase inhibitors, 5α-reductase inhibitors, aromatase inhibitors), leading to inhibition of androgen and oestrogen production (Foster, 2008). Finally, the binding of the ligands to their

receptors can be blocked by steroid receptor blockers (i.e., antiandrogens, antioestrogens).

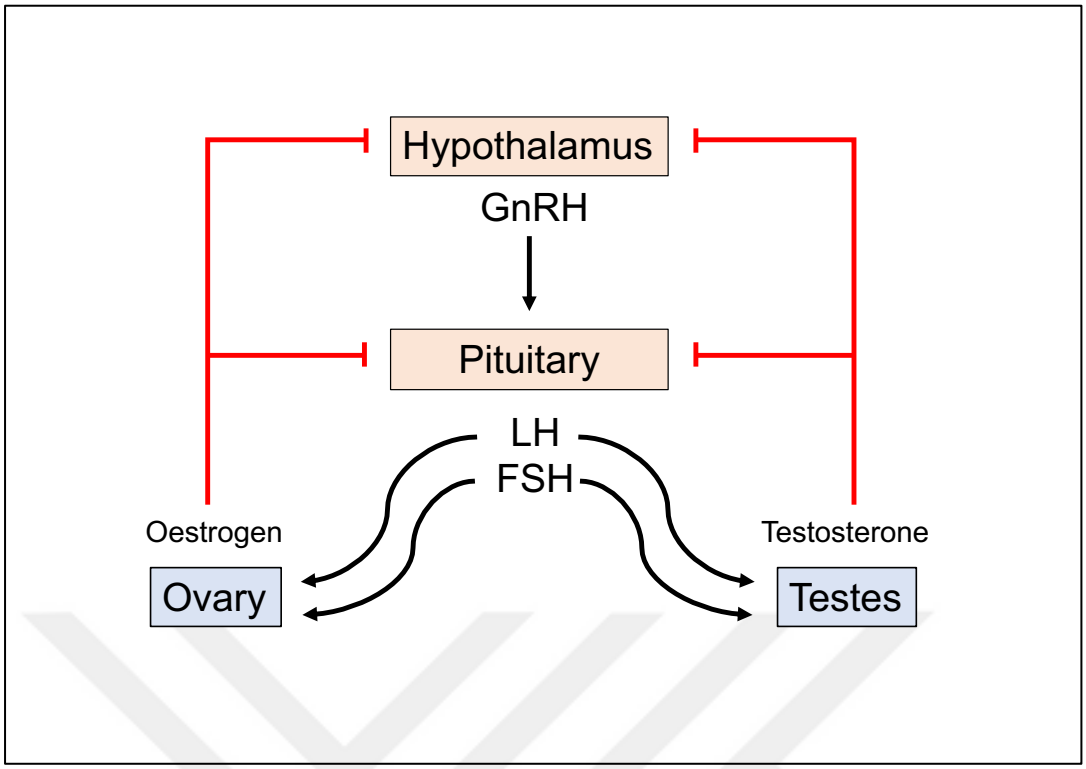

Figure 1-2 The hypothalamic-pituitary-gonadal axis

GnRH secreted by the hypothalamus stimulates the release of gonadotropins, LH and FSH. In men, LH stimulates testosterone production in the testes, and FSH stimulates sperm production. In women, LH and FSH stimulate production of oestrogen and progesterone in the ovary. Elevated oestrogen and testosterone levels stop GnRH and LH/FSH production in the hypothalamus and pituitary via negative feedback loop.

1.2.1 Steroidogenesis

Sex steroids are produced via the process called steroidogenesis (Figure 1-3) in the adrenal glands and gonads. Although oestrogens are the main hormones responsible for female sexual development (i.e. mammary and endometrial glands), androgens are secreted at a higher concentration than oestrogens in women (Burger, 2002). Further, it has been shown that in premenopausal women, androgen receptor (AR) is expressed more than oestrogen receptor α (ERα) in mammary gland (Li et al., 2010).

Three oestrogens are present in the blood of women: oestrone (E1), which is synthesized in the peripheral tissues from androgens secreted by the adrenal glands and ovaries; β-oestradiol (E2 or 17β-oestradiol), which is secreted by the ovaries; oestriol (E3), which is predominantly synthesized in the liver through 16α-hydroxylation (Cui et al., 2013). E2 is 12 times more potent than E1 and 80 times more potent than E3 (Hall, 2011b). During luteinisation phase, the theca cells in the ovary produce androstenedione (A) and testosterone (T) which are then converted into E1 and E2, respectively by the aromatase enzyme in the granulosa cells. FSH secretion stimulates the aromatisation. E3 is a weak oestrogen, derived from E2 via CYP3A4 in the liver (Hall, 2011b; Cui et al., 2013). A schematic representation of the steroidogenic pathways leading to oestrogen synthesis is represented in Figure 1-3.

Androgens are produced in women from the ovaries and adrenal glands (Burger, 2002). The main circulating androgens in women are dehydroepiandrosterone (DHEA), A, T, and dihydrotestosterone (DHT), from highest concentration to lowest concentration in the blood, respectively (Rahim and O'Regan, 2017). The enzymes in the zona reticularis of the adrenal gland convert pregnenolone to DHEA and progesterone to A (Burger, 2002). However, only T and DHT have the ability to bind to and activate the AR (Rahim and O'Regan, 2017). Steroid hormone levels, in circulating blood, changes throughout life mainly depending on menopausal status. For instance, because of reduced ovarian activity in post-menopausal women, oestrogen levels decrease significantly (Secreto et al., 2019).

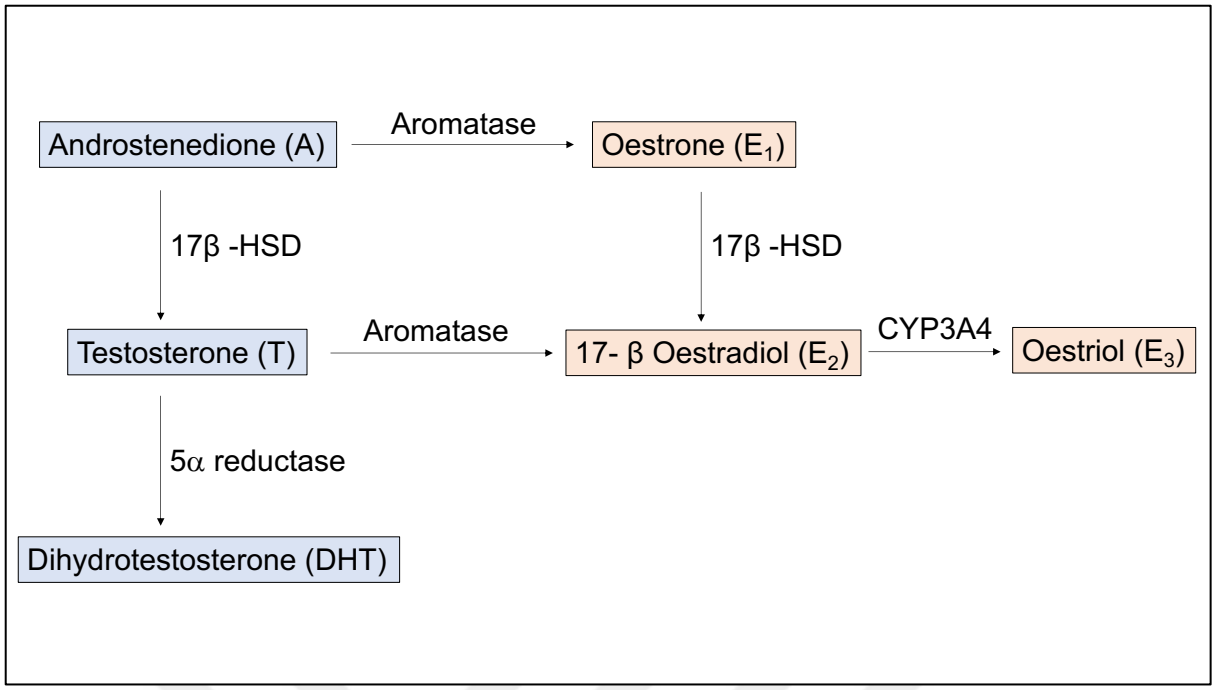

Figure 1-3 Synthesis of oestrogens from androgens

Schematic representation of the steroidogenic pathways leading to oestrogen synthesis from androgenic precursors. 17β-HSD, 17β-Hydroxysteroid Dehydrogenase; CYP3A4, Cytochrome P450 3A4.

Androgens are known to have an inhibitory effect on normal breast growth (Tiefenbacher and Daxenbichler, 2008), but excessive circulating androgen levels have been associated with increased breast cancer (BrCa) risk, specifically ERα-positive (Secreto et al., 2019). However, diseases that have increased androgen levels, such as polycystic ovarian syndrome (PCOS) are not associated with increased BrCa risk (Kotsopoulos and Narod, 2012). Therefore, this increase in BrCa risk could be because of ligand activated cell-specific AR activity, or intra-tumoral aromatase activity in BrCa (Secreto et al., 2019). Accordingly, it has been reported that BrCa tumours that have a BRCA1 (Breast Cancer 1, Early Onset) mutation also have enhanced aromatase activity in the tumour tissues (Kotsopoulos and Narod, 2012).

1.3 Breast Cancer

1.3.1 Breast Cancer Statistics

BrCa is the most common cancer in the UK (Cancer Research UK, 2018a), accounting for 15% of all new cancer cases, and is the second most common cancer in the world (WHO, 2018). There are approximately 2.09 million new BrCa cases every year and it is the 5th most common cause of cancer death (WHO, 2018). Although BrCa mortality rates have decreased by 38% (Cancer Research UK, 2016b) over the last 20 years, 11,482 women and 81 men died in the UK in 2016 as a result of BrCa (Cancer Research UK, 2016a).

1.3.2 Breast Cancer Risk Factors

The most significant risk factor for BrCa is gender, being approximately 100 times more common in women than men. There are multiple established and probable factors that also increase the risk of BrCa, including: older age, geographical location, early onset of menarche, late onset of menopause, nulliparity, late age to first pregnancy, history of BrCa in first relative, high intake of saturated fat, being overweight or obese after menopause, low Body Mass Index (BMI) in premenopausal women, use of oral contraceptive, inherited genetic changes such as BRCA1 and BRCA2 (Breast Cancer 2, Early Onset) mutations (McPherson et al., 2000; CDC,

2018). History of atypical hyperplasia, white women of non-Hispanic ancestry, postmenopausal hormone replacement therapy, history of endometrial carcinoma and environmental toxins such as organochlorine pesticides, which have oestrogenic activity, are additional factors that increase the risk of BrCa development (Kumar et al., 2013). A recent case-control study focussing on the dietary habits of BrCa patients found that drinking instant coffee for more than 10 years increases BrCa risk by 48% compared to the patients who has been drinking brewed coffee (Lee et al., 2019). In contrast, physical exercise, breast feeding and pregnancy at a young age, SERMs and aromatase inhibitors (AIs) are considered protective factors against BrCa development (National Cancer Institute (US), 2018).

BRCA1, BRCA2, p53 and CHEK2 (Checkpoint Kinase 2) are the most common single gene mutations associated with hereditary susceptibility to BrCa (Kumar et al., 2013). However, in a population-based case-control study, investigating BrCa risk factors, it was found that multiparity and young age for first pregnancy decreased the risk of Luminal A disease, but increased the risk of basal like disease (Millikan et al., 2008), suggesting that risk factors can vary according to the subtype (see Section 1.3.4 Breast Cancer Subtypes).

1.3.3 Breast Cancer Development

BrCa occurs through a series of changes in the epithelial cells; starting with hyperplasia, then evolving into *in situ* carcinomas, and eventually to invasive carcinomas (Arpino et al., 2005; Costa and Zanini, 2008; Rakha and Green, 2017). The changes in the epithelial cells before becoming invasive carcinomas are known as premalignant lesions (Feng et al., 2018). The terminal duct lobular unit is the most proliferative compartment of the mammary gland, where both luminal and myoepithelial cells of the breast originate from. Hence, it is thought that premalignant lesions arise from the terminal duct lobular unit, eventually becoming malignant (Feng et al., 2018).

The process of epithelial cells in the terminal duct lobular units undergoing proliferation can sometimes result with hyperplastic lesions (Costa and Zanini, 2008; Feng et al., 2018). The most common hyperplastic change is usual ductal hyperplasia, which overexpresses ERα as compared to normal breast epithelial cells, is well

differentiated, and is found in around one quarter of benign breast biopsies. There can also be atypical hyperplastic changes, such as atypical ductal hyperplasia, atypical lobular hyperplasia (Arpino et al., 2005; Lebeau, 2010). These atypical lesions then progress to *in situ* (non-invasive) carcinomas. *In situ* carcinomas are pre-invasive lesions (Arpino et al., 2005; Feng et al., 2018). They are confined to the normal breast lobules and ducts, and do not extend beyond basal membrane. Invasive carcinomas, on the other hand, spread outside of the basal membrane, and invade surrounding tissues, therefore, have the potential to metastasise to other parts of the body. Metastatic or advanced BrCas are late-stage cancers and have limited treatment options as the cancer is already spread to other organs such as lymph nodes, lungs, brain (Arpino et al., 2005; Costa and Zanini, 2008; Feng et al., 2018). Treatment options for BrCa patients are decided on the grade, stage, and molecular subtype of the disease (Rakha et al., 2010; Rakha and Green, 2017).

The grade of BrCa is a prognostic factor and represents the aggressiveness of a tumour (Kumar et al., 2013; Johns Hopkins Pathology, 2021). The lower the grade, the better the prognosis. In order to determine the grade of a tumour, different scoring systems have been in use. One of these is the Nottingham Scoring System which considers 3 factors: formation of the gland/tubule, nuclear pleomorphism, and mitotic activity (Table 1-1) (Johns Hopkins Pathology, 2021). A well differentiated tumour has a lower grade, whereas a poorly differentiated tumour has a higher grade, and the course of the disease tends to be more aggressive in these patients (Rakha et al., 2010). Another important classification is the molecular subtype of the disease which is discussed in detail in Section 1.3.4. To determine the stage of the disease based on the tumour size, lymph node metastasis and systemic metastasis, TNM scoring system is being used (see Section 1.3.5).

Table 1-1 Nottingham Histological Grade Scoring System

Score	Glandular/tubular differentiation	Nuclear pleomorphism	Mitotic count*
1	>75% of tumour forms glands	Uniform cells with small nuclei similar in size to normal breast epithelial cells	<7 mitoses per 10 high power fields
2	10-75% of tumour forms glands	Cells larger than normal with open vesicular nuclei, visible nucleoli, and moderate variability in size and shape	8-15 mitoses per 10 high power fields
3	<10% of tumour forms glands	Cells with vesicular nuclei, prominent nucleoli, marked variation in size and shape	>16 mitoses per 10 high power fields

*High power field diameter of 0.52mm.

The scores from all three categories above are added up to come up with the Overall Grade.

Total Score	Overall Grade
3-5	Grade I (Low)
6-7	Grade II (Intermediate)
8-9	Grade III (High)

1.3.4 Breast Cancer Subtypes

BrCa is a diverse disease, which has various gene expression profiles, therapy responses and phenotypes (Perou et al., 2000; Sørlie et al., 2001). Classification of BrCa is highly important, in terms of determining the treatment and patients' responsiveness to the therapy. Histologically, the majority of breast carcinomas (70-85%) are invasive carcinomas (NST), the remaining 15-30% are either ductal carcinoma *in situ* (DCIS or intraductal carcinoma) or lobular carcinoma *in situ* (LCIS) (Kumar et al., 2013). Carcinoma *in situ* means that disease is non-invasive and confined to the basal layer of ducts and lobules (Ward et al., 2015).

Over the past couple of decades, major advances in molecular biology have allowed us to classify invasive carcinomas by using immunohistochemistry (IHC) staining and gene expression profiling techniques (Prat et al., 2015). Canonical classification of distinct molecular subtypes of BrCa classifies tumours into Luminal A, Luminal B, HER2 enriched and basal-like (Table 1-2). These subtypes are defined by the expression of Oestrogen Receptor alpha (ERα), Progesterone Receptor (PR) and Human Epidermal Growth Factor Receptor 2 (HER2 or erythroblastosis oncogene B2, ErbB2), the expression of which have clinical importance for response to therapy and prognosis (Fioretti et al., 2014; Barnard et al., 2015).

The majority of BrCas, approximately 70%, are Luminal A and luminal B subtypes, defined as hormone receptor positive (Renoir et al., 2013). Carcinomas defined as luminal have similar characteristics to breast epithelial cells and are ERα-positive (Zwart et al., 2011). The Luminal A subtype, stains positive for ERα and negative for HER2 amplification, has the best therapy response and prognosis relative to other molecular subtypes (Zwart et al., 2011). Unlike Luminal A tumours, Luminal B tumours have HER2 amplification, more genomic mutations and express more proliferative genes (Prat et al., 2015). Therefore, it is more likely for Luminal B cancers to have lymph node metastases (Kumar et al., 2013). ERα-negative, HER2 enriched subtype account for 20% of breast tumours, have higher levels of genomic mutations and overexpress the HER2 oncogene (Zwart et al., 2011; Fioretti et al., 2014; Prat et al., 2015). These tumours tend to be more aggressive and proliferative, and to have a worse prognosis than luminal tumours (Fioretti et al., 2014).

The remaining 10% of BrCas are described as basal-like subtype, also known as triple negative BrCa (TNBC) because of the absence of ERα, PR and HER2. This subtype includes the medullary carcinomas and metaplastic carcinomas, and are more associated with BRCA1 mutations (Prat et al., 2015; Hon et al., 2016). The term basal means these cancers are positive for markers of basal breast epithelial cells (e.g., basal keratins, laminin) (Prat et al., 2015). The most distinct subtype of BrCa is basal-like, which highly expresses the marker of proliferation ki-67 and although these tumours do not usually express HER2, it has been reported that up to 17.4% of basal-like tumours might have *HER2* gene amplification (Prat et al., 2015). LCIS and invasive lobular carcinomas are associated with loss of E-cadherin, a cell adhesion molecule that functions as a tumour suppressor in epithelial cells, and PTEN (Phosphatase and Tensin Homolog) gene mutation (Pećina-Slaus, 2003; Boelens et al., 2016).

Table 1-2 Molecular subtypes of Breast Cancer

ERα, Oestrogen Receptor α; PR, Progesterone Receptor; HER2, Human Epidermal Growth Factor Receptor 2; TNBC, Triple Negative Breast Cancer

Subtype	ERα	PR	HER2
Luminal A	+	+	-
Luminal B	+	+/-	+
HER2 enriched	-	-	+
Basal like/TNBC	-	-	-

Analysis of primary BrCas by genomic DNA copy number, DNA methylation, exome sequencing, mRNAs, and protein arrays have provided key insights into molecular portraits of the disease (Cancer Genome Atlas Network, 2012). It was found that *PIK3CA*, *TP53*, *GATA3* were the most commonly mutated genes across all samples. HER2-enriched and basal like tumours had higher mutation rates as compared to luminal tumours. Luminal tumours had loss of 16q, gain of 1q, and had the luminal gene expression signature (*ESR1*, *GATA3*, *FOXA1*, *XBP1*, *MYB*). Basal like tumours showed loss of 5q, gain of 10p, and had the highest *TP53* mutation rate as compared to other subtypes. Another difference between the subtypes was the type of *TP53* mutations. For example, the majority of *TP53* mutations were nonsense and frameshift in basal like, whereas luminal tumours mostly harboured missense mutations. The analysis also revealed distinctive DNA methylation groups. The group with the lowest DNA methylation were similar to basal like subtype, whereas the group with the highest DNA methylation were similar with luminal B subtype. Finally, it was found that the epigenetic changes occur within the 4 molecular subtypes, and not across (Cancer Genome Atlas Network, 2012).

The use of BrCa subgrouping has improved disease outcomes; however, a more specific molecular portrait classification is much needed, but remains a challenge. Classifying tumours into additional subgroups could allow for more specialised and targeted treatments, resulting in better clinical outcomes for patients. For example, genomic analysis of 2000 BrCa tumours identified 10 distinct subgroups which were associated with definitive clinical characteristics and outcomes (Dawson et al., 2013). This subgrouping identified gene expression profiles that could be used for BrCa classification and presented a more comprehensive way of understanding the genomic landscapes of these tumours. For instance, one of the groups had amplification in 17q23 locus and high *GATA3* mutation frequency as compared to other groups. Another group, which had 11q13/14 amplification, consisted of luminal A and B tumours, and had the worst prognosis amongst all ERα-positive tumours. The group which had the best prognosis amongst these subgroups was the one with a low mutation rate in *TP53* but a high mutation frequency in *PIK3CA*. Although this group was mostly composed of Luminal A tumours, this profile suggests that this subgroup of patients could benefit from chemotherapy (Dawson et al., 2013). However, more clinical studies are needed to assess these different subgrouping systems before this can be applied into clinical practice.

1.3.5 Treatment options for Breast Cancer

The main treatment options for BrCa include various combinations of surgery, chemotherapy, hormonal therapy, radiotherapy, and targeted cancer drugs. Treatment options for BrCa depends on multiple prognostic factors such as size of the tumour, metastasis to lymph nodes or other organs, hormone receptor status, HER2 amplification, age and menopausal status (National Cancer Institute (US), 2018). The development of the molecular subtype classification system has allowed for the use of targeted endocrine therapies, which has led to a great reduction in BrCa associated mortalities, especially patients with early-stage tumours (Hickey, Dwyer, et al., 2021). The stage of the disease also needs to be defined at diagnosis in order to choose the best therapy option for the patient. A scoring system termed as TNM is being used to define the stage based on the tumour size, lymph node metastasis and systemic metastasis (Table 1-3, Table 1-4) (National Cancer Institute (US), 2018). Therefore, treatments are personalised for each patient and are dependent upon the tumour characteristics. However, despite the success with endocrine therapy options, metastatic BrCa mortality rates have not improved significantly over the years (Hickey, Dwyer, et al., 2021).

Table 1-3 TNM classification of Breast Cancer

T, Tumour; N, Lymph nodes; M, metastasis; c, clinical; p, pathological. Table is adapted from (AJCC, 2017).

T Category	**T Criteria**
TX	Primary tumour cannot be assessed
T0	No evidence of primary tumour
Tis (DCIS)	Ductal carcinoma in situ
Tis (Paget)	Paget disease not associated with invasive carcinoma or DCIS
T1	Tumour size ≤ 20 mm
T1mi	Tumour size ≤ 1 mm
T1a	Tumour size > 1 mm but ≤ 5 mm
T1b	Tumour size > 5 mm but ≤ 10 mm
T1c	Tumour size > 10 mm but ≤ 20 mm
T2	Tumour size > 20 mm but ≤ 50 mm
T3	Tumour size > 50 mm
T4	Tumour with direct extension to the chest wall and/or the skin with macroscopic changes
T4a	Tumour with chest wall invasion
T4b	Tumour with macroscopic skin changes including ulceration and/or satellite skin nodules and/or oedema
T4c	Tumour with criteria of both T4a and T4b
T4d	Inflammatory carcinoma
N Category	**N Criteria**
NX	Regional nodes cannot be assessed (previously removed)
N0	No regional nodes metastases
N1	Metastases to movable ipsilateral level I and/or level II axillary nodes
N1mi	Micro metastases
N2	Metastases to fixed or matted ipsilateral level I and/or level II axillary nodes, or metastases to ipsilateral internal mammary nodes without axillary metastases
N2a	Metastases to fixed or matted ipsilateral level I and/or level II axillary nodes
N2b	Metastases to ipsilateral internal mammary nodes without axillary metastases
N3	Metastases to ipsilateral level III axillary nodes with or without level I and/or level II axillary metastases ; or metastases to ipsilateral internal mammary nodes with level I and/or level II axillary metastases; or metastases to ipsilateral supraclavicular nodes
N3a	Metastases to ipsilateral level III axillary nodes with or without level I and/or level II axillary metastases
N3b	Metastases to ipsilateral internal mammary nodes with level I and/or level II axillary metastases
N3c	Metastases to ipsilateral supraclavicular nodes
M Category	**M Criteria**
M0	No clinical or imaging evidence of distant metastases
cM0(+)	No clinical or imaging evidence of distant metastases, but with tumour cells or deposits measuring ≤ 0.2 mm detected in circulating blood, bone marrow, or other nonregional nodal tissue in the absence of clinical signs and symptoms of metastases
cM1	Distant metastases on the basis of clinical or imaging findings
pM1	Histologically proven distant metastases in solid organs; or, if in nonregional nodes, metastases measuring > 0.2 mm

Table 1-4 Staging of Breast Cancer according to TNM classification

Stage	**TNM**
Stage 0	Tis, N0, M0
Stage IA	T1, N0, M0
Stage IB	T0, N1mi, M0
	T1, N1mi, M0
Stage IIA	T0, N1, M0
	T1, N1, M0
	T2, N0, M0
Stage IIB	T2, N1, M0
	T3, N0, M0
Stage IIIA	T0, N2, M0
	T1, N2, M0
	T2, N2, M0
	T3, N1, M0
	T3, N2, M0
Stage IIIB	T4, N0, M0
	T4, N1, M0
	T4, N2, M0
Stage IIIC	AnyT, N3, M0
Stage IV	AnyT, AnyN, M1

The most important factor for better therapy response and decreasing BrCa mortality rates is early detection and diagnosing (American Cancer Society, 2019). The American Cancer Society (ACS) recommends that women at average BrCa risk should get mammograms annually after 45 and have the opportunity to begin annual screening between the ages 40 and 44 years (Oeffinger et al., 2015). The suggestion for women at high risk of BrCa (i.e., to have a known *BRCA1* or *BRCA2* gene mutation, a first degree relative with these mutations or to have certain types of hereditary disorders that predisposes to cancer development) is that they should be screened from the age of 30, and that the person should get a Magnetic Resonance Imaging (MRI) and a mammogram annually (American Cancer Society, 2019).

1.3.5.1 Surgical options for Breast Cancer

Surgery options for BrCa patients include breast conserving surgery (lumpectomy), which aims to remove the tumour and the surrounding tissue; mastectomy, which aims to remove the breast with cancer; modified radical mastectomy, which is the removal of the breast with cancer and chest muscles and most or all of the lymph nodes in axillary area (Cancer Research UK, 2018c; National Cancer Institute (US), 2018). The treatment for DCIS is either lumpectomy or mastectomy followed by radiotherapy with or without endocrine therapy (National Cancer Institute (US), 2018). For early, localized BrCa, lumpectomy or modified radical mastectomy is performed initially. However, for locally advanced or inflammatory BrCa patients, a neoadjuvant therapy might be needed to downsize the tumour before surgery (National Cancer Institute (US), 2018). Following the removal of the tumour, an adjuvant therapy is usually required to prevent the systemic recurrence (Gonzalez-Angulo et al., 2007).

Another treatment approach for BrCa patients is to surgically remove the ovaries (oophorectomy) to stop oestrogen and progesterone production permanently (Lumachi et al., 2015). This suppression of ovarian function can also be achieved medically by GnRH or LHRH agonists, the effect of which is reversible (Goel et al., 2009).

1.3.5.2 Chemotherapy and Targeted Cancer Drugs for Breast Cancer

For the subtypes of BrCa which do not have targeted therapy options (i.e. endocrine therapies, AIs, Herceptin), chemotherapy still remains the only option as an adjuvant or neoadjuvant treatment (Ali and Coombes, 2002). Chemotherapy drugs are usually used in a combination rather than single agent therapy to prevent the recurrence and improve the treatment response. Anthracycline (i.e., doxorubicin, daunorubicin) and taxane (i.e., docetaxel, paclitaxel) combinations are preferred for patients who have lymph node metastasis to improve the survival rates (National Cancer Institute (US), 2018). A meta-analysis has demonstrated that anthracycline-taxane combination improved the disease-free survival and overall survival, and reduced the relapse risk for early BrCa patients at high risk (de Laurentiis et al., 2008).

Neoadjuvant chemotherapy regimens are also the same as adjuvant therapies, they usually consist anthracycline and/or taxane based therapies (National Cancer Institute (US), 2018). For example, doxorubicin/cyclophosphamide therapy was more effective when given as neoadjuvant treatment as compared to when given as adjuvant therapy (Wolmark et al., 2001). Another study showed that addition of docetaxel after cyclophosphamide as neoadjuvant therapy increased the response rates of operable BrCa patients as compared to cyclophosphamide only treatment (Bear et al., 2003). For HER2-positive patients neoadjuvant therapies consist of chemotherapeutics and HER2 targeted therapies (National Cancer Institute (US), 2018).

The main therapeutic option for TNBC is chemotherapy, as the tumour lacks the receptors, ERα and HER2, that are targeted by endocrine therapies and HER2-monoclonal antibody, respectively. Trastuzumab (Herceptin), a monoclonal antibody that specifically binds to the extracellular domain of HER2, has led to a significant improvement in patients with HER2-positive disease (Fioretti et al., 2014; Fabi et al., 2014). Moreover, combination of trastuzumab with another HER2 targeted drug, pertuzumab, which blocks the dimerization of HER2, significantly extended survival rates in comparison with trastuzumab only treatment in HER2-positive patients (Vorobiof, 2016). There are other cancer drugs that target other signalling pathways like tyrosine kinase, cyclin-dependent kinase (i.e., palbociclib, ribociclib, abemaciclib), mammalian target of rapamycin (mTOR) (everolimus) however, therapy resistance in

BrCa continues to be a significant clinical problem (Murphy and Dickler, 2016; National Cancer Institute (US), 2018).

1.3.5.3 Endocrine Therapies for Breast Cancer (Antioestrogens and Aromatase Inhibitors)

As previously stated, the majority of BrCas are hormone receptor positive and sensitive to endocrine therapies which can be used as a neoadjuvant therapy to shrink the size of the tumour before, or as an adjuvant therapy after, surgery (Cancer Research UK, 2018b). However, most of the neoadjuvant therapies are chemotherapy drugs rather than endocrine therapies in ERα-positive disease, as it was found to be more effective (Zhang et al., 2021). Endocrine therapies include AIs and antioestrogens. There are two types of antioestrogens: Selective Oestrogen Receptor Modulators (SERMs), for example tamoxifen (TAM), which acts as an antagonist or agonist depending on tissue context (Jordan, 2007), and Selective Oestrogen Receptor Down Regulators (SERDs), such as fulvestrant (FULV), which act as an antagonist in all tissues (Cardoso et al., 2013). In contrast, AIs (anastrozole, exemestane, letrozole) block oestradiol (E_2) synthesis. Not all patients respond to endocrine therapies (*de novo* resistance), and those who initially respond often become therapy resistant (acquired resistance) (Fan et al., 2015).

In general, when E_2 binds to ERα, the receptor undergoes a conformational change that facilitates the binding of coregulatory proteins that enhance the receptor's transcriptional activity. However, anti-oestrogens promote a different conformation that blocks these interactions and therefore inhibits the transcriptional activity of the receptor (Figure 1-4) and in the case of SERMs, which competitively bind to ERα and inhibit the downstream signalling in the oestrogen receptor signalling pathway, these effects can be cell-type specific (Higa and Fell, 2013). For example, TAM has agonistic effects in endometrial tissue, acts as a partial agonist in bone and as an antagonist in breast tissue (Martinkovich et al., 2014). Further, the oestrogenic effect of TAM on the endometrium is associated with increased endometrial cancer risk because of agonistic activity (Martinkovich et al., 2014). Hence, the use of TAM to prevent the occurrence of BrCa in high-risk patients have not been found to be beneficial, since the long-term usage of it increases endometrial proliferation and cancer risk (Vorobiof, 2016).

SERDs block and reduce ERα activity and act as pure antagonists (Cardoso et al., 2013). For example, when FULV binds to ERα, the ligand-receptor complex undergoes conformational changes resulting in a transcriptionally inactive form, blocking homodimerization and nuclear localisation and promotes degradation of the receptor (Hu et al., 2017). SERMs and SERDs are usually prescribed in premenopausal women as they are still able to produce E_2 via ovaries. In postmenopausal women, the main source of E2 is not ovaries but peripheral tissues (Higa and Fell, 2013).

Endocrine therapies are effective, at least initially, in 90% of primary BrCa and 50% of metastatic disease (Gonzalez-Angulo et al., 2007). Approximately 30-40% of treated primary BrCa patients have a systemic recurrence, which is metastatic in most cases (Gonzalez-Angulo et al., 2007; Lei et al., 2019), and once metastasis occurs, few treatment options are available. More than 90% of metastatic BrCa patients do not have curative therapy regimes and the overall survival for these patients is 2 to 3 years (Hu et al., 2017). AR overexpression is one of the mechanisms that has been associated with TAM resistance (de Amicis et al., 2010), suggesting that other signalling pathways may promote therapy failure. Resistance pathways are discussed in detail in Section 1.5.

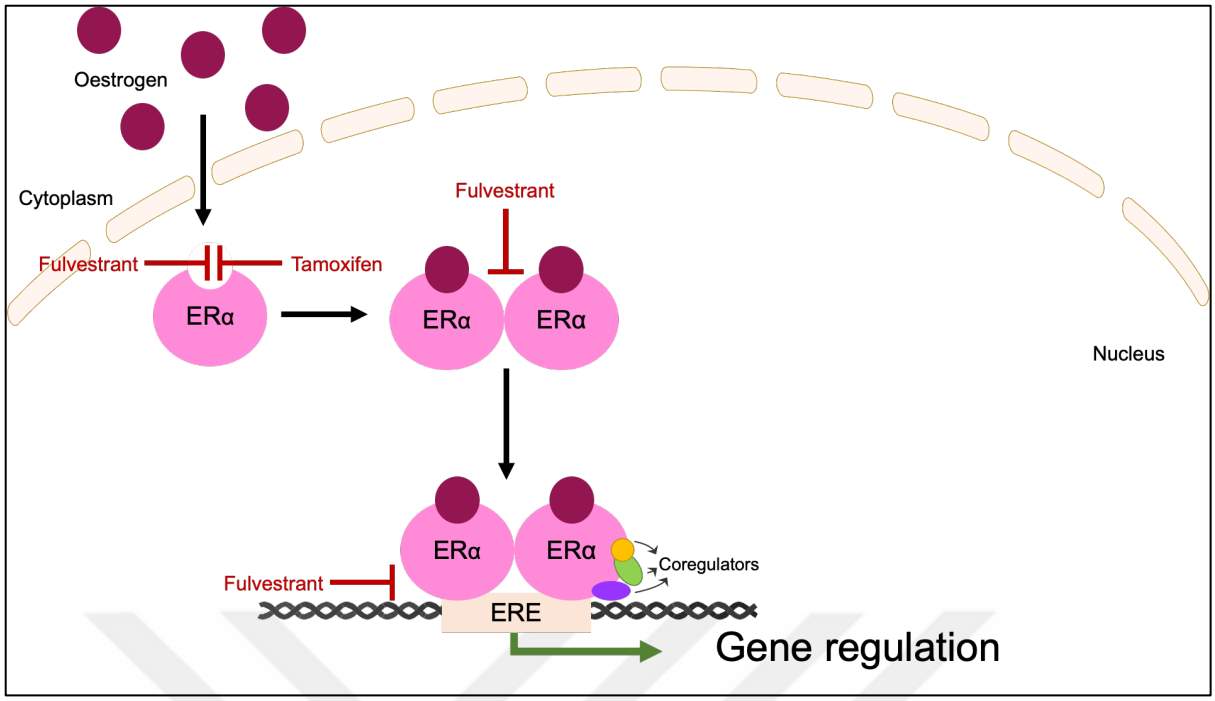

Figure 1-4 Oestrogen signalling pathway and the mechanism of action of Tamoxifen and Fulvestrant

Upon ligand (oestrogen) binding, Oestrogen Receptor α (ERα) forms a homodimer, and activates gene expression via binding to Oestrogen Response Elements (EREs) as part of a complex with coactivators. Tamoxifen blocks the binding of the ligand, and binds to ERα in a way that results in a confirmational change that antagonists receptor activity. Fulvestrant inhibits every step of the signalling pathway: the ligand binding, dimerization, coactivator recruitment and DNA binding.

1.3.5.4 GnRH Agonists for Breast Cancer

Inhibiting the release of GnRH from the hypothalamus, blocks the release of LH and production of oestrogen from the ovaries. Therefore, inhibition of E2 production can be achieved by inhibiting GnRH (Garner, 1994). GnRH agonists such as leuprolide and goserelin, which inhibit LH and FSH release, are FDA approved for BrCa treatment.

Antioestrogens not only bind to ERα in tumours but also bind to their receptors in the hypothalamus and pituitary, causing the disruption of negative feedback and resulting GnRH stimulation which might stimulate the production of oestrogens from the ovaries (Rau et al., 2005). Hence it was proposed that combining the GnRH agonists with antioestrogens or AIs might prevent this possible mechanism of resistance and have better treatment outcomes (Rau et al., 2005). In support of this, the combination treatment of GnRH agonists with AIs or TAM reduced relapse by 4.5-7.7%, compared to TAM only treatment (Nourmoussavi et al., 2017). However, it has been found that GnRH-agonists-induced-premature menopause is associated with long-term mortality risks (i.e., increase of ischaemic heart diseases) and the use of GnRH agonists is not cost-effective (Nourmoussavi et al., 2017).

1.4 Nuclear Receptors

The family of nuclear receptors (NR) function as ligand-dependent transcription factors (TFs) (Sever and Glass, 2013) and humans have 48 members (Table 1-5) (Robinson-Rechavi et al., 2003; le Maire et al., 2010). NRs have a modular structure (Figure 1-5) consisting of a highly variable N-terminal ligand-independent domain (NTD) which contains a region termed as Activation Function 1 (AF1); a DNA Binding Domain (DBD) which contains two highly conserved zinc-finger regions that have a high affinity and specificity for hormone response elements, the proximal box region (P-Box) for sequence specific DNA binding and the distal box region (D-Box) responsible for receptor dimerization; a hinge region responsible for nuclear translocation; a ligand-binding domain (LBD) composed of 12 α helixes and hosts Activation Function 2 (AF2) (Robinson-Rechavi et al., 2003; Sever and Glass, 2013; Pietri et al., 2016; Groner and Brown, 2017). Some NRs have a variable C-terminal

region following the LBD but the function of this domain is unclear for many receptors (Sever and Glass, 2013).

Lipid soluble hormones, such as thyroid hormones, adrenal and gonadal steroid hormones, retinoid hormones and vitamin D, can easily cross the lipid bilayer membrane and interact with their cognate receptors in the cytoplasm or nucleus (Hall, 2011a; Sever and Glass, 2013). After steroid hormone binding, the LBD switches the receptor status to active for transcription (Mangelsdorf et al., 1995). In almost all cases, hormones exert their effects in target tissues by forming a hormone receptor complex (Hall, 2011a). NRs regulate target gene expression via interaction with specific DNA sequences termed as hormone response elements (HREs) by forming a monomer, homodimer, or heterodimer (Robinson-Rechavi et al., 2003).

Table 1-5 Nuclear Receptor family members in humans

NRNC Symbol	Abbreviation	Name
NR1A1	TRα	Thyroid hormone receptor-α
NR1A2	TRβ	Thyroid hormone receptor-β
NR1B1	RARα	Retinoic acid receptor-α
NR1B2	RARβ	Retinoic acid receptor-β
NR1B3	RARγ	Retinoic acid receptor-γ
NR1C1	PPARα	Peroxisome proliferator-activated receptor-α
NR1C2	PPAR-β	Peroxisome proliferator-activated receptor-β
NR1C3	PPARγ	Peroxisome proliferator-activated receptor-γ
NR1D1	Rev-Erbα	Rev-Erbα
NR1D2	Rev-Erbβ	Rev-Erbβ
NR1F1	RORα	RAR-related orphan receptor-α
NR1F2	RORβ	RAR-related orphan receptor-β
NR1F3	RORγ	RAR-related orphan receptor-γ
NR1H2	LXRβ	Liver X receptor-β
NR1H3	LXRα	Liver X receptor-α
NR1H4	FXR	Farnesoid X receptor
NR1I1	VDR	Vitamin D receptor
NR1I2	PXR	Pregnane X receptor
NR1I3	CAR	Constitutive androstane receptor
NR2A1	HNF4α	Hepatocyte nuclear factor-4-α
NR2A2	HNF4γ	Hepatocyte nuclear factor-4-γ
NR2B1	RXRα	Retinoid X receptor-α
NR2B2	RXRβ	Retinoid X receptor-β
NR2B3	RXRγ	Retinoid X receptor-γ
NR2C1	TR2	Testicular receptor 2
NR2C2	TR4	Testicular receptor 4
NR2E1	TLX	Homologue of the Drosophila tailless gene
NR2E3	PNR	Photoreceptor cell-specific nuclear receptor
NR2F1	COUP-TFI	Chicken ovalbumin upstream promoter-transcription factor I
NR2F2	COUP-TFII	Chicken ovalbumin upstream promoter-transcription factor II
NR2F6	EAR-2	V-erbA-related
NR3A1	ERα	Oestrogen receptor-α
NR3A2	ERβ	Oestrogen receptor-β
NR3B1	ERRα	Oestrogen-related receptor-α
NR3B2	ERRβ	Oestrogen-related receptor-β
NR3B3	ERRγ	Oestrogen-related receptor-γ
NR3C1	GR	Glucocorticoid receptor
NR3C2	MR	Mineralocorticoid receptor
NR3C3	PR	Progesterone receptor
NR3C4	AR	Androgen receptor
NR4A1	NGFIB	Nerve Growth factor IB
NR4A2	NURR1	Nuclear receptor related 1
NR4A3	NOR1	Neuron-derived orphan receptor 1
NR5A1	SF1	Steroidogenic factor 1
NR5A2	LRH-1	Liver receptor homolog-1Tabe
NR6A1	GCNF	Germ cell nuclear factor
NR0B1	DAX1	Dosage-sensitive sex reversal, adrenal hypoplasia critical region, on chromosome X, gene 1
NR0B2	SHP	Small heterodimer partner

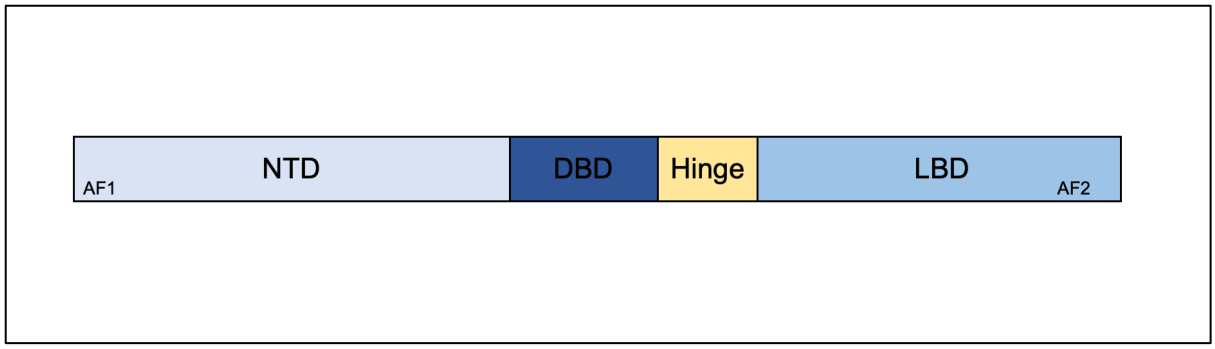

Figure 1-5 Schematic of common structure and domains for nuclear receptors

The general Nuclear Receptor structure consists of N-Terminal Domain (NTD) which contains Activation Function 1 (AF1), a DNA Binding Domain (DBD) with two conserved zinc-finger regions, a hinge region (Hinge) and a Ligand Binding Domain (LBD) containing Activation Function 2 (AF2) and a variable C-Terminal Domain.

1.4.1 Steroid Receptors

The steroid hormone receptor family is comprised of the oestrogen receptor (ER), androgen receptor (AR), progesterone receptor (PR), glucocorticoid receptor (GR) and mineralocorticoid receptor (MR) (Fioretti et al., 2014). Generally, steroid hormones pass through the cell membrane, bind to their specific protein receptors, form a hormone-receptor complex, bind to specific sites on DNA, activate the transcription of specific genes that regulate the metabolism, development and differentiation of the target cell (Figure 1-6) (Mangelsdorf et al., 1995; Pietri et al., 2016; Groner and Brown, 2017).

The transcriptional activity of steroid receptors is modified through interaction with transcriptional corepressors and coactivators (Groner and Brown, 2017). Unliganded steroid receptors are held in a ligand-binding competent state through interaction with chaperone proteins, for example heat-shock protein 90 (HSP90). Upon ligand binding, the receptors dissociate from the chaperone complex, translocate to the nucleus, dimerise and via the recruitment of a coregulator complex, regulate the expression of target genes (Figure 1-6) (Robinson-Rechavi et al., 2003; Sever and Glass, 2013; Pietri et al., 2016).

The functions and effects of steroid hormone receptors depend on tissue context. For example, oestrogen has a protective role in vascular endothelial cells, which has been associated with better vascular health outcomes and reduced risk of cardiovascular diseases in women before menopause (Usselman et al., 2016), whereas in the endometrium, oestrogen has a proliferative effect on the endometrial epithelial cells (Hapangama et al., 2015). This study will focus on 2 members of the steroid receptor family: AR and ERα.

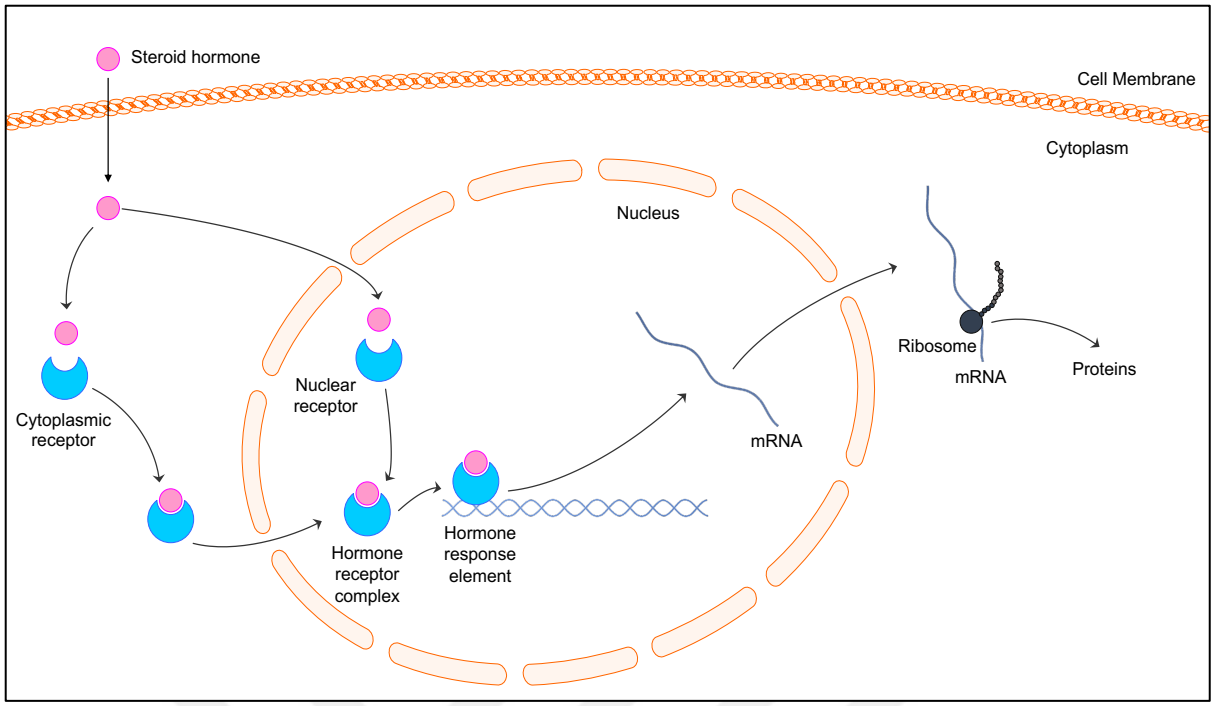

Figure 1-6 Mechanisms of steroid hormones with intracellular receptors in target cells

After a steroid hormone binds to its receptor, the hormone-receptor complex binds to the hormone receptor elements with coregulators. This mediates gene transcription and protein synthesis.

1.4.1.1 Oestrogen Receptor

There are two main ER variants that mediate the oestrogen signalling pathway: ERα and ERβ, which are encoded by genes located on different chromosomes, *ESR1* (*Oestrogen Receptor 1*) at 6q24-27 and *ESR2* at 14q21-22, respectively (Higa and Fell, 2013; Cui et al., 2013). ERβ expression is dominant in normal breast (Rahim and O'Regan, 2017) but the receptor that is oncogenic in ER-positive BrCa is ERα, which is a predictive and prognostic factor for the disease (Kumar et al., 2013).

Despite the fact that ERα and ERβ are encoded by two separate genes, they both have the main structure of a NR (Huang et al., 2010). In both receptors, the DBD is very similar but the AF1 and AF2 regions vary between the two variants (Higa and Fell, 2013). The transcriptional action of the AF1 and AF2 domains is promoter and tissue-specific (Rau et al., 2005). AF1 is also associated with MAPK induced phosphorylation on Ser-118 of ERα. This phosphorylation induces AF1 transcriptional activity in a ligand-independent manner (Kato et al., 1995), while the transcriptional activity of AF2 is ligand-dependent (Kato et al., 2000).

It has been demonstrated in the monkey mammary gland, that ERβ expression increases by 80%, and ERα expression decreases from 12.5% to 1.2% in lobules during the menstrual period (Cheng et al., 2005). These results are consistent with other research which found that ERβ is expressed (70-85%) more than ERα (%10) in the breast epithelial cells of premenopausal women (Li et al., 2010). However, it has been found that the survival rate for BrCa patients with ERα-positive or ERα-negative tumours is not affected by the presence of ERβ expression (Marotti et al., 2010).

1.4.1.2 Androgen Receptor

The *AR* gene is located on the X chromosome, q11-12, and consists of 8 exons just like ERα (Higa and Fell, 2013). Exon 1 encodes the NTD, exons 2 and 3 encode the DBD, and exons from 4 to 8 encode the hinge and LBD (Anestis et al., 2015) (Figure 1-7). The AR, like other members of the steroid hormone receptors, is a ligand-dependent TF, which regulates gene expression (Li et al., 2010). Ligand binding results in a conformational change in the AR, allowing the receptor to regulate downstream targets (Higa and Fell, 2013; Sever and Glass, 2013). Genomic AR

signalling has been associated with cell differentiation, proliferation, angiogenesis, and apoptosis in different tissues (Venema et al., 2019). The AR plays a role in normal mammary gland development (Peters et al., 2011) and pathological pathways that leads to cancer development in the breast (Rahim and O'Regan, 2017), however the biological role of androgens and the androgen signalling pathway in the breast is not fully understood.

Similar to the other nuclear receptors' structure, the AR has 4 main domains: NTD, DBD, hinge region and LBD (Higa and Fell, 2013). The NTD is mostly responsible for transactivation of the receptor. Unlike other steroid receptors, the NTD of AR primarily interacts with coactivators which facilitate and regulate AR transcriptional activity (Sever and Glass, 2013; Cano et al., 2013; Yu et al., 2020). The NTD harbours AF1 which constitutes two important transactivation units (TAU), TAU1 and TAU5, that are shown to be important regions for coactivator recruitment (Dehm and Tindall, 2007). CAG repeats (polyglutamine tract) in the NTD also have been reported to regulate AR's biological function and activity (Gottlieb et al., 2012). For example, Kennedy's disease (spinal bulbar muscular dystrophy) is characterized by long CAG repeats in the *AR* gene (Coffey and Robson, 2012).

The DBD is the most conserved domain of AR and consists of 8 cysteine residues, 2 zinc-finger regions for binding to AREs with high affinity, P-Box for sequence specific DNA binding, and D-Box for receptor dimerization (Sever and Glass, 2013). Androgen response elements (AREs) in DNA often consist of 2 palindromic sequences (Higa and Fell, 2013) and the number of AREs in a gene's promoter region positively correlates with AR specifity (Sever and Glass, 2013).

The LBD consists of 12 α-helixes and ligand binding results in helix 12 relocating to close the ligand bound pocket. Upon ligand binding, helix 12 primarily contacts helices 4, 5, and 10, and these conformational changes facilitate the recruitment of coregulator proteins and interaction with the NTD (Robinson-Rechavi et al., 2003; Sever and Glass, 2013; Pietri et al., 2016; Groner and Brown, 2017). T and DHT are the endogenous ligands of AR, and these are products of steroidogenesis (Rahim and O'Regan, 2017).

Even though the AR and ER belong to the same receptor family and share a common nuclear receptor structure, there are differences between the two receptors. For example, ER has isoforms; ERα and ERβ, whereas AR has splice variants (Rau et al., 2005; Higa and Fell, 2013). The length of AR is 919 amino acids, while ER is

composed of 595 amino acids (Gelmann, 2002). AR can only form dimers with AR, and this homodimerization is necessary and critical for the function of the receptor. ERα, on the other hand, has been shown to be able to form heterodimers with ERβ isoforms. In contrast with C terminal domain of ERα, the first 12 amino acids of the AR's C terminal domain are essential for AR to bind DNA (Higa and Fell, 2013). Another difference between AR and ERα is the structural changes in the receptor upon ligand binding. Ligand binding to the receptor makes AR more stable, whereas ER's stability degrades (Rau et al., 2005). AF2 region in LBD of ERα is the primary site for coactivator recruitment, whereas in AR, after ligand binding to LBD, AF2 interacts with NTD and NTD becomes the coactivator recruitment site of the receptor (Jenster et al., 1995; Heery et al., 1997).

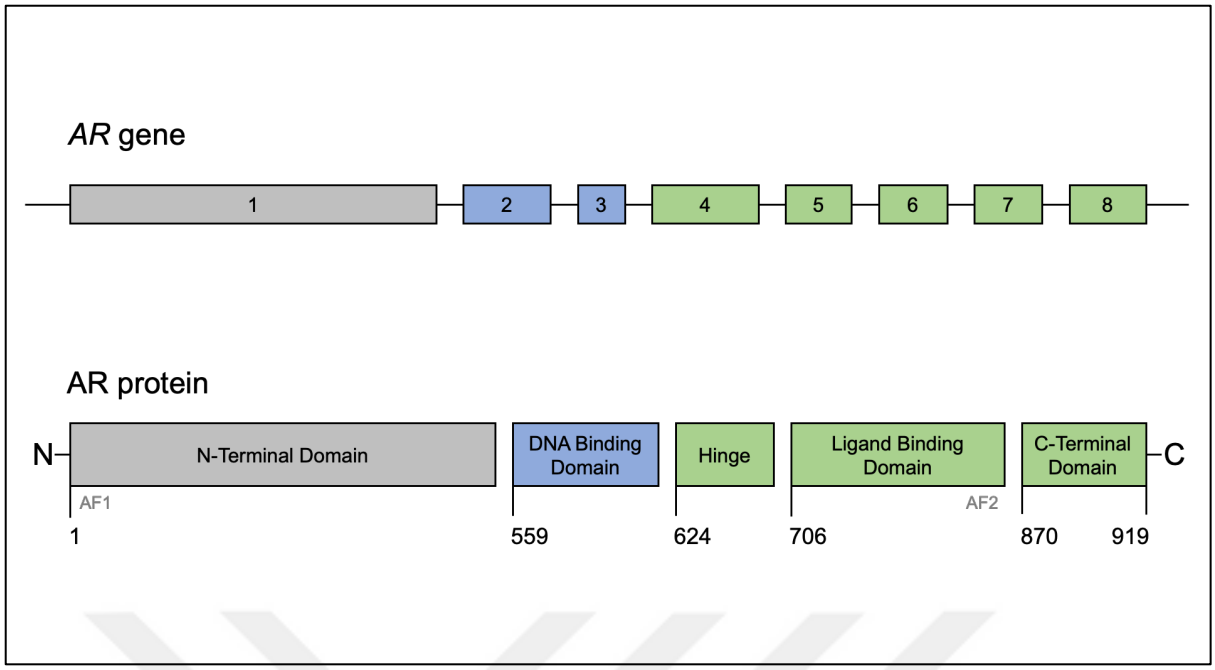

Figure 1-7 Schematic representation of AR gene and AR protein

The AR gene consists of 8 exons and at the protein level contains 4 main domains. The domains of AR and the exon(s) that encode that domain are colour matched.

Like other steroid receptors, AR activity is mediated by cofactors with repressor or activator activity (Sever and Glass, 2013). Upon binding of the ligand to the receptor, the hormone-receptor complex forms and interacts with coactivator molecules that promotes binding to the regulatory regions of target genes (Sever and Glass, 2013). For instance, transcription in acetylated chromatin regions increase. The coactivator proteins either have or recruit proteins that have histone acetyltransferase activity to relax the chromatin, facilitating and enhancing the binding of the receptor complex to DNA (Groner and Brown, 2017).

In addition to the direct regulation of gene transcription, the AR also appears to regulate cellular activity in a non-genomic manner. For example, in AR-positive LNCaP cells, kinase signalling cascades were found to be activated within minutes of exposure to the synthetic androgen methyltrienolone (Heinlein and Chang, 2002). It was therefore postulated that this effect of androgens on prostate cancer (PrCa) cells is a result of nongenomic AR signalling (Heinlein and Chang, 2002). Further, this effect appears to be via the activation of the Mitogen-Activated Protein Kinase (MAPK) signalling pathway, a family of serine/threonine protein kinases involved in cellular proliferation (Heinlein and Chang, 2002).

1.4.1.2.1 AR coregulators

The unliganded AR is located in the cytoplasm as a complex of proteins with heat shock proteins and other chaperons (Cano et al., 2013). Upon ligand binding, the receptor undergoes conformational changes which results in the dissociation of chaperones and heat shock proteins (Tan et al., 2015). Subsequently, AR translocates to the nucleus, forms a homodimer, binds to AREs and initiates target gene expression (Sever and Glass, 2013; Tan et al., 2015; Groner and Brown, 2017). The transcription of ligand bound AR is mediated by coregulators which are divided into two categories: coactivators and corepressors. The balance between these two groups is important for the regulation of AR signalling and the subsequent regulation of cell differentiation, proliferation, and disease progression (Shang et al., 2002; Cano et al., 2013).

Coactivators facilitate the transcriptional activity of the receptor depending on the bound ligand and cell type (Tan et al., 2015). Two main regions have an essential and a critical role for coactivator recruitment: AF1 in the NTD and AF2 in the LBD. For

example, the p160 coactivator protein complex is recruited to AF2, relaxing the structure of chromatin, and enhancing the binding of AR to DNA (He et al., 2002; Groner and Brown, 2017). The Steroid Receptor coactivator (SRC) family also forms a scaffold to attract more coactivators for histone modification (Xu and Li, 2003). SRC1 and SRC3 are known to have histone acetylase activity, whereas SRC2 does not feature this (Bevan et al., 1999; He et al., 2002). A structural study that investigated the interaction of AR and coactivator complexes showed that AR can directly recruit p300 coactivator complex without needing the assistance of SRC3, in contrast with ERα which needs SRC3 first to recruit the p300 complex (Yu et al., 2020). Moreover, ChIP analysis of the p300 coactivator complex in BrCa cells has demonstrated that activation of AR could re-distribute ERα-recruited p300 binding sites to ARE binding sites (Hickey, Selth, et al., 2021).

Corepressors, in contrast with coactivators, supress AR transcriptional activity via various mechanisms, including inhibiting DNA binding or nuclear translocation of AR, disrupting the forming of an AR-coactivator complex, inhibiting N/C interaction, recruiting histone deacetylases (Wang et al., 2005; Sharifi et al., 2010). For example, ARR19 (Androgen Receptor Corepressor, 19 kDa) represses AR activity by recruiting HDAC4 (histone deacetylase 4), whereas SHP (Short Heterodimer Protein) interacts with the AR LBD and AR NTD, disrupting the AR N/C interaction (Wang et al., 2005).

However, there are also coregulators which act as a corepressor or coactivator depending on the tissue. For example, it has been demonstrated that Akt can inhibit AR transactivation through phosphorylation of the receptor and inhibiting the recruitment of ARA70, an AR coactivator (Lin et al., 2001). It has also been suggested that Akt can lead to a ligand-independent constitutively active AR in PrCa, and therefore promote cell growth (Sarker et al., 2009; Anestis et al., 2020).

1.4.2 Posttranslational modifications of AR

There are a number of different posttranslational modifications that the AR undergoes. Phosphorylation is one of the most studied post-translational modifications of AR, as it has been demonstrated that phosphorylation of AR on certain cites can affect the agonistic or antagonistic activity of ligands (Coffey and Robson, 2012). A schematic of AR phosphorylation sites can be found in Figure 1-8. AR could be

phosphorylated by Protein Kinases (PK), Cyclin Dependent Kinases (CDK1, CDK5, CDK7, CDK9), MAPK, or Akt, and dephosphorylation occurs via PP2A, PP1 (Lin et al., 2001; Coffey and Robson, 2012). The effects of these have a variety of implications on AR function, affecting coactivator recruitment, DNA binding, nuclear localisation, and receptor stability (Coffey and Robson, 2012; van der Steen et al., 2013).

AR Acetylation in the hinge region was found to be important for receptor function upon ligand binding (van der Steen et al., 2013). 3 acetylation sites have been identified in the AR (K630, K632, K633) and these sites were reported to be acetylated by p300 (Coffey and Robson, 2012). K845 and K847, in the AR LBD, have been shown to be a target site for ubiquitination (van der Steen et al., 2013) and this post-translational modification has been linked to the development of castrate resistant PrCa (CRPC). It was postulated that when AR is not ubiquitinated, AR levels increase and this hypersensitizes the cells to androgens, promoting cell growth and proliferation (Xu et al., 2009). An addition of small ubiquitination like modifier (SUMO) (approximately 100 amino acid in length) to lysine residues in AR (K520), termed SUMOylation, is thought to take place in the nucleus (van der Steen et al., 2013). This modification can affect the cellular localisation and transcriptional activity of AR. Further, when SUMOylation site cannot be SUMOylated, this results a decrease in the half-life of the AR (van der Steen et al., 2013). Posttranslational modification sites on the AR can be found in Figure 1-8.

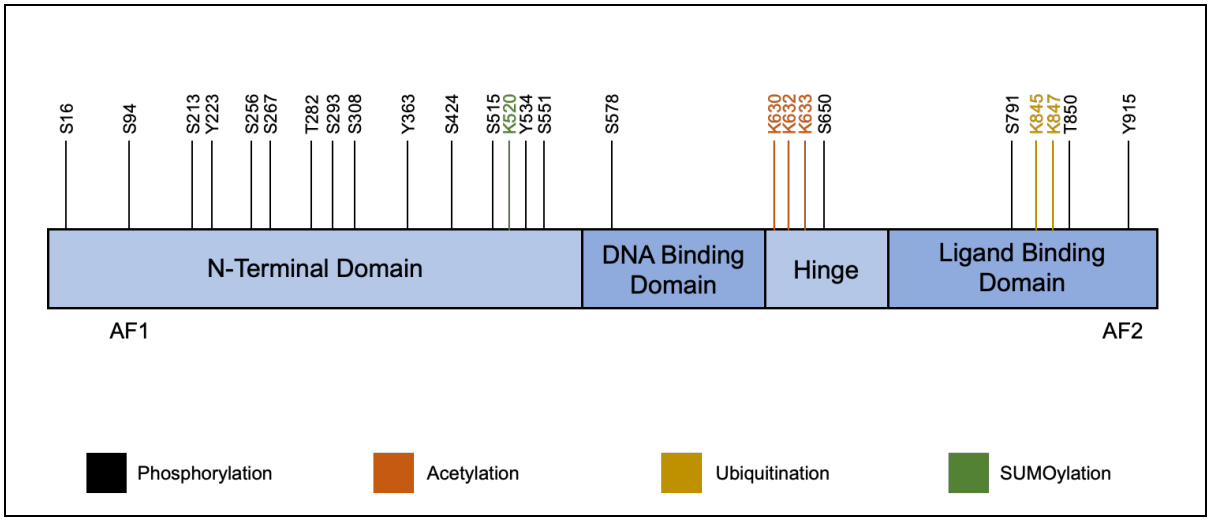

Figure 1-8 Identified posttranslational modification sites and their locations in the domains of AR

AF1, Activation Function 1; AF2, Activation Function 2. The numbering represents the amino acid position.

1.5 Endocrine Resistance

The mortality rates of hormone receptor positive BrCa patients significantly decreased following the introduction of antioestrogens and AIs (Haque and Desai, 2019). However, around 40% of the primary BrCa tumours which initially respond to endocrine therapies acquire resistance over time (Gonzalez-Angulo et al., 2007; Lei et al., 2019), and for metastatic BrCa patients, endocrine therapy resistance is almost inevitable (Hanker et al., 2020). In this section, some of the most common acquired mechanisms for endocrine resistance will be discussed.

1.5.1 Regulation of ER

As mentioned previously, ER has two subtypes: ERα, which facilitates tumorigenesis and promotes proliferation of BrCa tumours; ERβ, which appears to have an anti-proliferative role in breast tumour development (Haque and Desai, 2019). Many studies have investigated the predictive role of ERβ as an independent prognostic factor in BrCa, however there does not seem to be a consensus in findings regarding its role as a prognostic/predictive marker (Zhou and Liu, 2020). It was also thought that the ERα/ERβ ratio could be used as a predictive marker for therapy response and survival. However, due to alterations in their expression profiles and alternative splicing, the effect of this interaction on tumour progression is still not fully understood (Taylor et al., 2010; Zhou and Liu, 2020). Interestingly, it has also been found that, compared to TAM sensitive tumour samples, TAM resistant BrCa samples have higher level of ERβ expression (Speirs et al., 1999). Tumours can also become resistant to TAM by modifying ERα levels, reducing the effects of TAM via ERα inhibition (Chang, 2012).

One of the possible mechanisms for TAM resistance is the nongenomic activation of ERα within the cell (Fan et al., 2007). In a study by Fan et al. 2007, 6 months of exposure to TAM resulted in cells that were resistant to this antioestrogen. Interestingly, the localisation of ERα, which is mainly an intranuclear steroid receptor, was found to be in extranuclear sites with increased cooperation with epidermal growth factor receptor (EGFR) (Fan et al., 2007).

Another alteration in the oestrogen signalling pathway that leads to TAM resistance is mutations that occur in ERα (Alluri et al., 2014). ERα mutations are usually detected in metastatic BrCa patients who have undergone AI therapies, in advanced stage endocrine therapy resistant tumours, and are rarely seen in early-stage primary breast tumours (Alluri et al., 2014). For example, whole genome sequencing performed on 46 ERα-positive primary breast tumours found no mutations in the *ESR1* gene (Ellis et al., 2012). In accordance with this, genome sequencing analyses of 390 hormone receptor positive primary tumours did not reveal any mutations in the *ESR1* gene (Cancer Genome Atlas Network, 2012). However, exome and transcriptome analysis of 11 hormone receptor positive patients, who received endocrine therapies, showed that 6 out of those 11 patients had mutations in the *ESR1* gene and these were found to be located in the LBD region of the receptor (Robinson et al., 2013). Confirming this, another study found that 20% of metastatic ERα-positive BrCa cases whose tumours spread to new sites during hormonal therapy treatment had *ESR1* mutations affecting the LBD (Toy et al., 2013).

When oestrogen binds to ERα, the receptor undergoes conformational changes creating a pocket that coregulators can bind to (Sever and Glass, 2013; Haque and Desai, 2019). Helix 12 plays a critical role in the formation of this pocket, and mutations in this region usually result in an alteration in ERα activity (Szostakowska et al., 2019). For example, mutants Y537S and D538G were found to be constitutively active and to increase the interaction of ERα with the coactivator SRC1 (Merenbakh-Lamin et al., 2013; Alluri et al., 2014; Fanning et al., 2016).

1.5.2 Modifying coregulator proteins

Recruitment of coactivators by ERα increases in BrCa (Haque and Desai, 2019), and it was thought that upregulation in the expression of coactivators could lead to an increase in the agonist activity of TAM, hence promoting TAM resistance (Chang, 2012). For example, upregulation of TRAM1 (Thyroid Hormone Receptor Activator Molecule 1), a coactivator of ERα, was found to be associated with enhanced agonist activity of TAM (Weiner et al., 2013). Increased SRY-box-9 (SOX9) levels were also associated with endocrine therapy resistance (Chang, 2012). Additionally, decreased Nuclear receptor Corepressor 1 (NCoR) levels were found to enhance the agonistic

activity of TAM and this change in expression has been associated with acquired TAM resistance (Lavinsky et al., 1998). Further, the coactivator, FOXA1, which is a key regulatory TF in CRPC, was also highly expressed in TAM resistant BrCa cells (Robinson and Carroll, 2012; Michmerhuizen et al., 2020).

1.5.3 MicroRNAs (miRNAs)

MicroRNAs (miRNAs) are noncoding RNAs, 18-22 bp in length, that regulate gene expression. The way that miRNAs regulate gene expression is via the degradation of the target mRNA or the inhibition of gene translation (Haque and Desai, 2019). Multiple miRNAs have been found to be associated with therapy resistance (Muluhngwi and Klinge, 2015). For example, miR-221/222 were increased in endocrine resistant HER2 positive tumours and overexpressed in TAM resistant cell lines (Muluhngwi and Klinge, 2015). Further, in TAM resistant MCF7 cells, miR-873 levels were decreased, and it was postulated that this downregulation of miR-873 led to enhanced ERα activity (Muluhngwi and Klinge, 2015). However, the regulation of miRNAs and their effect on endocrine therapy resistance is still in its infancy and requires further investigation.

1.5.4 Long noncoding RNAs (lncRNAs)

Similar to miRNAs, long noncoding RNAs (lncRNAs) are a group of non-protein coding RNAs, transcribed from the genome. LncRNAs are usually more than 200 bps and they are involved in many processes in tumour cells such as gene regulation, proliferation, oncogenesis, and metastasis (Zhang et al., 2019). Many lncRNAs have been shown to be important in BrCa pathogenesis, being associated with tumour development and progression, as well as resistance to endocrine therapies (Tian et al., 2021). For instance, it was found that lncRNAs HOTAIR, BLACAT1 and HOXA1 are upregulated in tamoxifen resistant tumour cells. These lncRNAs promote therapy resistance via different mechanisms, including activation of ERα signalling and other proliferative cell signalling pathways, inhibition of other lncRNAs and inhibition of miRNAs related to cell proliferation (Tian et al., 2021). Although it seems that lncRNAs play an important role in tumour cell biology, their mechanism of action in BrCa

progression still needs further exploration before they can be exploited as predictive biomarkers for tumour prognosis, drug resistance and/or therapeutic targets.

1.5.5 Crosstalk of ERα Signalling Pathway with Other Signalling Pathways

One of the mechanisms that was suggested to drive endocrine therapy resistance in BrCa is the activation of ERα via the overexpression of growth factor signalling pathways (Haque and Desai, 2019). Overexpression of receptors like EGFR, insulin like growth factor receptor (IGFR) and HER2 results in ERα phosphorylation which stimulates the activation of the receptor in a ligand-independent manner (Nicholson et al., 2007). It was demonstrated that endocrine resistant MCF7 cells had a significant increase, both at protein and mRNA level, in EGFR and HER2 expression (Nicholson et al., 2007). The heterodimerisation of HER2/EGFR also activates PI3K-AKT and MAPK signalling pathways, facilitating TAM resistant tumour growth (Nicholson et al., 2007). Additionally, in another study, TAM was unable to inhibit E2-stimulated growth in EGFR expressing MCF7 cells (Moerkens et al., 2014).

Pathway analysis of endocrine resistant MCF7 cells has shown that the NOTCH pathway was significantly more active in therapy resistant cells compared to endocrine sensitive cells. siRNA depletion of NOTCH resulted in inhibition of the endocrine resistant cells, suggesting that NOTCH drives endocrine therapy resistance in BrCa cells (Magnani et al., 2013).

Androgen receptor signalling has also been associated with TAM resistance (de Amicis et al., 2010). The role of AR in BrCa and endocrine resistance is discussed in more depth in Section 1.7.

1.6 AR in Normal Breast

It is well known that the AR is necessary for the development and function of the male reproductive system (Walters et al., 2010). For example, knocking-out *AR* led to sterility in male mice, by perturbating spermatogenesis (Walters et al., 2010). However, studies in the last couple of decades have also shed some light about its role in female reproductive system. Studies on rodent and primate mammary glands have played an important role in furthering our understanding of breast tissue

characteristics and function (Cheng et al., 2005; Walters et al., 2010; Macias and Hinck, 2012). It was demonstrated that in monkeys, the AR is expressed more highly than ERα in the mammary gland during the menstrual cycle, gestation, and lactation (Cheng et al., 2005). *In vivo* studies have also shown that AR plays a key role in mammary gland development. For example, in female mice, with *AR* knockout in the mammary gland, ductal branching was reduced and lobuloalveolar development decreased in prepubertal and pubertal periods (Yeh et al., 2003), demonstrating that a functioning AR is necessary for normal breast development. It has also been found in the primate mammary gland that, throughout the menstrual period, AR is expressed in up to 71% of lobular epithelial cells and in up to 75% of ductal epithelial cells (Cheng et al., 2005). Further, in breast tissues of premenopausal women, AR is expressed in a greater proportion of cells than ERα (Li et al., 2010).

It has also been demonstrated that a functional AR is necessary for a functional and healthy female reproductive system. *AR* knockout in female mice disrupted the development of follicles in the ovaries, and deteriorated ovulation (Walters et al., 2010). However, androgens are known to have an antagonistic effect on normal breast development (Tiefenbacher and Daxenbichler, 2008). For example, gene ontology analysis of patient derived *ex vivo* cultures of normal breast that were treated with oestrogen identified an activation of proliferative and cell cycle related pathways, and co-treatment with androgen reversed this effect (Hickey, Selth, et al., 2021). Hence it seems that AR is essential for breast development, but androgen activation of AR is inhibitory in normal breast.

1.7 AR in Breast Cancer

The AR is expressed in almost all cases of BrCa, occurring in up to 90% of all tumours (Rahim and O'Regan, 2017), whereas ERα is expressed in 50-80% (Peters et al., 2009). In a study that examined 413 BrCa patients' samples, 78.4% of AR-positive patients stained positive for ERα (Park et al., 2010). While the role of the AR in BrCa development and growth is not fully understood, it appears that the AR plays different roles depending on the stage and molecular subtype of the disease (Gucalp et al., 2013; Pietri et al., 2016).

It has been shown that AR expression in early BrCa is associated with better disease-free survival and overall survival in hormone receptor positive and negative tumours (Vera-Badillo et al., 2014). In a meta-analysis, the risk of cancer recurrence was lower in ERα-positive tumours which expresses AR, and it has been shown that these tumours have improved overall survival, compared to ERα-positive, AR-negative tumours (Qu et al., 2013). For this reason, it has been proposed that BrCa be divided into 3 different subtypes based on ERα and AR expression which are luminal (ERα-positive AR-negative), basal (ERα-negative AR-negative) and molecular apocrine (ERα-negative AR-positive) (Farmer et al., 2005). Consequently, several mechanisms have been suggested to explain the effect of AR in ERα-positive tumours which will be discussed further in the next section.

1.7.1 AR in ERα-positive Breast Cancer

Recent studies have demonstrated that there is an important association between AR and ERα function in BrCa (Pietri et al., 2016; Rahim and O'Regan, 2017). The prevalence of AR was found to be approximately 90% in ERα-positive disease (Vera-Badillo et al., 2014). In a study, AR expression was found to be an independent prognostic factor of better outcome for disease specific survival in ERα-positive BrCa patients (Castellano et al., 2010). Another study found that in ERα-positive BrCa, tumour relapses and cancer-associated deaths increased by 3-fold and 4.6-fold higher in patients with low AR expression compared to those with high AR expression (Peters et al., 2009). Further, it was also shown that staining positive for AR correlates with small tumour size, absence of lymph node metastases and lower grade tumours (Castellano et al., 2010; Kensler et al., 2019). In contrast, a retrospective study of 7,693 BrCa patients found AR expression to be associated with low ki-67 index (used as a marker of proliferation) but not associated with grade and size of the tumour, lymph node metastases or nodal status (Vera-Badillo et al., 2014).

In vitro studies with BrCa cell lines (T47D and ZR-75-1), that express both ERα and AR endogenously, have demonstrated that their growth is induced by oestrogen treatment, and proliferation is inhibited by androgen treatment (Poulin et al., 1988; Birrell et al., 1995), suggesting an inhibitory role for AR in ERα-positive BrCa. In contrast, another study showed that androgen induced the proliferation of 4 different

ERα-positive BrCa cell lines (T47D, ZR-75-1, MCF7, BCK4); the proliferation of BCK4 and MCF7 cells was found to be responsive to DHT treatment and ENZA was able to inhibit this DHT-stimulated growth (Cochrane et al., 2014).

Further evidence for this inhibitory crosstalk comes from ERα-positive primary tumours that were cultured *ex vivo*. The effect of oestrogen only treatment or androgen and oestrogen treatments on the proliferation of these model tumours was assessed by comparing the ki67 levels and bromodeoxyuridine (BRDU, an analogue of thymidine) incorporation (Hickey, Selth, et al., 2021). It was found that tumour models treated with oestrogen-only had higher ki67 and BRDU levels compared to the ones that were additionally treated with androgen, suggesting an antagonistic activity for AR in ERα-positive BrCa (Hickey, Selth, et al., 2021).

The AR/ERα ratio may also have prognostic value in ERα-positive BrCa patients (Rangel et al., 2018). It was found that IHC determined AR/ERα ratio that is equal or higher than 2 might identify patients with a worse prognosis, as it was shown that this subgroup of patients had higher histological grade, more lymph node metastases, worse disease-free interval, and survival rates as compared to the ones that had a ratio of less than 2 (Rangel et al., 2018).

A study sub-grouped 47 ERα-positive patients using a cut-off value of 2 for the AR/ERα ratio, by evaluating a combination of protein levels by IHC and mRNA levels by qPCR analysis. The results demonstrated that tumours with an AR/ERα ≥ 2 ratio had higher proliferation rates independent of *HER2* overexpression (Rangel et al., 2020). The association between some of the genes involved in BrCa proliferation (*AURKA*, *BIRC5*, *CCNB1*, *MKI67* and *UBE2C*) and high AR/ERα ratio has also been assessed and it was found that this subgroup of patients with AR/ERα ≥ 2 ratio had higher levels of expression of these genes as compared to the ones with a AR/ERα < 2 (Rangel et al., 2020).

A retrospective study which investigated AR expression in 42 DCIS patients treated with surgery followed by radiotherapy that had been followed up for 95 months (Ravaioli et al., 2017), found that AR/ERα ratios were higher in patients that had disease relapse compared to non-relapse. The reason why AR/ERα ratios in relapsed patients was found to be higher could be attributed to the fact that relapsed patients not only had higher AR levels, but also lower ERα levels. Also, ki67 expression in the relapsed patients' was found to be 50% higher compared to non-relapsed patients (Ravaioli et al., 2017), which is again another poor prognosis indicator. Moreover, it

was found that a cut-off value of 1.1 for AR/ERα ratio could predict almost 4 out of 5 patients' *in situ* disease relapse or progression to invasiveness (Ravaioli et al., 2017).

AR expression has also been investigated as a potential prognostic value for disease progression and prediction of treatment response. A retrospective study, that investigated 913 BrCa patient samples, found that the prediction of prognosis and treatment response was improved when both AR and ERα expression were evaluated (Elebro et al., 2015). That study also found that in ERα-positive disease, negative AR staining was able to predict treatment failure with AI, suggesting a predictive role for AR in therapy response in postmenopausal women, a population which is usually treated with AI rather than antioestrogens.

The effects of androgen and oestrogen on tumour proliferation have also been investigated *in vivo* (Hickey, Selth, et al., 2021). Mice xenografts models created with ZR-75-1 cells, and animals were treated with E2 or E2 and DHT for 90 days. It was shown that E2 and DHT co-treated mice had smaller tumours as compared to E2 stimulated tumours at the end of the treatment period, suggesting an inhibitory effect for androgen in hormone receptor positive BrCa.

As several studies have demonstrated that AR has an antiproliferative effect on tumour growth in the presence of ERα (Peters et al., 2009; Need et al., 2012; Fioretti et al., 2014; Hickey, Selth, et al., 2021), multiple mechanisms have been proposed to explain this inhibitory activity of AR in ERα-positive BrCa. It has been shown that the AR DBD binds with 3 to 10 times higher affinity to nonspecific hormone response elements compared to other steroid hormone receptors (Shaffer et al., 2004), and AR can bind to EREs in BrCa (Peters et al., 2009). In accordance with this, it was found that AR and ERα crosstalk increases at the genomic level in BrCa as compared to normal breast tissue (Hickey, Selth, et al., 2021). AR and ERα colocalisation was measured in normal, and oncologic breast tissues (DCIS, invasive ductal carcinoma, lymph node metastases) via a tissue microarray based dual-label immunofluorescence method, and approximately 25% of normal breast tissue samples showed AR and ERα colocalisation in the nuclei, whereas this was more than 60% for malignant lesions (Hickey, Selth, et al., 2021), suggesting that the two receptors interact at the genomic level to a greater extent in BrCa. ERα binds to 5'-AGGTCA-3' response elements, which is very similar to the DNA binding sequence of AR (5'-AGAACA-3') (Fioretti et al., 2014). Thus, one of the suggested mechanisms for

ERα and AR crosstalk is that AR competes for EREs resulting in downregulation of ERα activity (Peters et al., 2009).

A study that combined ChIP and transcriptome analysis of the luminal BrCa cell line ZR-75-1 (ERα and AR positive), demonstrated that E_2 and DHT target genes can be antagonised by their co-treatment and binding of one receptor blocks the binding of the other receptor when response elements were shared or closely located (within 10 kb of the other) (Need et al., 2012). This analysis demonstrated that when cells were co-treated with both hormones, the AR was recruited to 40% of ERα-binding sites, suggesting that the AR might directly regulate the transcriptional activity of ERα via altering the ERα cistrome (Hickey, Selth, et al., 2021). It has also been observed that the proliferation of MCF-7 cells, transfected with AR, was inhibited in response to androgen and that this inhibition was reversed when cells were co-treated with the antiandrogens bicalutamide (BIC) or hydroxyflutamide (Szelei et al., 1997). These findings broadly support the antiproliferative effect of AR on ERα-positive breast tumours.

Analysis of ZR-75-1 cells has shown that some well-known ERα targets (such as *MYB* and *BCL2*) were downregulated, and ERα binding sites in these regions were lost, upon androgen co-treatment as compared to oestrogen only treatment (Hickey, Selth, et al., 2021). Further, it was found that some AR target and binding sites (i.e., *ZBTB16* and *SEC14L2*) also showed an increase in ERα binding following AR activation by androgen, suggesting that AR could perturbate ERα signalling in BrCa by redistributing ERα on chromatin. However, when ERα is inhibited with anti-oestrogens, the AR can facilitate proliferation in an androgen-dependent manner, promoting therapy resistance (de Amicis et al., 2010). For example, it has been demonstrated that in MCF-7 cells overexpressing AR, treatment with TAM does not decrease Cyclin D1 expression, which is a transcriptional target for ERα (de Amicis et al., 2010). Hence it could be postulated that in the presence of antioestrogens, AR mimics ERα to drive tumour growth. It has also been shown that in AR overexpressing ERα-positive TAM resistant cells (ZR-75-B and MCF-7), the antiandrogen enzalutamide (ENZA) blocked the agonistic activity of TAM on ERα signalling (Ciupek et al., 2015). In the same study, it was postulated that the interaction of AR nongenomic signalling with EGFR resulted in ERα phosphorylation and ligand-independent activation of the receptor (Ciupek et al., 2015). AR knockdown in TAM resistant MCF7 cells reversed this resistance, and cells became sensitive to TAM

treatment, whereas treatment with an AR antagonist ENZA did not (Chia et al., 2019). Therefore, activation of the AR signalling pathway could be an adaptive mechanism that develops under selective pressure of endocrine therapy, and the inhibition of AR could be a way to prevent this mechanism of therapy resistance from developing.

Although AR expression was correlated with good tumour characteristics, a recent study found high AR expression to correlate with endocrine resistance (Michmerhuizen et al., 2020). Analysis of the tumours from 192 ERα-positive BrCa patient samples who received tamoxifen as an adjuvant therapy demonstrated that an AR/ERα ratio ≥ 2 was an indicator of tamoxifen therapy failure, and this indicatory effect of AR/ERα ratio was independent of the proportion of positive ERα staining (Cochrane et al., 2014).

Another mechanism that has been proposed to explain AR and ERα crosstalk is competition for shared coregulators. For example, coimmunoprecipitation assays in MCF-7 cells has shown that the AR coactivator ARA70 can interact with ERα in an oestradiol dependent manner (Lanzino et al., 2005). Further, in LNCaP cells AR signalling has been found to be modulated by Forkhead box protein A1 (FOXA1), a pioneer TF that also regulates ERα binding in the genome (Pomerantz et al., 2015). Competition for this pioneer factor may therefore inhibit receptor activity. The relationship between AR and another coregulatory TF for DNA binding, p300, has also been investigated. P300 is recruited by ERα to enhancer regions of ERα regulated genes (Lasko et al., 2017), and regulated AR activity in PrCa cells (Murakami et al., 2017). In BrCa cells, the E2-induced distribution of p300 has been found to be perturbated significantly by the addition of androgen (Hickey, Selth, et al., 2021), suggesting that this factor is being sequestered by the AR.

It was thought that AR might inhibit ERα by reducing DNA binding. Confirming this, it was found that for AR to be able to inhibit ERα binding to DNA, binding of AR to the DNA is necessary. ChIP experiments were performed on the ERE binding sites in *MYB* and *CCND1* genes in MCF7 cells that were transduced with an expression vector that encodes a constitutively active AR and an AR mutant which was not capable of binding to DNA (Hickey, Selth, et al., 2021). Following oestrogen treatment, while the constitutively active AR was able to inhibit ERα from binding to DNA, the mutant AR did not have an effect on ERα binding to the EREs. A summary of the role of AR in ERα-positive BrCa can be found in Table 1-6.

Table 1-6 The role of AR In ERα-positive Breast Cancer

AR in ERα-positive Breast Cancer	
AR expression in primary breast cancer	• Low AR expression is associated with tumour relapses and increased cancer associated deaths in ERα-positive BrCa (Peters et al., 2009) • AR positivity is associated with low ki-67 index, small tumour size, absence of lymph node metastases, lower grade tumours (Castellano et al., 2010; Vera-Badillo et al., 2014; Kensler et al., 2019) • Evaluation of both AR and ERα improves the prediction of prognosis and treatment response (Elebro et al., 2015)
Androgen effects	• The growth of ERα-positive, AR-positive cell lines (ZR-75-1, T47D) are inhibited by androgen (Poulin et al., 1988; Birrell et al., 1995) • Androgen treated ERα-positive ex vivo tumours have low levels of proliferation markers, and smaller tumours (Hickey, Selth, et al., 2021) • AR transfected MCF7 cells are responsive to androgen for proliferation (Szelei et al., 1997) • Androgen treatment downregulates ERα and results with loss of ERα binding in ERα binding sites in ZR-75-1 (Hickey, Selth, et al., 2021)
AR/ERα ratio	• Patients with AR/ERα ≥ 2 has worse prognosis, higher histological grade, more lymph node metastasis (Rangel et al., 2018) • BrCa proliferative genes are highly expressed in tumours with high AR/ERα ratio (Rangel et al., 2020) • AR/ERα ratio is higher in relapsed patients (Ravaioli et al., 2017) • AR/ERα ≥ 2 indicates TAM therapy failure (Cochrane et al., 2014)
AR-ERα crosstalk	• AR competes for EREs and can bind to EREs (Peters et al., 2009) • AR-ERα colocalisation in the nuclei increases in breast malignancies as compared to normal breast tissue (Hickey, Selth, et al., 2021) • Binding of one receptor blocks the binding of other receptor when response elements were shared or closely located (Need et al., 2012) • AR is recruited to 40% of ERα binding sites (Hickey, Selth, et al., 2021) • Nongenomic AR signalling interacts with EGFR and results with ligand independent activation of ERα (Ciupek et al., 2015) • ARA70 (AR coactivator) can interact with ERα (Lanzino et al., 2005) • FOXA1 mediates AR and ERα signalling (Pomerantz et al., 2015) • P300 is recruited by ERα to enhancer regions in BrCa, and to AREs by AR in PrCa (Lasko et al., 2017; Murakami et al., 2017) • Androgen perturbates p300 distribution in BrCa (Hickey, Selth, et al., 2021) • A mutant AR that cannot bind to DNA cannot inhibit ERα binding to DNA (Hickey, Selth, et al., 2021)
Endocrine resistance	• TAM cannot inhibit cyclin D1 expression in MCF7-AR overexpressing cells (de Amicis et al., 2010) • ENZA blocks the agonistic activity of TAM on ERα signalling in TAM resistant cells (Ciupek et al., 2015) • AR knockdown resensitises the TAM resistant cells to TAM treatment (Chia et al., 2019) • Staining negative for AR predicts treatment failure with AI (Elebro et al., 2015) • High AR expression correlates with endocrine resistance (Michmerhuizen et al., 2020)

1.7.2 AR in ERα-negative Breast Cancer

In BrCa, *BRCA1* mutations usually correlate with *TP53* mutations and tumours bearing these alterations have a high proliferation rate (Sorlie et al., 2003). TNBC is usually associated with BRCA1 mutations, and a poor survival rate compared to other BrCa subtypes (Rahim and O'Regan, 2017). It is a heterogenous disease which has been categorised into subgroups by different research studies to better determine the treatment options, predict the outcomes of the disease and therapy response. For instance, after gene expression profiling of 587 TNBC cases, 6 distinct TNBC subtypes have been identified including; basal like 1 (BL1), basal like 2 (BL2), luminal androgen receptor (LAR), mesenchymal (Me), mesenchymal stem like (MSL), immunomodulatory (IM) (Lehmann et al., 2011). The LAR subtype is AR-positive and has a gene expression profile similar to luminal tumours (Lehmann et al., 2011). Another study evaluated the implications of these subtypes into clinical outcomes by assessing the pathological complete responses of patients in these subgroups (Masuda et al., 2013). Evaluation of 146 TNBC patients identified a strong association between pathological complete response and the TNBC subtype, with BL1 having the best and LAR having the worst rate (Masuda et al., 2013). It was also found that classification of TNBC patients into these distinct subgroups was better at predicting pathological complete response than when they are classified as basal-like and non-basal-like.

Preclinical studies play an important role in furthering our understanding of the role of AR signalling in ERα-negative BrCa. Many studies have shown that AR signalling regulates BrCa proliferation, and this might have particular importance in ERα-negative tumours (Peters et al., 2009; Robinson et al., 2011; Lehmann et al., 2011; Barton et al., 2015; Rangel et al., 2020). For example, it was shown that MDA-MB-453 (AR-positive, ERα-negative, HER2-positive) cells were responsive to DHT and R1881 for growth, and co-treatment with BIC was able to reverse this androgen-induced growth and induce apoptosis (Doane et al., 2006; Ni et al., 2011). Interestingly, MDA-MB-453 cells were found to have the highest AR-v7 protein levels among different BrCa cell lines tested, and over-expression of AR-v7 reversed the inhibitory effect of ENZA in these cells (Hickey et al., 2015). ChIP-Seq analysis of androgen treated MDA-MB-453 cells, revealed that 20% of AR binding sites overlap

with those found in LNCaP cells (Ni et al., 2011), demonstrating the difference in AR target sites between breast and prostate cancer cell lines. Comparison of AR binding sites in MDA-MB-453 cells to MCF7 ERα binding cites found only a 7% overlap (Ni et al., 2011), suggesting that the mechanism and genomic landscape of AR signalling might differ in the presence/absence of ERα.

It has also been thought that posttranslational modifications (i.e. phosphorylation) modulate AR activity and its role in cellular actions. It was suggested that phosphorylation of AR at Ser-515 by CDK1 could lead to AR overexpression (Shah and Bradbury, 2015). In a study conducted with 332 invasive ductal cancer patient samples, it was found that phosphorylation of AR at Ser-515 was associated with improved cancer specific survival in ERα-positive disease, but was associated with poor patient survival in TNBC patients (Roseweir et al., 2017). It has also been found that TNBC patients with phosphorylated Ser-515 have increased lymphatic invasion, proliferation and tumour budding (Roseweir et al., 2017), suggesting that AR is a potential therapeutic target and prognostic marker for TNBC patients.

TNBC tumours expressing AR is clinically defined as molecular apocrine tumours. In the absence of ERα pathway intervention, when exposed to androgens, HER2 enriched tumours proliferate due to crosstalk between the HER2 and AR pathways (Doane et al., 2006). Treatment with androgen in Sum-190 and MDA-MB-453 (ERα-negative AR-positive HER2 expressed) cell lines resulted in HER2 overexpression (Naderi and Hughes-Davies, 2008), the effect of which in MDA-MB-453 cells was blocked by the antiandrogen flutamide (Chia et al., 2011). These results are in accordance with a meta-analysis indicating that there is a significant overlap between the AR and HER2 pathways (Sanga et al., 2009). Activation of AR has also been demonstrated to enhance the HER2/HER3 pathways, which facilitates transcriptional activation of Myc, promoting proliferation and oncogenesis in molecular apocrine BrCa (Ni et al., 2011).

It has been demonstrated that, in molecular apocrine tumours, FOXA1 is required for AR to bind hormone response elements (Robinson et al., 2011). Interestingly, ChIP-seq analysis of MDA-MB-453 cells, demonstrated that AR binding sites overlapped with 98.1% of FOXA1 binding sites, whereas the overlap between ERα and FOXA1 was only 50% (Robinson et al., 2011). Another nuclear TF that regulates cell differentiation and proliferation, termed as cyclic-AMP Responsive Element Binding Protein 1 (CREB1), which is a mediator of AR in PrCa, has also been

shown to bind to AR promoter regions in BrCa, facilitating gene regulation (Chia et al., 2011).

1.7.3 AR Mutations in Breast Cancer

The progression and proliferation of prostate cancer (PrCa) is mainly driven by the AR signalling pathway (Brooke and Bevan, 2009; Crumbaker et al., 2017). There are a number of endocrine therapies for PrCa that target the AR signalling pathway (Brooke and Bevan, 2009). Hence, the majority of information about AR as a therapeutic target comes from PrCa studies. Like BrCa, endocrine therapies for PrCa are effective initially, but often fail and the disease progresses to the endocrine resistant stage. One of the mechanisms that has been proposed for the tumour to reach therapy resistant (hormone-independent) stage is AR mutations (Brooke and Bevan, 2009).

More than 150 different somatic mutations have been identified in PrCa patients (Gottlieb et al., 2012). It was found that some of the identified mutants result in a constitutively active receptor, resulting in ligand-independent proliferation of the tumour (Brooke and Bevan, 2009). The incidence of AR mutations is low in early stage PrCa but significantly increased in castrate resistant disease (Brooke and Bevan, 2009). As previously mentioned, molecular apocrine tumours are dependent upon AR for growth and proliferation (Naderi and Hughes-Davies, 2008; Robinson et al., 2011), and that antiandrogens can block this effect (Chia et al., 2011). It was demonstrated that ERα-positive tumours can develop mutations in ERα to become therapy resistant (Alluri et al., 2014). It is therefore possible that AR-dependent tumours can also develop mutations to become resistant to existing therapies and continue to proliferate in a ligand-independent manner.

The MDA-MB-453 cell line contains a mutant AR (AR-Q865H) which in reporter assays has been demonstrated to have a decreased sensitivity to androgen (DHT) and medroxyprogesterone acetate (MPA). AR mutations affect ligand sensitivity and specifity, and might alter cell proliferation pathways in a BrCa tumour cell, depending on the subtype (Moore et al., 2012). Interestingly, TCGA and METABRIC studies have shown that only 1% of the samples had alterations in the *AR* gene and the majority of

these were amplification of the *AR* (Curtis et al., 2012; Cancer Genome Atlas Network, 2012). However, little is known about the role of AR mutations in BrCa.

1.8 AR in Prostate Cancer

Prostate cancer (PrCa) is the most common cancer amongst men (Cancer Research UK, 2021), and activation of AR signalling is one of the main mechanisms for PrCa tumour development, and progression (Brooke and Bevan, 2009). The majority of PrCa cases are diagnosed when the disease is at an advanced stage, meaning that the tumour has already spread to neighbouring tissues, or metastasized to other parts of the body (Brooke and Bevan, 2009). Hence, surgery options are limited for these patients. Androgen ablation therapies, inhibiting the AR signalling pathway before/after the surgery is the mainstay of treatment for patients with advanced PrCa (Michmerhuizen et al., 2020). Therapy resistance is another common problem amongst PrCa patients who receive AR targeted therapies (Brooke and Bevan, 2009). Therefore, most of the knowledge about oncogenic AR signalling and AR targeted therapies comes from PrCa research. For example, the development of non-steroidal anti-androgen therapeutics (i.e., Flutamide, BIC, ENZA) have significantly increased PrCa survival rates (Dehm and Tindall, 2007; Tan et al., 2015).

In addition to AR signalling, a number of other signalling pathways have been shown to be involved in PrCa development and progression (Tan et al., 2015). For instance, activation of Phosphatidylinositol 3-Kinase (PI3K) leads to the phosphorylation of Akt (Protein Kinase B) and the activation of downstream signalling cascades (Sarker et al., 2009). *PTEN* loss leads to an elevation in Akt phosphorylation which correlates with poor prognosis, advanced tumour stage and grade of PrCa (Ayala et al., 2004). It has been proposed that the downstream effects of the PI3K/Akt pathway in PrCa could lead to activation of AR in a ligand-independent way either via regulation of phosphorylation of the receptor or via modification of coregulators (Sarker et al., 2009; Anestis et al., 2020). As such, Wnt/β-catenin, mTOR, extracellular signal regulated kinase (ERK) have also been associated with AR signalling (Anestis et al., 2020).

1.9 AR as a predictor and therapeutic target

Several studies have looked into AR expression in BrCa to investigate whether it could be used to predict a patient's responsiveness to endocrine therapies, clinical outcomes, or therapy failure. For example, AR expression was found to be correlated with better clinical outcomes, and low recurrence rates in ERα-positive patients (Qu et al., 2013; Vera-Badillo et al., 2014), and also in ERα-negative patients (Thike et al., 2014). In contrast, a phase III trial conducted with 3021 ERα-positive postmenopausal women, demonstrated that AR expression was not a good indicator of therapy response to tamoxifen or letrozole treatment (Kensler et al., 2019). However, AR/ERα ratio seemed to be a better predictive indicator compared to AR expression alone (Cochrane et al., 2014; Ravaioli et al., 2017; Rangel et al., 2018; Rangel et al., 2020).

Tissue microarray analysis of 699 TNBC patients was used to divide patients into AR-negative and AR-positive groups (Thike et al., 2014). IHC staining of nuclear AR in tumour cells (cut-off: 1%) was defined as the AR-positive subgroup, and it was found that TNBC patients with AR-positive tumours had better disease-free survival rates compared to AR-negative patients (Thike et al., 2014). Another study, which used the same cut-off value (1%) (Thike et al., 2014) for staining positive for AR, assessed the differences between a total of 135 TNBC patients, based on variable clinical characteristics (tumour size, lymph node metastasis, EGFR, ki67, disease-free survival rate etc.). That study found that classifying TNBC patients based on their EGFR and AR status could better predict the treatment outcomes by grouping patients into 3 risk groups: low (AR+/EGFR-), intermediate (AR+/EGFR+, AR-/EGFR-), and high (AR-/EGFR+) (Astvatsaturyan et al., 2018). This subgrouping of TNBC patients may help with choosing targeted therapies to achieve better clinical outcomes, and preferably prevent therapy resistance and tumour recurrences. Therefore, further clinical studies are necessary to evaluate the implications of these findings.

A study which investigated circulating tumour cells (CTCs) from blood samples of patients with advanced stage ERα-positive tumours, found that AR splice variant (AR-v7) expression in CTCs was associated with bone metastases (Aceto et al., 2018). The balance between AR and AR-v7 is known to be altered in CRPC, an aggressive stage of PrCa, which the cancer stops responding to the treatment, and the disease progresses and metastases despite of the low androgen levels

(Michmerhuizen et al., 2020). AR-v7 was also detected in almost half of 54 primary BrCa tumours (Hickey et al., 2015). Transcript levels of AR-v7 has been compared with full length AR levels in different BrCa cell lines (MDA-MB-453, ZR-75-1, T47D, MCF7, MDA-MB-231) by qPCR; ZR-75-1 and MDA-MB-453 had the highest AR-v7 transcript levels (Hickey et al., 2015). Thus, the AR splice variant AR-v7 could potentially be used as a predictor of bone metastases in BrCa patients, and could potentially have a role to predict antiandrogen resistance in AR-positive TNBC.

There is also emerging evidence that the AR signalling pathway plays a key role in BrCa, therefore it is a potential therapeutic target. It is thought that targeting the AR could lead to better clinical outcomes and prevent the occurrence of endocrine resistance in patients (Vera-Badillo et al., 2014). *In vivo* studies of xenograft models have shown that ENZA decreases the proliferation not only in LAR subtype but also in non-LAR TNBC subtypes (Barton et al., 2015). A study which used MCF7 xenograft models, demonstrated that ENZA can inhibit ERα-positive tumour growth (Cochrane et al., 2014). In the study, MCF7 luminescent cells were injected into ovariectomized mice, and mice were split into 2 different treatment groups: one receiving DHT-only, and the other DHT and ENZA. At the end of the treatment period, luminescence was measured, and the results showed that the group that received ENZA had a reduction of almost 85% in tumour mass in comparison with DHT-only group (Cochrane et al., 2014). In the same study, the ERα-negative line MDA-MB-453 was injected into mice and at the end of the treatment period, the size of tumour was measured with callipers. DHT and ENZA treated mice had smaller tumours than the mice treated with DHT. It has also been reported that a 55-year-old woman with metastatic TNBC and AR expression, after 4 months of treatment with 150 mg BIC daily, has achieved a complete clinical response (Arce-Salinas et al., 2016), suggesting that TNBC patients can benefit from antiandrogen therapy.

In a phase II study, out of 424 HR-negative cancer cases, 26 were found to be AR-positive and patients with AR-positive disease received 150mg BIC treatment daily (Gucalp et al., 2013). The progression free survival was 12 weeks and 6-month clinical benefit rate was 19% for patients who received BIC treatment (Gucalp et al., 2013). In another phase II study, patients with locally advanced or metastatic AR-positive TNBC received 160 mg ENZA daily and the clinical beneficial rate at 16 weeks was 25% (Traina et al., 2018). There is also an ongoing phase 2 study that assesses the efficacy

of ENZA and trastuzumab combination in HER2-enriched AR-positive metastatic BrCa patients (NCT02091960).

A phase II study (NCT02953860), which recruited 32 ERα-positive HER2-negative metastatic BrCa patients to test the efficacy of the combination of fulvestrant and ENZA has also been completed, however the results of this study has not been published yet. Some of the current ongoing trials for antiandrogen therapy in BrCa patients, as a single agent or in combination with other cancer drugs, are listed in Table 1-7.

Table 1-7 Ongoing clinical trials for antiandrogen therapy in Breast Cancer

The information about clinical trials was obtained from https://clinicaltrials.gov/ (Latest access: 18/09/2021).

Trial ID	Agent(s)	Treatments	Patient Population	Study Design
NCT00468715	Bicalutamide	AR antagonist	AR-positive, ERα-negative, metastatic BrCa	Open-label, Phase II, feasibility
NCT01889238	Enzalutamide	AR antagonist	Advanced, AR-positive, TNBC	Open-label, Phase II
NCT02750358	Enzalutamide	AR antagonist	Early stage, AR-positive, TNBC	Non-randomized, open-label, feasibility
NCT02457910	Enzalutamide & Taselisib	AR antagonist & PI3K inhibitor	AR-positive, metastatic TNBC	Partially randomized, open-label, phase I/II
NCT02605486	Bicalutamide & Palbociclib	AR antagonist & CDK4/6 inhibitor	AR-positive, metastatic BrCa	Non-randomized, open-label, phase I/II
NCT02091960	Enzalutamide & Trastuzumab	AR antagonist & HER2 monoclonal antibody	AR-positive, HER2 enriched metastatic or locally advanced BrCa	Non-randomized open-label, phase II
NCT02689427	Enzalutamide & Paclitaxel	AR antagonist & Taxane	AR-positive, TNBC	Non-randomized, open-label, phase II
NCT03207529	Enzalutamide + Alpelisib	AR antagonist & PI3K inhibitor	Metastatic AR-positive, PTEN positive BrCa	Not yet recruiting
NCT02955394	Neoadjuvant fulvestrant +/- Enzalutamide	AR antagonist & SERD	ERα-positive, HER2-negative BrCa	Phase II
NCT02007512	Exemestane +/- Enzalutamide	Aromatase inhibitor & AR antagonist	Metastatic HR-positive, HER2-negative BrCa	Phase II
NCT02676986	Enzalutamide +/- Exemestane	Aromatase inhibitor & AR antagonist	Primary ERα-positive BrCa	Phase II

1.10 Project Objectives

The AR has been shown to be an important regulator of BrCa progression. AR expression was not only associated with better tumour characteristics and disease-free survival in ERα-positive tumours, but also endocrine resistance. Therefore, questions remain about the role of the AR signalling in BrCa. Preclinical and clinical data have demonstrated that targeting AR could be beneficial in BrCa patients. However, identifying patients that can benefit from such therapies is important. In order to have better outcomes and prognosis, prevent therapy resistance and disease recurrence, understanding the role of the AR is essential. Therefore, this project aims to

- characterise AR and ERα crosstalk (Chapter 3),
- characterise the transcriptomic changes by AR-ERα crosstalk (Chapter 4),
- and investigate the role of AR mutations in BrCa (Chapter 5).

Chapter 2
Materials and Methods

Materials and Methods

2.1 Reagents and Kits

Each reagent and kit used throughout this work is listed in Table 2-1.

Table 2-1 Reagents and kits

Product	Company	Catalogue Number
Agarose	Melford	A20090
Acrylamide/Bis-acrylamide 30%	Sigma-Aldrich	A3699
Ammonium persulphate	Sigma-Aldrich	A3678
Ampicillin sodium salt	Sigma-Aldrich	A9518
Bovine serum albumin	Sigma-Aldrich	A2153
$CaCl_2$	Sigma-Aldrich	223506
Chloroform	VWR Chemicals	22711.34
Crystal violet	Sigma-Aldrich	46364
Detergent Compatible (DC) protein assay	Bio-Rad	5000112
ddH_2O	HyClone	SH30538
DMEM	Lonza	12-604F
DMEM (without phenol red or L-glutamine)	Lonza	12-917F
*Dpn*I	Fisher Scientific	10140690
Dual-Glo Luciferase Assay Reagent	Promega	E2920
Dual Light β-galactosidase assay	Applied Biosciences	BD100LP, BD300LP, BD2000LP
FCS	First Link	02-00-850
FuGENE HD transfection reagent	Promega	E2311
Glacial acetic acid	Fisher Scientific	A/0400/PB17
Glucose	Fisher Scientific	G/0500/53
Glycine	Fisher Scientific	G/0800/60
Glycoblue	Thermo Fisher	AM9516
Igepal CA-630	Sigma-Aldrich	I3021
Isopropanol	VWR Chemicals	20842.323
Kanamycin	Sigma-Aldrich	K4000
KCl	Sigma-Aldrich	P9541
L-Glutamine-Penicillin-Streptomycin Solution	Sigma-Aldrich	G1146
Lennox L Broth, granules	Melford	L24066
Luciferase assays	Promega	E1500
Luna Script Reverse Transcriptase Super Mix Kit	New England Biolabs	E3010L
Luna Universal qPCR Master Mix	New England Biolabs	M3003L
Luria agar, powder	Melford	L24020

$MgCl_2$	Fisher Scientific	M/0600/53
Monarch Plasmid Miniprep Kit	New England Biolabs	T1010L
Monarch Total RNA Miniprep Kit	New England Biolabs	T2010S
MycoAlert Mycoplasma Detection Kit	Lonza	LT07-701
NaCl	Sigma-Aldrich	S/3160/60
NaCl 5M	Alfa Aesar	J60434
N,N,N',N' - Tetramethyl ethylenediamine	Sigma-Aldrich	T9281
Opti-MEM	Thermo Fisher	31985070
Page Ruler Pre-stained Protein Ladder	Thermo Fisher	26616
PBS tablets	Melford	P32080
PFA	Sigma-Aldrich	16005
Phenol:chloroform:isoamyl alcohol	Thermo Fisher	P2069
Plasmid Midiprep Kit	Qiagen	12143
Plasmid Maxiprep Kit	Qiagen	12163
Polyvinylidene difluoride (PVDF) membrane	Millipore	IPVH00010
Protease Inhibitor Cocktail	Melford	P50750-1
Proteinase K	Thermo Fisher	AM2546
Protein G Dynabeads	Invitrogen	10003D
Qubit RNA IQ assay	Thermo Fisher	Q33221
QuickChange II Site directed mutagenesis	Agilent	200524
RPMI-1640	Lonza	BE04-558F
RPMI-1640 (without phenol red and L-glutamine)	Lonza	12-918F
Sodium deoxycholate	Sigma-Aldrich	D6750
SYBR Safe	Invitrogen	S33102
TBE	Melford	T32020
Tris base	Fisher Scientific	BP152-1
Triton X-100	Sigma-Aldrich	T8787
TRIzol	Invitrogen	15596018
Tryptone	Oxoid	LP0042
Tween-20	Sigma-Aldrich	P1379
Yeast extract	Oxoid	LP0021
2X RNA loading dye	Thermo Fisher	R0641
4X Laemmli protein sample buffer	Bio-Rad	1610747
5x Reporter Lysis Buffer	Promega	E397A
20% N-Lauroylsarcosine	Sigma-Aldrich	L7414
100X TE buffer	Sigma-Aldrich	T9285

2.2 Solutions and Buffers

Table 2-2 Preparation recipes for solutions and buffers

Solutions and Buffers

Buffer/Solution	Recipe	Sterilisation	Storage
4% Paraformaldehyde (PFA)	8 g of PFA (Sigma-Aldrich) dissolved in sterile ddH_2O to a final volume of 200 mL, whilst heated on a stirring plate inside a fume cupboard.	-	-20°C, in 50 mL aliquots
Phosphate buffered saline (PBS)	8 PBS tablets (Melford) dissolved in sterile ddH_2O to a final volume of 800 mL.	Autoclave	RT (room temperature)
PBS-0.1%-Tween (PBS-T)	800 µL of Tween-20 (Sigma-Aldrich) in a total of 800 mL PBS.	-	RT
0.04% Crystal violet	16 mg crystal violet (Sigma-Aldrich) in a final volume of 40 mL sterile ddH_2O.	0.22 µm filter sterilise	RT

Agarose Gel Electrophoresis

Gel	Recipe	Sterilisation	Storage
1% Agarose gels	1 g (1%) of agarose (Melford) dissolved in 100 mL of 1X TAE for DNA, 1X TBE for RNA, via boiling. Following this, it was briefly allowed to cool prior to the addition of 1 µL of SYBR Safe (10,000X in DMSO, Invitrogen) and casting.	-	Freshly made before use

1X Tris-acetate-EDTA (TAE)	40 mM Tris base (4.846 g, Fisher Scientific), 1.114 mL glacial acetic acid (Fisher Scientific) and 1 mM EDTA (2 mL of 0.5 M stock), in a total of 1 L sterile ddH_2O.	-	RT
1X Tris-Borate-EDTA (TBE)	100 mL of 10X TBE (Melford) in a total of 1 L sterile filtered (0.1 µm), nuclease-free ddH_2O (HyClone).	-	RT

Bacterial Culture

Solution	**Recipe**	**Sterilisation**	**Storage**
100 mg/mL Ampicillin stock	1 g ampicillin sodium salt (Sigma-Aldrich) to a final volume of 10 mL ddH_2O. Added to LB broth/agar to a final concentration of 100 µg/mL.	0.22 µm filter sterilise	-20°C in 1 mL aliquots
50 mg/mL Kanamycin stock	0.5 g kanamycin (Sigma-Aldrich) to a final volume of 10 mL ddH_2O. Added to LB broth/agar to a final concentration of 50 µg/mL.	0.22 µm filter sterilise	-20°C in 1 mL aliquots
1 M Glucose stock	18 g of Glucose (Fisher Scientific) in a final volume of 100 mL ddH_2O.	0.22 µm filter sterilise	RT
Luria Broth (LB)	4 g LB Broth (Lennox L Broth, granules, Melford) dissolved in a total of 200 mL of ddH_2O, with the pH adjusted to 7.2 where necessary. When required,	Autoclave	4°C

	supplemented using antibiotics.		
1 M Magnesium chloride ($MgCl_2$) stock	9.5 g of $MgCl_2$ (Fisher Scientific) in a final volume of 100 mL ddH_2O.	Autoclave	RT
LB agar plates	7 g of LB Agar (Luria agar, powder, Melford) to a final volume of 200 mL ddH_2O, supplemented if required with antibiotics. Melted prior to use and poured to make agar plates whilst still liquified.	Autoclave	4°C
Super Optimal broth with Catabolite repression (SOC) media	20 g of Tryptone (Oxoid), 5 g of yeast extract (Oxoid), 0.5 g of NaCl (10mM, Sigma-Aldrich), 0.18 g KCl (2.5 mM, Sigma-Aldrich), 10 mL of 1 M $MgCl_2$ stock, 10 mL of 1 M $MgSO_4$ stock, and 20 mL of 1 M Glucose stock, dissolved in ddH_2O up to 1 L.	Autoclave (prior to adding glucose)	4°C

Western Blotting

Solution/Buffer	**Recipe**	**Sterilisation**	**Storage**
10% Ammonium persulphate (APS)	1 g of APS (Sigma-Aldrich) dissolved in a total volume of 10 mL ddH_2O.	-	-20°C, in 1 mL aliquots
Blocking buffer	2.5 g (5%) dried skimmed milk powder (Marvel) to a total of 50 mL in PBS-T.	-	4°C, used within 24 hours.
10% Polyacrylamide Gel	Per gel, a 10% resolving gel was made, consisting of 1.65 mL Acrylamide/Bis-	-	4°C, kept moist and used within

	acrylamide 30% solution (Sigma-Aldrich), 1.875 mL of 1 M Tris/HCl at pH 8.9, 1.375 mL of ddH_2O and 50 µL of 10% SDS. Immediately prior to pouring, 50 µL of 10% APS stock and 5 µL N,N,N',N' - Tetramethyl ethylenediamine (TEMED, Sigma-Aldrich) were added.		3 days
Stacking gel	Per gel, 425 µL of Acrylamide/Bis-acrylamide 30% solution (Sigma-Aldrich), 937.5 µL of 1 M Tris/HCl at pH 6.8, 1.0875 mL of ddH_2O and 25 µL of 10% SDS were added. Immediately prior to pouring, 25 µL of 10% APS and 2.5 µL TEMED were added.	-	4°C, kept moist and used within 3 days
Radioimmunoprecipitation Assay (RIPA) buffer	0.5 mL of 1 M Tris-HCl (pH 8.0) stock (10 mM), 20 mg of EDTA (1 mM, Fisher Scientific), 0.5 mL of Triton X- 100 (1%, Sigma-Aldrich), 50 mg of Sodium deoxycholate (0.1%, Sigma-Aldrich), 0.5 mL of 10% SDS stock solution (0.1%) and 0.41 g of NaCl (Sigma-Aldrich). Supplemented with 10 µL of Halt Protease Inhibitor Cocktail (PIC)	0.22 µm filter sterilise	4°C, used within 4 weeks

	(Melford) per 1 mL of RIPA immediately prior to use.		
1 X Running Buffer	3 g of Tris base (25 mM, Fisher Scientific), 14.45 g of Glycine (0.2 M, Fisher Scientific) and 0.5 g of SDS (0.05%, Fisher Scientific) were dissolved in a total volume of 1 L ddH_2O.	-	RT
10% Sodium dodecyl sulphate (SDS)	50 g of SDS (Fisher Scientific) dissolved in a total volume of 500 mL ddH_2O.	-	RT
Semi-Dry Transfer Buffer	11.26 g Glycine (150 mM, Fisher Scientific), 2.44 g Tris base (20 mM) and 200 ml of Methanol (20%, MeOH, Fisher Scientific), dissolved in a total volume of 1 L ddH_2O.	-	RT

Transfections

Solution	**Recipe**	**Sterilisation**	**Storage**
N,N-Bis(2-hydroxyethyl)-2-aminoethanesulphonic acid (BES)-buffered saline (BBS) 2 X solution	50 mM BES (10.66 g, Sigma-Aldrich), 280 mM NaCl (16.36 g, Sigma- Aldrich), 1.5 mM Sodium phosphate dibasic (Na_2HPO_4, 0.21 g, Sigma- Aldrich), to a final volume of 1 L using ddH_2O, adjusted to pH 6.95 using 5 M NaOH stock solution.	0.22 µm filter sterilise	-20°C, in 50 mL aliquots
2.5 M Calcium Chloride ($CaCl_2$)	138.73 g of anhydrous granular $CaCl_2$ (Sigma-	0.22 µm filter sterilise	-20°C, in 50 mL aliquots

	Aldrich) to a total of 500 mL in ddH_2O.		

Chromatin Immunoprecipitation

Block solution	0.5% BSA (Bovine serum albumin) (Sigma-Aldrich) in PBS.	0.22 µm filter sterilise	4°C, used within a week
2.5 M glycine	18.7 g glycine (Fisher Scientific) in 100 mL ddH_2O.	0.22 µm filter sterilise	RT, used within 4 weeks.
1X Tris-EDTA (TE) Buffer	100X TE buffer (Sigma-Aldrich) diluted 1:100 with ddH_2O.	0.22 µm filter sterilise	RT, freshly made before use.
Lysis Buffer 1 (LyB1)	For 50 mL buffer, 2.5 mL of 1M HEPES-KOH pH 7.5 (50 mM), 1.4 mL of 5M NaCl (Sigma-Aldrich) (140 mM), 0.1 mL of 0.5 M EDTA (Fisher Scientific) (1 mM), 5 mL of Glycerol (10%), 0.25 mL of Igepal CA-630 (Sigma-Aldrich) (0.5%), 0.125 mL of Triton X-100 (Sigma-Aldrich) (0.25%), 40.625 mL of ddH_2O. Supplemented with 10 µL of Halt Protease Inhibitor Cocktail (PIC) (Melford) per 1 mL of LyB1 immediately prior to use.	0.22 µm filter sterilise	4°C, used within 4 weeks
Lysis Buffer 2 (LyB2)	For 50 mL buffer, 0.5 mL of 1M Tris-HCl at pH 8 (10mM), 2 mL of 5M NaCl (Sigma-Aldrich) (200mM), 0.1 mL of	0.22 µm filter sterilise	4°C, used within 4 weeks

	0.5 M EDTA (Fisher Scientific) (1mM), 0.125 mL of 0.2 M EGTA (0.5mM), 47.275 mL of ddH_2O. Supplemented with 10 µL of Halt Protease Inhibitor Cocktail (PIC) (Melford) per 1 mL of LyB2 immediately prior to use.		
Lysis Buffer 3 (LyB3)	For 50 mL buffer, 0.5 mL of 1M Tris-HCl at pH 8 (10 mM), 1 mL of 5 M NaCl (Sigma-Aldrich) (100 mM), 0.1 mL of 0.5 M EDTA (Fisher Scientific) (1 mM), 0.125 mL of 0.2 M EGTA (0.5 mM), 0.5 mL of 10% Sodium deoxycholate (Sigma-Aldrich) (0.1%), 1.25 mL of 20% N-Lauroylsarcosine (Sigma-Aldrich) (0.5%), 46.525 mL of ddH_2O. Supplemented with 10 µL of Halt Protease Inhibitor Cocktail (PIC) (Melford) per 1 mL of LyB3 immediately prior to use.	0.22 µm filter sterilise	4°C, used within 4 weeks
Radioimmunoprecipitation Assay - ChIP (RIPA-C) Buffer	For 100 mL buffer, 5 mL of 1 M HEPES-KOH at pH 7.5 (50 mM), 50 mL of 1 M LiCl (500 mM), 0.2 mL of 0.5 M EDTA (Fisher Scientific) (1 mM), 1 mL of Igepal CA-630 (Sigma-Aldrich) (1%), 7 mL of 10%	0.22 µm filter sterilise	4°C, used within 4 weeks

	Sodium deoxycholate (Sigma-Aldrich) (0.7%), 36.8 mL of ddH_2O.		
Tris-buffered Saline (TBS) Buffer	For 50 mL buffer, 1 mL of 1 M Tris-HCl at pH 7.6 (20mM), 1.5 mL of 5 M NaCl (Sigma-Aldrich) (150mM), 47.5 mL of ddH_2O.	0.22 µm filter sterilise	RT, freshly made before use.
Elution buffer	For 5 mL buffer, 0.25 mL of 1 M Tris-HCl at pH 8 (50 mM), 0.1 mL of 0.5 M EDTA (Fisher Scientific) (10 mM), 0.5 mL of 10% SDS (1%), 4.15 mL of ddH_2O.	0.22 µm filter sterilise	RT, freshly made before use.

2.3 Mammalian Cell Culture

MCF7, T47D and COS-1 cells were originally obtained from American Type Culture Collection (ATCC), and were cultured in their relevant normal media (Table 2-3) at 37°C, 5% CO_2. Cells were monitored regularly under microscopes for confluency and health. Cell passaging was performed twice a week. Cells were regularly checked for mycoplasma using MycoAlert Mycoplasma Detection Kit (Lonza), following manufacturer's protocol.

72 hours before exposure to ligands, MCF7 and T47D cells were cultured in hormone-depleted media. The receptor status (AR/ERα/PR/HER2) of cell lines, their relevant media and supplements are listed in Table 2-3 and Table 2-4.

Table 2-3 Mammalian cell lines used in the study

Cell Line	AR	ERα	PR	HER2	Normal Media	Hormone-depleted Media
T47D	+	+	+	-	RPMI	Phenol-red free RPMI
MCF7	+	+	+	-	DMEM	Phenol-red free DMEM
COS-1	-	-	-	-	DMEM	Phenol-red free DMEM

Table 2-4 Cell culture media

Media	Supplements
DMEM	10% FCS, 1% PSG (100 U penicillin, 2 mM glutamine, and 0.1 mg/mL streptomycin)
RPMI	10% FCS, 1% PSG (100 U penicillin, 2 mM glutamine, and 0.1 mg/mL streptomycin)
Phenol-red free DMEM	2% sFCS (double charcoal stripped foetal calf serum), 1% PSG (100 U penicillin, 2 mM glutamine, and 0.1 mg/mL streptomycin)
Phenol-red free RPMI	5% sFCS (double charcoal stripped foetal calf serum), 1% PSG (100 U penicillin, 2 mM glutamine, and 0.1 mg/mL streptomycin)

2.4 Gene Expression Analysis

Cells were seeded at 70% confluency (approximately 2 x 10^5 cells) in 12-well plates and grown for 72 hours in hormone-depleted media before exposure to ligands. Cells were then treated with the required ligand or drug concentration for 8 or 24 hours.

2.4.1 RNA Extraction

After treatment, cells were washed with PBS and lysed using 400 µL of TRIzol Reagent (Invitrogen). 80 µL of chloroform was added to the samples, incubated for 2 minutes at room temperature (RT) and spun for 15 minutes at 12,000 g, 4°C. The aqueous layer was transferred to a new microcentrifuge tube, 200 µL isopropanol and 1 µL glycogen blue were added, mixed, and incubated at RT for 10 minutes. After incubation, samples were spun for 10 minutes at 12,000 g, 4°C. The RNA pellets were washed twice with 75% ethanol (EtOH) and were spun for 5 minutes at 7,500 g, 4°C, then air dried and resuspended in 30 µL RNase-free ddH_2O. The RNA concentration and quality were checked using a NanoDrop Spectrophotometer (Nanodrop, LabTech).

2.4.2 Reverse Transcriptase PCR (cDNA Synthesis)

250 ng RNA was reverse transcribed using the Luna Script Reverse Transcriptase Super Mix Kit (New England Biolabs). The reactions were incubated following the manufacturer's protocol in a BioRad thermocycler and the resulting cDNA was diluted 1:4 with RNase-free ddH_2O prior to use.

2.4.3 Primer Design

Genomic and mRNA FASTA sequences of the interest of genes were obtained from National Centre for Biotechnology Information (NCBI) and primers for gene expression analysis were designed using Primer Bank (https://pga.mgh.harvard.edu/primerbank/). Primers that were approximately 20 bp

length, an amplicon size or approximately 100 bp, and preferably spanning intron boundaries were chosen for qPCR.

2.4.4 Quantitative PCR (qPCR)

qPCR was conducted using 2 µL of synthesised cDNA with the Luna Universal qPCR Master Mix (New England Biolabs), following the manufacturer's protocol with a LightCycler 96 (Roche). Melt curves for each reaction were evaluated. Gene expression was normalised using the RPL19 ribosomal protein (L19) reference gene and alterations in gene expression calculated using the delta-delta Ct (ΔΔCt) method. The primers used are provided in Table 2-5.

Table 2-5 Sequences of gene expression primers for use with qPCR

Gene	Primer Sequences (5'-3')	
RPL19	F	GCGGAAGGGTACAGCCAAT
	R	GCAGCCGGCGCAAA
TFF1	F	GGAGAACAAGGTGATCTGCG
	R	TTATTTGCACACTGGGAGGG
CXCL12	F	GAGAAAGCTTTAAACAAGAGGTTCA
	R	CCTTCCCTAACACTGGTTTCAG
MYB	F	ATCTCCCGAATCGAACAGATGT
	R	TGCTTGGCAATAACAGACCAAC
KCNK5	F	TCACAGGGAACCAGACCTTC
	R	GCCACATTGCCATATCCAATG
PSCA	F	TGCTGCTTGCCCTGTTGAT
	R	CCTGTGAGTCATCCACGCA
C1orf116	F	CATCTCTGCCCTTTGAAACAAAA
	R	GGGCATCACCCGAAACAAG
ZBTB16	F	CTGGATAGTTTGCGGCTGAG
	R	ATGTCAGTGCCAGTATGGGT

2.5 Chromatin Immunoprecipitation (ChIP)

1 x 10^6 cells were seeded in 15 cm culture dishes, cultured in hormone-depleted media for 72 hours and treated with ethanol (vehicle), MIB (1 nM), E_2 (1 nM), TAM (100 nM) and FULV (100 nM) for 4 hours. To crosslink DNA-protein complexes, cells were treated with 1% formaldehyde in PBS for 10 minutes and the reaction was quenched using glycine to a final concentration of 250 µM. Cells were washed twice with ice cold PBS, scraped on ice in 1.6ml ice cold PBS (with PIC) and transferred into pre-chilled 2ml Eppendorf tubes. Cells were then spun at 2000 rpm at 4°C for 10 minutes, and the supernatant was removed, pellets were stored at -80°C before cell lysis.

Protein G Dynabeads (Invitrogen) were washed three times with 1 mL of block solution using a magnetic stand. Dynabeads were then resuspended in block solution and 4 µg AR antibody were added in a final volume of 250 µl (supplemented with 10 µL of PIC), and incubated overnight on a rotating platform at 4°C.

For lysis, cell pellets were resuspended in 1 mL of LyB1, tubes were rotated at 4°C for 10 minutes, and spun at 2000 rpm for 5 minutes at 4°C. The same procedure was repeated for LyB2 before resuspension in 1 mL of LyB3. Lysates were split into 500 µl volume, DNA was sonicated for 25 cycles of 30 seconds on and 30 seconds off at 4°C using a Biorupter Plus (Diagenode) to approximately 200 bp size fragments. Lysates were then combined and spun at high speed for 10 minutes at 4°C, and the supernatant was transferred into new pre-chilled Eppendorf tubes. 50 µl of the lysates were retained as input and the rest was used for the immunoprecipitation. The fragments were analysed using 1% agarose gel electrophoresis for successful sonication.

To pull down DNA target sites, antibody-Dynabeads complexes were washed three times using block solution to remove unbound antibodies. Antibody-bead complexes were resuspended in 100 µl of block solution (supplemented with PIC), 1 mL of sonicated cell lysates were added, and incubated overnight on a rotating platform at 4°C. The next day, tubes were washed with RIPA-C buffer six times using a magnetic stand to collect the beads. 1 mL of TBS was added, samples were spun at 2000 rpm for 30 seconds, and TBS was removed using a magnetic stand before adding 200 µl of elution buffer to the beads. Reverse crosslinking was performed at

65°C for 6 hours for input and ChIP samples. Subsequently, beads were removed, and the supernatant was transferred to fresh Eppendorf tubes, containing 4 µl of 20 mg/ml proteinase K (Thermo Fisher), and 200 µl of TE buffer. Samples were incubated at 55°C for 2 hours. Next, 400 µl of phenol:chloroform:isoamyl alcohol (Thermo Fisher) was added and the samples were centrifuged at 14,800 rpm for 5 minutes at 4°C. The aqueous layer was transferred to a new centrifuge tube, 16 µl of 5 M NaCl (Sigma-Aldrich), 1 mL of 100% ethanol and 1 µl of glycoblue (Thermo Fisher) were added and the tubes centrifuged at 14,800 rpm for 30 minutes at 4°C to pellet the DNA. Pellets were left to air dry and resuspended in 25 µl of nuclease-free ddH_2O. Input samples were diluted 1:125 for qPCR. The DNA concentration and quality were checked using a NanoDrop Spectrophotometer (Nanodrop, LabTech). ChIP-qPCR was performed (primer sequences are listed in Table 2-6) as described in Section 2.4.4 to assess binding to the AR response elements and control regions.

Table 2-6 Sequences of primers used to investigate Androgen Receptor binding sites

Description	Primer Sequence (5'-3')	
ZBTB16 ARE+	F	ATGCCCTGCGTCTGTACTCATT
	R	TGTTCTGATGAGATCTGCACGCCT
ZBTB16 ARE-	F	GTCCTGTCTCCCA TTCCAGA
	R	GAGAAGCCCAAT CGCAATAA
PSCA ARE+	F	CCACTGCCTTACAGCAATC
	R	GTCTCTGTGTTCAAGGTGC
PSCA ARE-	F	CTGCCCAAATAAGCCTGTG
	R	AGAGGACAGTGAGGGGTTAG

2.6 Bacterial Cultures, Transformation and DNA Preparation

2.6.1 Bacterial strains and culture

For transformation procedures, the max efficiency XL1-Blue *Escherichia coli* (*E. coli*) strain of competent cells was used (Agilent). All bacterial work was performed in sterile conditions. Bacterial suspensions were incubated in a shaker at 225 rpm, at 37°C.

2.6.2 Transformation

50 µL of competent *E. coli* cells were defrosted on ice and gently mixed with 50 ng of plasmid DNA and the mixture was incubated on ice for 30 minutes. Next, the mixture was heat shocked for 45 seconds in a 42°C water bath. The cells were immediately placed on ice for 3 minutes and then incubated in 450 µL of pre-warmed SOC media for 1 hour at 37°C in a shaker at 300 rpm as a recovery period. The required amount of bacteria suspension was spread onto LB agar plates, containing the appropriate antibiotics, and incubated overnight at 37°C.

2.6.3 DNA Preparation (Miniprep, Midiprep and Maxiprep)

A single colony was selected from the bacterial plate using a sterile pipette tip. The colony was used to inoculate 5 mL of LB broth supplemented with the appropriate antibiotic, overnight at 37°C with shaking. For plasmid verification, the plasmid DNA was initially purified using the Monarch Plasmid Miniprep Kit (New England Biolabs), following the manufacturer's protocol. To verify the cloning, Sanger sequencing (Eurofins) was performed with harvested DNA plasmids. Once verified, the cloned transformed bacteria were stored at -80°C as glycerol stocks (combining 200 µL of glycerol with 800 µL of bacterial culture).

For higher quantities of DNA, glycerol stocks were spread onto LB agar plates containing the appropriate antibiotic and grown overnight. A single bacterial colony was used to inoculate 5 mL of LB broth supplemented with the appropriate antibiotic overnight at 37°C with shaking. The culture was transferred into 200 mL of LB broth

supplemented with the appropriate antibiotic and incubated overnight at 37°C while shaking. The plasmids were harvested using the Plasmid Midiprep/Maxiprep Kit (Qiagen), following the manufacturer's protocol. After mini/midi/maxi DNA preparation, DNA concentrations were quantified using the NanoDrop Spectrophotometer (Nanodrop, Labtech).

2.7 Plasmids

Table 2-7 Plasmids used in this work

Plasmid	**Antibiotic resistance**
pSV-AR	Ampicillin
GFP-AR	Kanamycin
Bos-β-galactosidase	Ampicillin
TAT-GRE-EIB-LUC (ARE-luciferase)	Ampicillin
3xERE-TATA-LUC (ERE-luciferase)	Ampicillin
pSG5-ERα	Ampicillin
pSG5-Empty	Ampicillin
Renilla	Ampicillin

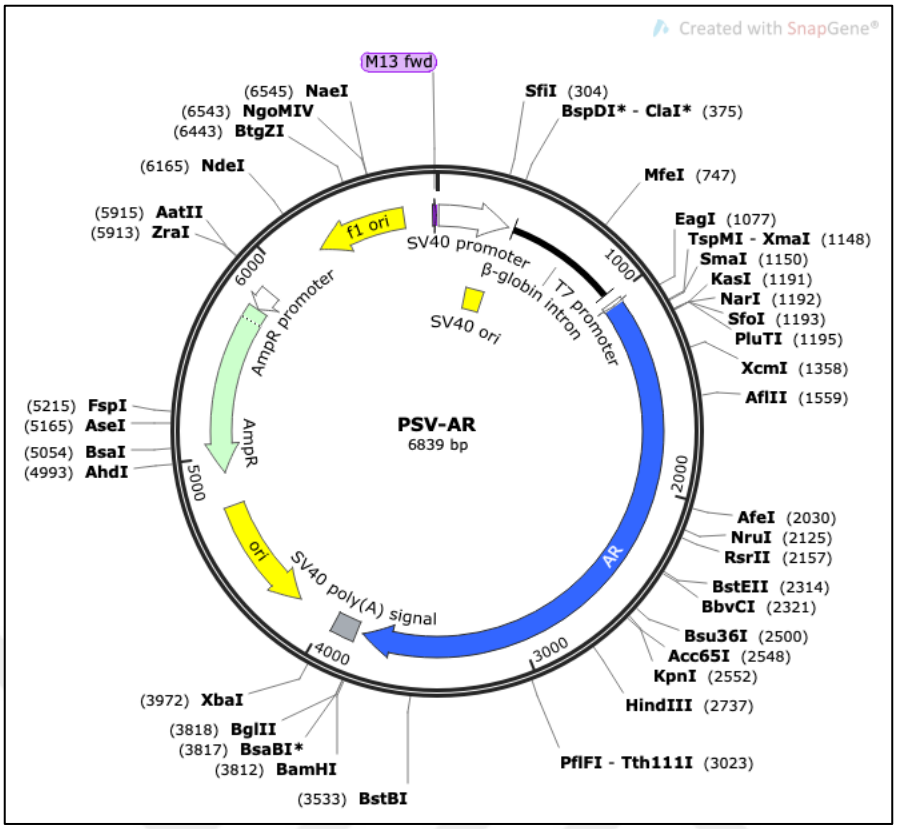

Figure 2-1 Plasmid map of pSV-AR

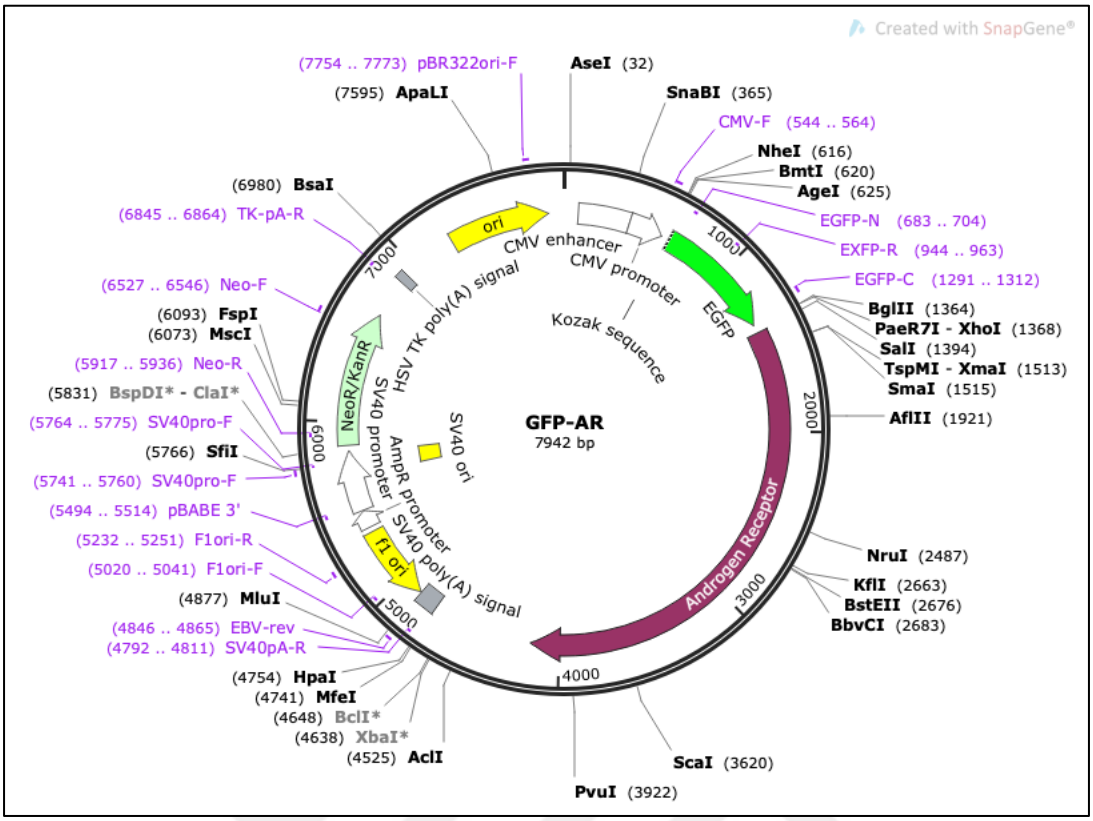

Figure 2-2 Plasmid map of GFP-AR

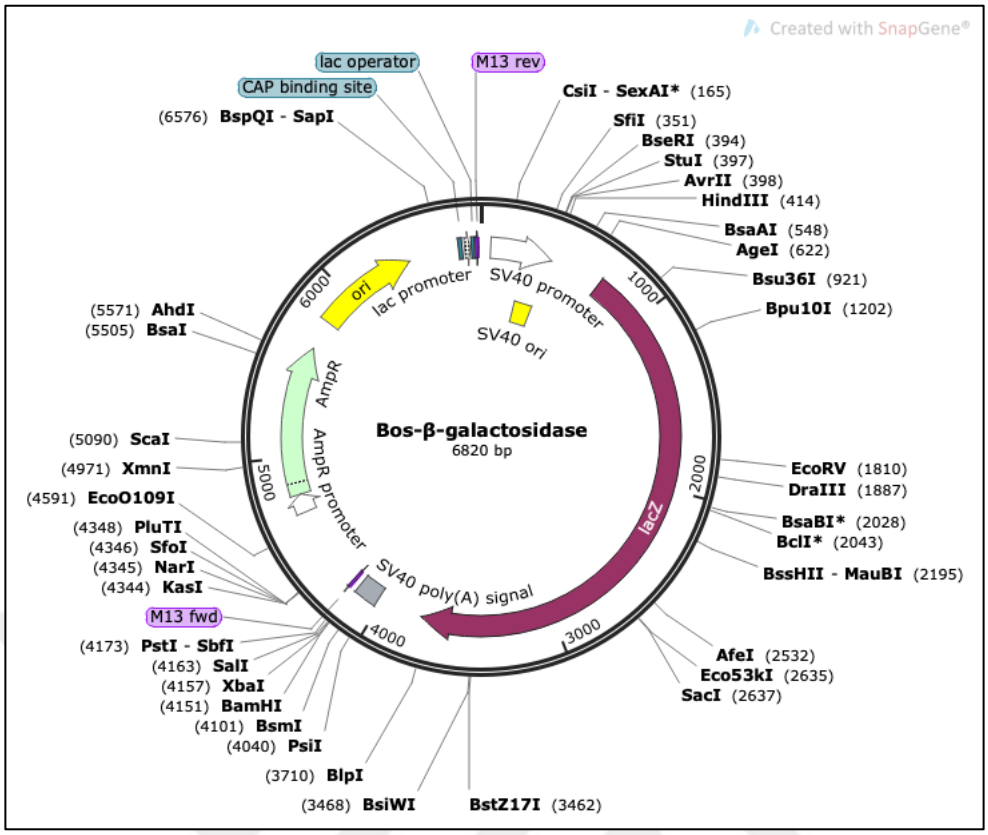

Figure 2-3 Plasmid map of Bos-β-galactosidase

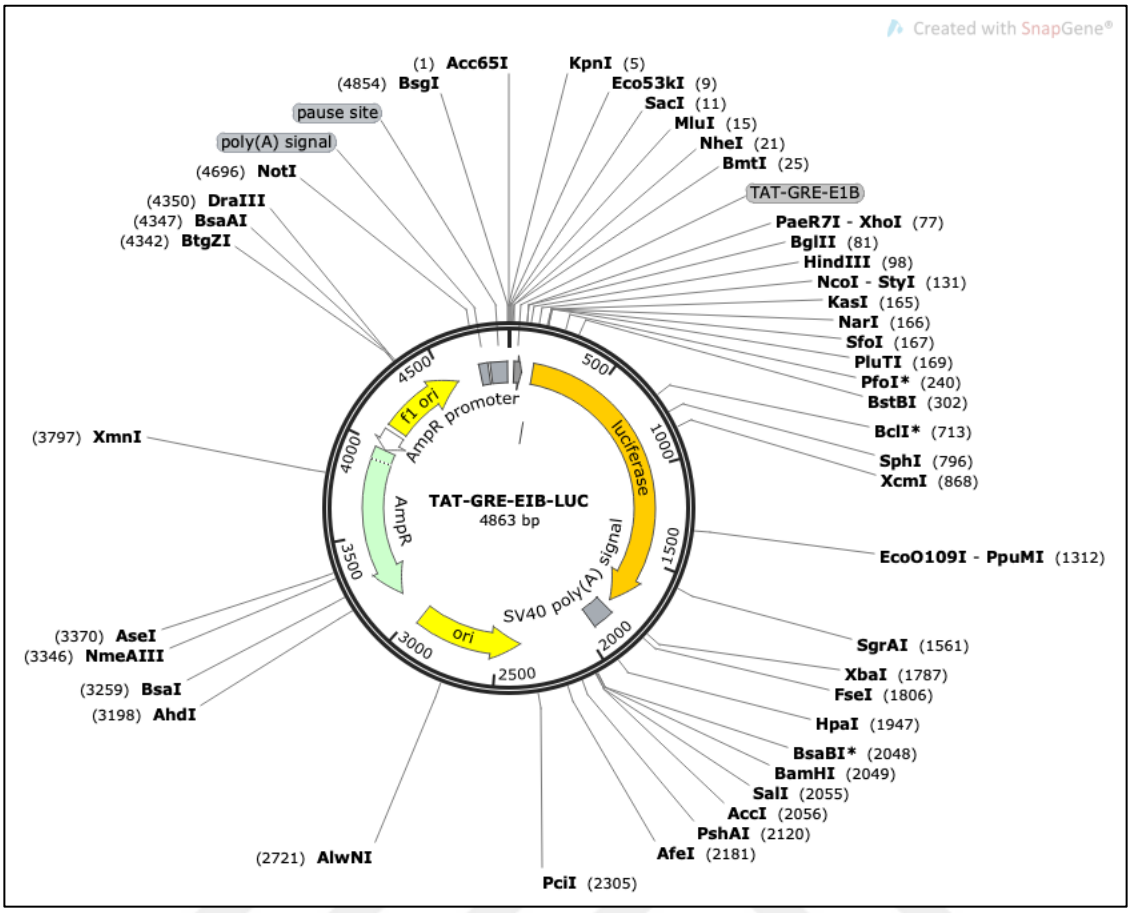

Figure 2-4 Plasmid map of TAT-GRE-EIB-LUC

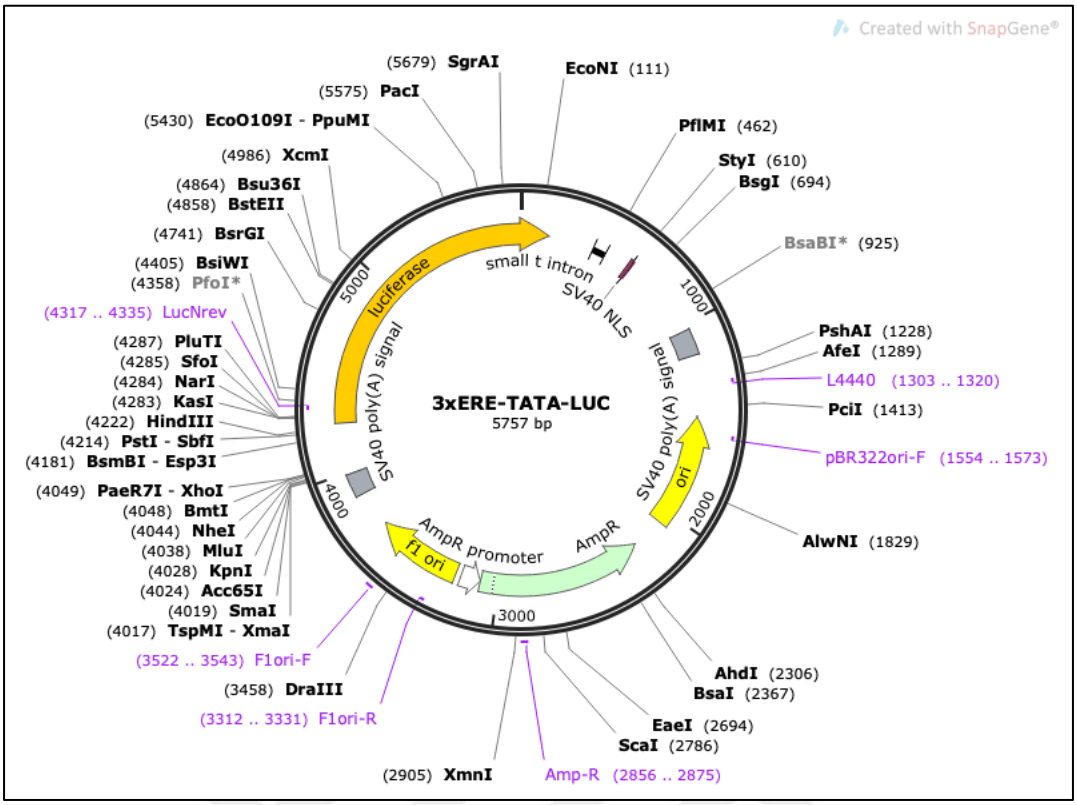

Figure 2-5 Plasmid map of 3xERE-TATA-LUC

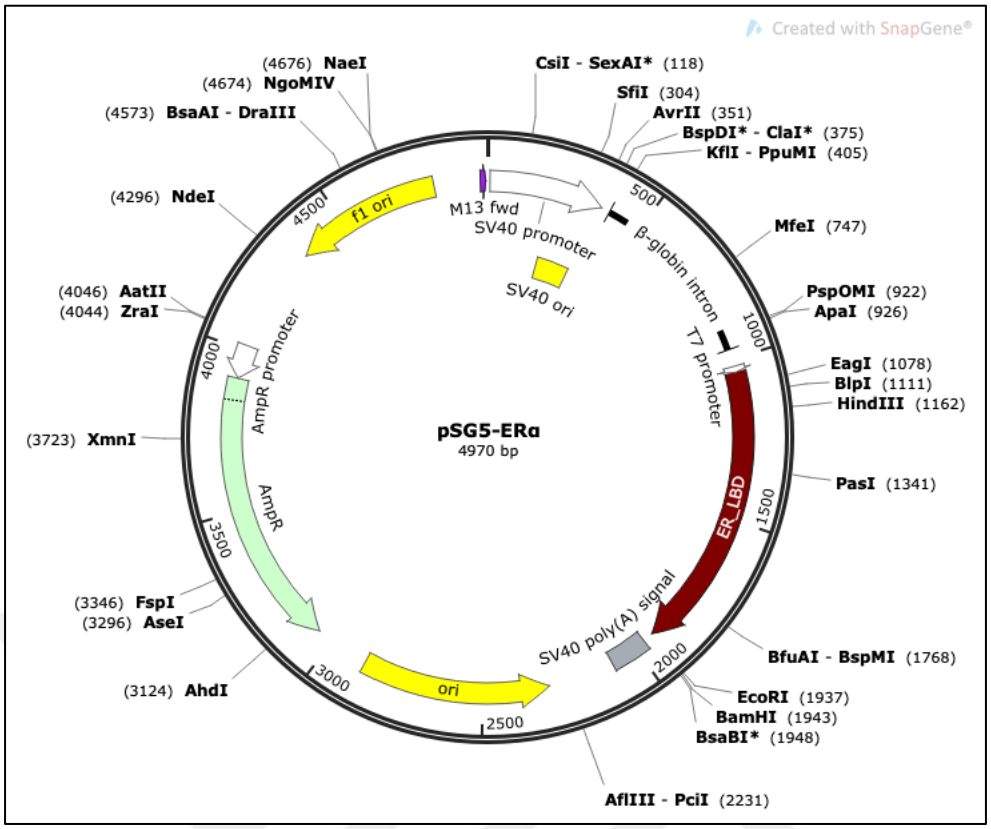

Figure 2-6 Plasmid map of pSG5-ERα

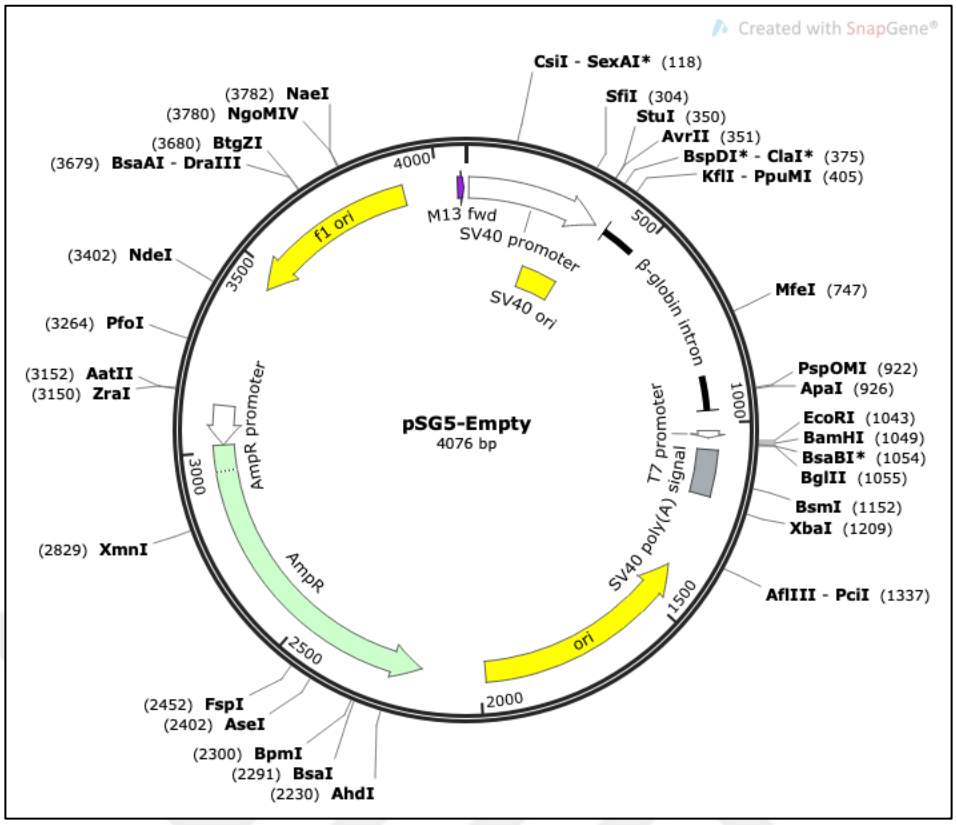

Figure 2-7 Plasmid map of pSG5-Empty

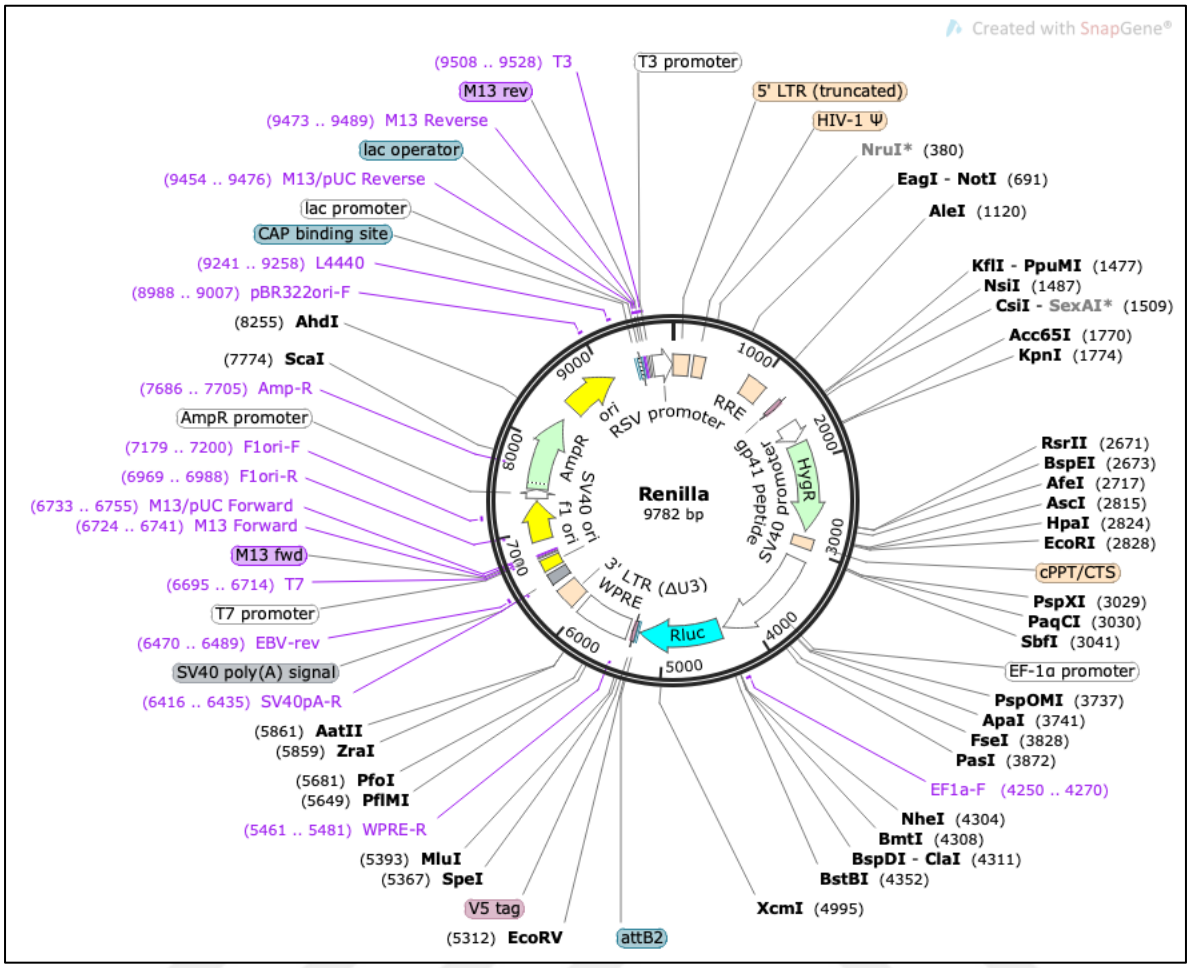

Figure 2-8 Plasmid map of Renilla

2.8 Site directed mutagenesis

Site directed mutagenesis (QuickChange II, Agilent DE, USA) was conducted to introduce mutations into the AR expression plasmids (pSV-AR or GFP-AR) following the preparation (Table 2-8) and reaction instructions (Table 2-9). The primer sequences for mutagenesis are listed in Table 2-10. Amplified plasmids were incubated with *Dpn*I at 37 °C for 1 hour, then transformed into XL1-Blue *E. coli* and bacterial colonies were grown on LB agar plates containing the appropriate antibiotic overnight at 37°C in the incubator. The purification of plasmid DNA was conducted using the Monarch Plasmid Miniprep Kit (New England Biolabs) and mutations were confirmed by Sanger sequencing (Eurofins). Successful mutagenesis was confirmed by visualisation of the sequencing chromatogram in SnapGene Viewer (version 4.2.11).

Table 2-8 PCR reaction ingredients

Sample	**Volume (µL)**	
	GFP-AR reactions	**pSV-AR reactions**
Nuclease free ddH_2O water	19.6	21.1
PFU buffer (10X)	3	3
DMSO	1.8	1.8
dNTP	0.6	0.6
Template plasmid (20ng/µL)	2.5	1
F primer (75ng/µL)	1	1
R primer (75ng/µL)	1	1
PFU DNA polymerase	0.5	0.5
Total	30	

Table 2-9 PCR conditions for mutagenesis reactions

Temperature (°C)	**GFP-AR reactions**		**pSV-AR reactions**	
	Number of cycles	**Duration**	**Number of cycles**	**Duration**
95	1	2 minutes	1	2 minutes
95	20	50 seconds	15	50 seconds
55		1 minute		1 minute
68		8 minutes		4 minutes
68	1	15 minutes	1	15 minutes
12	1	4 minutes	1	4 minutes
4	Hold			

Table 2-10 List of primers for AR mutagenesis

Mutation	Melting Temperatures	Primer Sequences (5'-3')	
R13W (C37T)	78.25°C	F	GGAAGGGTCTACCCTTGGCCGCCG
		R	CGGCGGCCAAGGGTAGACCCTTCC
R31H (G92A)	80.38°C	F	CTGTTCCAGAGCGTGCACGAAGTGATCCAGAAC
		R	GTTCTGGATCACTTCGTGCACGCTCTGGAACAG
L57Q (T170A)	80.22°C	F	CAGTTTGCTGCTGCAGCAGCAGCAGCAGC
		R	GCTGCTGCTGCTGCTGCAGCAGCAAACTG
E81Q (G241C)	80.22°C	F	CAGCAGCAGCAGCAACAGACTAGCCCCAG
		R	CTGGGGCTAGTCTGTTGCTGCTGCTGCTG
E187Q (G559C)	78.81°C	F	AAGACATCCTGAGCCAGGCCAGCACCATG
		R	CATGGTGCTGGCCTGGCTCAGGATGTCTT
E304K (G910A)	79.27°C	F	GCGCAGGCAAGAGCACTAAAGATACTGCTGAGTAT
		R	ATACTCAGCAGTATCTTTAGTGCTCTTGCCTGCGC
S336P (T1006C)	78.38°C	F	GCAGCAGGGAGCCCCGGGACACTTG
		R	CAAGTGTCCCGGGGCTCCCTGCTGC
T338I (C1013T)	78.71°C	F	CAGGGAGCTCCGGGATACTTGAACTGCC
		R	GGCAGTTCAAGTATCCCGGAGCTCCCTG
S361N (G1082A)	80.27°C	F	GAGGCAGCTGCGTACCAGAATCGCGACTAC
		R	GTAGTCGCGATTCTGGTACGCAGCTGCCTC
R386G (C1156G)	78.50°C	F	CCCATCCCCACGCTGGCATCAAGCTG
		R	CAGCTTGATGCCAGCGTGGGGATGGG
G409R (G1225C)	78.25°C	F	GCGCAGTGCCGCTATCGGGACCTG
		R	CAGGTCCCGATAGCGGCACTGCGC
A430T (G1288A)	78.61°C	F	GTCACCCTCAGCCACCGCTTCCTCATC
		R	GATGAGGAAGCGGTGGCTGAGGGTGAC
Q445P (A1334C)	80.31°C	F	CAGCCGAAGAAGGCCCGTTGTATGGACCGTG
		R	CACGGTCCATACAACGGGCCTTCTTCGGCTG
Q488* (C1462T)	78.38°C	F	TACACTCGGCCCCCTTAGGGGCTGG
		R	CCAGCCCCTAAGGGGGCCGAGTGTA
G525A (G1574C)	80.38°C	F	GTCAAAAGCGAAATGGCCCCCTGGATGGATAGC
		R	GCTATCCATCCAGGGGGCCATTTCGCTTTTGAC
L561M (C1681A)	78.98°C	F	CCCCAGAAGACCTGCATGATCTGTGGAGATG
		R	CATCTCCACAGATCATGCAGGTCTTCTGGGG
A810V (C2429T)	78.45°C	F	GAATTCCTGTGCATGAAAGTACTGCTACTCTTCAGCATT
		R	AATGCTGAAGAGTAGCAGTACTTTCATGCACAGGAATTC
E830K (G2488A)	79.12°C	F	TGGATGGGCTGAAAAATCAAAAATTCTTTGATAAACTTCGAATGAACTAC
		R	GTAGTTCATTCGAAGTTTATCAAAGAATTTTTGATTTTTCAGCCCATCCA
R856C (C2566T)	79.06°C	F	CCACATCCTGCTCAAGATGCTTCTACCAGCTC
		R	GAGCTGGTAGAAGCATCTTGAGCAGGATGTGG
H875Y (C2623T)	79.39°C	F	CCTATTGCGAGAGAGCTGTATCAGTTCACTTTTGACC
		R	GGTCAAAAGTGAACTGATACAGCTCTCTCGCAATAGG

2.9 Reporter assays

2.9.1 Luciferase and β-galactosidase reporter assays

COS-1 cells were grown in 24-well plates to approximately 70% confluence in hormone-depleted media for 24 hours prior to transfection. Cells were transfected with 100 ng pSV-AR, 25 ng p-BOS-β-gal, 1 µg TAT-GRE-EIB-LUC (ARE luciferase reporter) using the Calcium Phosphate method (Chen and Okayama, 1987). 24 hours after transfection, cells were washed twice with pre-warmed PBS and then incubated for a further 24 hours in hormone-depleted media with the desired concentration of hormone/drug/vehicle. Cells were washed twice with ice cold PBS, lysed by adding 60 µL of 1x Reporter Lysis Buffer (Promega) and kept at -80 ^{o}C for storage before the analysis. Luciferase assays (Promega) were performed on 20 µL of defrosted lysate alongside the β-galactosidase assay (Applied Biosciences) on 5 µL of lysate for normalisation, following the manufacturer's guidelines. Luminescence was measured using a FLUOstar Omega Plate reader (BMG Labtech).

2.9.2 Dual-Glo Luciferase and Renilla reporter assays

COS-1 cells (1 x 10^4 cells/well) were seeded in 96-well plates in hormone-depleted media for 24 hours prior to transfection. For each well, 10 ng pSV-AR or pSG5-ERα, 10 ng renilla, 150 ng TAT-GRE-EIB-LUC (ARE-luciferase) or 3xERE-TATA-LUC (ERE-luciferase), and 0.51 µL FuGENE HD transfection reagent (Promega) were mixed in 4.5 µL Opti-MEM (Thermo Fisher) and incubated for 5 minutes prior to transfection. 24 hours after transfection, cells were treated with the desired concentration of hormone/drug/vehicle. 24 hours after treatment, the media in each well was removed leaving approximately 25 µL of media per well. Cells were lysed by the addition of 25 µL Dual-Glo Luciferase Assay Reagent (Promega) and incubated for 10 minutes with gentle shaking, then 40 µL of the mixture in each well was transferred into a 96-well microplate (Lumitrac, Greiner Bio-One), luminescence was measured using a FLUOstar Omega Plate reader (BMG Labtech). Next, 20 µL of Dual-Glo Stop & Glo Reagent (Promega) was added, incubated for a further 10

minutes with gentle shaking, and renilla luminescence was measured for normalisation using a FLUOstar Omega Plate reader (BMG Labtech).

2.10 Crystal violet proliferation assays

Cells were seeded (approximately 5 x 10^4 cells) in a 96-well plate with the relevant hormone-depleted culture media (Table 2-3), and after 24 hours, treated with the desired concentration of vehicle, hormone, or drug for different time periods (72, 120 and 168 hours). Cells were fixed with 100 µL of 2% PFA for an hour at RT, washed three times with ddH_2O and left 2 hours to air dry. Cells were subsequently stained using 100 µL of 0.04% crystal violet at RT. The plates were washed three times with ddH_2O and left 2 hours to air dry. Following the air drying, the plates were scanned. After visualisation, 100 µL of 10% acetic acid was added to all wells and the plates were gently rocked for 1 hour. Cell density in each well was quantified by measuring the resulting absorbance (λ = 595 nm) with a FLUOstar Omega plate reader (BMG Labtech).

2.11 Colony formation assays

Cells were seeded at a low confluency (approximately 2 x 10^4 cells) in 6 well plates in the relevant hormone-depleted media (Table 2-3). Cells were cultured in the presence of vehicle/ligand/drug, and the media and treatments changed every 72 hours, for 4 weeks. The wells were washed three times using PBS, fixed at RT with 1 ml of 2% PFA for an hour, washed a further three times with PBS and left overnight to air dry. Fixed cells were stained using 500 µL of 0.08% crystal violet at RT for one hour. Wells were washed three times with ddH_2O and following the air drying overnight, plates were photographed using a scanner. After visualisation, 100 µL of 10% acetic acid was added to all wells and the plates were gently rocked for 1 hour. Cell density in each well was quantified by measuring the resulting absorbance (λ = 595 nm) with a FLUOstar Omega plate reader (BMG Labtech).

2.12 Protein analysis

2.12.1 Cell Lysis

Cells were washed twice with ice cold PBS, detached by scraping with fresh PBS and centrifuged at 13,000 rpm for 1 minute at 4 ^{o}C. After that the supernatant was discarded and the cell pellet was frozen and kept at -80 ^{o}C. When required, cell pellets were resuspended in radioimmunoprecipitation (RIPA) buffer with protease inhibitor cocktail (PIC) (Melford) added. Lysates were sonicated for 3 cycles on high of 30 seconds on and 30 seconds off using a Biorupter Plus (Diagenode). The lysates were then centrifuged at 13,000 rpm for 10 minutes at 4 ^{o}C and the supernatant was transferred to a pre-chilled 1.5 ml tube.

2.12.2 DC Protein Assay

The protein concentration was measured with the Detergent Compatible (DC) protein assay (Bio-Rad), using 5 µL of sample against standard concentrations of BSA as a reference protein, following the manufacturer's guideline. Protein concentrations were measured (at absorbance λ = 750 nm) using a FLUOstar Omega Plate Reader (BMG Labtech). Samples were diluted to an equal volume of protein per set (10–20 µg per 12 µL of sample) with 4 x Laemmli protein sample buffer (Bio-Rad).

2.12.3 SDS-Page

Cell lysates were vortexed and incubated at 95 ^{o}C for 5 minutes and following this, the tubes were immediately placed on ice for at least 10 minutes to cool. After cooling period, tubes were briefly vortexed and 16 µL of lysate was loaded per well of a 10% polyacrylamide gel, against 4 µL of the Page Ruler Pre-stained Protein Ladder (Thermo Fisher). Sodium dodecyl sulphate polyacrylamide gel electrophoresis (SDS-PAGE) was conducted at 130 V for 2.5 hours with pre-made running buffer.

2.12.4 Immunoblotting

Proteins were transferred onto a polyvinylidene difluoride (PVDF) membrane (Immobilion P, Millipore Inc., hydrated using 100% Methanol, MeOH) via semi-dry transfer. The transfer was performed at 15 V and 100 mA for 2 hours, using a semi-dry electroblotting apparatus (Bio-Rad) and pre-made transfer buffer. Following this, the membranes were incubated with blocking buffer for 1 hour at RT with gentle shaking. Next, the membranes were probed with the desired primary (1^{o}) antibody (Table 2-11) overnight, diluted in blocking buffer, at 4 ^{o}C with gentle rocking. The membranes were washed 3 times with PBS-T for 5 minutes with gentle shaking before the incubation with the appropriate secondary (2^{o}) antibody (Table 2-11) for 1 hour at RT with gentle rocking. The membranes were then washed for a further 3 times with PBS-T for 5 minutes with gentle shaking. Next, an additional wash with PBS was conducted for 5 minutes with gentle rocking. After that, the membranes were visualised via chemiluminescence using Luminata TM Forte (Millipore) with the Fusion FX imager (Vilber Lourmat).

Table 2-11 Antibodies used in this study

Antibody	**Company**	**Lot number**	**Dilution**
AR rabbit IgG (ab108341)	abcam	GR3233428-1	1:2,000
ERα rabbit IgG (HC20)	Santa Cruz	Sc-543	1:2,000
α–Tubulin mouse IgG (T5168)	Sigma	039M4769V	1:10,000
2^{o} rabbit IgG (A6154)	Sigma	SLBK2462V	1:2,000
2^{o} mouse IgG (A90-116-P)	Bethyl	A90-116P-42	1:10,000

2.13 Transient Transfection of Mammalian Cells

2.13.1 Calcium phosphate

The calcium phosphate method was performed as described in (Chen and Okayama, 1987). Per well, the desired concentration of DNA was diluted to 45 µL using ddH_2O. Following this, 5 µL of 2.5 M $CaCl_2$ and 50 µL of BBS were added and then gently mixed by bubbling with a Gilson pipette. Master mixes were used to ensure consistency between wells. The transfection mixture was gently mixed and incubated at RT for 15 minutes before being added to each well of a 24-well plate in a drop-wise manner.

2.13.2 FuGENE HD transfection of cells for fluorescent microscopy

Cells were seeded at a low confluency (approximately 2 x 10^4 cells/well in 24-well plates) on coverslips in the relevant hormone-depleted media, and incubated for 24 hours. Subsequently, cells were transfected using FuGENE HD transfection reagent (Promega) according to the standard protocol. After 24 hours, the media was changed, and cells were incubated in the hormone-depleted media for a further 24 hours. Next, cells were treated with the required hormones for 2 hours and fixed with 4% Paraformaldehyde (PFA) for 10 minutes, then washed three times with PBS. Coverslips were fixed onto microscope slides using Vectashield mountant (Vector Laboratories) and Fixogum rubber cement (Marabu). Slides were visualised using confocal microscopy.

2.14 Wound Healing Assays

Cells were seeded at 85-90% confluency (approximately 1.2 x 10^6 cells) in 6-well plates in the relevant hormone-depleted media (Table 2-3). After 48 hours, the surface of the wells was scraped with a p200 pipette tip and a cell-free space was created (0-hour). After scraping, the media was removed and washed twice with PBS to dispose of any cell debris, then fresh media containing the relevant treatments were added. The scratched area was photographed under a microscope at 0-, 24- and 48-hour time

points and the images were processed using ImageJ (version 1.53) to measure the change in wound areas.

2.15 Freezing and Defrosting Cells

To freeze, cells were split as normal and resuspended in 10 ml of media and transferred into a 15 ml falcon tube and spun at 1,500 rpm for 3 minutes. The supernatant was discarded, and the cells were resuspended in freezing media (10% DMSO, 90% FCS). The mixture was transferred into cryotubes as 1 ml per tube. The tubes were covered with insulating material and kept at -80 ^{o}C for short term storage. For longer term storage the tubes were transferred to liquid nitrogen.

To defrost, stocks were defrosted at 37 ^{o}C and cells immediately transferred into a 15 ml falcon tube with 5 ml of pre-warmed media. The cell suspension was spun at 1,500 rpm for 3 minutes. The supernatant was removed, and the cells resuspended in 5 ml of fresh media before being transferred into a flask for culture conditions. The media was changed after 24 hours.

2.16 RNA preparation for sequencing analysis

2.16.1 RNA Preparation

Total RNA was extracted from cells treated with different ligands using the Monarch Total RNA Miniprep Kit (T2010S). Subsequently, cDNA was synthesised, and qPCR was performed as described in Section 2.4.2 and 2.4.4 to validate the effects of these treatments on gene expression levels in T47D and MCF7 cells.

2.16.2 Quality Assessment of RNA

The quality of RNA was checked by running samples on a 1% agarose TBE RNA gel (Table 2-2). Samples were diluted 1:1 with 2X RNA loading dye (Thermo Fisher) and were separated using gel electrophoresis at 100 V for 45 minutes. Each sample was quantified by Qubit RNA IQ assay (Thermo Fisher) and the RNA integrity numbers (RIN) were recorded.

2.17 Analysis of RNA-Seq

RNA-Seq was performed by Novogene and raw data files were downloaded to the University of Essex High Performance Cluster (http://hpc.essex.ac.uk). The quality of the reads was checked using fastQC (version 0.11.7), and adaptors were trimmed using cutadapt (version 1.18). For total RNA-Seq samples, reads were aligned to the human genome (GRCh38) using the STAR (version 2.7.3a) alignment tool. For microRNA analysis, after removal of the adapters, reads were aligned to a hairpin annotation file of human microRNAs, obtained from miRbase (https://www.mirbase.org, database release 22.1, October 2018), using bowtie2 (version 2.3.4.1). Read counts per sample were downloaded into R (version 4.0.3) and differential gene expression analyses were performed using the DeSeq2 (version 1.28.1) package.

2.18 Statistical Analysis

Unless otherwise stated, three independent biological repeats were performed for every experiment. All values were written as mean value ± SE. ANOVA tests were performed to determine the significant differences in values, using GraphPad Prism Software (version 9). P values were adjusted for multiple testing and values less than 0.05 were considered to be significant.

Chapter 3
AR and ERα crosstalk

AR-ERα crosstalk

3.1 Introduction

The AR is expressed in almost all BrCa subtypes, and it was thought that it plays an important role in pathological pathways that drive BrCa development and outcome (Rahim and O'Regan, 2017; Rangel et al., 2018). Several studies have shown that there is a strong association between ERα and AR expression in BrCa (Castellano et al., 2010; Park et al., 2011; Rangel et al., 2018; Vidula et al., 2019). It has been shown that AR expression in early BrCa is associated with better disease-free survival and overall survival in hormone receptor positive and negative tumours (Vera-Badillo et al., 2014). It has also been shown that the risk of relapse and cancer-associated deaths is higher in hormone sensitive BrCa patients that have low AR expression (Peters et al., 2009). Therefore, it can be postulated that ERα and AR could regulate each other's activity. Because of the emerging evidence of AR expression in BrCa, AR-targeted therapies used for the treatment of PrCa have been tested on BrCa patients in clinical trials (Gucalp et al., 2013; Pietri et al., 2016). However, our knowledge of the crosstalk between AR and ERα is limited and the role of androgen signalling pathway in BrCa has not been fully characterised.

The aim of this chapter is to further our understanding of AR-ERα crosstalk and to characterise the effects of endocrine therapies and AR-targeted drugs on this crosstalk, using endocrine sensitive BrCa cells.

3.2 The crosstalk between AR and ERα in endocrine sensitive breast cancer cells

3.2.1 The regulation of AR and ERα target genes differs in response to varying oestrogen and androgen concentrations

The circulating hormone levels of androgen and oestrogen, and the balance of these steroids changes throughout life, mainly depending on the menstrual cycle and menopausal status (Secreto et al., 2019). Conditions such as early menarche, nulliparity, late menopause, and obesity which lead the body to be exposed to longer and higher levels of oestrogen, are known to be risk factors (Adly et al., 2006; Kotsopoulos and Narod, 2012). Therefore, it was shown that people with higher endogenous circulating oestrogen serum levels are predisposed to BrCa; however, the link between the levels of circulating androgens and BrCa risk are not known or are yet to be elucidated.

To investigate the effect of different concentrations of androgen and different concentrations of oestrogen upon target gene expression in endocrine sensitive BrCa cells, gene expression analysis (qPCR) was performed on different AR and ERα target genes, using MIB (Mibolerone) and E2 at varying concentrations. MIB was chosen for this study because it is a potent anabolic androgenic steroid that cannot be metabolised further to oestrogen. MCF7 and T47D cells were starved of hormones for 72 hours before being exposed to MIB or E2 (1, 10, 100 nM) for 8 hours and 24 hours. QPCR was performed to assess the changes in the expression of AR target genes: *C1orf116* (*Chromosome 1 open reading frame 116*), *PSCA* (*Prostate Stem Cell Antigen*), *ZBTB16* (*Zinc Finger And BTB Domain Containing 16*); and in ERα target genes: *CXCL12* (*C-X-C Motif Chemokine Ligand 12*), *MYB* (*MYB Proto-Oncogene, Transcription Factor*), *KCNK5* (*Potassium Two Pore Domain channel subfamily K Member 5*). The target genes were selected through the analysis of a microarray-based gene expression dataset which investigated the effects of E2 (10 nM) and DHT (10 nM) treatment in T47D cells (GEO accession number: GSE62243). Their role in cancer is summarised in Table 3-1. Primers for gene expression analysis were designed using Primer Bank (https://pga.mgh.harvard.edu/primerbank/). Primers that were approximately 20 bp length, an amplicon size or approximately 100 bp, and preferably spinning intron boundaries were chosen.

Table 3-1 The AR and ERα target genes, and associated roles in cancer, selected for study using qPCR

Gene	Role
CXCL12	• Upregulation enhances invasiveness of the BrCa tumour (Boimel et al., 2012) • Promotes tumour growth and metastasis in BrCa (Zhao et al., 2014) • Overexpressed in metastasis sites, correlated with poor overall survival in BrCa (Wu et al., 2015) • Possible tumour marker in BrCa patients (Dąbrowska et al., 2020)
KCNK5	• ERα regulated, associated with proliferation in hormone receptor positive BrCa (Alvarez-Baron et al., 2011) • Upregulated in oesophageal, breast and lung cancers (Dookeran and Auer, 2017) • Upregulation is associated with poor outcome in basal-like BrCa subtype (Clarke et al., 2013)
MYB	• Upregulated by ERα, involved in BrCa metastasis and progression, associated with cell cycle regulators (Drabsch et al., 2007; Cicirò and Sala, 2021)
C1orf116	• Under-expression is associated with poor prognosis in lung and prostate cancer patients, increased in higher grades of BrCa (Parsana et al., 2017)
PSCA	• Upregulated in BrCa tumours, correlates with HER2 overexpression (Link et al., 2017) • Upregulated in PrCa (Zhigang and Wenlv, 2004)
ZBTB16	• Upregulated by AR in molecular apocrine BrCa (Robinson et al., 2011) • Possible tumour suppressor, overexpression inhibits BrCa cell proliferation (He et al., 2020)

CXCL12 expression was significantly increased by E2 treatment in response to all of the concentrations tested and at both time points in T47D (Figure 3-1A, B). *MYB* expression was also significantly upregulated by ERα, with the exception of 100 nM E2 at 24 hours in T47D (Figure 3-1C, D). The expression of *KCNK5*, another ERα target, was upregulated significantly by E2 in T47D at both time points studied (Figure 3-1E, F).

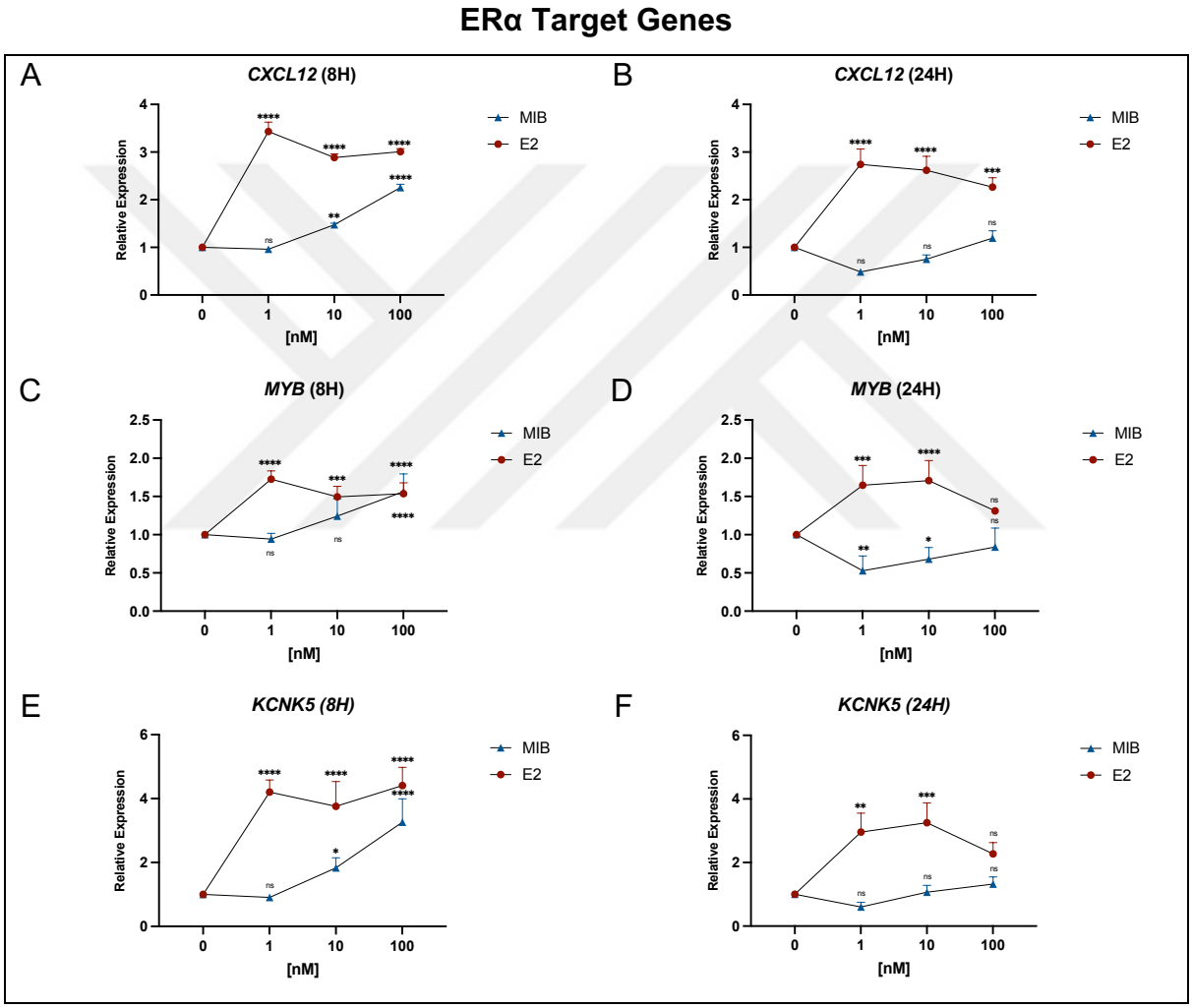

Figure 3-1 The responsiveness of ERα target genes in response to varying androgen and oestrogen concentrations in T47D cells

*T47D cells were incubated in hormone-depleted media for 72 hours, treated with varying concentrations of E2 or MIB (0, 1, 10, 100 nM) for 8 or 24 hours. RNA was harvested, reverse transcribed into cDNA, and qPCR was performed using SYBR green to measure the expression level of ERα target genes (A, B) CXCL12, (C, D) MYB, (E, F) KCNK5. Expression was normalised to RPL19 and changes in expression calculated using $2^{-\Delta\Delta Ct}$. Expression was made relative to control. Graphs are the average of 3 individual replicates, and generated with GraphPad Prism 9 software. ANOVA. ns = not significant, *p ≤ 0.05, **p ≤ 0.01, ***p ≤ 0.001, ****p ≤ 0.0001. Mean ± 1SE.*

The increase in *C1orf116* (AR target gene) expression was found to be dramatic in T47D cells, and as expected exposure to oestrogen did not affect its expression (Figure 3-2A, B). The induction of *PSCA* was found to be well regulated by androgen in T47D, and E2 treatment significantly inhibited the expression of *PSCA* regardless of the concentration and exposure time in T47D (Figure 3-2C, D). It was found that high androgen concentrations were needed for *ZBTB16* to be significantly regulated in T47D (Figure 3-2E, F).

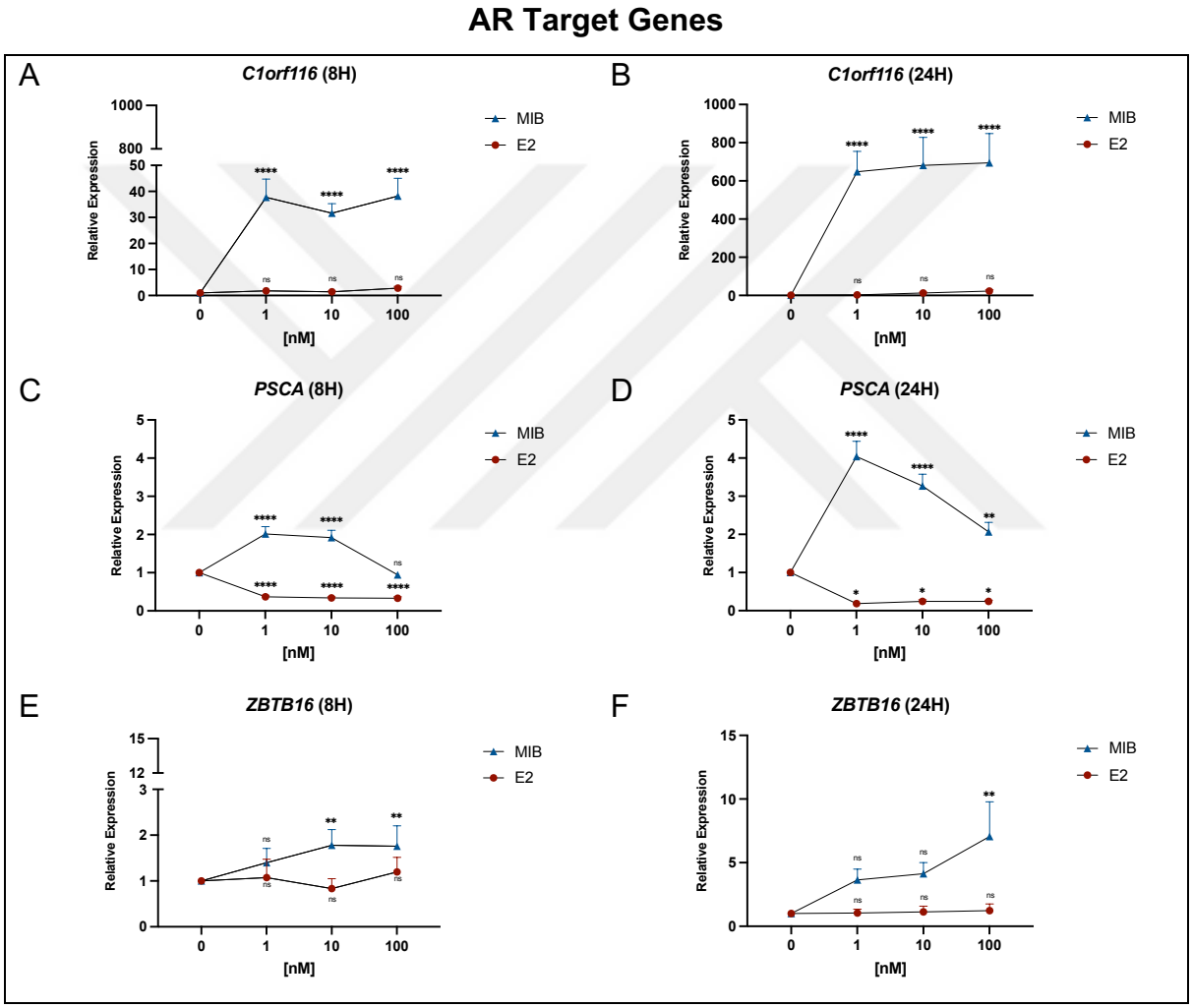

Figure 3-2 The responsiveness of AR target genes in response to varying androgen and oestrogen concentrations in T47D cells

*T47D cells were incubated in hormone-depleted media for 72 hours, treated with varying concentrations of E2 or MIB (0, 1, 10, 100 nM) for 8 or 24 hours. RNA was harvested, reverse transcribed into cDNA, and qPCR was performed using SYBR green to measure the expression level of AR target genes (A, B) C1orf116, (C, D) PSCA, (E, F) ZBTB16. Expression was normalised to RPL19 and changes in expression calculated using $2^{-\Delta\Delta Ct}$. Expression was made relative to control. Graphs are the average of 3 individual replicates, and generated with GraphPad Prism 9 software. ANOVA. ns = not significant, * p ≤ 0.05, **p ≤ 0.01, ***p ≤ 0.001, ****p ≤ 0.0001. Mean ± 1SE.*

The expression of *CXCL12* in MCF7 in response to E2, was found to have a similar trend as it had in T47D (Figure 3-3A, B). *CXCL12* expression was significantly increased by E2 treatment in response to all of the concentrations tested at both time points in MCF7. *MYB* expression was also significantly upregulated in response to E2, with the exceptions of 1 nM E2 (8 hours, Figure 3-3C), and 10 nM E2 (24 hours, Figure 3-3D). The expression of *KCNK5* differed in MCF7 as compared to T47D in response to treatment with E2 for 24 hours. Higher E2 concentrations were needed for a significant increase in expression (Figure 3-3E), whereas no regulation in response to E2 was evident at the 24 hour timepoint (Figure 3-3F).

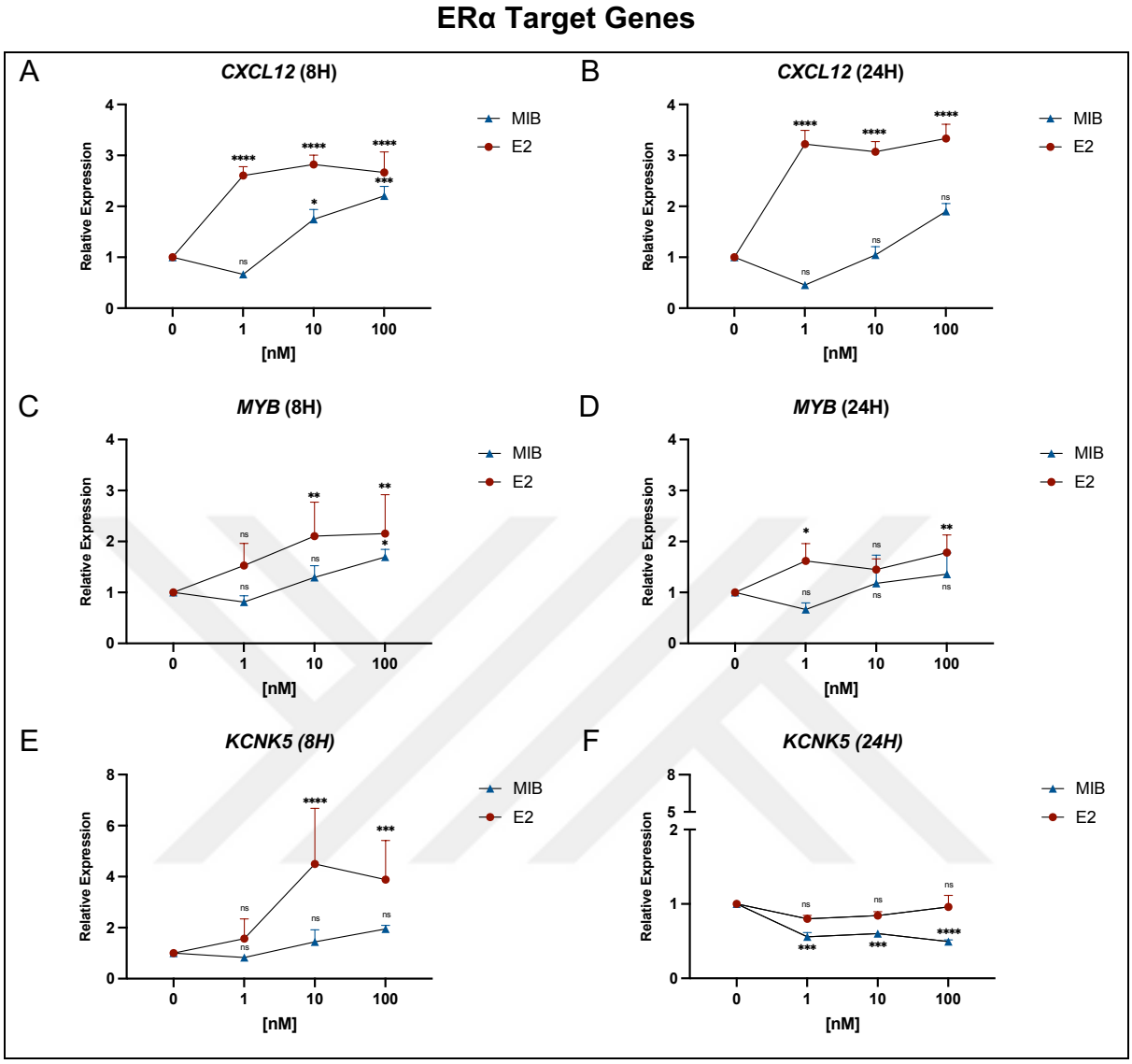

Figure 3-3 The responsiveness of ERα target genes in response to varying androgen and oestrogen concentrations in MCF7 cells

*MCF7 cells were incubated in hormone-depleted media for 72 hours, treated with varying concentrations of E2 or MIB (0, 1, 10, 100 nM) for 8 or 24 hours. RNA was harvested, reverse transcribed into cDNA, and qPCR was performed using SYBR green to measure the expression level of ERα target genes (A, B) CXCL12, (C, D) MYB, (E, F) KCNK5. Expression was normalised to RPL19 and changes in expression calculated using $2^{-\Delta\Delta Ct}$. Expression was made relative to control. Graphs are the average of 3 individual replicates, and generated with GraphPad Prism 9 software. ANOVA. ns = not significant, *p ≤ 0.05, **p ≤ 0.01, ***p ≤ 0.001, ****p ≤ 0.0001. Mean ± 1SE.*

C1orf116 expression was less dramatic in MCF7 in response to MIB as compared to T47D (Figure 3-4A, B). *PSCA* was also less well-regulated in MCF7 as compared to T47D, and longer exposure of E2 was needed for the inhibition of the gene expression to be seen (Figure 3-4C, D). *ZBTB16* was significantly upregulated by MIB regardless of androgen concentration in MCF7 cells (Figure 3-4E, F), whereas higher androgen concentrations were needed for it to be significantly regulated in T47D.

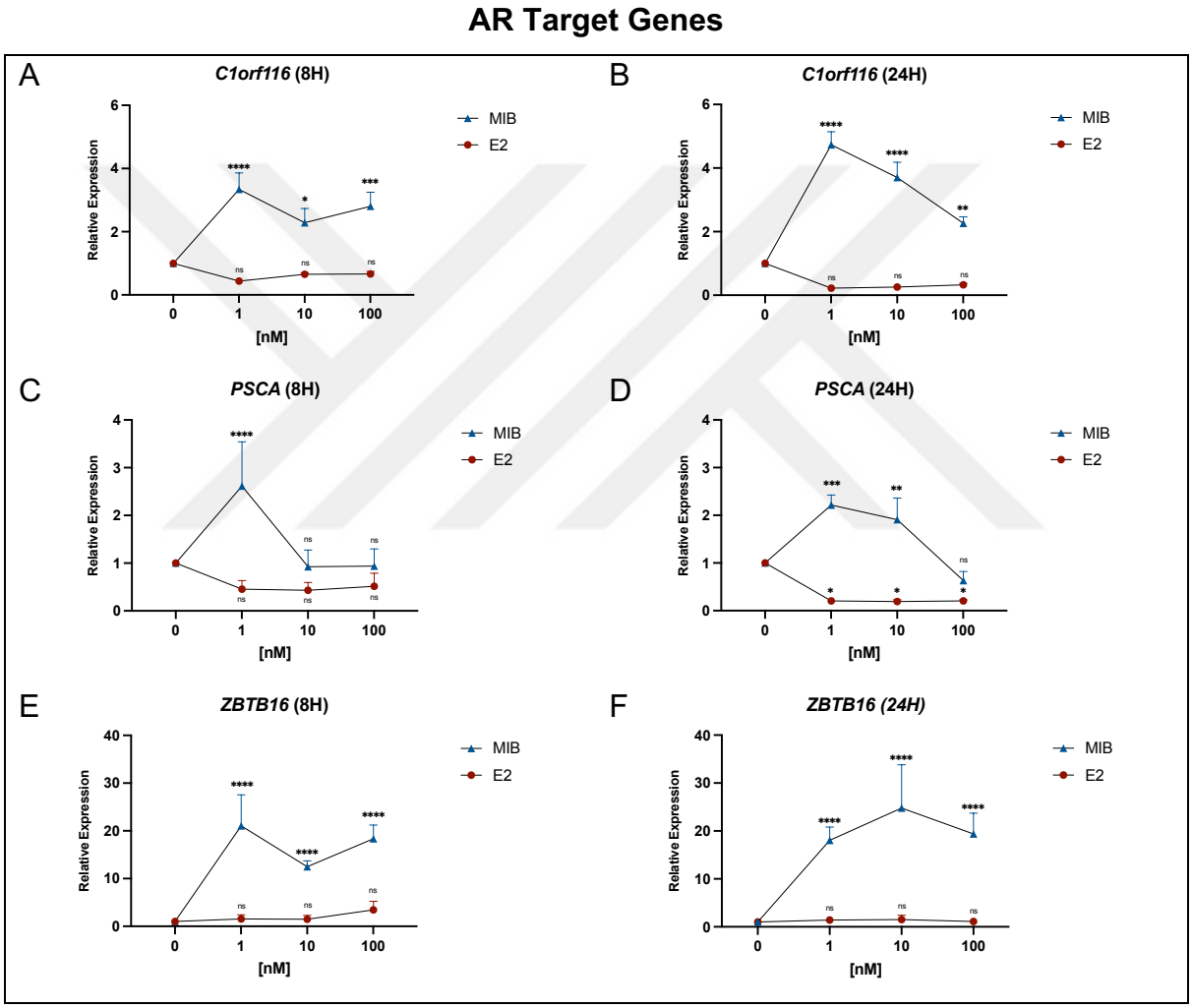

Figure 3-4 The responsiveness of AR target genes in response to varying androgen and oestrogen concentrations in MCF7 cells

*MCF7 cells were incubated in hormone-depleted media for 72 hours, treated with varying concentrations of E2 or MIB (0, 1, 10, 100 nM) for 8 or 24 hours. RNA was harvested, reverse transcribed into cDNA, and qPCR was performed using SYBR green to measure the expression level of ERα target genes (A, B) C1orf116, (C, D) PSCA, (E, F) ZBTB16. Expression was normalised to RPL19 and changes in expression calculated using $2^{-\Delta\Delta Ct}$. Expression was made relative to control. Graphs are the average of 3 individual replicates, and generated with GraphPad Prism 9 software. ANOVA. ns = not significant, * p ≤ 0.05, **p ≤ 0.01, ***p ≤ 0.001, ****p ≤ 0.0001. Mean ± 1SE.*

Surprisingly, even though *CXCL12* is an ERα regulated gene, higher androgen concentrations also induced its expression, although this was not found to be significant at 24 hours of treatment. Furthermore, androgen was able to weakly enhance the expression of *MYB* at 8 hours, and *KCNK5* expression was induced by MIB at high concentrations in T47D. Additionally, AR seemed to have an inhibitory effect on *MYB* in T47D cells at 1 and 10 nM at the 24-hour timepoint. This significant inhibitory effect of AR was also found for *KCNK5* in MCF7 at all concentrations of androgen tested at the 24-hour timepoint. Table 3-2 summarises the findings of gene expression analyses. These findings suggest that higher circulating androgen levels might initiate the transcription of some ERα regulated genes in BrCa, thus mimicking the oestrogen signalling program. However, at longer time points, the AR may switch to negatively regulate some of the genes.

Table 3-2 Summary of gene expression analysis of AR and ERα targets in response to different treatments

↑: increased expression, ↓: decreased expression, -: no effect.

Cell line	Genes	Time	MIB			E2		
			1nM	10nM	100nM	1nM	10nM	100nM
T47D	*CXCL12*	8h	-	↑	↑	↑	↑	↑
		24h	-	-	-	↑	↑	↑
	MYB	8h	-	-	↑	↑	↑	↑
		24h	↓	↓	-	↑	↑	-
	KCNK5	8h	-	↑	↑	↑	↑	↑
		24h	-	-	-	↑	↑	-
MCF7	*CXCL12*	8h	-	↑	↑	↑	↑	↑
		24h	-	-	-	↑	↑	↑
	MYB	8h	-	-	↑	-	↑	↑
		24h	-	-	-	↑	-	↑
	KCNK5	8h	-	-	-	-	↑	↑
		24h	↓	↓	↓	-	-	-
T47D	*C1orf116*	8h	↑	↑	↑	-	-	-
		24h	↑	↑	↑	-	-	-
	PSCA	8h	↑	↑	-	↓	↓	↓
		24h	↑	↑	↑	↓	↓	↓
	ZBTB16	8h	-	↑	↑	-	-	-
		24h	-	-	↑	-	-	-
MCF7	*C1orf116*	8h	↑	↑	↑	-	-	-
		24h	↑	↑	↑	-	-	-
	PSCA	8h	↑	-	-	-	-	-
		24h	↑	↑	-	↓	↓	↓
	ZBTB16	8h	↑	↑	↑	-	-	-
		24h	↑	↑	↑	-	-	-

It appears that concentrations and exposure times of hormones have different effects on target gene expression, which could mean that fluctuations in circulating hormone levels could modulate the effects of AR and ERα on the transcriptome. Both AR and ERα regulate specific genes, but there seems to be an overlap in the regulation of these target genes. Interestingly, the AR also upregulates a number of ERα target genes, whereas ERα appears to inhibit the expression of a number of AR target genes.

3.2.2 AR and ERα crosstalk is inhibitory to target gene expression

When cells were exposed to the individual hormones, AR and ERα regulated target gene expression. However, in physiological conditions both receptors' ligands are present, thus both receptors are active at the same time. To investigate the effect of receptor crosstalk on gene expression, qPCR was performed on the same AR and ERα target genes, co-treating cells with their ligands simultaneously. Endocrine sensitive MCF7 and T47D cells were incubated in hormone-depleted media for 72 hours before cells were co-treated with MIB (1 nM) and E2 (1 nM) for 24 hours.

AR significantly inhibited the majority of E2-induced genes (Figure 3-5A, B, C, Figure 3-6A, C), with the exception of *MYB* in MCF7 (Figure 3-6B). Similarly, ERα inhibited 2 of the AR regulated genes significantly, *C1orf116* and *PSCA* in T47D and MCF7 (Figure 3-5D, E, Figure 3-6D, E). The expression of *ZBTB16* was also reduced by 27.2%, and by 31.1%, in T47D and MCF7, respectively (Figure 3-5F, Figure 3-6F); however, this was not found to be statistically significant. The gene expression results demonstrated that the AR-ERα crosstalk is inhibitory in endocrine sensitive BrCa.

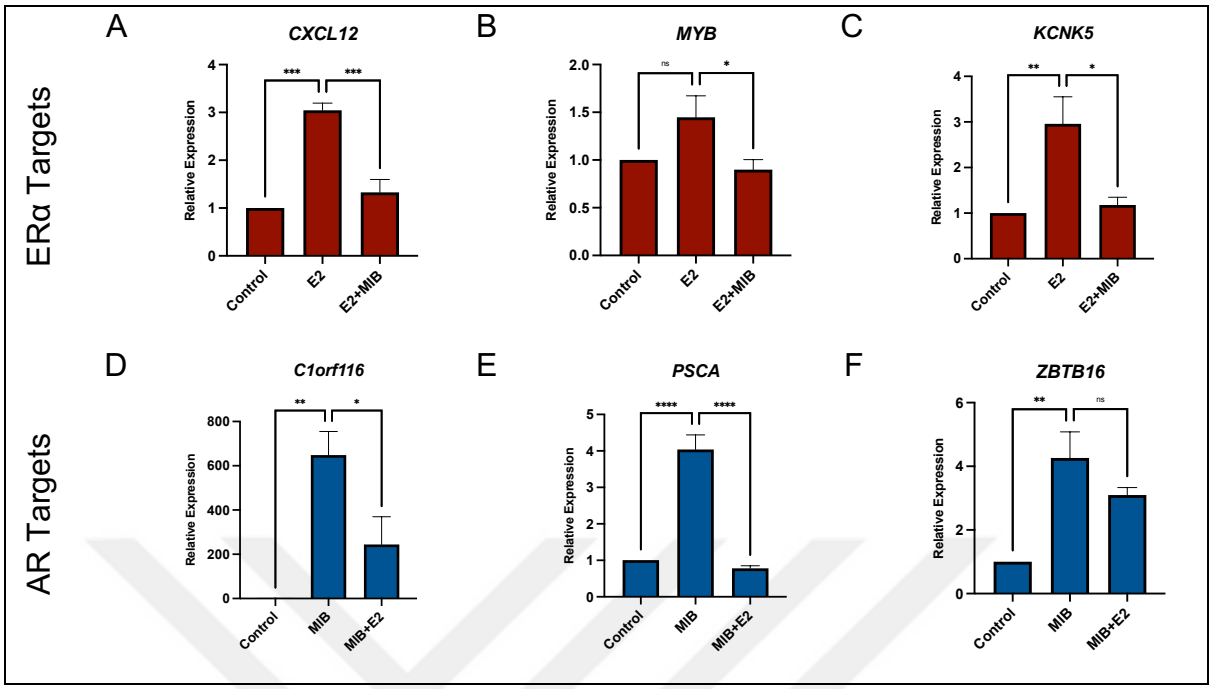

Figure 3-5 Co-treatment with androgen and oestrogen is inhibitory on ERα/AR target gene expression in T47D cells

*T47D cells were incubated in hormone-depleted media for 72 hours, treated with vehicle control (EtOH), or E2 (1 nM) with or without MIB (1 nM) for 24 hours. RNA was harvested, reverse transcribed into cDNA, and qPCR was performed using SYBR green to measure the expression level of ERα target genes (A) CXCL12, (B) MYB, (C) KCNK5; AR target genes (D) C1orf116, (E) PSCA, (F) ZBTB16. Expression was normalised to RPL19 and changes in expression calculated using $2^{-\Delta\Delta Ct}$. Expression was made relative to control. Graphs are the average of 3 individual replicates, and generated with GraphPad Prism 9 software. ANOVA. ns = not significant, * p ≤ 0.05, **p ≤ 0.01, ***p ≤ 0.001, ****p ≤ 0.0001. Mean ± 1SE.*

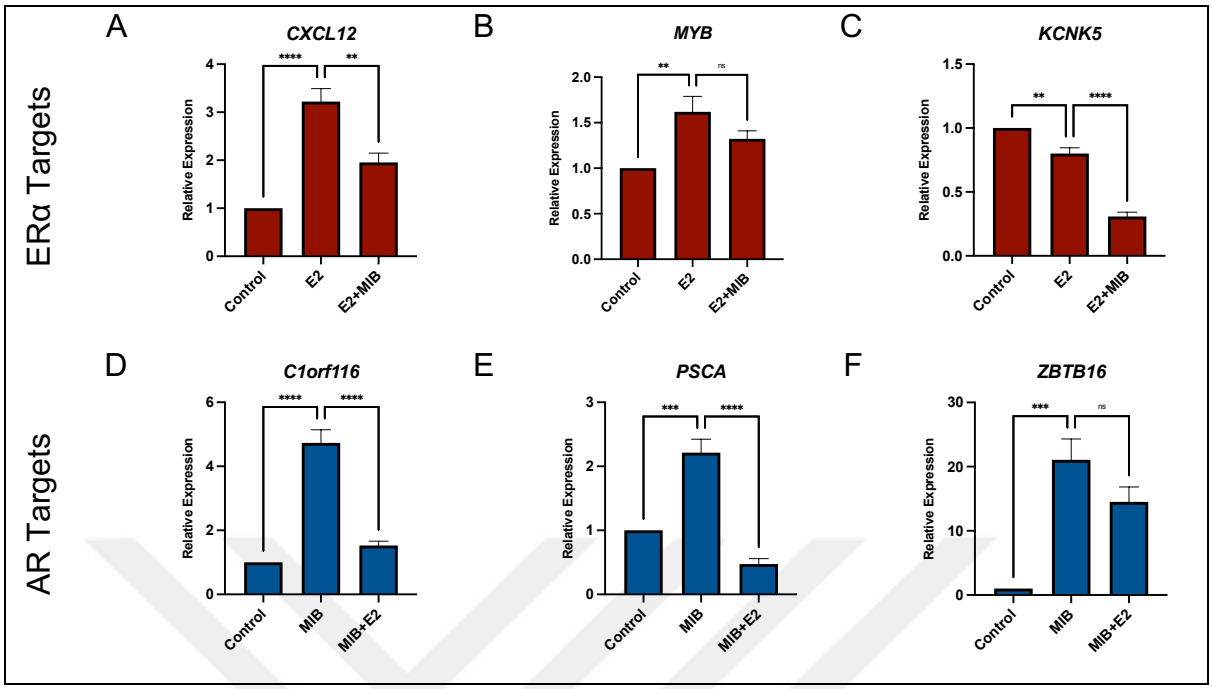

Figure 3-6 Co-treatment with androgen and oestrogen is inhibitory on ERα/AR target gene expression in MCF7 cells

MCF7 cells were incubated in hormone-depleted media for 72 hours, treated with vehicle control (EtOH), or E2 (1 nM) with or without MIB (1 nM) for 24 hours. RNA was harvested, reverse transcribed into cDNA, and qPCR was performed using SYBR green to measure the expression level of ERα target genes (A) CXCL12, (B) MYB, (C) KCNK5; AR target genes (D) C1orf116, (E) PSCA, (F) ZBTB16. Expression was normalised to RPL19 and changes in expression calculated using $2^{-\Delta\Delta Ct}$*. Expression was made relative to control. Graphs are the average of 3 individual replicates, and generated with GraphPad Prism 9 software. ANOVA. ns = not significant, * p ≤ 0.05, **p ≤ 0.01, ***p ≤ 0.001, ****p ≤ 0.0001. Mean ± 1SE.*

3.2.3 The effect of AR/ERα ratio on the transcriptional activity of AR

A retrospective study that was performed on 402 ERα-positive BrCa tumours, demonstrated that tumours that had an AR/ERα ratio equal or greater than 2, were larger in size, had higher histological grade, and had more lymph node metastases as compared to the cases with a AR/ERα ratio that was less than 2 (Rangel et al., 2018). To investigate the effects of different ratios of AR and ERα upon AR transcriptional activity, reporter assays were performed. COS-1 cells, negative for AR and ERα, were seeded in hormone-depleted media and transfected with different amounts of AR and ERα expression plasmids, along with an ARE reporter.

The results demonstrated that AR activity was significantly increased following MIB and E2 treatment (Figure 3-7). The lowest amount of pSG5-ERα (1 ng) was able to inhibit AR activity at 5 and 20 ng (Figure 3-7A, C), but not at 10 ng (Figure 3-7B). Transfections with 5 and 10 ng of pSG5-ERα were also found to significantly reduce AR transcriptional activity at all amounts tested. Interestingly, the highest pSG5-ERα amount (20 ng) only partially reduced AR activity at 10 ng, which was not significant. These results show that ERα inhibits AR activity, even at low levels of expression. However, because of the nature of reporter assays there are some limitations to these findings. For example, a different reporter to measure AR's transcriptional activity might show more or less dramatic inhibition as compared to the reporter used in this experiment. The volumes of the plasmids, transfection efficiency, and background are other important components of this assay that also affect the results.

To ensure that the ARE activity is only activated by AR, cells were transfected with an ARE reporter along with either AR, ERα, or empty vector (EV), and treated with control, MIB, or E2 separately. It was shown that the ARE reporter is only activated by AR, and not by ERα or EV (Figure 3-8), demonstrating the specificity of the reporter.

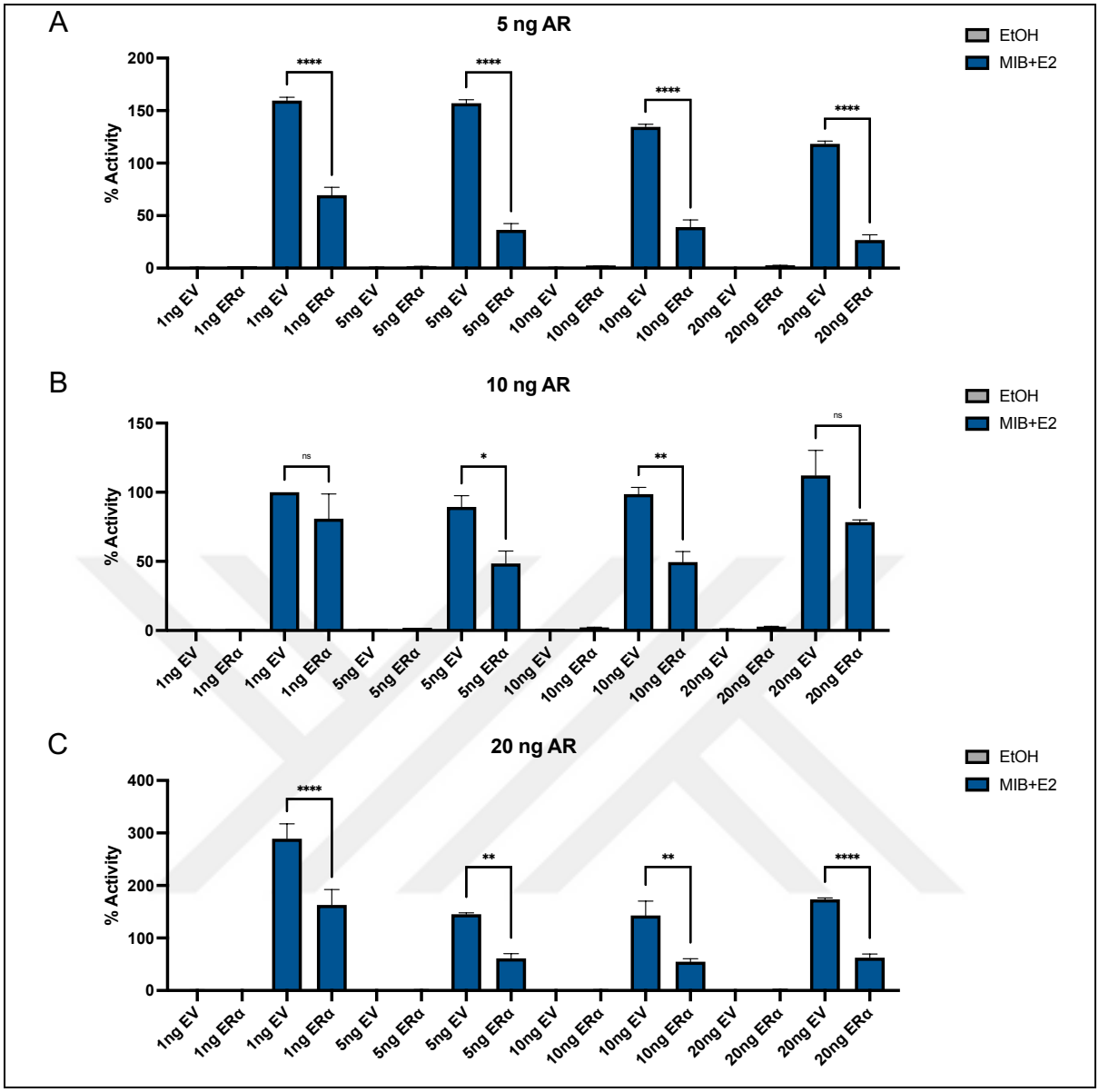

Figure 3-7 The AR's transcriptional activity is inhibited by different ERα levels

*COS-1 cells were seeded in 96-well plates in hormone-depleted media, incubated for 24 hours, and transfected with ARE luciferase reporter (TAT-GRE-EIB-LUC), renilla expression plasmid, and pSV-AR expression plasmid in varying amounts (5 ng, 10 ng, 20 ng), along with either an empty vector (EV), or an expression plasmid for ERα (pSG5-ERα) in different amounts (1 ng, 5 ng, 10 ng, 20 ng). Cells were incubated in hormone-depleted media for another 24 hours prior to treatment. Cells were treated with EtOH (ethanol), or Mibolerone (MIB, 1 nM) and Oestradiol (E2, 1 nM) for 24 hours. Luciferase activity was normalised to renilla activity and results were made relative to 10 ng AR activity in the presence of MIB+E2 treatment. Graphs are the average of 3 individual experiments, each with triplicate repeats and generated with GraphPad Prism 9 software. ANOVA. ns = not significant , * p ≤ 0.05, **p ≤ 0.01, ****p ≤ 0.0001. Mean ± 1SE.*

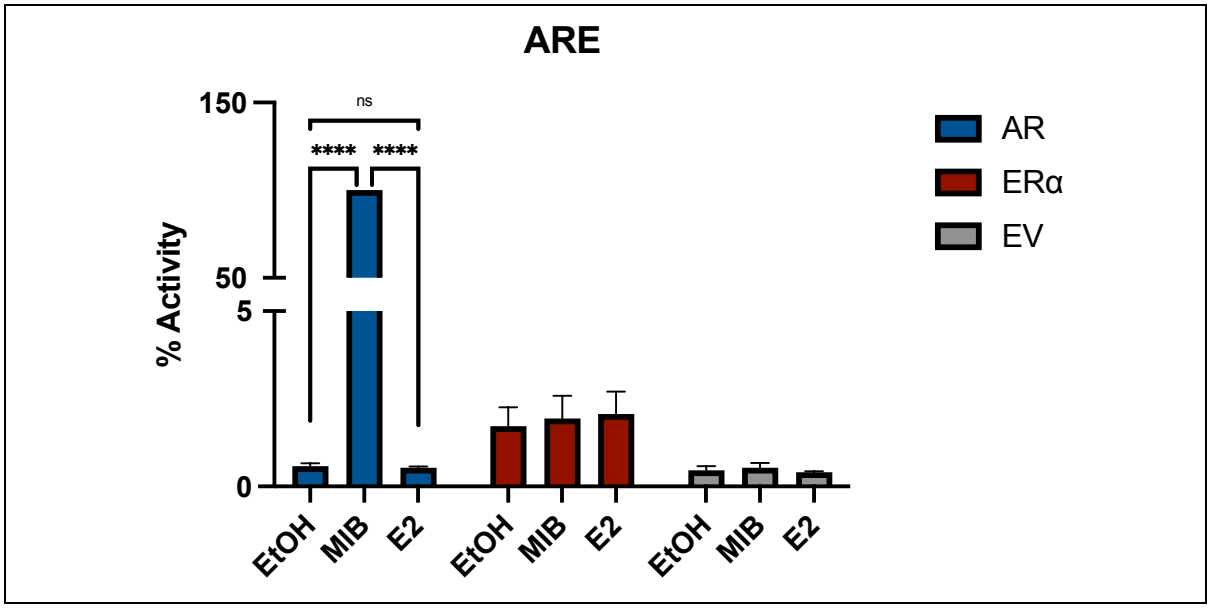

Figure 3-8 The ARE is only activated by AR in the presence of its ligand

*COS-1 cells were seeded in 96-well plates in hormone-depleted media, incubated for 24 hours, and transfected with ARE luciferase reporter (TAT-GRE-EIB-LUC), renilla expression plasmid, along with one of the plasmids: AR (pSV-AR), empty vector (EV), or ERα (pSG5-ERα). Cells were incubated in hormone-depleted media for another 24 hours prior to treatment. Cells were treated with EtOH (ethanol), MIB (1 nM) or E2 (1 nM) for 24 hours. Luciferase activity was normalised to renilla activity and results were made relative to AR activity in the presence of MIB treatment. The graph is the average of 3 individual experiments, each with triplicate repeats and generated with GraphPad Prism 9 software. ANOVA. ns = not significant, ****p ≤ 0.0001. Mean ± 1SE.*

3.3 The effect of antioestrogen treatment on the crosstalk between AR and ERα in endocrine sensitive cells

3.3.1 The effect of antioestrogen treatment on AR and ERα regulated genes

It appears that ERα inhibits the transcriptional activity of AR. To investigate how this crosstalk is affected upon antioestrogen treatment, qPCR was performed in MCF7 and T47D cells. In addition to genes that were checked in Section 3.2, a further AR target gene *NDRG1* (*N-Myc Downstream Regulated Gene 1*), which has been found to negatively correlate with metastasis in BrCa (Bandyopadhyay et al., 2004) was investigated. Similarly, an additional ERα-regulated gene, *TFF1* (*Trefoil Factor 1*), that was shown to be involved in chemoresistance *in vitro* (Pelden et al., 2013) was also included. MCF7 and T47D cells were grown in hormone-depleted media for 72 hours and treated with E2 and/or MIB and/or TAM or FULV for 24 hours.

As expected, the expression of target genes regulated by AR or ERα increased significantly in response to the receptor's cognate ligand. Amongst the AR regulated genes investigated, *ZBTB16* regulation by MIB was found to be the strongest in both MCF7 and T47D (Figure 3-9C, Figure 3-10A). In MCF7, while the co-treatment of MIB with E2 decreased the expression of *C1orf116*, *PSCA*, *ZBTB16* significantly (Figure 3-9A, B, C), it was unable to reduce the expression of *NDRG* (Figure 3-9D), the regulation of which was weak compared to the other AR target genes. For *C1orf116*, *PSCA* and *NDRG,* the addition of TAM had no significant effect on the inhibitory crosstalk when cells were treated with E2 and MIB. However, this inhibitory effect of ERα on AR-induced expression of *ZBTB16* was significantly reversed by TAM (Figure 3-9C). More strikingly, the inhibition of ERα by FULV led to a dramatic increase in the expression of *C1orf116*, *PSCA*, *ZBTB16*. For *PSCA*, and *C1orf116*, this induction, in response to co-treatment with FULV, was found to be even greater than when the genes were only induced with MIB. The expression of *C1orf116* increased 2.24-fold, *PSCA* 45.5-fold, *ZBTB16* 216.7-fold, in comparison with co-treatment with MIB and E2 (Figure 3-9A, B, C), suggesting that when ERα is fully inhibited, the AR becomes more active. The addition of both TAM and FULV did not cause any change in the expression of *NDRG* in MCF7 (Figure 3-9D).

MCF7

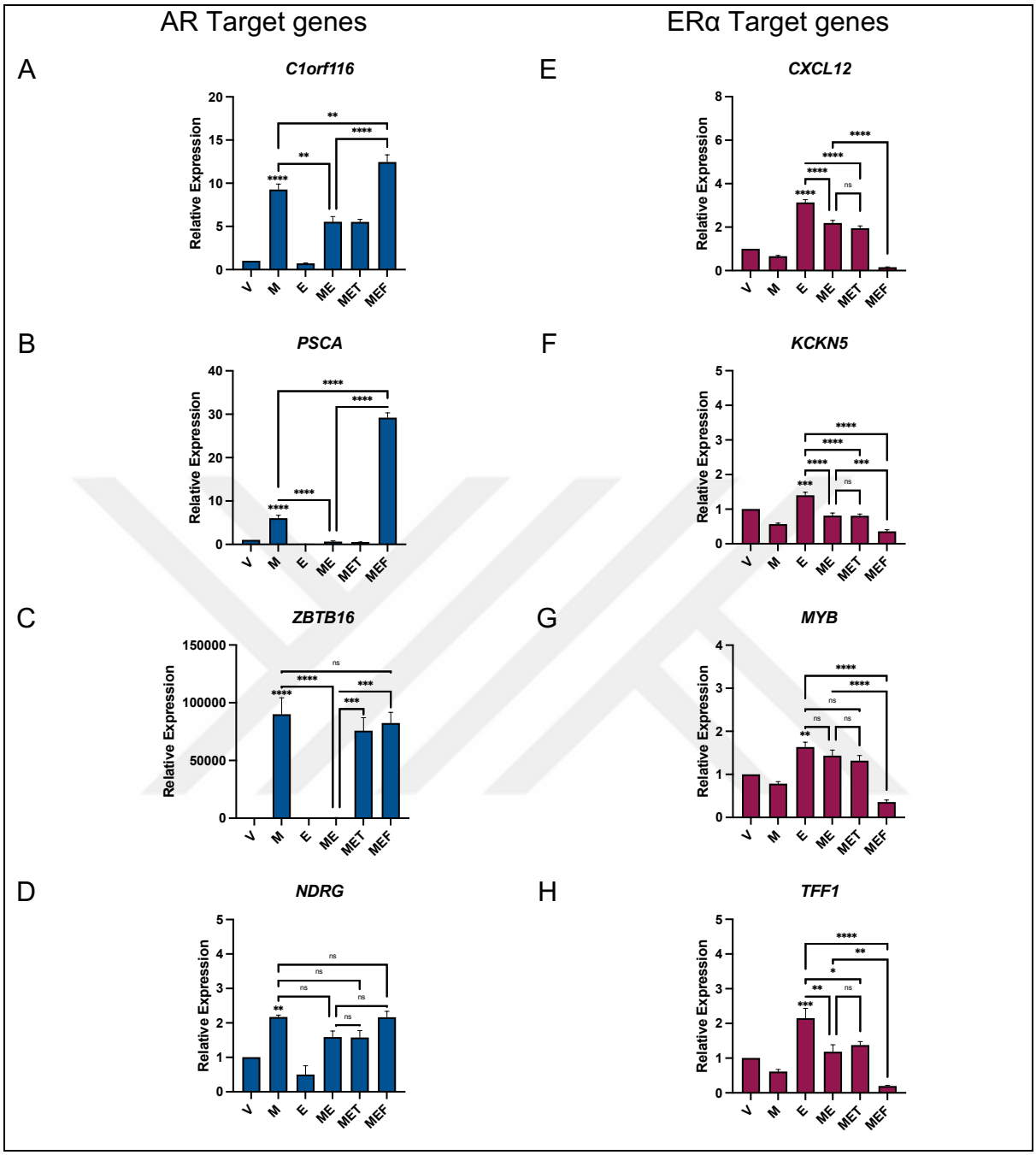

Figure 3-9 Antioestrogens lift the inhibitory effect of ERα on AR target gene expression in MCF7 cells

*MCF7 cells were incubated in hormone-depleted media for 72 hours, treated with vehicle control (V, EtOH), or varying combinations of oestradiol (E, 1 nM), Mibolerone (M, 1 nM), tamoxifen (T, 100 nM), fulvestrant (F, 100 nM) for 24 hours. RNA was harvested, reverse transcribed into cDNA, and qPCR was performed using SYBR green to measure the expression level of AR target genes (A) C1orf116, (B) PSCA, (C) ZBTB16, (D) NDRG1; ERα target genes (E) CXCL12, (F) MYB, (G) KCNK5, (H) TFF1. Expression was normalised to RPL19 and changes in expression calculated using $2^{-\Delta\Delta Ct}$. Expression was made relative to control treatment. Graphs are the average of 3 individual replicates, and generated with GraphPad Prism 9 software. ANOVA. ns = not significant, * p ≤ 0.05, **p ≤ 0.01, ***p ≤ 0.001, ****p ≤ 0.0001. Mean ± 1SE.*

T47D

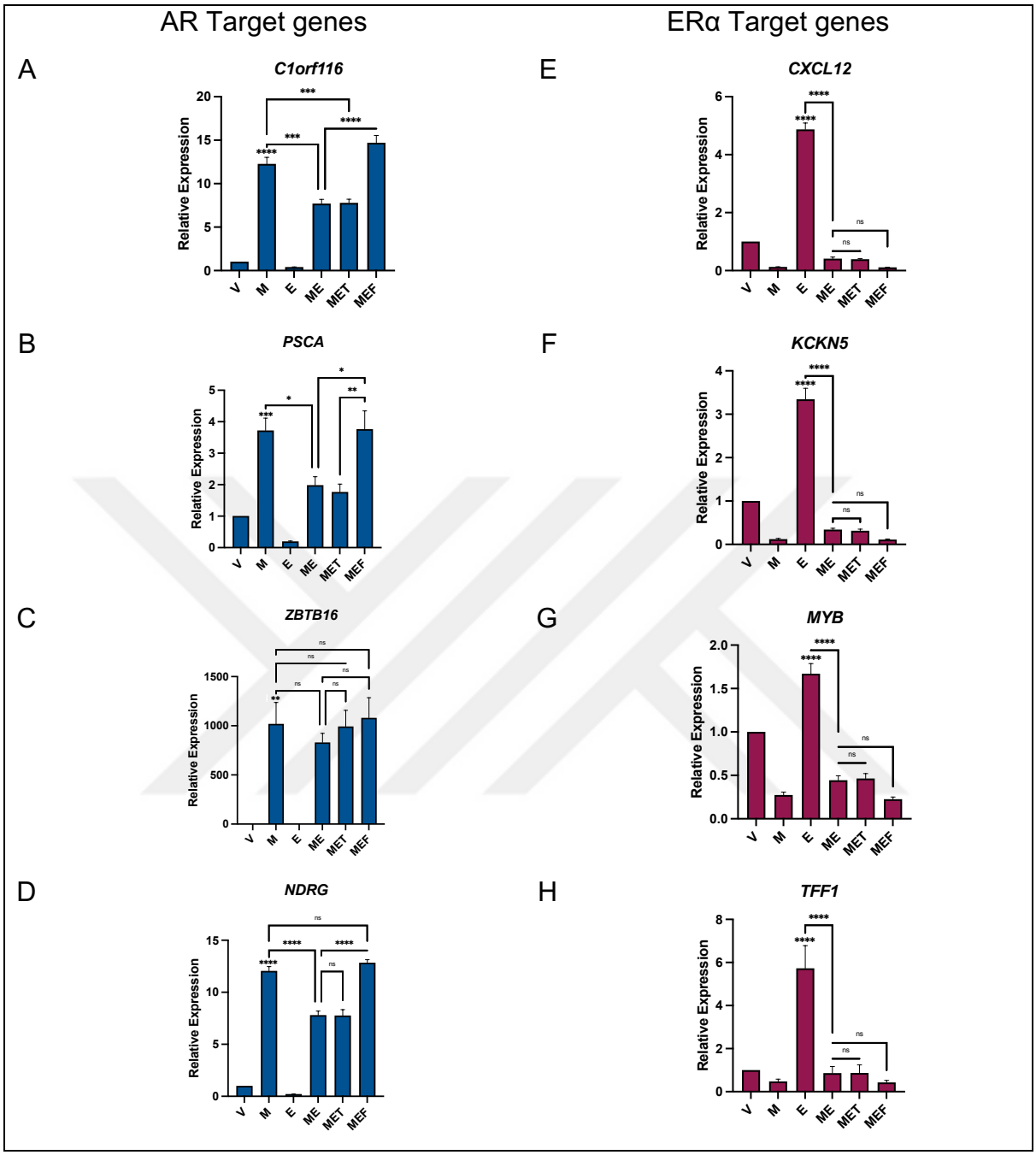

Figure 3-10 Antioestrogens lift the inhibitory effect of ERα on AR target gene expression in T47D cells

*T47D cells were incubated in hormone-depleted media for 72 hours, treated with vehicle control (V, EtOH), or varying combinations of oestradiol (E, 1 nM), Mibolerone (M, 1 nM), tamoxifen (T, 100 nM), fulvestrant (F, 100 nM) for 24 hours. RNA was harvested, reverse transcribed into cDNA, and qPCR was performed using SYBR green to measure the expression level of AR target genes (A) C1orf116, (B) PSCA, (C) ZBTB16, (D) NDRG1; ERα target genes (E) CXCL12, (F) MYB, (G) KCNK5, (H) TFF1. Expression was normalised to RPL19 and changes in expression calculated using $2^{-\Delta\Delta Ct}$. Expression was made relative to control treatment. Graphs are the average of 3 individual replicates, and generated with GraphPad Prism 9 software. ANOVA. ns = not significant, * p ≤ 0.05, **p ≤ 0.01, ***p ≤ 0.001, ****p ≤ 0.0001. Mean ± 1SE.*

Similar to MCF7, E2 was able to reduce the MIB-induced expression of *C1orf116*, *PSCA*, and *NDRG* significantly in T47D (Figure 3-10A, B, D). The expression level of *ZBTB16* was also slightly reduced by E2, but it was not found to be significant (Figure 3-10C). Similar to the MCF7 results, the expression levels of the AR-regulated genes were also not significantly affected by TAM, in comparison with MIB and E2 co-treatment, in T47D. However, FULV once again was able to reverse the inhibitory effect of ERα on *C1orf116*, *PSCA* and *NDRG* (Figure 3-10A, B, D), confirming that in ERα-positive disease when the ERα is inhibited by a full antagonist, the AR becomes more active.

To investigate the effect of antioestrogens and AR-ERα crosstalk upon oestrogen target genes, qPCR was repeated for the genes known to be regulated by ERα. In MCF7, the presence of MIB caused a significant reduction in the E2-induced expression of *CXCL12*, *KCNK5* and *TFF1*, but this effect was not seen for *MYB* (Figure 3-9E, F, G, H). Interestingly, the expression levels of these genes were not further reduced following the addition of TAM, in comparison with co-treatment with MIB and E2.

The E2-induction of ERα regulated genes (*CXCL12*, *KCNK5*, *MYB*, *TFF1*) were downregulated significantly in response to co-treatment of E2 with MIB in T47D cells (Figure 3-10E, F, G, H), in agreement with the results obtained in MCF7. Again, inhibition by TAM did not change the expression of ERα target genes, in comparison with co-treatment of MIB and E2. Further inhibition of E2-induced genes by FULV were seen in MCF7 and T47D. In conclusion, the crosstalk between AR and ERα was found to be inhibitory. However, antioestrogens, in particular FULV, reduced this repressive crosstalk, leading to a more active AR.

3.3.2 The effect of antioestrogens on binding of AR to DNA

The previous data demonstrates that AR and ERα inhibit each other's activity, and the transcriptional activity of AR appears to be enhanced via the inhibition of ERα by antioestrogens. To see if AR and ERα inhibit each other's activity via competition for binding to response elements, ChIP assays were performed on AR regulated genes: *ZBTB16* and *PSCA*. *ZBTB16* has been shown to be regulated by AR in molecular apocrine BrCa and PrCa (van de Wijngaart et al., 2009; Robinson et al.,

2011). PSCA was suggested as a biomarker in PrCa patients, and its expression was associated with increased proliferative characteristics in BrCa patient tumour samples (Link et al., 2017). Both were also regulated in endocrine sensitive disease and their expression was inhibited by ERα (Section 3.3.1). In addition to investigating the effect of co-treatment with MIB and E2, the antioestrogens, TAM and FULV, were also included to investigate AR DNA occupancy following inhibition of ERα.

MCF7 and T47D cells were grown in hormone-depleted media for 72 hours, then treated with the ligands MIB (1 nM), E2 (1 nM), TAM (100 nM) and/or FULV (100 nM) for 4 hours. Cells were crosslinked with formaldehyde, quenched with glycine, and the DNA was sonicated to approximately 100-200 bp fragments (Figure 3-11A). AR enriched DNA regions were pulled down using an AR-specific antibody (ab108341) and qPCR performed for an AR response element (ARE+) and a negative control region (ARE-) (Figure 3-11B, Figure 3-12A).

It was found that AR bound to the ZBTB16 ARE+ in response to MIB treatment, and the enhancement by MIB was higher in MCF7 cells as compared to T47D (Figure 3-11C and Figure 3-11D). This MIB-enhanced binding of AR to the response element appears to be weakly inhibited following treatment with E2 in both cell lines. This reduction in binding was reversed following treatment with the antioestrogens, especially with FULV. The reversion by TAM was not found to be significant; however, the inhibition of ERα by FULV led to a striking enhancement in the AR binding to the DNA, not only as compared to co-treatment of MIB and E2, but also in comparison to MIB-only treatment. The binding enhancement of AR in the presence of FULV as compared to MIB and E2 treated samples increased by 566.6% in T47D and 458.6% in MCF7.

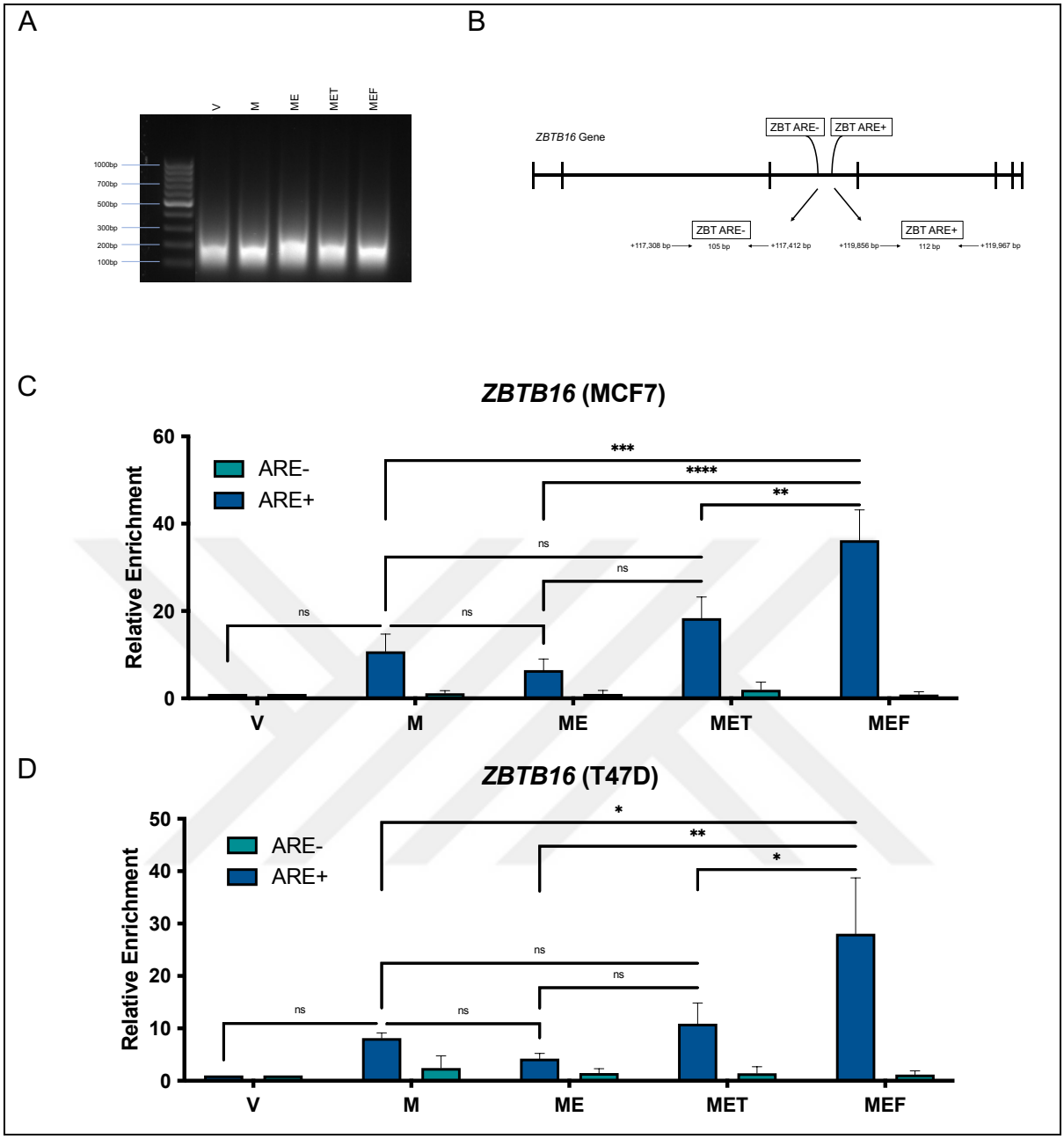

Figure 3-11 Antioestrogens, especially fulvestrant, reverse ERα inhibition of AR binding to an ARE within ZBTB16 gene in endocrine sensitive cells

*Cells were grown in hormone depleted media for 72 hours, then treated with the ligands MIB (M) (1 nM), E2 (E) (1 nM), TAM (T) (100 nM), FULV (F) (100 nM) for 4 hours. EtOH was used as vehicle control (V). Cells were crosslinked using formaldehyde and (A) sonicated to approximately 200 bp. ChIP assays were performed using an antibody specific for the AR (ab108341). Subsequent qPCR was conducted to identify DNA enrichment at a known androgen response element (ARE) within the ZBTB16 gene (ZBT ARE+) and its relative negative control region (ZBT ARE-). Enrichment values were made relative to the control (V). (B) A schematic of ZBT ARE and its negative region. (C) MCF7 (D) T47D. Graph is the average of 3 individual repeats for MCF7, 2 individual repeats for T47D, and generated with GraphPad Prism 9 software. ANOVA. ns = not significant, **p ≤ 0.01, ***p ≤ 0.001, ****p ≤ 0.0001. Mean ± 1SE.*

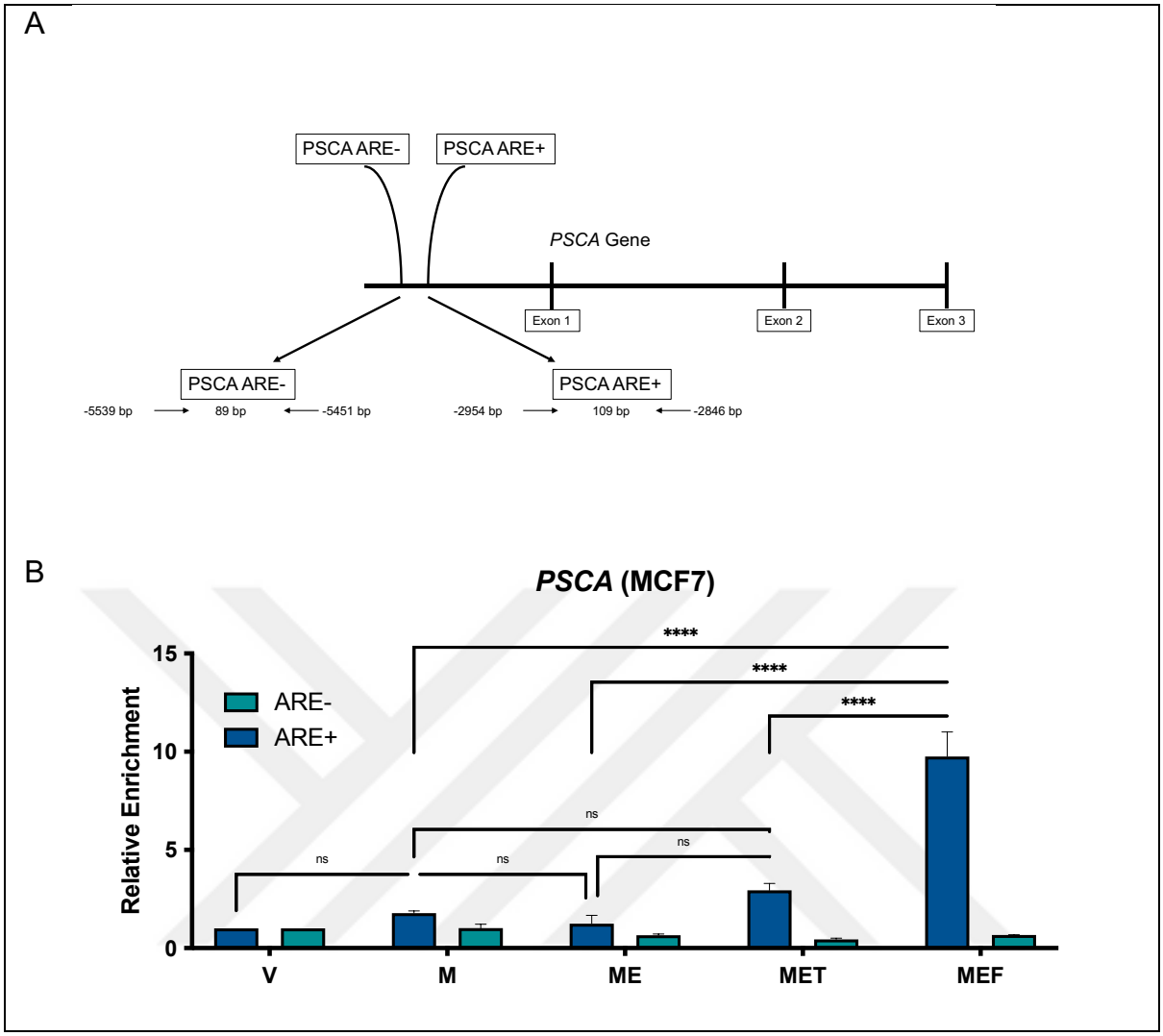

Figure 3-12 Antioestrogens, especially fulvestrant, reverse ERα inhibition of AR binding to an ARE in the promoter region of PSCA gene in MCF7 cells

*Cells were grown in hormone depleted media for 72 hours, then treated with the ligands MIB (M) (1 nM), E2 (E) (1 nM), TAM (T) (100 nM), FULV (F) (100 nM) for 4 hours. EtOH was used as vehicle control (V). Cells were crosslinked using formaldehyde and sonicated to approximately 200 bp. ChIP assays were performed using an antibody specific for the AR (ab108341). Subsequent qPCR was conducted to identify DNA enrichment at a previously established high affinity androgen response element (ARE) in the promoter region of the PSCA gene (PSCA ARE+) and its relative negative control region (PSCA ARE-). Enrichment values were made relative to the control (V). (A) A schematic of PSCE ARE and its negative region. (B) Representative graph of MCF7 ChIP assays. Graph is the average of 2 individual repeats, and generated with GraphPad Prism 9 software. ANOVA. ns = not significant, ****p ≤ 0.0001. Mean ± 1SE.*

To investigate this observed enhancement in DNA binding further, recruitment of AR to an ARE upstream of the *PSCA* gene was also investigated in MCF7 cells. In LNCaP cells, a high affinity ARE (5'-CCTGGAACTTTCCGTCCTCAAATA-3') has previously been identified in the promoter region of *PSCA* (~3kb upstream) (Jain et al., 2002). Using UCSC Genome Browser, the location of the ARE was identified, and primers were designed to cover a 102 bp long region which harbours the ARE, 2954-2846 bp upstream of *PSCA* gene (PSCA ARE+). Primers for a negative control region (PSCA ARE-), 2496 bp upstream, were also designed (Figure 3-12A). Additionally, to verify that the chosen ARE- region was indeed negative for androgen response elements, the AR binding motif (MA0007.2) from the JASPAR motif database was obtained, and using FIMO (Grant et al., 2011) potential matches were also investigated in the 7 kb upstream of the *PSCA* gene. This analysis demonstrated that only one motif exists ($p < 0.0001$), which coincides with the motif identified by Jain et al., 2002.

Interestingly, MIB did not significantly increase AR binding to the response element compared to control treatment (Figure 3-12B). Again, the addition of E2 inhibited this enhancement partially. In accordance with the previous findings observed for ZBTB16 ARE, AR binding was enhanced following the addition of TAM and FULV, 233% and 786.2%, respectively. However, only the enhancement in the presence of FULV was found to be statistically significant. Hence, in support of the previously shown data, these findings suggest that ERα inhibits AR binding to DNA and that antioestrogens can reverse this, especially FULV, leading to activation of androgen signalling in hormone receptor positive BrCa cell line models.

3.3.3 Inhibiting AR with an antiandrogen, ENZA, enhances the inhibitory effect of antioestrogens on ERα expression

To investigate how the crosstalk between AR and ERα affects the receptor expression at the protein level, western blotting was performed. MCF7 cells were treated with different combinations of MIB, E2, antioestrogens (TAM, FULV), and the antiandrogen ENZA for different time periods (3, 5, and 7 days). ENZA, a second-generation AR antagonist, which is being used for the treatment of metastatic PrCa, blocks androgen binding to AR, inhibits nuclear translocation and DNA binding (Vera-Badillo et al., 2014), was chosen for AR inhibition.

AR levels were found to increase in response to MIB treatment at all time points. In contrast, E2-only treatment led to a reduction in AR expression, and this inhibition was more visible after 7 days (Figure 3-13C and F). However, the addition of E2 to MIB did not have a noticeable impact on AR expression, and protein levels varied across time points. Interestingly, when ERα was inhibited by TAM, AR levels were also slightly reduced in comparison with control, but this effect was lost over time (Figure 3-13A, B, C). In contrast, fulvestrant inhibition of ERα resulted in an increase in AR protein levels, even in the absence of androgen (Figure 3-13D). As expected (Siciliano et al., 2021), AR levels decreased following ENZA treatment.

ERα levels varied across samples following E2 treatment, with only half of the E2-treated samples having an increase in ERα expression (Figure 3-13C, E, F). MIB treatment resulted in a decrease in ERα levels (Figure 3-13A, B, C, D, F) and co-treatment of E2 with MIB also reduced ERα levels (Figure 3-13A, B, E, F). The addition of the antioestrogens also reduced ERα levels, and this reduction was more significant following FULV treatment. However, when cells were treated with MIB, E2 and an antioestrogen, the expression of ERα varied as compared to co-treatment of MIB and E2. Most importantly, inhibition of AR by ENZA, facilitated the down-regulatory effect of the antioestrogens on ERα levels.

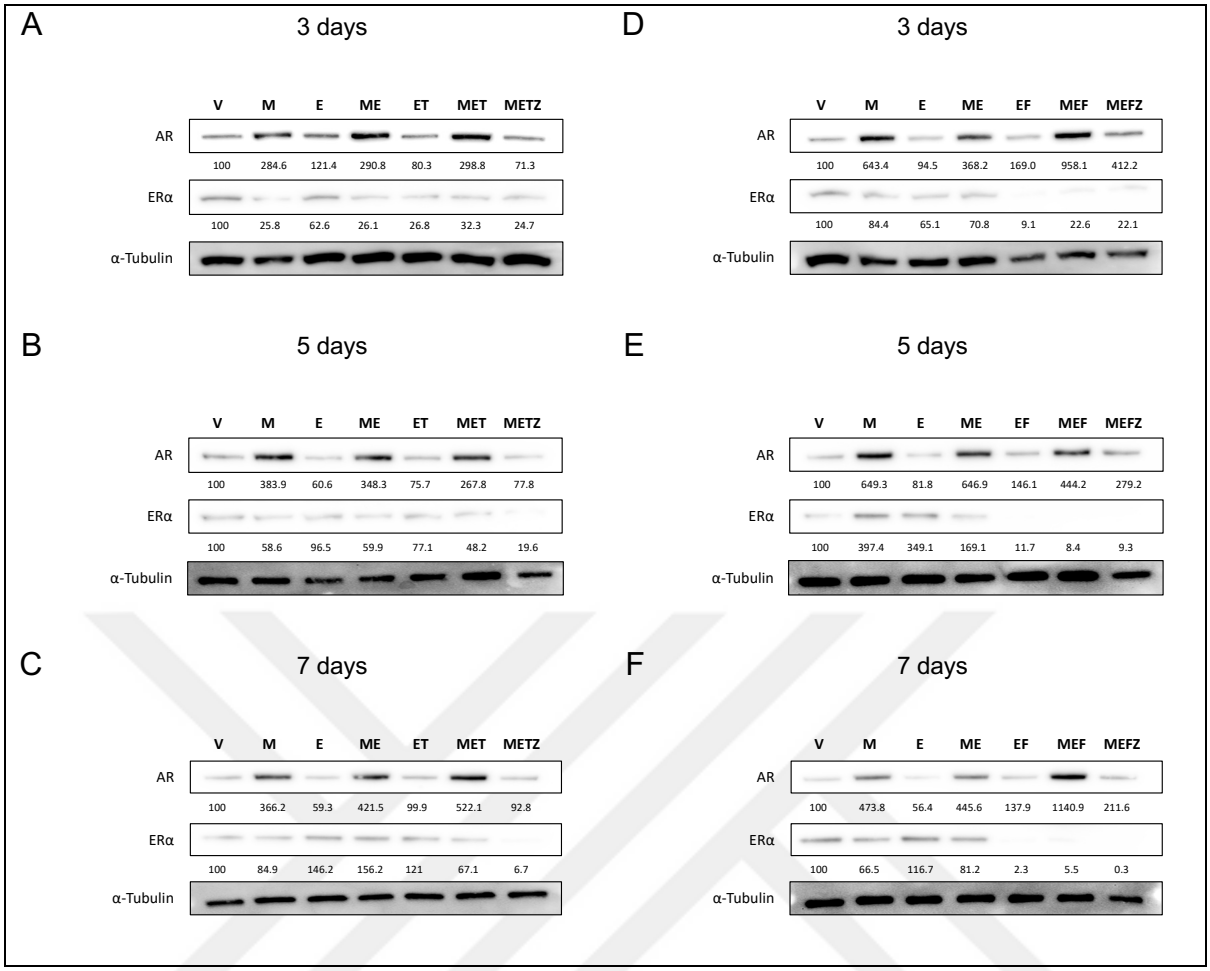

Figure 3-13 Inhibition of AR enhances the inhibitory effect of antioestrogens on ERα protein expression in MCF7

MCF7 cells were grown in hormone-depleted media for 24 hours, then treated with different combinations of Mibolerone (M, 1 nM), 17-β-Oestradiol (E, 1 nM), Tamoxifen (T, 100 nM), Fulvestrant (F, 100 nM) or Enzalutamide (Z, 10 μM) for (A, D) 3, (B, E) 5 or (C, F) 7 days. Ethanol treatment was used as a vehicle control (V). Cells were collected, lysed, and immunoblotting conducted to examine AR and ERα expression. α-Tubulin was used as a loading control. Densitometry analysis was performed using Image J (Version 1.53) software and results were represented as the percentage of vehicle control for AR and ERα expression.

3.3.4 Investigation of the motility of breast cancer cells in response to androgen when ERα is inhibited by antioestrogens

The overexpression of AR in circulating BrCa tumour cells has been associated with increased bone metastases (Aceto et al., 2018). Further, it has been shown that enhanced AR signalling is a common feature of circulating tumour cells obtained from patients with metastatic ERα-positive BrCa (Aceto et al., 2018). The results presented here have shown that ERα can inhibit AR's target gene expression and that antioestrogens can reverse this inhibitory effect of ERα on AR. Additionally, AR's binding to the DNA increases when ERα is inhibited by antioestrogens. To see the effect of androgen on cell migration when ERα is inhibited by antioestrogen treatments, wound healing assays were performed with MCF7 and T47D cells (Figure 3-14). In the absence of ligands, the wounds closed by approximately 15% and 45% after 24 hours for MCF7 and T47D, respectively (Figure 3-14A, B, C). However, treatments with the different ligands did not significantly affect wound closure in either of the cell lines. Although AR-ERα signalling and crosstalk has an effect upon gene expression, this does not appear to affect cell motility.

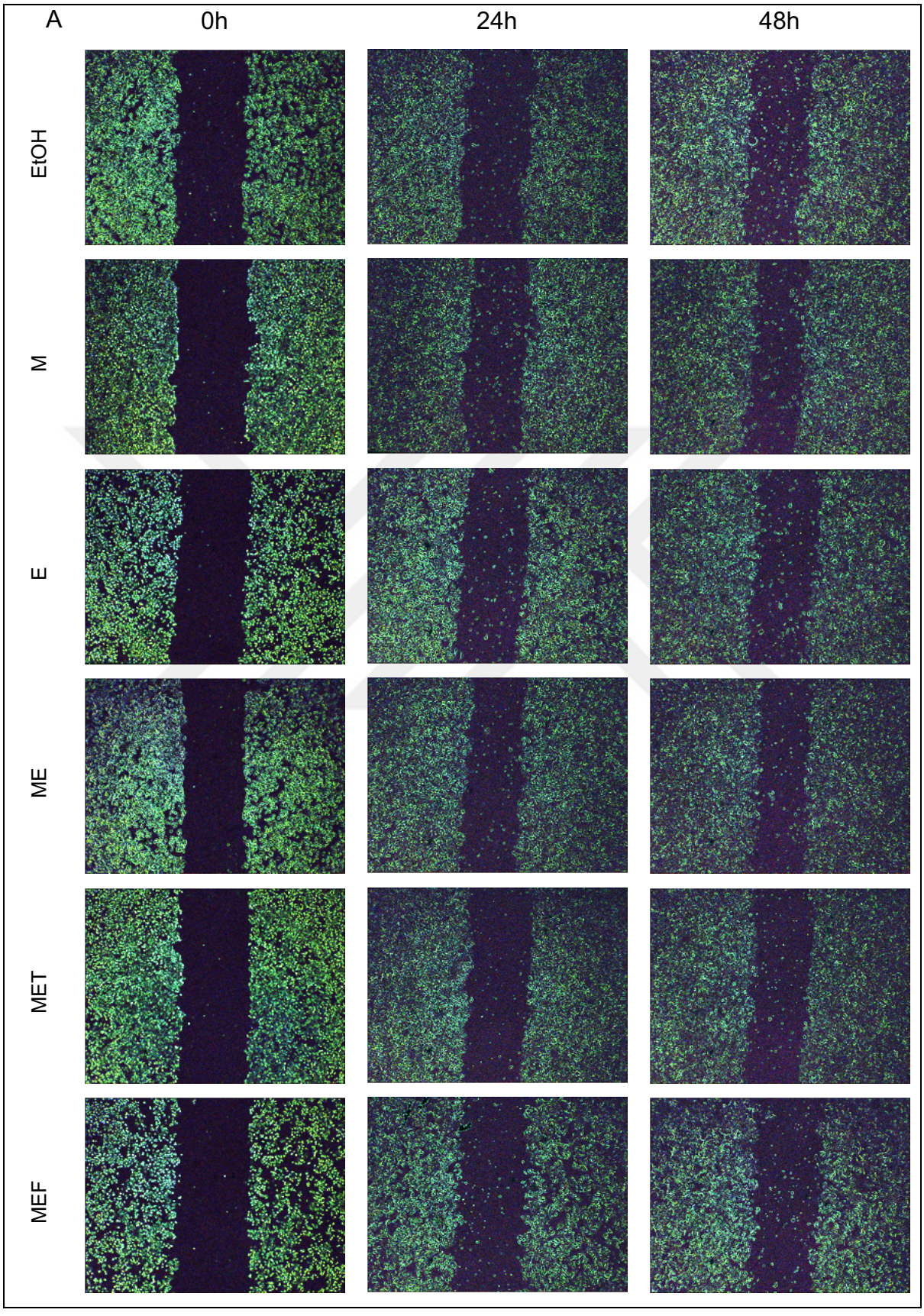
A
0h
24h
48h
EtOH
M
E
ME
MET
MEF

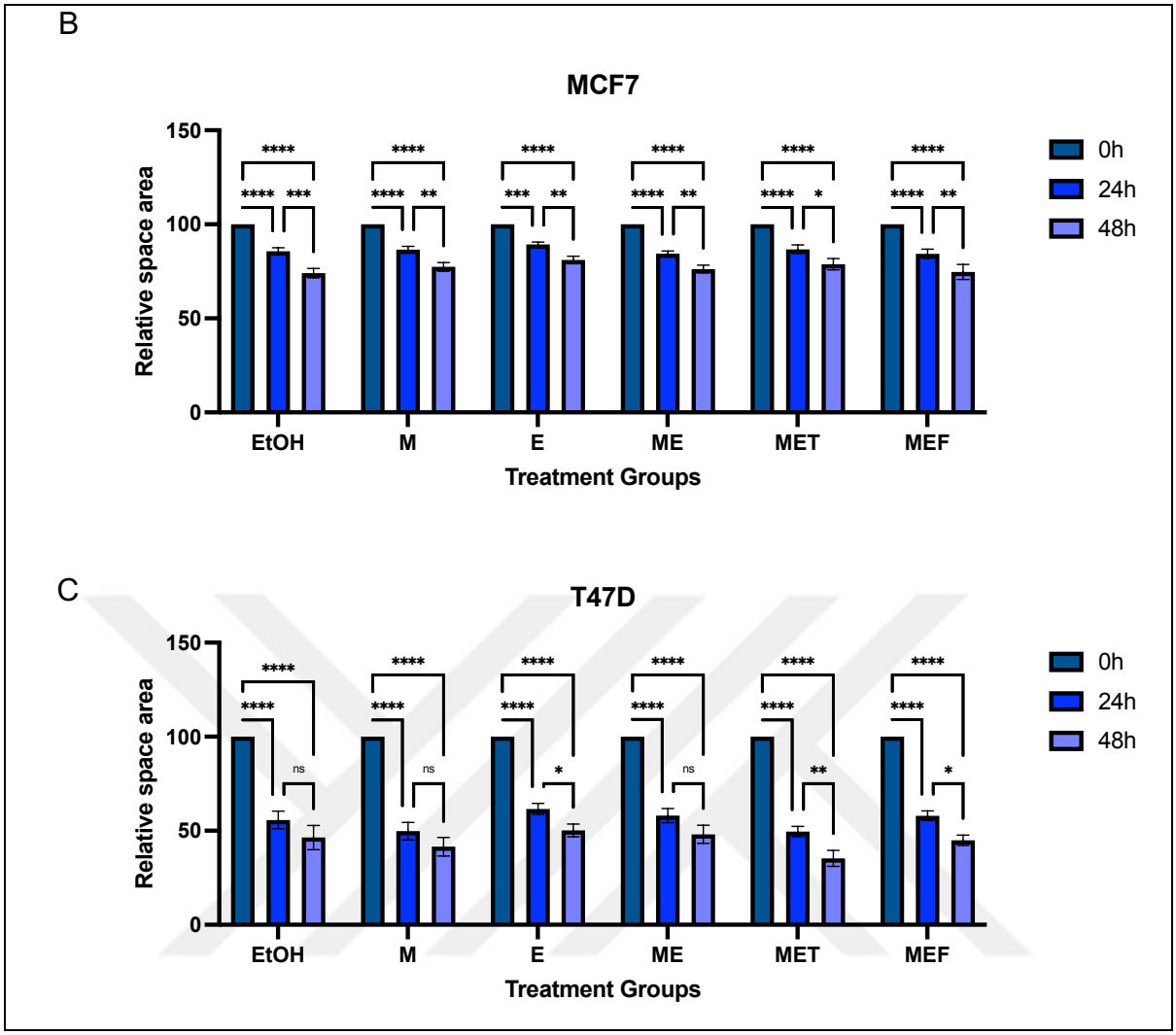

Figure 3-14 Androgen does not affect the motility of MCF7 and T47D cells in response to antioestrogen treatments

*Cells were seeded in 6-well plates at 90% confluency in hormone-depleted media. After 48 hours, the surface of the wells was scraped with a p200 pipette tip, the media was removed and washed twice with PBS, then fresh media containing the different combinations of EtOH, Mibolerone (M, 1 nM), oestradiol (E, 1 nM), Tamoxifen (T, 100 nM), Fulvestrant (F, 100 nM) were added (0h). (A) Per replicate, three different points of the scratched area were imaged under a microscope at 0-, 24- and 48-hour time points (representative images provided). For (B) MCF7 and (C) T47D , the images were processed using ImageJ (Version 1.53) to measure the change in wound areas. Measured areas are represented as a percentage of 0h measurements of each treatment groups. Data are the average of 3 individual repeats and generated with GraphPad Prism 9. ANOVA. ns = not significant, * p ≤ 0.05, **p ≤ 0.01, ***p ≤ 0.001, ****p ≤ 0.0001. Mean ± 1SE.*

3.3.5 The effect of antiandrogen treatment on the proliferation of endocrine sensitive cells

The emerging evidence of AR expression and its association with better clinical outcomes (Venema et al., 2019) has meant that the receptor has emerged as a therapeutic target for BrCa. It has been demonstrated that simultaneous inhibition of both receptors, through the use of antioestrogens and antiandrogens, reduces both AR and ERα expression significantly, as compared to antioestrogen treatment only. To investigate the effects of AR and ERα crosstalk on cell proliferation, proliferation assays were conducted, when the receptors are induced by their ligands or inhibited by antiandrogen/antioestrogen. MCF7 cells were seeded in 96-well plates in hormone-depleted media, and after 24 hours treated with different combinations of MIB, E2, TAM, FULV and/or ENZA. Subsequently, the cells were left in the incubator for 3, 5 or 7 days and crystal violet assays performed.

As it can clearly be seen, proliferation of MCF7 cells were found to be significantly induced by E2 at all the times points investigated (Figure 3-15A, B, C, D, E, F). It was also expected that MIB would inhibit E2-induced cell proliferation, as AR was found to inhibit ERα transcriptional activity in MCF7 (Section 3.2.2). However, MIB was not able to reduce E2-induced proliferation initially, and it was found that at least 5 days was necessary for the inhibitory effect of MIB on E2-induced proliferation to be significant, and this inhibitory effect of MIB was lost at the 7-day time point. Interestingly, MIB was able to induce cell proliferation on day 7 (Figure 3-15C, F), which suggest that endocrine sensitive cells can use androgen to promote cell proliferation when deprived from E2.

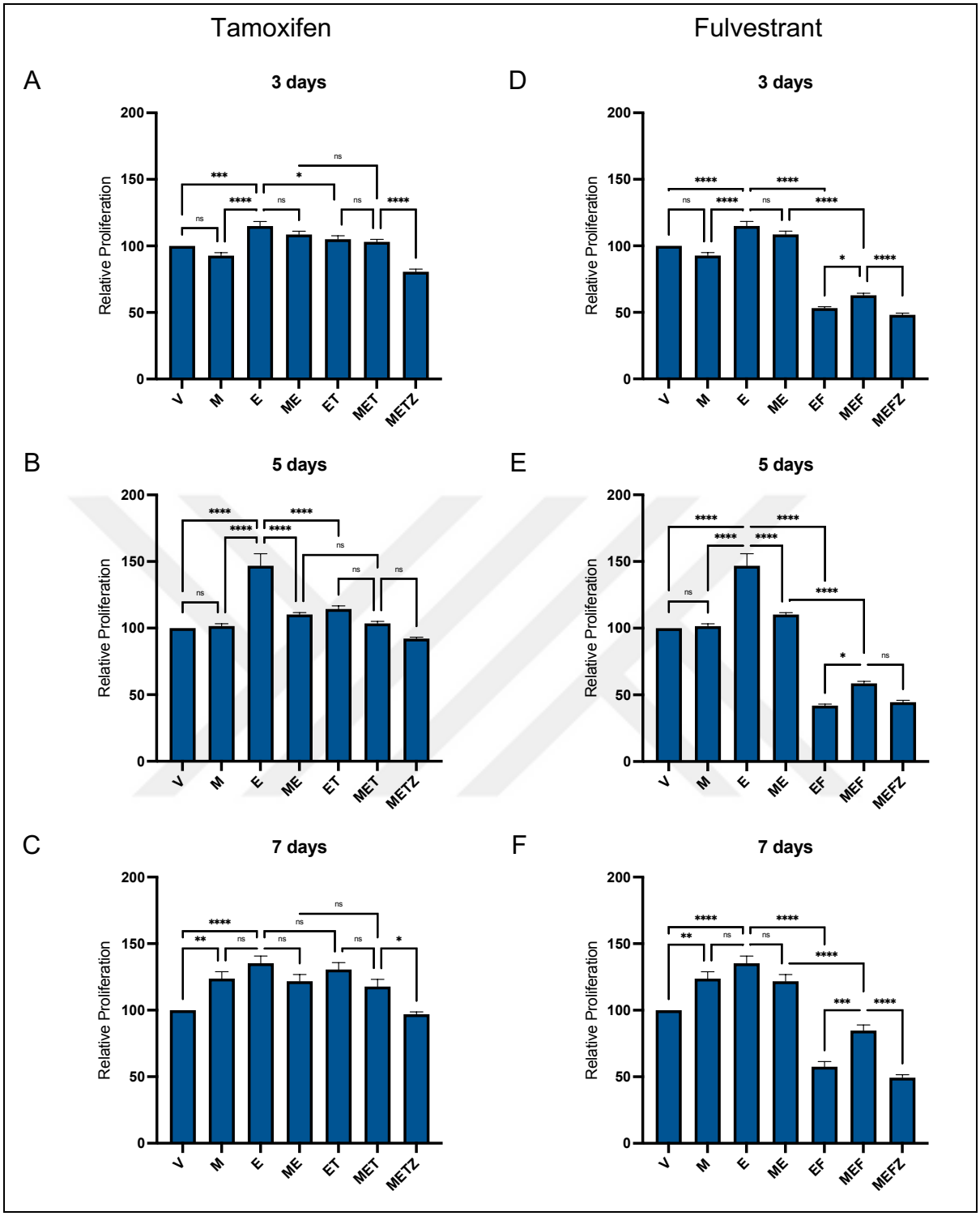

Figure 3-15 Antiandrogen treatment enhances the inhibitory effect of fulvestrant on cell proliferation in short term in MCF7 cells

*MCF7 cells were incubated in hormone-depleted media for 24 hours, followed by different combinations of treatment with Mibolerone (M) (1 nM), 17-β-Oestradiol (E) (1 nM), Tamoxifen (T) (100 nM), Fulvestrant (F) (100 nM) or Enzalutamide (Z) (10 μM) for (A, D) 3 days, (B, E) 5 days, or (C, F) 7 days. Ethanol treatment was used as a vehicle control (V). Six different wells were seeded per treatment condition, three independent proliferation assays were conducted, and the cells fixed with 2% Paraformaldehyde and stained using 0.04% crystal violet. Cell proliferation was assessed by measuring the resulting absorbance (λ = 595 nm) on a FLUOstar Omega plate reader (BMG Labtech). Results were presented as percentage of control absorbance. ANOVA. ns = not significant, * p ≤ 0.05, **p ≤ 0.01, ***p ≤ 0.001, ****p ≤ 0.0001. Mean ± 1SE.*

Cell proliferation was inhibited by antioestrogens, TAM and FULV. However, TAM was only able to reduce E2-induced cell proliferation at the early time points, and this effect was lost after 7 days. The addition of MIB also did not have a significant effect upon the TAM inhibition of E2-induced growth (Figure 3-15A, B, C). However, when AR was inhibited with ENZA, MCF7 proliferation was further reduced.

More importantly, FULV was not only able to inhibit E2-induced growth, but also decreased cell proliferation significantly in comparison with control. Interestingly, addition of MIB reversed the inhibitory effects of FULV (Figure 3-15D, E, F), and this increase was significant at all time points, most evident on the 7th day. Furthermore, ENZA inhibited this MIB-induced effect, leading to a significant decrease in the proliferation. Thus, it could be postulated that an active AR might promote growth, and this could be prevented by inhibition of the receptor. This therefore suggests that the combination of an antiandrogen with an antioestrogen could be an effective method to inhibit BrCa proliferation, compared to when these molecules are used as a monotherapy.

To expand upon the proliferation assays, which showed the effects of antiandrogen, and antioestrogen treatments on endocrine sensitive BrCa cells in at relatively short time-points, colony formation assays were conducted, to see the effects of the different ligands on BrCa proliferation in the longer term. MCF7 and T47D cells were seeded in 6-well plates at 10% confluency in hormone-depleted media, and treated with different combinations of MIB, E2, TAM, FULV, and ENZA every 72 hours for 4 weeks (Figure 3-16A, Figure 3-17A). The results demonstrated that the proliferation of T47D cells were significantly inhibited by MIB in comparison with E2, but not with control (Figure 3-16B). Interestingly, addition of MIB to E2 did not significantly alter cell growth when compared to E2-induced growth. Surprisingly, TAM was also not able to reduce E2-induced T47D cell growth. On the other hand, FULV significantly inhibited this. Additionally, MIB appears to enhance the antioestrogens efficacy, leading to a stronger inhibition of growth. The combination of antioestrogens with ENZA resulted in a further decrease in cell growth, and this inhibition was found to be significant for TAM.

MCF7 cells responded similarly to E2 and MIB. As was observed in T47D cells, co-treatment with both hormones did not have an inhibitory effect on E2-induced proliferation (Figure 3-17B). Again, TAM was unable to reduce E2-induced proliferation, whereas FULV did, and the addition of MIB did not increase proliferation

of MCF7 cells. However, compared to the MIB, E2 and antioestrogen treated cells, the growth of MCF7 cells was significantly reduced following co-treatment with ENZA.

In conclusion, it appears that the inhibitory effect of MIB on E2-induced cell growth is visible in short term proliferation assays but not in longer term assays. Further, in the short term MIB appears to reverse the anti-proliferative effect of antioestrogens on cell proliferation, but in the longer term this effect of MIB was lost.

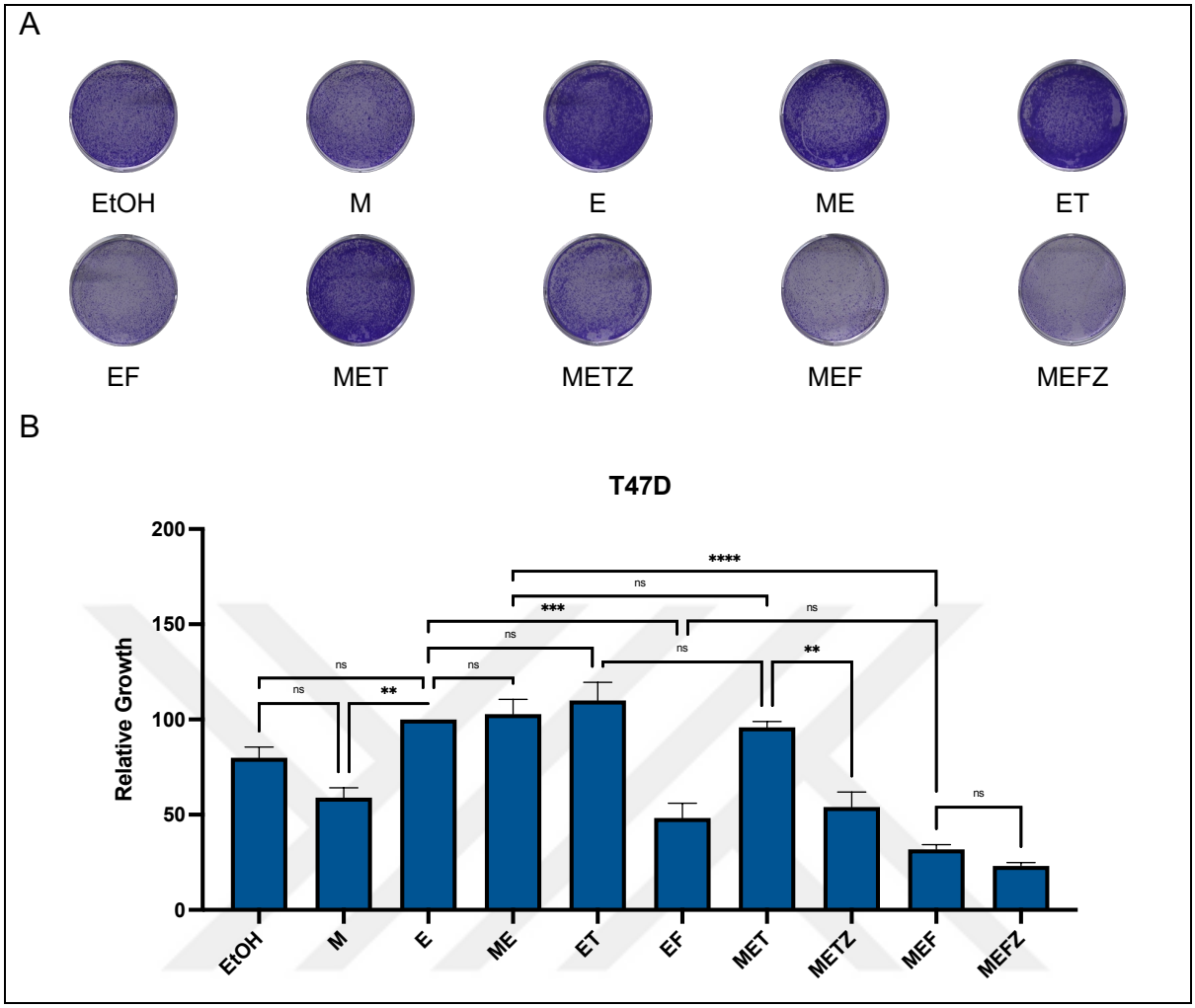

Figure 3-16 Combination of antioestrogen and antiandrogen treatment inhibits growth in T47D cells in the long term

*(A) T47D cells were treated for 4 weeks in hormone-depleted media with 1 nM of Mibolerone (M) or 17-β-Oestradiol (E) separately and in different combinations with 100 nM Tamoxifen (T), Fulvestrant (F), 10 μM Enzalutamide (Z). Ethanol (EtOH) treatment was used as a vehicle control. Three independent colony formation assays were conducted, and the cells fixed with 2% paraformaldehyde and stained using 0.04% crystal violet. (B) Cell proliferation was assessed by measuring the resulting absorbance (λ = 595 nm) on a FLUOstar Omega plate reader (BMG Labtech). Results were made relative to E absorbance. ANOVA. ns = not significant, **p ≤ 0.01, ***p ≤ 0.001, ****p ≤ 0.0001. Mean ± 1SE.*

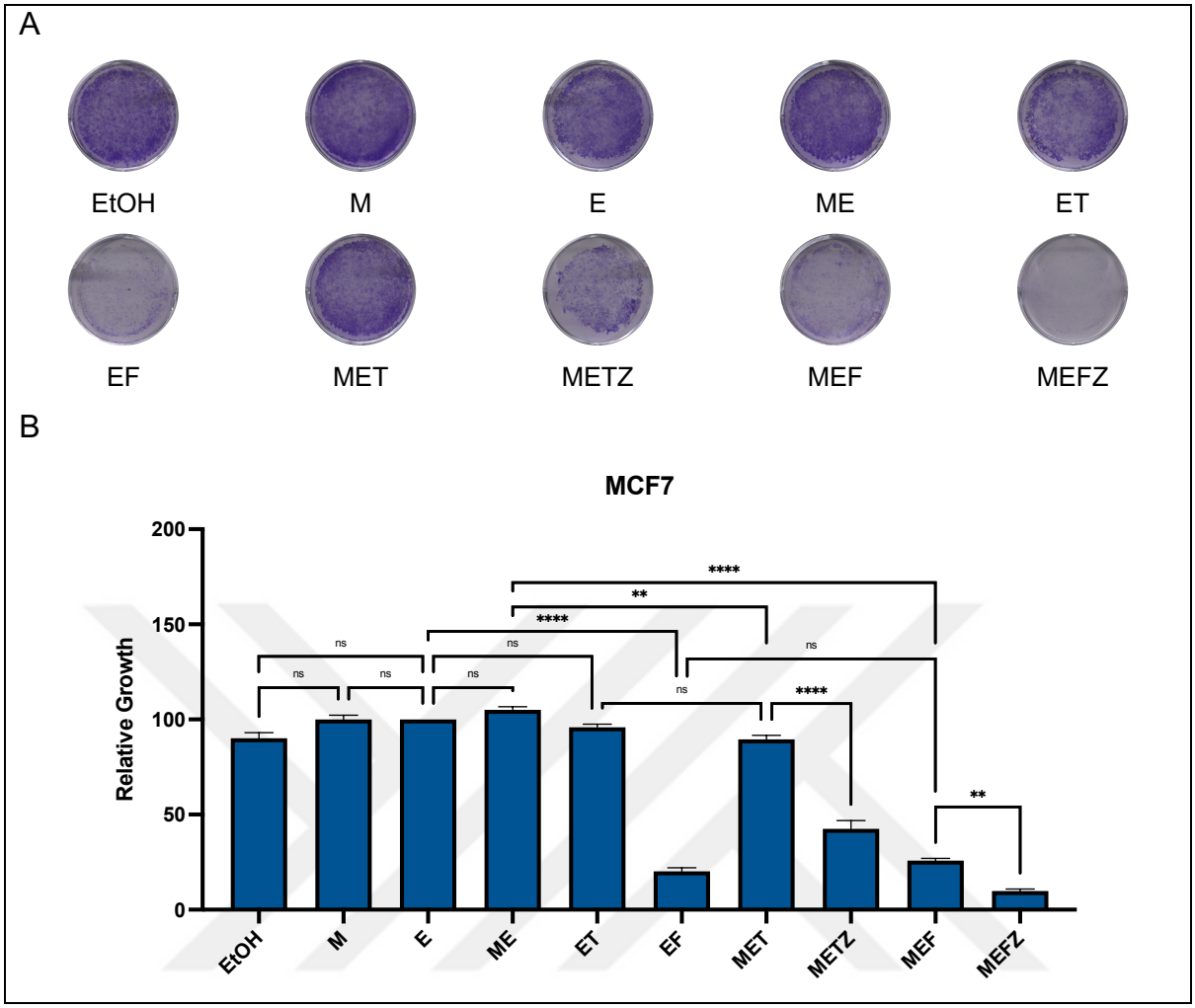

Figure 3-17 Combination of antioestrogen and antiandrogen treatment inhibits growth in MCF7 cells in the long term

*(A) MCF7 cells were treated for 4 weeks in hormone-depleted media with 1 nM of Mibolerone (M) or 17-β-Oestradiol (E) separately and in different combinations with 100 nM Tamoxifen (T), Fulvestrant (F), 10 μM Enzalutamide (Z). Ethanol (EtOH) treatment was used as a vehicle control. Three independent colony formation assays were conducted, and the cells fixed with 2% paraformaldehyde and stained using 0.04% crystal violet. (B) Cell proliferation was assessed by measuring the resulting absorbance (λ = 595 nm) on a FLUOstar Omega plate reader (BMG Labtech). Results were made relative to E absorbance. ANOVA. ns = not significant, **p ≤ 0.01, ****p ≤ 0.0001. Mean ± 1SE.*

3.4 Discussion

The majority of BrCa cases are ERα-positive (Sørlie et al., 2001; Ali and Coombes, 2002; Zwart et al., 2011; Fan et al., 2015; Hickey, Dwyer, et al., 2021). This BrCa subtype is dependent on ERα signalling, which promotes oncogenesis, cancer cell growth, and tumour proliferation (Eccles et al., 2013; Venema et al., 2019). ERα transcriptional activity is activated in response to ligand binding (Sever and Glass, 2013), and diseases that result in high circulating oestrogen levels predisposes BrCa risk (McPherson et al., 2000). This ligand-dependent ERα signalling is the mainstay therapeutic target in ERα-positive BrCa (Zwart et al., 2011; Szostakowska et al., 2019). Even though antioestrogens (SERMs and SERDs) have led to an improvement in the mortality rates of patients with early stage BrCa, a significant amount of those who initially respond to endocrine therapies develop resistance to these molecules. Further, there has been limited progress in treatment outcomes for BrCa patients with metastatic disease (Zwart et al., 2011; Murphy and Dickler, 2016; Szostakowska et al., 2019). Consequently, research is needed to further our understanding of the molecular mechanisms that drive BrCa development and progression as these may represent markers that predict disease outcome, recurrence, treatment response or failure, and targets that can be inhibited to overcome disease recurrence and therapy resistance.

The AR is expressed in many tissues in the body, albeit at different expression levels, suggesting that the receptor might play a role in the anatomical and physiological functions of these tissues, and breast epithelium is one of these (Dimitrakakis and Bondy, 2009). It has also been demonstrated that AR is expressed in the majority of ERα-positive BrCas (Vera-Badillo et al., 2014; Wu and Vadgama, 2017; Venema et al., 2019). AR positivity in ERα-positive patients has been associated with favourable tumour characteristics and better clinical outcomes (Castellano et al., 2010; Kensler et al., 2019; Anestis et al., 2020). Hence, AR signalling has emerged as a promising biomarker, and also therapeutic target, for BrCa. However, the role of AR signalling in BrCa has not been fully characterised. This study provides further understanding of the role of AR signalling in ERα-positive BrCa.

3.4.1 The effect of hormone levels on AR and ERα crosstalk

The effects of androgen on breast epithelial cells are inhibitory, whereas high circulating androgen levels are associated with an increase in BrCa risk, in particular ERα-positive BrCa (Dimitrakakis and Bondy, 2009; Kotsopoulos and Narod, 2012). For example, meta-analysis of 7 prospective studies with pre-menopausal women's circulating sex hormone levels has shown that increased testosterone levels were associated with BrCa risk (Endogenous Hormones and Breast Cancer Collaborative Group et al., 2013). It was also shown that high circulating androgen levels were associated with ERα positivity, suggesting that AR might also play a role in dysplastic progression of normal breast epithelial cells to cancer cells (Secreto et al., 2011). Additionally, the imbalance between circulating androgen and oestrogen hormone levels have also been proposed as a predisposing factor for BrCa tumour development (Secreto et al., 2019). However, it is known that testosterone can be converted to oestrogen via aromatisation in breast epithelial cells, and BrCa cells have excessive expression of aromatase within the tumour tissue (Suzuki et al., 2007; Suzuki et al., 2008). Therefore, circulating androgens could be converted into oestrogens locally which could lead to cell proliferation and cancer development. Confirming this, it was also demonstrated that oestrogen levels within tumour tissues were significantly higher in ERα-positive tumours as compared to ERα-negative tumours, although the circulating oestrogen levels were found to be similar in both patient groups (Kakugawa et al., 2017). To circumvent the issues of androgen being metabolised to E2, a synthetic non-aromatisable androgen (MIB) was used to in the experiments presented here.

It has been found that AR can facilitate BrCa proliferation via the induction of proliferative genes or via the regulation of alternative signalling pathways (Cochrane et al., 2014; Gerratana et al., 2018). Analysis of AR and ERα target genes, in response to MIB and E2, have shown that different concentrations of the hormones have differential effects upon the expression of the other receptor's target genes. ERα genes that are associated with invasion, tumour growth, metastasis in BrCa (*CXCL12*, *MYB*) were upregulated by higher concentrations of MIB (Alvarez-Baron et al., 2011; Boimel et al., 2012; Zhao et al., 2014; Wu et al., 2015; Cicirò and Sala, 2021). This upregulation of pro-proliferative ERα target genes by AR could be explained by several

different mechanisms. It could be because the activation of the receptor in response to excessive ligand exposure alters the AR cistrome, allowing the receptor to bind to additional sites (potentially EREs) present in the genome. Alternatively, it is possible that these genes have AREs in the regulatory regions of the target genes, which could be assessed through analysis of ChIP-Seq datasets.

Analysis of DHT concentrations in tumour samples from 38 BrCa patients showed that the 5α-reductase activity was increased and levels of DHT in the tumour tissues were higher in pre-menopausal women compared to post-menopausal women, and in ERα-positive tumours compared to ERα-negative tumours (Suzuki et al., 2007). Therefore, when the patients with ERα-positive tumours are treated with antioestrogens or AIs, intra-tumoural androgen levels could increase, causing the tumour to shift from oestrogen-dependent for growth to androgen-dependent. In support of this hypothesis, post-menopausal patients who receive TAM, have a reduction in circulating oestrogen levels and an increase in androgen levels (Baumgart et al., 2014). As the AR is the most commonly expressed steroid receptor in BrCa (Kotsopoulos and Narod, 2012), this change in hormone levels could result in enhanced AR signalling. However, this needs further investigation. Comparison of circulating androgen levels with intra-tumoral concentrations of androgen, androgen levels in BrCa tumour samples before and after antioestrogen treatment, AR and ERα expression status, and gene expression profiles in tumours with different androgen levels would further our understanding of this interplay between hormone levels in BrCa development and progression.

3.4.2 AR and ERα crosstalk is inhibitory and antioestrogens enhances AR activity

AR expression is associated with better clinical features (low proliferation, small tumour size, absence of lymph node metastases and lower grade tumours) and better outcomes for ERα-positive BrCa patients (Castellano et al., 2010; Vera-Badillo et al., 2014; Giovannelli et al., 2018). The work presented here suggests that this may be due to inhibitory crosstalk between the AR and ERα. For example, gene expression analyses of ERα and AR target genes, and reporter assays, found that the receptors inhibit each other's activity at the transcriptional level. The inhibitory effect of AR on ERα targets was found to be more significant in T47D cells, as compared to MCF7

cells. One possible explanation for that might be the different AR expression levels in these cell lines, as MCF7 cells are known to express low AR levels as compared to T47D (Birrell et al., 1995; Hickey, Selth, et al., 2021).

Short term proliferation assays showed that MCF7 cells were not only responsive to E2, but also became responsive to MIB for proliferation. This androgen-induced proliferation of MCF7 cells was observed in previous studies using different types of proliferation assays (i.e., cell count, methylene blue staining), and was reversed by the antiandrogen hydroxyflutamide, and also seen in the presence of DHT (Birrell et al., 1995; Somboonporn et al., 2004; Garay and Park, 2012). However, when cells were co-treated with MIB and E2, E2-induced proliferation decreased, confirming that the AR is inhibitory towards E2-induced proliferation. This inhibitory crosstalk of AR and ERα could explain the positive tumour characteristics and clinical outcomes observed in the aforementioned studies.

Elevated AR target gene expression has been found to correlate with high grades of BrCa and tumour growth (Robinson et al., 2011; Parsana et al., 2017; Link et al., 2017). The work presented here demonstrates that the expression of AR target genes is increased when ERα is inhibited by antioestrogens. This enhanced transcriptional AR activity is likely to be because the inhibitory ERα crosstalk is lost due to the action of the antioestrogens. For example, the AR may have enhanced binding to DNA and/or the AR may bind more readily to coactivators that would have been sequestered by the active ERα (Panet-Raymond et al., 2000; Peters et al., 2009). To investigate if the crosstalk between the receptors affects DNA binding, ChIP experiments were performed. These demonstrated that AR binding to DNA is enhanced when ERα is inhibited by antioestrogens, especially FULV.

Throughout the experiments, FULV was found to have a more potent effect upon AR-ERα crosstalk compared to TAM. This difference between the two antioestrogens could be attributed to several factors. Firstly, the mechanism of ERα inhibition by TAM is different to FULV. TAM binds to ERα and folds the ligand pocket in a way that results in a confirmational change that antagonists receptor activity, but DNA binding is still possible (Patel and Bihani, 2018). In contrast, FULV inhibits every step of the ERα signalling pathway (i.e., inhibition of dimerization, coactivator recruitment and DNA binding, and enhances ERα degradation). Secondly, because ERα is inhibited, and cannot interact with AR or AREs, AR can bind to response elements more readily.

Thirdly, because ERα cannot recruit any of the shared cofactors, AR can recruit them and become more active.

It has been reported that AR expression levels remains relatively similar throughout disease progression from primary tumours to metastasis sites (Hickey, Selth, et al., 2021), and the AR/ERα ratio could be a potential predictor for disease progression (Rangel et al., 2018). To investigate what effect hormones and antioestrogens had on receptor levels immunoblotting was performed. These assays demonstrated that AR levels remained relatively similar in TAM treated samples, and ERα levels decreased to a lesser extent as compared to FULV treated samples. On the other hand, AR levels increased significantly in samples that were treated with FULV, in which ERα expression levels decreased significantly. It has been suggested that AR can mimic ERα's function and facilitate the transcription of proliferative ERα targets, when ERα is expressed at low levels or not expressed at all (Rangel et al., 2020). In agreement with this, it has also been shown that AR drives the proliferation and aggressiveness of molecular apocrine tumours (Doane et al., 2006). Indeed, the proliferation assays data presented here have also demonstrated that AR can reverse the inhibitory effect of antioestrogen FULV, on E2-induced BrCa cell proliferation.

Long term colony formation assays that were conducted with MCF7 and T47D showed that, long term exposure to the ligands have different effects on these cell lines. For example, MIB was found to be inhibitory to T47D cell growth as compared to control and E2 treatment, whereas the proliferation of MCF7 cells in response to MIB was similar to control or E2-treated samples. Interestingly, MIB did not have an inhibitory effect on E2-induced proliferation in either cell line in these longer-term assays. Hence, it could be postulated that BrCa cells can overcome the antagonistic effect of AR on ERα over time.

Interestingly, the inhibitory effect of TAM on E2-induced proliferation was significant initially but lost after 5 days in the short-term assays. The effects of TAM upon ERα protein levels also changed over time; immunoblots demonstrated that TAM initially decreased ERα expression levels, but this was reversed by the 7^{th} day exposure. Additionally, TAM was also not able to inhibit E2-induced proliferation in the longer-term assays. It has been shown that TAM can induce pluripotent genes for proliferation in T47D and MCF7, as early as 3 hours after administration (Notas et al., 2015). Long term incubation of endocrine sensitive BrCa cell lines with TAM resulted in resistance to the antioestrogen (Fan et al., 2007; Watanabe et al., 2021). Therefore,

it is possible that the cells can develop mechanisms to overcome tamoxifen inhibition in the long term.

3.4.3 The antiandrogen enzalutamide enhances the inhibitory effect of antioestrogens

Antioestrogen inhibition of ERα, leads to an increase in AR levels, enhanced DNA binding, increased target gene expression and proliferation. In ERα-negative cells, activation of AR by DHT or MIB stimulated cell growth significantly and this was reversed by antiandrogens (Birrell et al., 1995; Garay and Park, 2012). For this reason, the effects of inhibiting AR, using the antiandrogen ENZA, was investigated in MCF7 and T47D. Short term proliferation assays demonstrated that the MIB-induced proliferation of MCF7 cells, when ERα is inhibited by FULV, could be successfully reversed through the addition of ENZA. This also confirmed that this pro-proliferative effect of MIB was mediated by AR.

Western blots showed a marked increase in AR levels in the presence of the antioestrogens, especially FULV. This increase in AR levels was abrogated by the addition of ENZA. Interestingly, patients who have received AI therapy for a long period were found to have higher AR levels (Aceto et al., 2018). Overexpression of AR has also been shown to promote TAM resistance (de Amicis et al., 2010). The immunoblots presented here also showed that AR expression increases in samples that were treated with antioestrogens as compared to MIB and E2 treated samples. Further, the proliferation assays demonstrated that MIB could reverse the inhibitory effect of the antioestrogen FULV on E2-induced BrCa cell proliferation. Therefore, increasing AR levels could be a mechanism of therapy resistance in ERα-dependent tumours, when ERα is inhibited.

The results demonstrated that the addition of ENZA to TAM and FULV treated samples inhibited the proliferation of cells in long term colony formation assays. Inhibition of AR alongside with ERα could therefore be a viable option to treat ERα-positive BrCa and prevent therapy resistance.

Chapter 4

Transcriptome Analysis of AR-ERα crosstalk in MCF7 and T47D

Transcriptome Analysis of AR-ERα crosstalk in MCF7 and T47D

4.1 Introduction

It has been shown that patients with ERα-positive tumours, which express high AR levels, have better outcome in terms of disease-free survival, lower tumour grade, and low lymph node metastasis (Peters et al., 2009; Vera-Badillo et al., 2014). However, it was found that AR expression in patients, who received adjuvant endocrine therapy, was lower in metastases compared to the primary tumour (Schrijver et al., 2017). It was also shown that patients treated with AI for a long time (average = 725 days) were found to have higher AR levels than those who had received AI treatment for a shorter time period (average = 85 days). Further, AR signalling was the most activated pathway in circulating tumour cells (CTCs) derived from bone metastases in ERα-positive patients' bloods (Aceto et al., 2018). These studies suggest that the crosstalk between AR and ERα is affected by endocrine therapies and that this could change the transcriptome in BrCa cells which may therefore affect tumour aggressiveness/progression and alternative therapeutic approaches could be more beneficial for patients.

To date, more than 1,900 microRNAs (miRNAs) have been identified in the human genome (miRBase database release 22.1, October 2018), and it has been shown that miRNAs play a key role in gene expression, cell differentiation and development, regulation of various biological pathways including oncogenic signalling, acting as a tumour suppressor (tsmiR) or as an oncogene (oncomiR) (Peng and Croce, 2016). Studies have shown that oncomiRs are mostly upregulated, and tsmiRs mostly downregulated in BrCa (Singh and Mo, 2013; Loh et al., 2019). For this reason, miRNA have been proposed as potential diagnostic/prognostic biomarkers and also therapeutic targets. The AR has also emerged as a possible therapeutic target in BrCa; however, little is known about the relationship between microRNAs and AR in the disease. This chapter will focus on the transcriptomic changes as a result of AR-ERα crosstalk, and miRNA regulation by androgen and oestrogen in MCF7 and T47D cells.

4.2 RNA-Seq Analysis of the effects of fulvestrant treatment on AR signalling in endocrine sensitive breast cancer cells

As it has been demonstrated in Chapter 3, the AR becomes more active in the presence of a SERD. To further analyse the effects of FULV on AR-ERα crosstalk on the transcriptome of endocrine sensitive BrCa cell lines, RNA-Seq analysis was performed on MCF7 and T47D. Cells were grown in hormone-depleted media for 72 hours, treated with different combinations of the ligands EtOH (control), MIB (1 nM), E2 (1 nM) and/or FULV (100 nM) for 24 hours. Total RNA was extracted, cDNA synthesis and qPCR analysis of AR and ERα target genes was performed prior to the samples being sent for sequencing. The quality of RNA was visualised by running the samples on a 1% agarose TBE gel. Two clear bands for ribosomal RNA were confirmed, and degradation was not observed (Figure 4-1). The RNA integrity number (RIN) of each sample was also quantified using a Qubit (Table 4-1) and all were found to be above the required cut-off of 6. 3 independent replicates per treatment group were sent for library preparation and sequencing (Novogene, UK). The quality of raw reads was checked with fastQC (Version 0.11.7) (Ewels et al., 2016) (Appendix Figure 7-1) and reads were mapped to a reference human genome (GRCh38) using the STAR tool (Version 2.7.3a). Subsequently, read counts of the genes were used to calculate differentially expressed genes (DEGs) by DESeq2 (Version 1.28.1) in R (Version 4.0.3). The distribution of the normalised reads for each group comparison were visualised using MA plots. Only genes with a large mean normalised count were considered to be significant. A representative plot for each cell line has been provided (Appendix Figure 7-2). Genes with adjusted p-value (padj) < 0.01 and $\log_2$ Fold Change (log2FC) > 1 were accepted as DEGs. The number of DEGs across all group comparisons are summarised in Table 4-2.

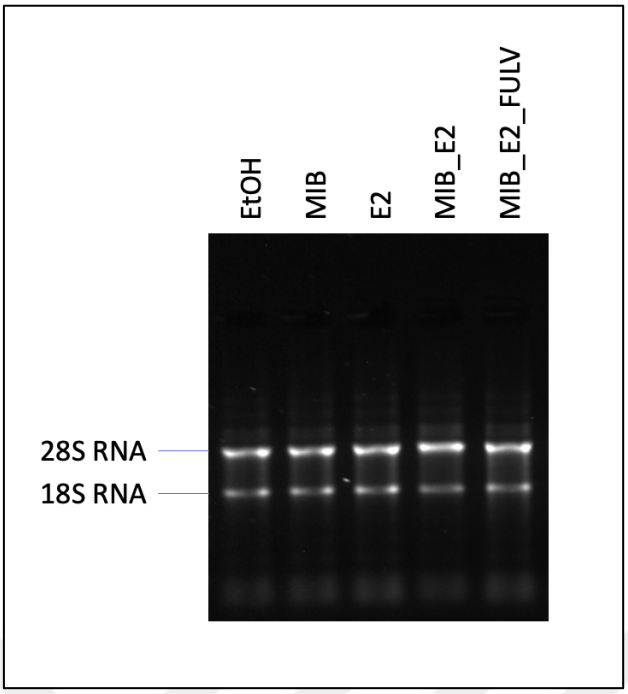

Figure 4-1 Gel electrophoresis of RNA-Seq samples

Cells were incubated in hormone-depleted media for 72 hours. Cells were then treated with vehicle control (Ethanol, EtOH) or different combinations of MIB (Mibolerone, 1 nM), E2 (Oestradiol, 1 nM), FULV (Fulvestrant, 1 nM) for 24 hours. RNA was harvested using New England Biolab Total RNA extraction kit. 2 µg of extracted total RNA samples were run on a 1% TBE agarose gel and samples were visualised using a gel doc system. The 18S and 28S ribosomal RNA bands were visualised for each RNA sample (Representative image provided).

Table 4-1 RNA Integrity Numbers of RNA samples

Control: EtOH, MIB: Mibolerone, E2: Oestradiol, MIB_E2: Mibolerone + Oestradiol, MIB_E2_FULV: Mibolerone + Oestradiol + Fulvestrant

Sample	RIN Scores					
	T47D			MCF7		
	Replicate 1	Replicate 2	Replicate 3	Replicate 1	Replicate 2	Replicate 3
EtOH (Control)	8.3	8.3	8	8.1	7.2	8.2
MIB	7.5	7.6	7.8	8	7.7	7.9
E2	7.9	7.6	8.2	8.1	7.8	8.2
MIB_E2	9	7.7	8.4	6.9	8.3	8.4
MIB_E2_FULV	7.5	8	8.2	6	7.7	8

Table 4-2 Number of Differentially Expressed Genes Across Treatment Groups

MCF7 and T47D cells were incubated in hormone-depleted media for 72 hours. Cells were treated with vehicle control (Ethanol, EtOH) or different combinations of MIB (Mibolerone, 1 nM), E2 (Oestradiol, 1 nM), FULV (Fulvestrant, 1 nM) for 24 hours, and RNA harvested. 3 independent replicates per treatment group were sent for library preparation and sequencing (Novogene). The quality of raw reads was checked with fastQC (Version 0.11.7), and reads were mapped to a reference human genome (GRCh38) using the STAR tool (Version 2.7.3a). Subsequently, read counts were used to calculate differentially expressed genes (DEGs) using DESeq2 (Version 1.28.1) in R (Version 4.0.3). Genes with adjusted p-value (padj) < 0.01 and log_2 Fold Change (log2FC) > 1 were accepted as DEGs. Up: Upregulated genes, Down: Downregulated Genes.

Group comparisons	MCF7			T47D		
	Up	Down	Total	Up	Down	Total
MIB vs CONTROL	148	39	187	711	522	1233
E2 vs CONTROL	68	24	92	337	250	587
MIB_E2 vs CONTROL	207	101	308	879	797	1676
MIB_E2_FULV vs CONTROL	183	208	391	836	819	1655
E2 vs MIB	137	213	350	657	739	1396
MIB_E2 vs MIB	62	33	95	148	77	225
MIB_E2_FULV vs MIB	6	111	117	22	22	44
MIB_E2 vs E2	114	31	145	736	636	1372
MIB_E2_FULV vs E2	373	442	815	771	756	1527
MIB_E2_FULV vs MIB_E2	216	363	579	14	102	116

PCA plots demonstrated that the variation in the gene expression data across samples is driven primarily by the treatment (Figure 4-2). The most distinct groups in both T47D and MCF7 are E2-treated cells and cells treated with MIB_E2_FULV, suggesting that the transcriptome changes most significantly when ERα is inhibited by FULV, and AR is activated by its ligand (Figure 4-2A, B). Interestingly co-treatment of MIB and E2 had a more similar projection with control in MCF7, whereas in T47D the projection of MIB_E2 were closer to MIB and MIB_E2_FULV.

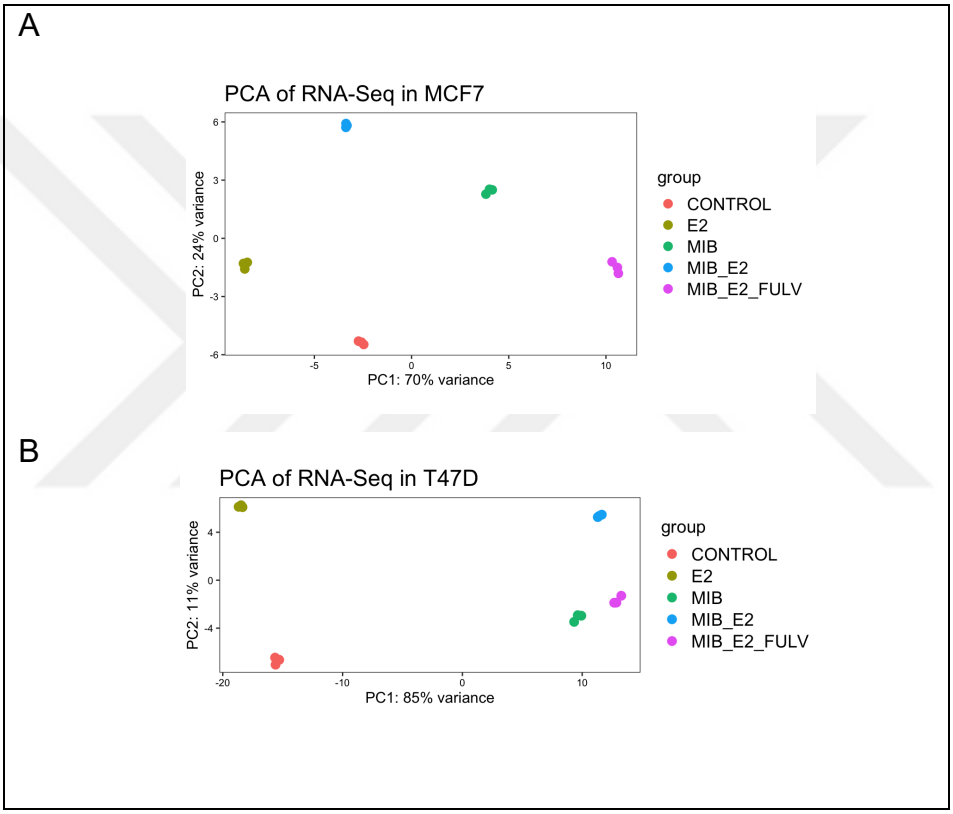

Figure 4-2 Principal Component Analysis of Treatment Groups

Variation in the gene expression data across samples is driven by different treatment groups. Read counts of the genes in different treatment groups in (A) MCF7 and (B) T47D cells were transformed to the log2 scale using rlog and then plotted using plotPCA (DESeq2 version 1.28.1). Numbers in parentheses indicate the percentage of variance explained by each axis. (Control: EtOH, MIB: Mibolerone, E2: Oestradiol, MIB_E2: Mibolerone + Oestradiol, MIB_E2_FULV: Mibolerone + Oestradiol + Fulvestrant)

To identify DEGs, the treatment groups were compared to the control samples and each other, and a heatmap with unsupervised clustering was generated for each cell line. It was found that across samples, T47D had 2936 DEGs, and MCF7 had 1162 DEGs. The DEGs for MIB, MIB_E2 and MIB_E2_FULV groups showed a similar pattern in T47D (Figure 4-3), whereas in MCF7 it can clearly be seen that the genes that were upregulated by MIB were upregulated further in MIB_E2_FULV, and the genes that were downregulated by MIB were downregulated further in MIB_E2_FULV (Figure 4-4).

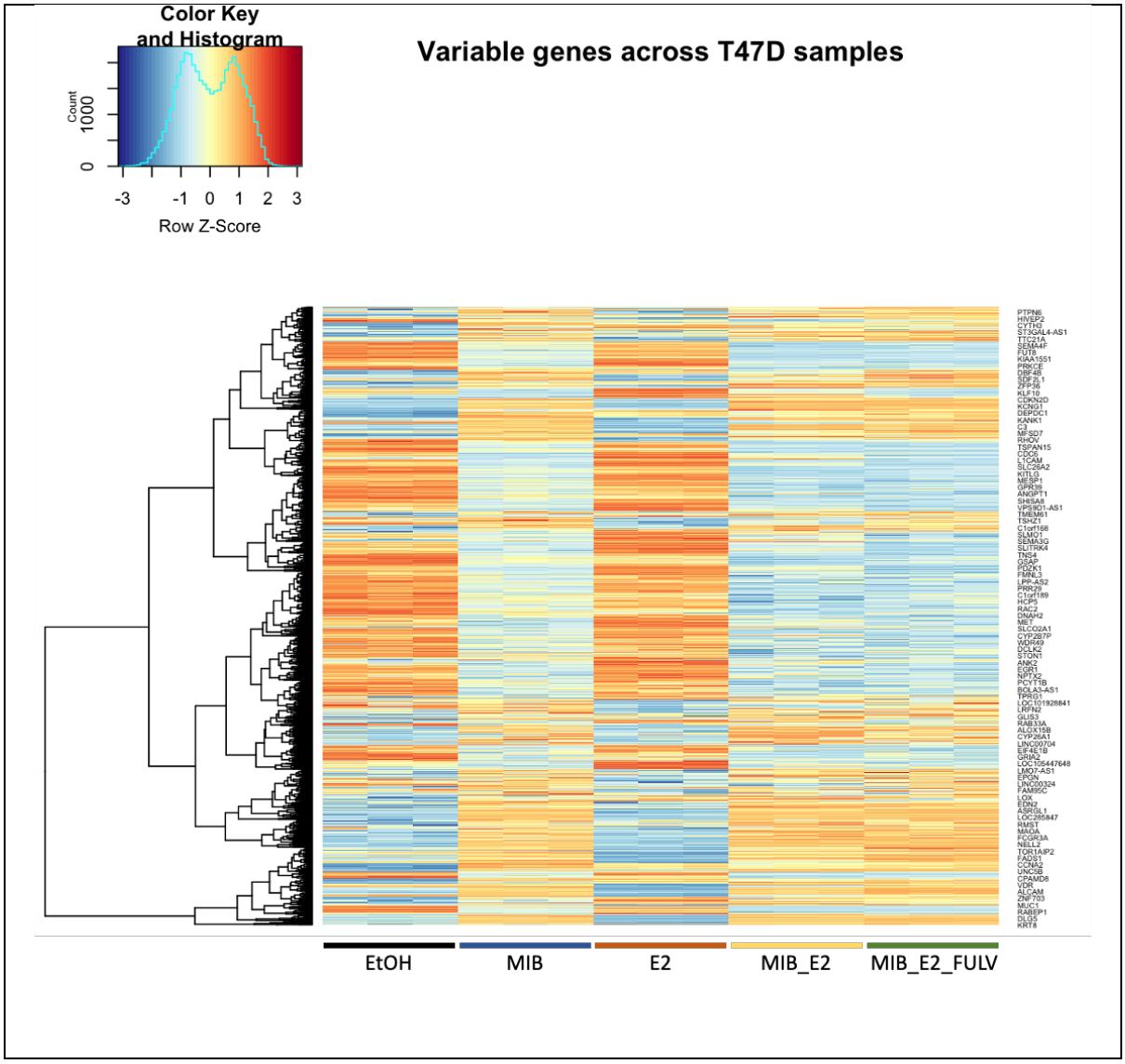

Figure 4-3 Heatmap of differentially expressed genes in T47D cells

The transcriptome changes in response to different treatment groups were analysed by RNA-Seq. Differential expressed genes (DEGs) were analysed using DESeq2. Genes with padj < 0.01 and log2Fold Change > 1 were considered as DEGs. A heatmap indicating all the DEGs in across different treatment group samples (n = 2936). Control: EtOH, MIB: Mibolerone, E2: Oestradiol, MIB_E2: Mibolerone + Oestradiol, MIB_E2_FULV: Mibolerone + Oestradiol + Fulvestrant.

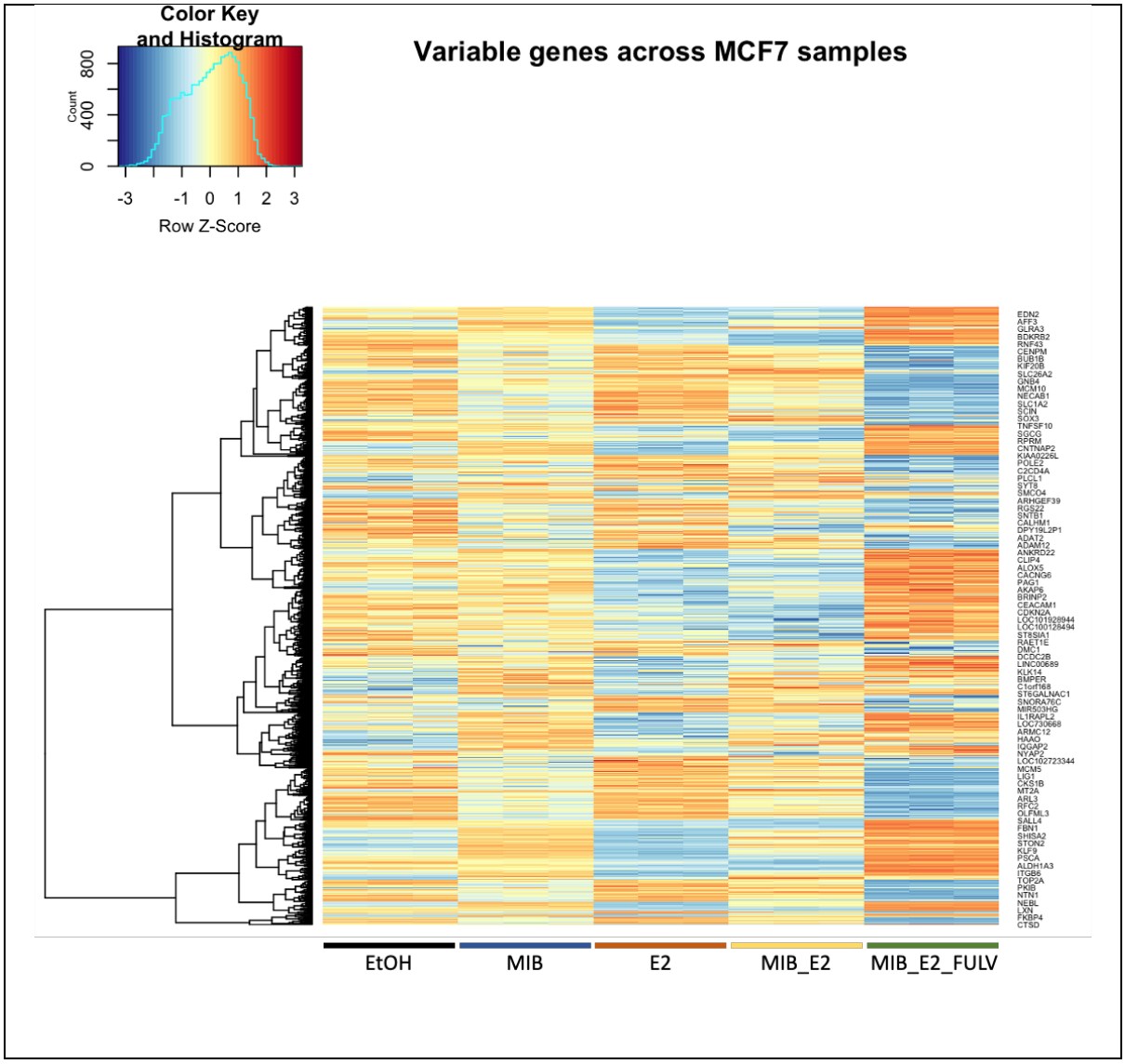

Figure 4-4 Heatmap of differentially expressed genes in MCF7 cells

The transcriptome changes in response to different treatment groups were analysed by RNA-Seq. Differential expressed genes were analysed using DESeq2. Genes with padj < 0.01 and log2FoldChange > 1 were considered as differentially expressed genes (DEGs). A heatmap indicating all the DEGs in across different treatment group samples (n = 1162). Control: EtOH, MIB: Mibolerone, E2: Oestradiol, MIB_E2: Mibolerone + Oestradiol, MIB_E2_FULV: Mibolerone + Oestradiol + Fulvestrant.

The DEGs for each treatment group, as compared to control, were analysed for intersections to further see the effects of treatments on the transcriptome, and identify the genes that are regulated by AR when the ERα inhibition is lifted by FULV in MCF7 and T47D. The intersection graphs show the number of DEGs for a treatment group and how many of those DEGs are unique to that treatment arm, or overlap with other treatment groups. The greatest number of unique DEGs was found following treatment MIB_E2_FULV, for both MCF7 and T47D (235 and 228 DEGs respectively) (Figure 4-5, Figure 4-6). 68% of MIB-only regulated DEGs (129 out of 187) were common with DEGs in MIB_E2_FULV in MCF7, and 88% (1097 out of 1233) in T47D. In MCF7, 22 genes were found to be regulated by MIB and E2 mutually. As the overall number of DEGs was higher in T47D, this overlap in genes was also found to be higher for T47D; 232 genes were found to be regulated by both MIB and E2.

Surprisingly, when the gene expression profiles of each treatment group were interrogated further (analysed as up- or downregulated DEGs) the expression of none of the E2-upregulated DEGs and only 1 E2-downregulated DEG (*AKAP12*) was reversed in response to co-treatment with MIB (E2 v E2_MIB) in MCF7 (Figure 4-7). However, in T47D, 13 of the E2-upregulated DEGs were downregulated, and 21 E2-downregulated DEGs were upregulated by following co-treatment with MIB (Figure 4-8). Similarly, none of the MIB-upregulated DEGs were downregulated by MIB_E2 in MCF7 and there were only 2 DEGs down-regulated in T47D. Further, none of the MIB-downregulated genes were upregulated by MIB_E2 in either of the cell lines. The small number of genes found to be regulated when comparing the mono-treatment versus the co-treatment might be because these DEGs were identified when comparing the treatment groups with control. However, 24 E2-upregulated DEGs were found to be downregulated in the presence of FULV in MCF7 and this was 44 for T47D. Further, in T47D 28 E2-downregulated DEGs were upregulated in response to MIB_E2_FULV, whereas only 3 DEGs followed this trend in MCF7 (Figure 4-7, Figure 4-8).

In conclusion, it was found that number of genes which were regulated by AR in MIB_E2_FULV were unique to this condition only, demonstrating that the AR becomes transcriptionally more active when ERα is inhibited by FULV.

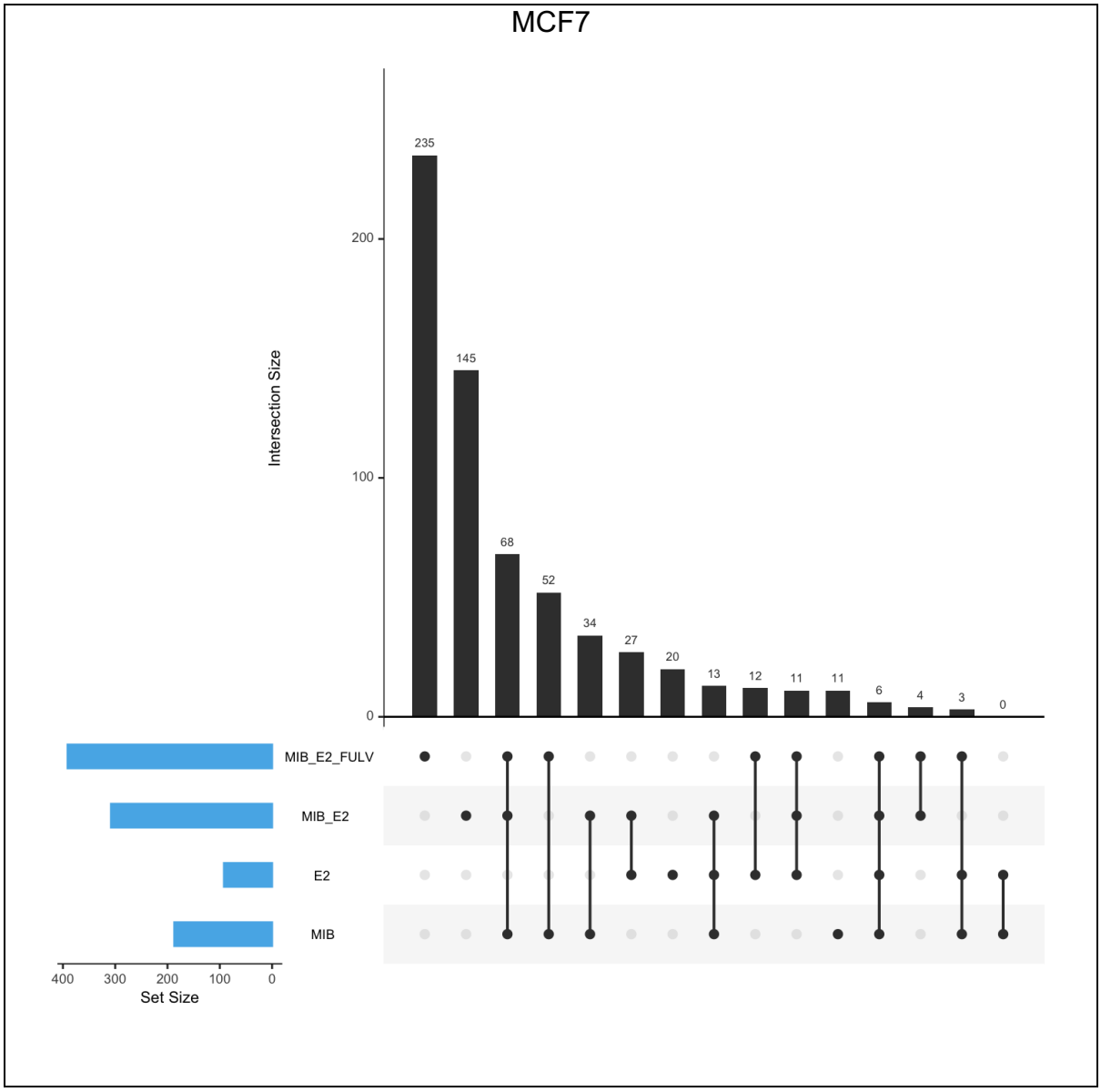

Figure 4-5 Comparison of differentially expressed genes across treatment groups in MCF7

The transcriptome changes in response to different treatment groups were analysed by RNA-Seq. Differentially expressed genes (DEGs) were analysed using DESeq2. Genes with padj < 0.01 and log2FoldChange > 1 were considered as DEGs. A bar chart indicating all the common and unique DEGs across treatment groups samples (n = 641). Control: EtOH, MIB: Mibolerone, E2: Oestradiol, MIB_E2: Mibolerone + Oestradiol, MIB_E2_FULV: Mibolerone + Oestradiol + Fulvestrant.

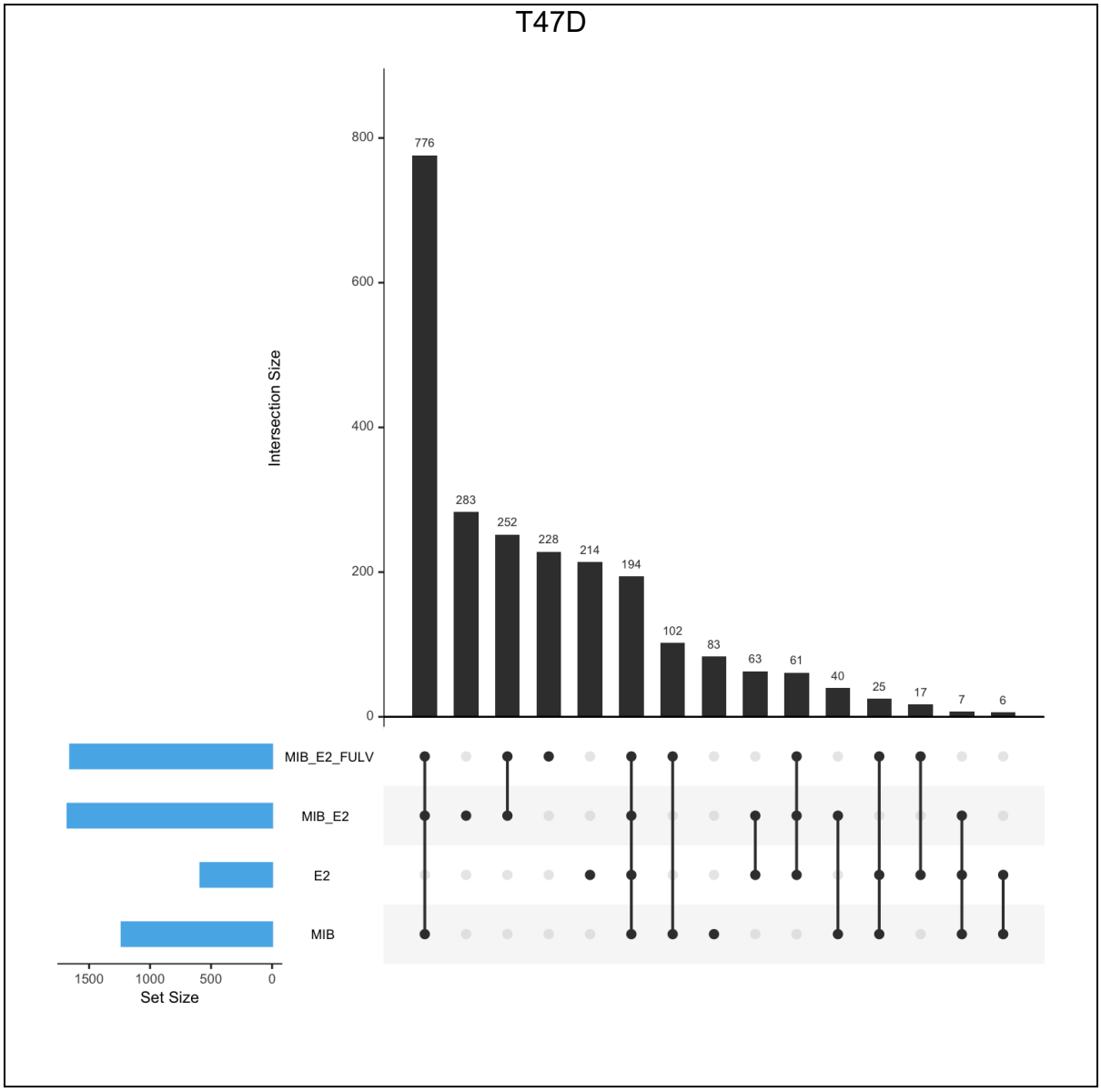

Figure 4-6 Comparison of differentially expressed genes across treatment groups in T47D

The transcriptome changes in response to different treatment groups were analysed by RNA-Seq. Differential expressed genes (DEGs) were analysed using DESeq2. Genes with padj < 0.01 and log2Fold Change > 1 were considered as DEGs. A bar chart indicating all the common and unique DEGs across treatment groups samples (n=2351). MIB: Mibolerone, E2: Oestradiol, MIB_E2: Mibolerone + Oestradiol, MIB_E2_FULV: Mibolerone + Oestradiol + Fulvestrant.

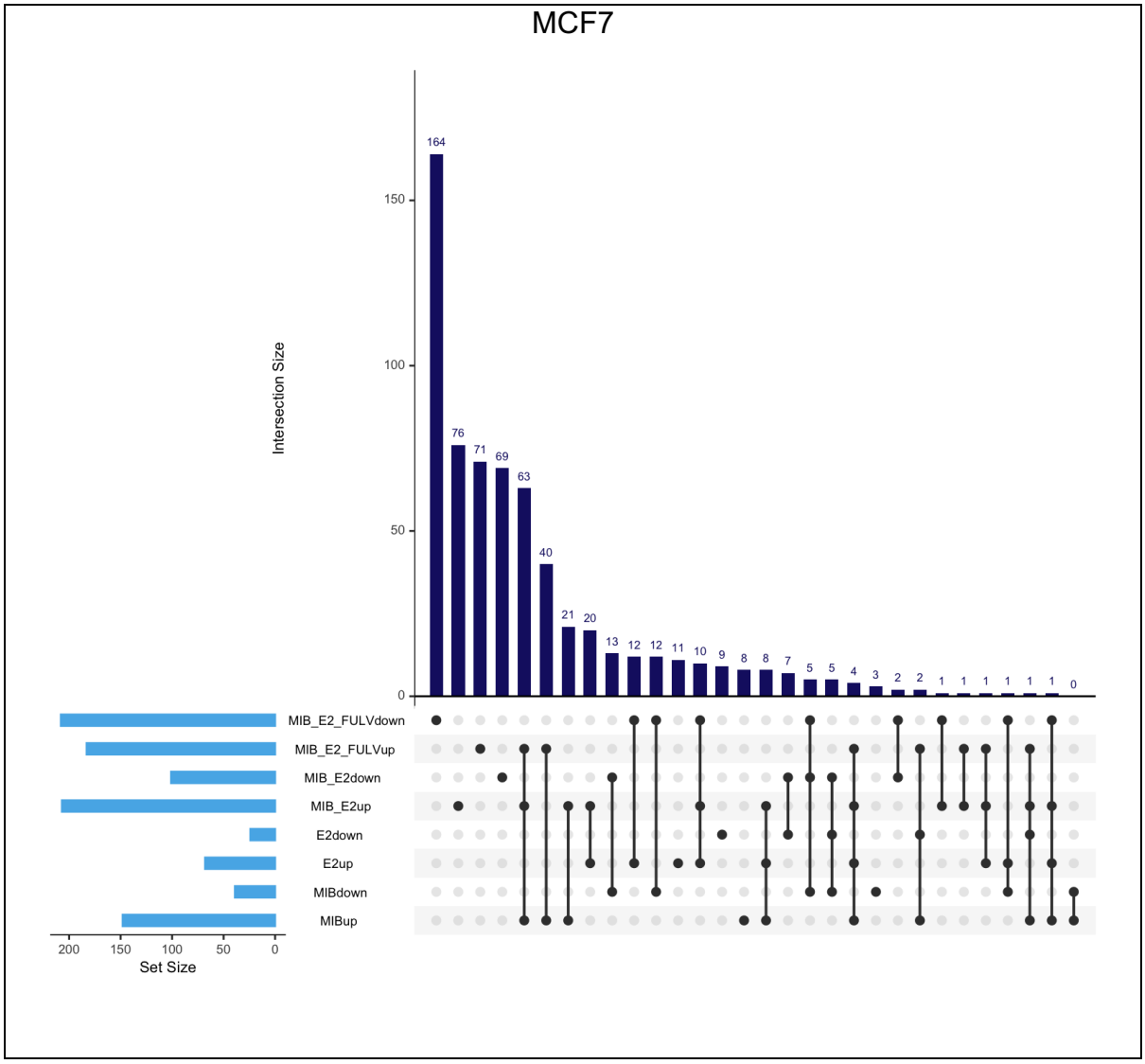

Figure 4-7 Comparison of up and downregulated gene numbers under different treatments in MCF7

The transcriptome changes in response to different treatment groups were analysed by RNA-Seq. Differentially expressed genes (DEGs) were analysed using DESeq2. Genes with padj < 0.01 and log2FoldChange > 1 were considered as DEGs. List of DEGs were extracted from the comparison of different treatments to control. A bar chart indicating all the common and unique DEGs across treatment groups samples (n = 641). MIB: Mibolerone, E2: Oestradiol, MIB_E2: Mibolerone + Oestradiol, MIB_E2_FULV: Mibolerone + Oestradiol + Fulvestrant. Up: upregulated DEGs, down: downregulated DEGs.

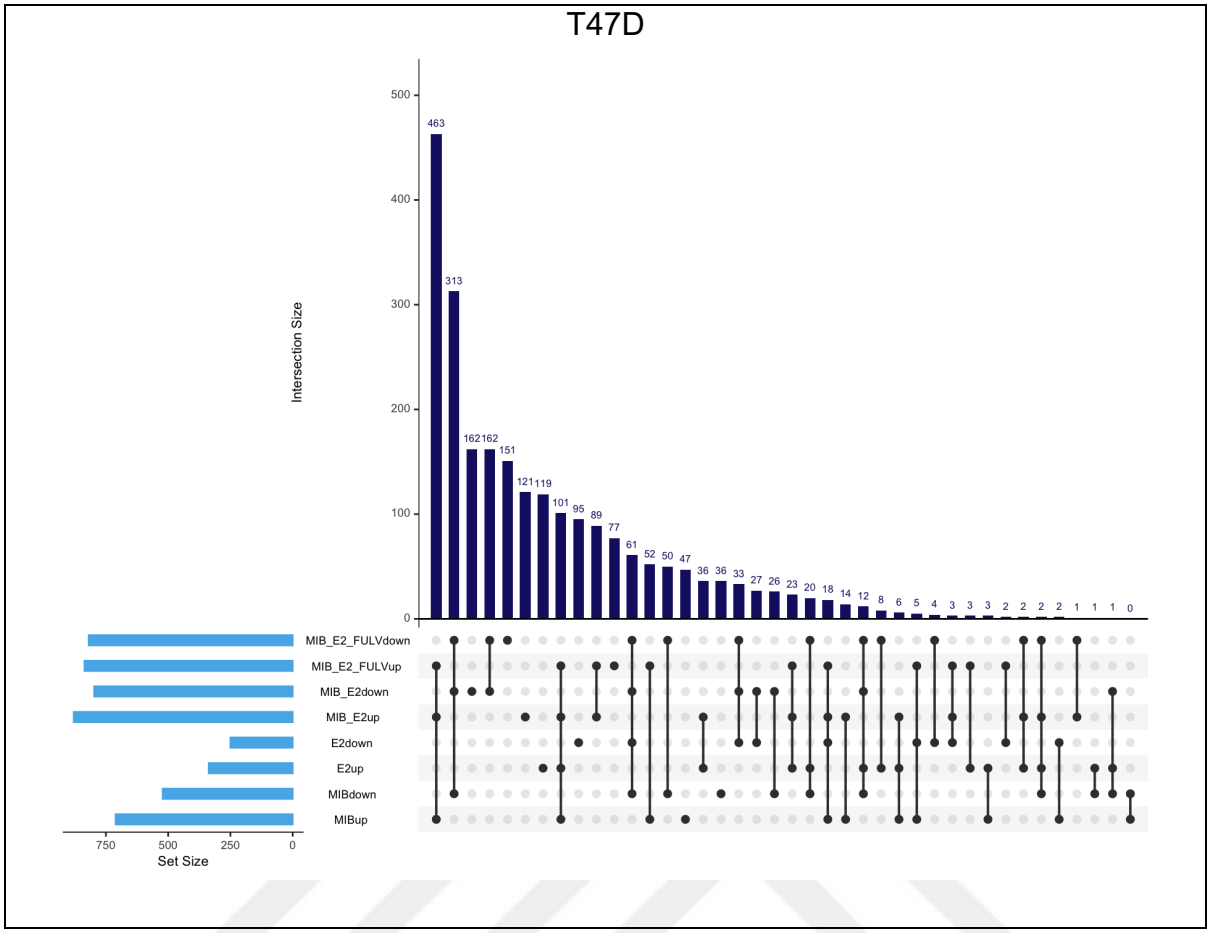

Figure 4-8 Comparison of up and downregulated gene numbers under different treatments in T47D

The transcriptome changes in response to different treatment groups were analysed by RNA-Seq. Differentially expressed genes (DEGs) were analysed using DESeq2. Genes with padj < 0.01 and log2FoldChange > 1 were considered as DEGs. List of DEGs were extracted from the comparison of different treatments to control. A bar chart indicating all the common and unique DEGs across treatment groups samples (n = 2351). MIB: Mibolerone, E2: Oestradiol, MIB_E2: Mibolerone + Oestradiol, MIB_E2_FULV: Mibolerone + Oestradiol + Fulvestrant. Up: upregulated DEGs, down: downregulated DEGs.

4.3 The effects of FULV on androgen and oestrogen regulated DEGs in T47D and MCF7 cells

To investigate the changes in MIB- or E2-regulated transcriptomes 3 subsequent comparisons were made. Firstly, MIB or E2 treated samples were compared to the control samples; secondly, MIB_E2 samples were compared to MIB or E2 samples; and thirdly, MIB_E2_FULV samples were compared to MIB_E2 samples (Appendix Table 7-1, Table 7-2, Table 7-3, Table 7-4).

4.3.1 The effects of FULV on androgen and oestrogen regulated DEGs in T47D cells

To visualise gene expression changes, volcano plots were generated (Figure 4-9) and to investigate potential overlaps in gene expression profiles, intersection graphs were plotted (Figure 4-10). Comparison of MIB and control-treated cells found that AR target genes such as *ZBTB16*, *PSCA* were upregulated and some ERα targets (*CXCL12*, *KCNK5*) were downregulated in response to the androgen (Figure 4-9A). Co-treatment of E2 and MIB regulation of gene expression was similar to MIB only, evidenced by fewer genes found to be differentially regulated (Figure 4-9B, Figure 4-10). To investigate what effect antioestrogens have on this crosstalk, the samples treated with MIB, E2 and FULV (MIB_E2_FULV) were compared to those treated with MIB_E2 (Figure 4-9C). The addition of FULV resulted in an increase in the number of genes found to be downregulated. Interestingly, comparison of MIB_E2_FULV with MIB, found that both treatment conditions had similar effects on the transcriptome of T47D cells (Figure 4-9D). In total, only 44 genes were found to be differentially expressed between the 2 treatment groups (22 upregulated, 22 downregulated). Comparison of E2 and control samples found that E2 downregulated 250 genes and upregulated total of 337 genes including proliferative genes such as *CXCL12*, *SERPINA6*, *GATA4* (Figure 4-9E), which were downregulated in MIB_E2 compared to E2 samples. The addition of MIB to E2-treated samples altered the number of genes significantly, a total of 736 genes were upregulated, including genes that are related to other signalling pathways such as *NOTCH2*, *CYP27A1*; and 636 were downregulated including genes such as *PIK3CD*, *BCL2*, *TGFB2* (Figure 4-9F).

DEGs were then analysed further, to investigate the ones that were solely induced by MIB, common amongst treatment groups, had no change in their expression in response to E2, and following ERα inhibition in response to FULV treatment (Figure 4-10).

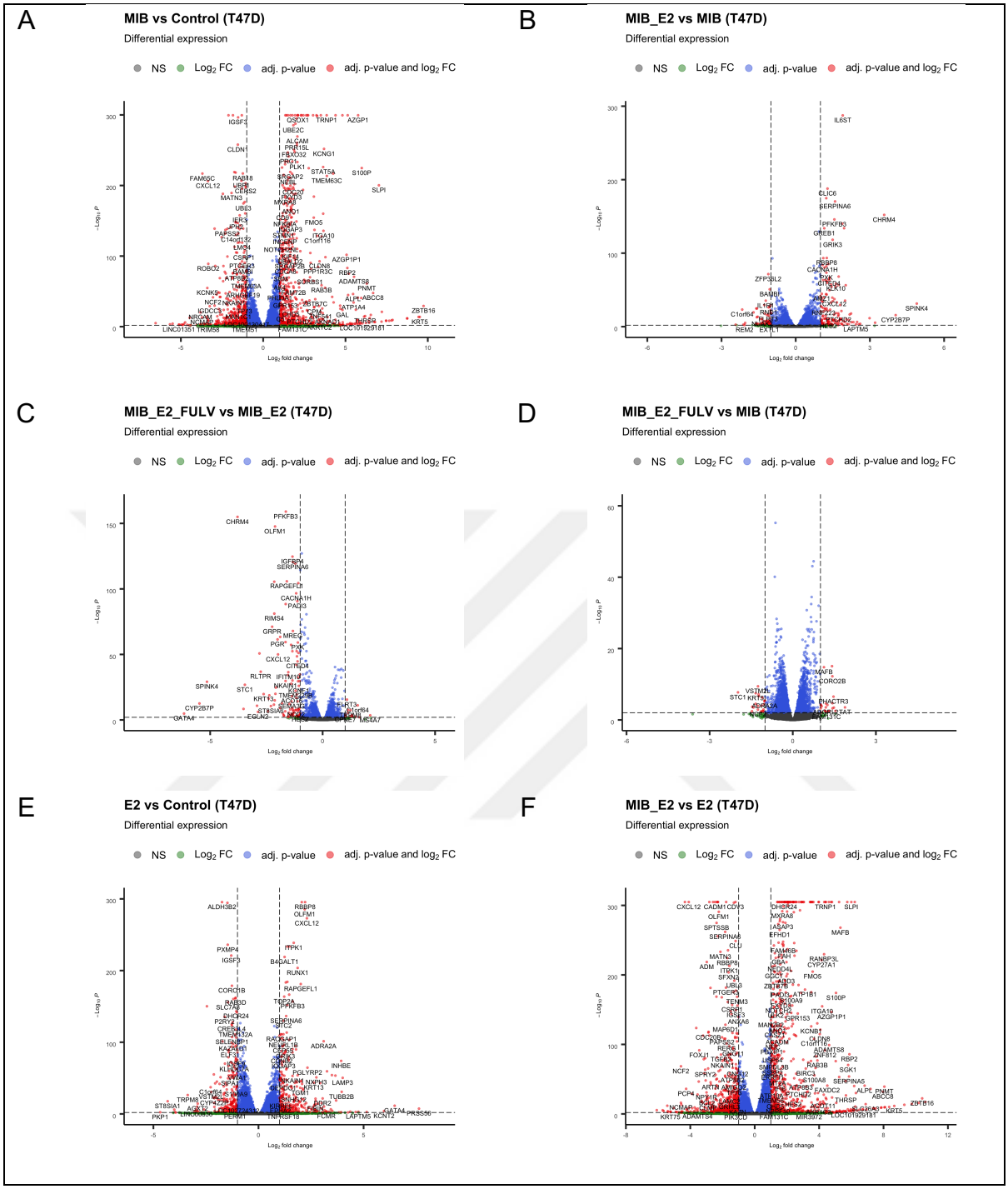

Figure 4-9 The effects of androgen, oestrogen and fulvestrant treatments on the T47D transcriptome

T47D cells were incubated in hormone-depleted media for 72 hours. Cells were then treated with vehicle control (Ethanol, EtOH) or different combinations of MIB (Mibolerone, 1 nM), E2 (Oestradiol, 1 nM), FULV (Fulvestrant, 1 nM) for 24 hours. RNA was harvested. 3 independent replicates per treatment group were conducted. The transcriptome changes in response to different treatments were analysed by RNA-Seq. Differentially expressed genes (DEGs) were analysed using DESeq2 (version 1.28.1) and visualised as volcano plots using EnhancedVolcano (Version 1.6.0). Cut-off values are padj < 0.01 and log2FoldChange > 1. Volcano plots showing DEGs, comparing (A) MIB versus control, (B) MIB_E2 versus MIB, (C) MIB_E2_FULV versus MIB_E2, (D) MIB _E2_FULV versus MIB, (E) E2 versus control, (F) MIB_E2 versus E2. Control: EtOH, MIB: Mibolerone, E2: Oestradiol, MIB_E2: Mibolerone + Oestradiol, MIB_E2_FULV: Mibolerone + Oestradiol + Fulvestrant.

The majority of the genes that were upregulated by MIB were not affected by E2 in either of the cell lines. In T47D, only 6 MIB-induced genes in total were found to be downregulated when E2 was added (*CPNE7*, *FLRT3*, *TM4SF18*, *SORBS1*, *TSPEAR*, *PRICKLE4*), 3 of which were upregulated again when the ERα was inhibited by FULV (*CPNE7*, *FLRT3*, *TM4SF18*). For these genes therefore, when ERα is inhibited, the repressive crosstalk upon AR was found to be lost, leading to the transcription of these factors (Figure 4-10).

In T47D, 27.8% of E2-upregulated DEGs were found to be downregulated in MIB_E2, and 25.2% of E2-downregulated DEGs were found to be upregulated in MIB_E2 in T47D (Figure 4-11). Three genes that were downregulated in response to E2 (*C1orf64*, *KCNC1*, *MS4A7*) were upregulated when ERα was inhibited (MIB_E2_FULV). 32 additional DEGs were found in MIB_E2_FULV, as compared to MIB_E2.

Seventeen genes (*PTCHD2*, *ACOT11*, *TNNI2*, *RLTPR*, *KLK10*, *TUBA3E*, *DEFB132*, *MAP1B*, *MAN1A1*, *GJA1*, *ADGRA2*, *KRT5*, TGM2, *COL6A2*, *ASPHD2*, *SEC14L2*, *CMTM7*) which were upregulated by MIB only treatment, were found to be downregulated in MIB_E2_FULV; and some genes (*C1orf64*, *KCNC1*, *FOXN*, *MS4A7*, *KRT81*) that were downregulated by MIB, were upregulated in MIB_E2_FULV in T47D (Figure 4-10). This suggests that the transcriptional activity of certain genes can change from upregulatory to downregulatory when ERα is inhibited, and vice versa.

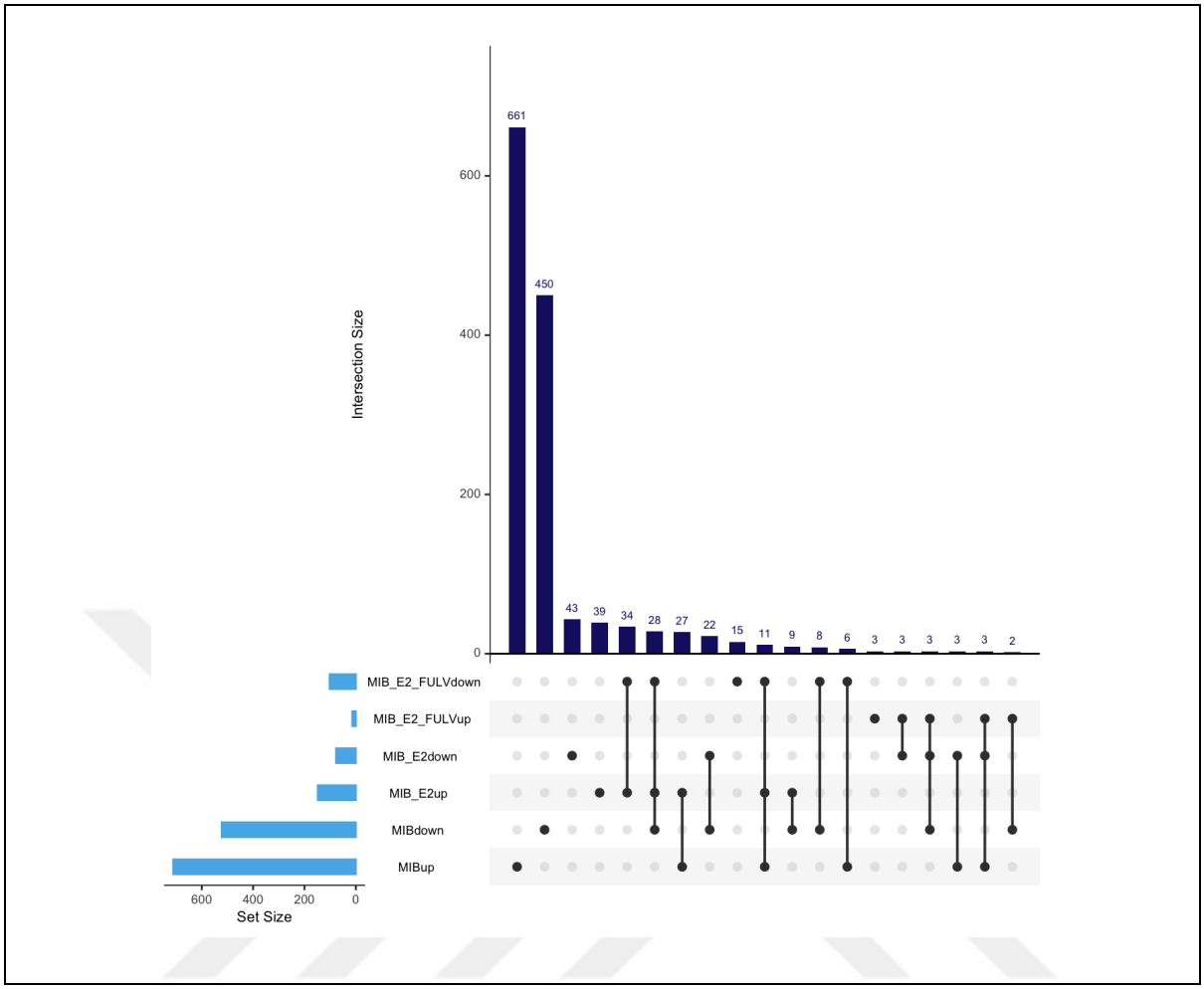

Figure 4-10 Identification of DEGs commonly regulated by MIB, and additional treatment combinations, in T47D

T47D cells were incubated in hormone-depleted media for 72 hours. Cells were then treated with vehicle control (Ethanol, EtOH) or different combinations of MIB (Mibolerone, 1 nM), E2 (Oestradiol, 1 nM), FULV (Fulvestrant, 1 nM) for 24 hours. RNA was harvested. 3 independent replicates per treatment group were conducted. The transcriptome changes in response to different treatments were analysed by RNA-Seq. Differentially expressed genes (DEGs) were analysed using DESeq2 (version 1.28.1) and visualised as an UpSetR plot (Version 1.4.0). Common genes between groups are represented as number of intersections via connected dots. Cut-off values for DEGS are padj < 0.01 and log2FoldChange > 1. MIB: Mibolerone, MIB_E2: Mibolerone + Oestradiol, MIB_E2_FULV: Mibolerone + Oestradiol + Fulvestrant. Up: upregulated DEGs, down: downregulated DEGs.

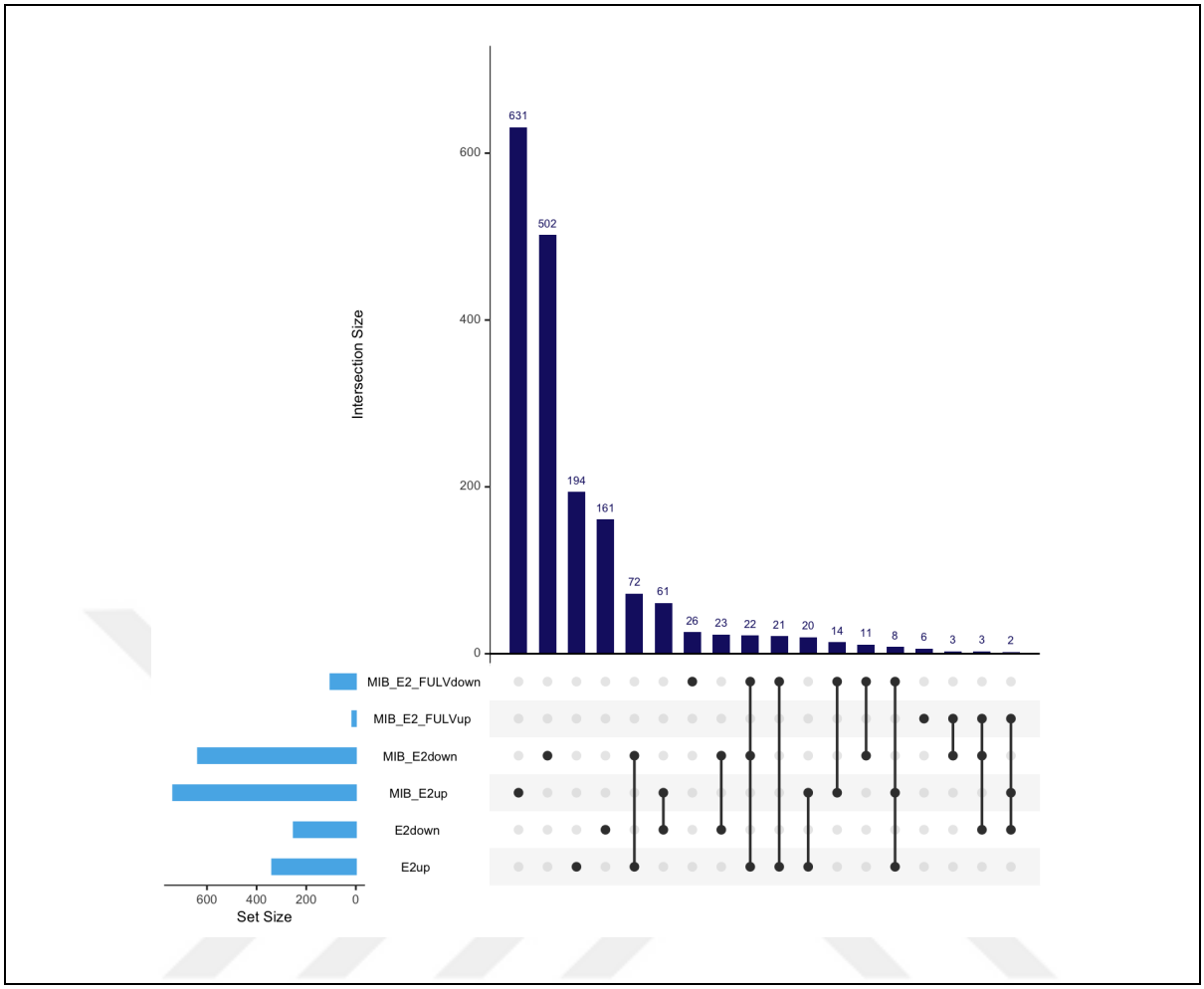

Figure 4-11 Identification of DEGs commonly regulated by E2, and additional treatment combinations, in T47D

T47D cells were incubated in hormone-depleted media for 72 hours. Cells were then treated with vehicle control (Ethanol, EtOH) or different combinations of MIB (Mibolerone, 1 nM), E2 (Oestradiol, 1 nM), FULV (Fulvestrant, 1 nM) for 24 hours. RNA was harvested. 3 independent replicates per treatment group were conducted. The transcriptome changes in response to different treatments were analysed by RNA-Seq. Differentially expressed genes (DEGs) were analysed using DESeq2 (version 1.28.1) and visualised as an UpSetR plot (Version 1.4.0). Common genes between groups are represented as number of intersections via connected dots. Cut-off values for DEGS are padj < 0.01 and log2FoldChange > 1. E2: Oestradiol, MIB_E2: Mibolerone + Oestradiol, MIB_E2_FULV: Mibolerone + Oestradiol + Fulvestrant. Up: upregulated DEGs, down: downregulated DEGs.

4.3.2 The effects of FULV on androgen and oestrogen regulated DEGs in MCF7 cells

In MCF7 cells, MIB was found to upregulate the expression of well-known target genes such as *ZBTB16*, *SEC14L2*, *FKBP5* (Figure 4-12A). Similarly, E2 was also found to upregulate well-known ERα targets (i.e., *CXCL12*, *PGR*, *GREB1*) (Figure 4-12E), validating the approach. Co-treatment of E2 to MIB resulted in the downregulation of several MIB upregulated genes, and E2 upregulated genes (Figure 4-12B). MIB-upregulated DEGs shifted to being predominantly down-regulated when cells were co-treated with MIB, E2 and FULV (Figure 4-12C). Further, the number of genes down-regulated by AR in MIB_E2_FULV was found to be higher than MIB-only treatment, when these treatment groups were compared (Figure 4-12D). Comparison of E2-treated samples to control samples showed that E2 also upregulates some MIB upregulated genes in MCF7 (e.g., *MYBL1*) (Figure 4-12E). Similar to T47D, the addition of MIB to E2 led to an upregulation of AR targets (Figure 4-12F).

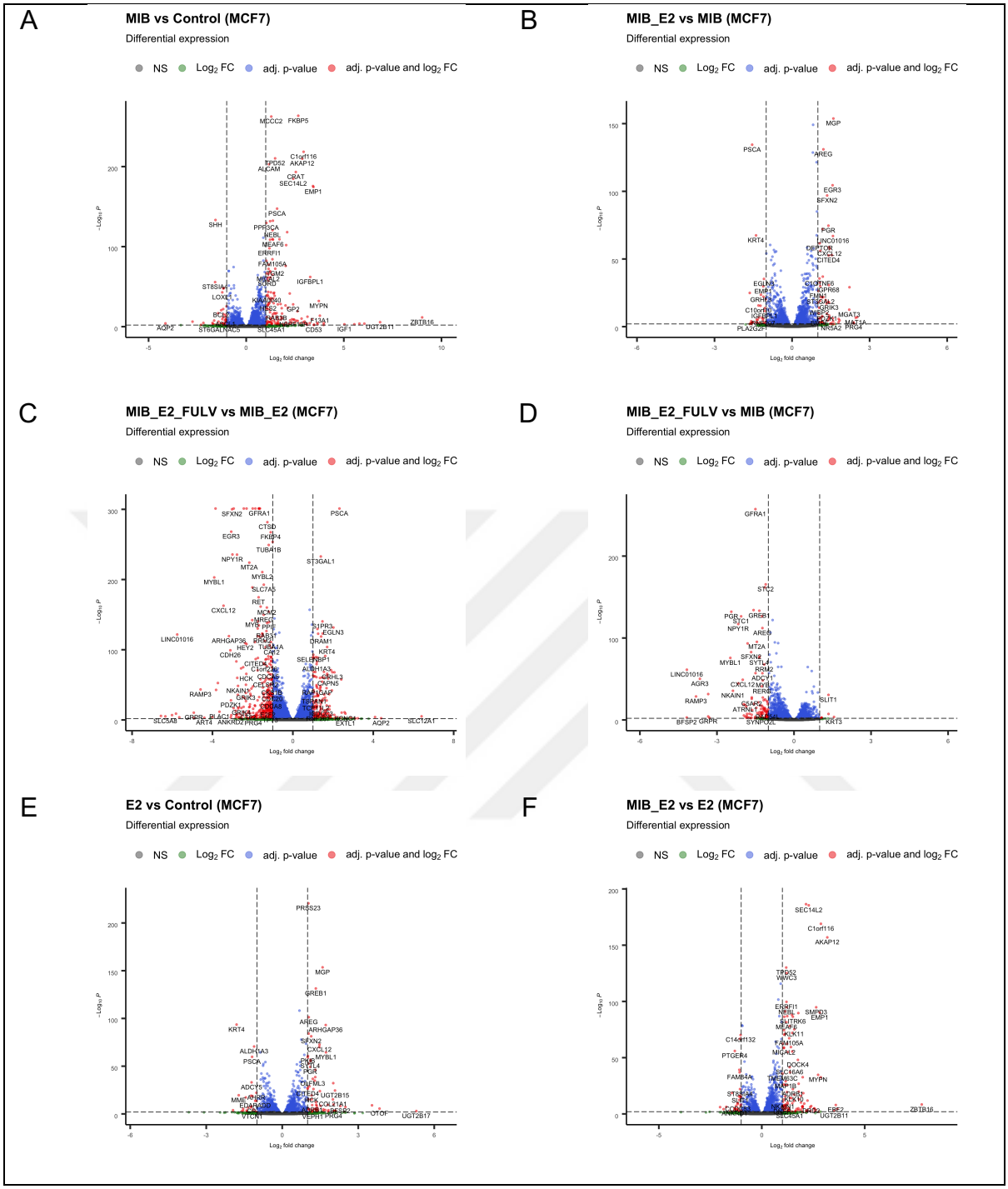

Figure 4-12 The effects of androgen, oestrogen and fulvestrant treatments on the MCF7 transcriptome

MCF7 cells were incubated in hormone-depleted media for 72 hours. Cells were then treated with vehicle control (Ethanol, EtOH) or different combinations of MIB (Mibolerone, 1 nM), E2 (Oestradiol, 1 nM), FULV (Fulvestrant, 1 nM) for 24 hours. RNA was harvested. 3 independent replicates per treatment group were conducted. The transcriptome changes in response to different treatments were analysed by RNA-Seq. Differentially expressed genes (DEGs) were analysed using DESeq2 (version 1.28.1) and visualised as volcano plots using EnhancedVolcano (Version 1.6.0). Cut-off values are padj < 0.01 and log2FoldChange > 1. Volcano plots showing DEGs, comparing (A) MIB versus control, (B) MIB_E2 versus MIB, (C) MIB_E2_FULV versus MIB_E2, (D) MIB _E2_FULV versus MIB, (E) E2 versus control, (F) MIB_E2 versus E2. Control: EtOH, MIB: Mibolerone, E2: Oestradiol, MIB_E2: Mibolerone + Oestradiol, MIB_E2_FULV: Mibolerone + Oestradiol + Fulvestrant.

Only 10 MIB-induced genes were inhibited by E2, and this inhibition was reversed when ERα was inhibited by FULV (Figure 4-13). 4 MIB-responsive genes (*ADRB1*, *VWA2*, SGK1, *MYBL1*) were found to be downregulated in MIB_E2_FULV, and 8 (*WNT11*, *AQP2*, *LOC101927318*, *VAT1L*, *RPRM*, *DAB2*, *ASB9*, *CP*) were found to be upregulated in MIB_E2_FULV (Figure 4-13). This therefore demonstrates that when ERα is inhibited, transcriptional regulation of these genes might shift from upregulatory to downregulatory or from downregulatory to upregulatory. Some genes such as *MYPN*, *VMA2*, *EPGN*, *F13A1* remained stable and upregulated irrespective of the combination treatments.

Out of 68 E2-upregulated DEGs, only 2 were downregulated when cells were co-treated with MIB (E2 vs E2_MIB, Figure 4-14). However, the regulation of 85% of E2-upregulated DEGs and 87.5% of E2-downregulated DEGs was reversed when cells were treated with MIB_E2_FULV, showing the inhibitory effect of FULV on ERα targets (Figure 4-14). It is also possible that MIB and FULV work synergistically to inhibit ERα signalling; however, a comparison of E2, and co-treatment of E2 and FULV treatment is needed to confirm this, which was not included in this study. These findings suggest that the transcriptional role of AR is important in patients who receive FULV therapy, as the AR can become more transcriptionally active and regulates some ERα targets. However, whether this regulation is due to the AR binding to EREs or via an alternative mechanism, needs to be examined further.

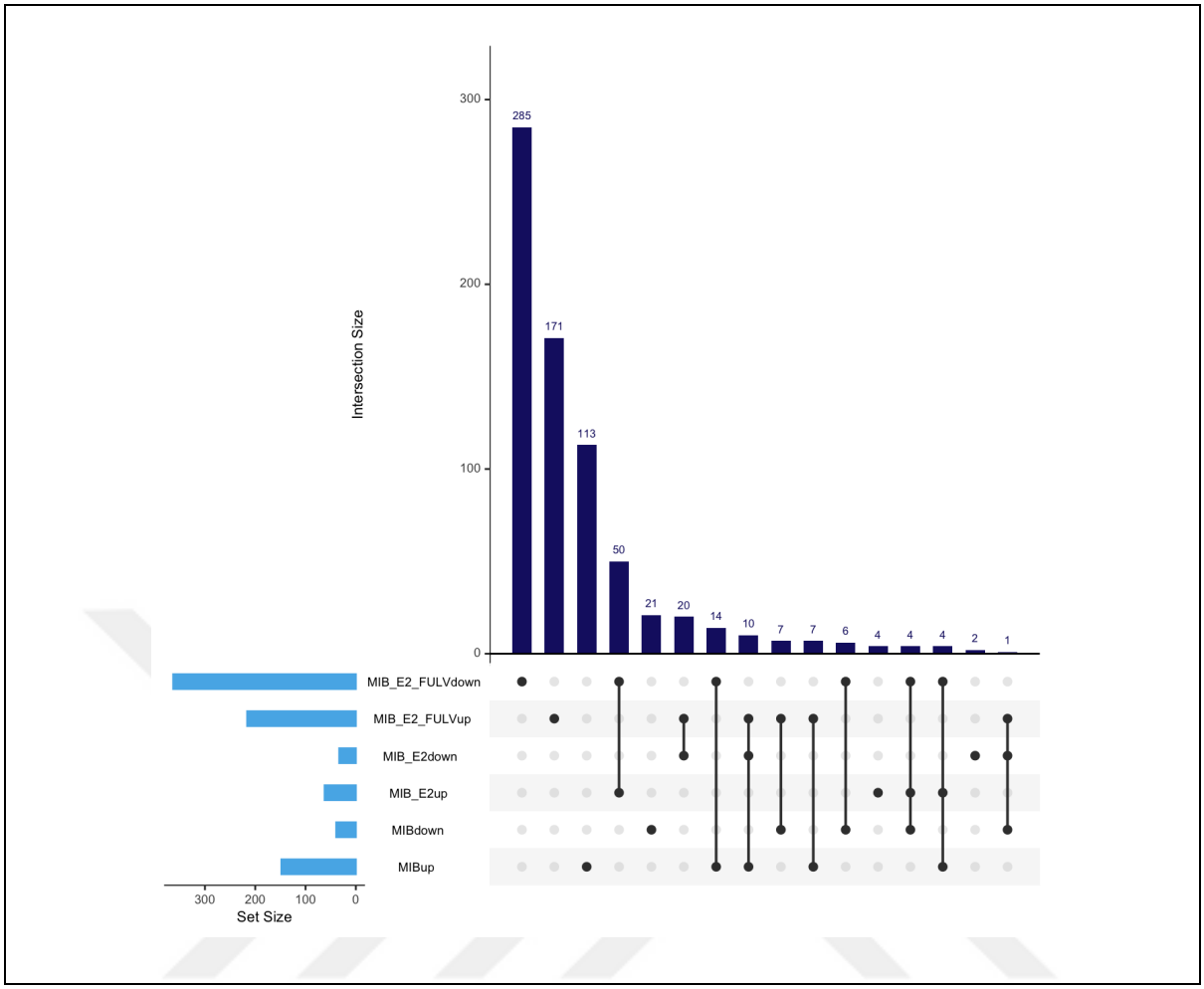

Figure 4-13 Identification of DEGs commonly regulated by MIB, and additional treatment combinations, in MCF7

MCF7 cells were incubated in hormone-depleted media for 72 hours. Cells were then treated with vehicle control (Ethanol, EtOH) or different combinations of MIB (Mibolerone, 1 nM), E2 (Oestradiol, 1 nM), FULV (Fulvestrant, 1 nM) for 24 hours. RNA was harvested. 3 independent replicates per treatment group were conducted. The transcriptome changes in response to different treatments were analysed by RNA-Seq. Differentially expressed genes (DEGs) were analysed using DESeq2 (version 1.28.1) and visualised as an UpSetR plot (Version 1.4.0). Common genes between groups are represented as number of intersections via connected dots. Cut-off values for DEGS are padj < 0.01 and log2FoldChange > 1. MIB: Mibolerone, E2: Oestradiol, MIB_E2: Mibolerone + Oestradiol, MIB_E2_FULV: Mibolerone + Oestradiol + Fulvestrant. Up: upregulated DEGs, down: downregulated DEGs.

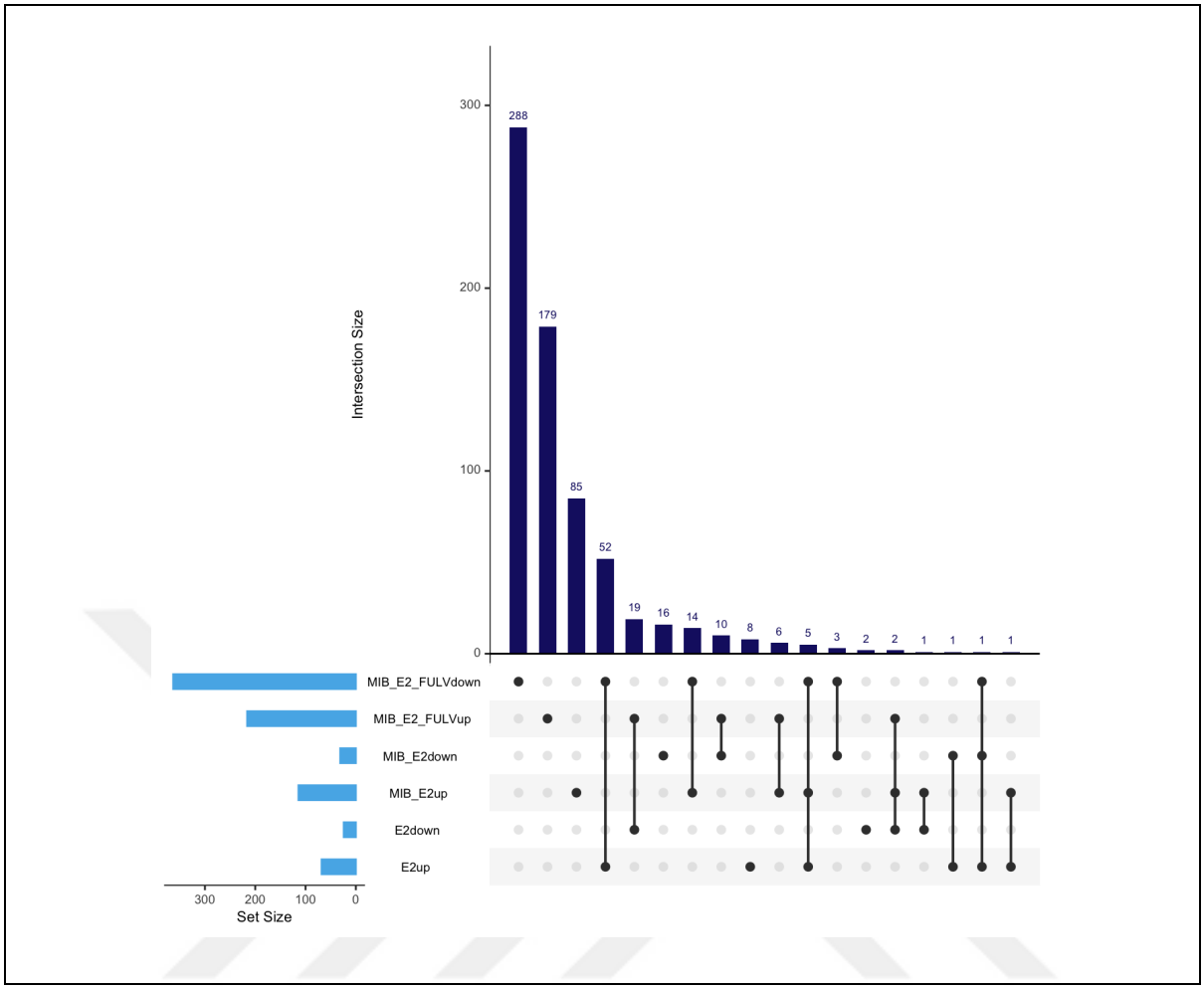

Figure 4-14 Identification of DEGs commonly regulated by E2, and additional treatment combinations, in MCF7

MCF7 cells were incubated in hormone-depleted media for 72 hours. Cells were then treated with vehicle control (Ethanol, EtOH) or different combinations of MIB (Mibolerone, 1 nM), E2 (Oestradiol, 1 nM), FULV (Fulvestrant, 1 nM) for 24 hours. RNA was harvested. 3 independent replicates per treatment group were conducted. The transcriptome changes in response to different treatments were analysed by RNA-Seq. Differentially expressed genes (DEGs) were analysed using DESeq2 (version 1.28.1) and visualised as an UpSetR plot (Version 1.4.0). Common genes between groups are represented as number of intersections via connected dots. Cut-off values for DEGS are padj < 0.01 and log2FoldChange > 1. E2: Oestradiol, MIB_E2: Mibolerone + Oestradiol, MIB_E2_FULV: Mibolerone + Oestradiol + Fulvestrant. Up: upregulated DEGs, down: downregulated DEGs.

4.3.3 MIB can regulate cell division in T47D, growth and cell differentiation in MCF7

To better understand what effect the different treatment arms have on the cells, Gene Ontology term enrichment analysis were conducted using Go.db (Version 3.11.4), GOstats (Version 2.54.0) and org.Hs.eg.db (Version 3.11.4) packages in R (Version 4.0.3). GO terms were sorted by their p values and the top 10 most significant terms are provided (Figure 4-15, Figure 4-16, Figure 4-17). MIB induced DEGs were involved in processes that are related to cell division, chromosome segragation, and cell cycle in T47D cells (Figure 4-15A). Addition of E2 to MIB resulted in pathways such as cell-cell signalling networks, hormone responsiveness, and cell transport regulatory mechanisms, and tyrosine kinase activity being regulated (Figure 4-15B). In MCF7 cells, MIB treatment was positively correlated with regulation of different metabolic processes, cell proliferation and growth (Figure 4-15C). Addition of E2 resulted in the regulation of genes involved in epithelial cell differentiation, development, and proliferation, organisation of cellular skeletal components (Figure 4-15D).

In T47D, E2-only treatment led to the activation of biological pathways related to cell differentiation, cell division, and chromosome segragation which was expected considering the fact that ERα is the main oncogenic driver in these tumour cells (Figure 4-16A). Co-treatment with MIB resulted in pathways related to biosynthetic, metabolic and cellular transport mechanisms being modulated (Figure 4-16B). In MCF7, E2 was found to regulate pathways involved in organ morphogenesis, muscular differentiation and epithelial proliferation (Figure 4-16C), and MIB co-treatment shifted the processes towards regulation of growth, organogenesis and morphogenesis (Figure 4-16D). Co-treatment of T47D with MIB, E2 and FULV found that terms such as regulation of hormone responsivenes, and different pathways such as ErbB, steroid receptor and phosphorylation were enriched (Figure 4-17A). In MCF7 cells, the top terms that were enriched in response to these treatments were cell and epithelial differentiation (Figure 4-17B).

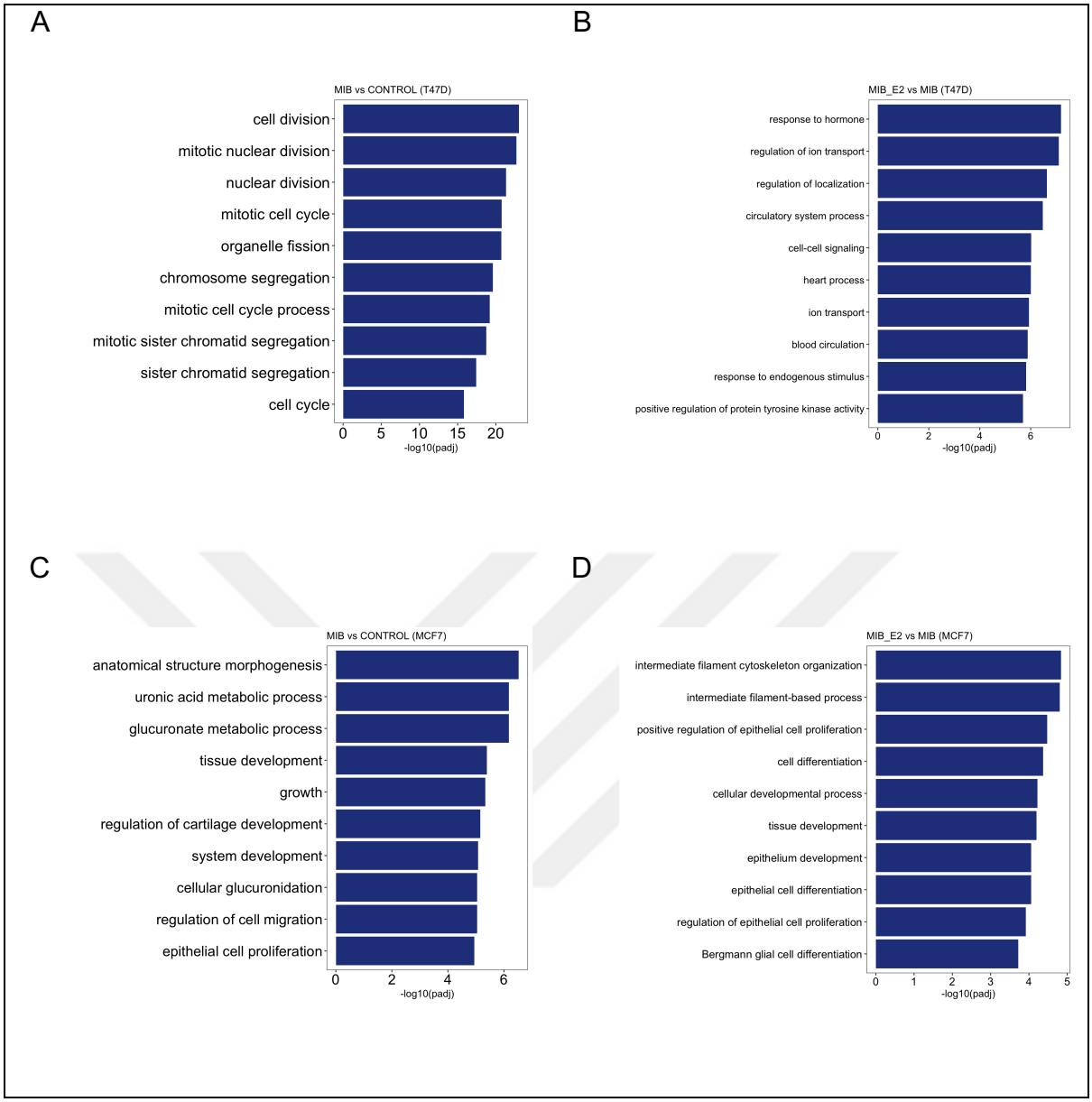

Figure 4-15 GO term enrichment analysis of MIB-regulated DEGs and the effect of co-treatment with E2 in MCF7 and T47D

Gene Ontology term enrichment analysis were conducted using Go.db (Version 3.11.4), GOstats (Version 2.54.0) and org.Hs.eg.db (Version 3.11.4) packages in R (Version 4.0.3). GO terms were sorted by their p values and the top 10 terms were demonstrated for each group comparison. Bar graphs showing the top 10 GO terms that were most significantly overrepresented in a term enrichment analysis of DEGs from the comparison between MIB vs Control in (A) T47D, (C) MCF7, and MIB_E2 vs MIB in (B) T47D, (D) MCF7. Control: EtOH, MIB: Mibolerone, E2: Oestradiol.

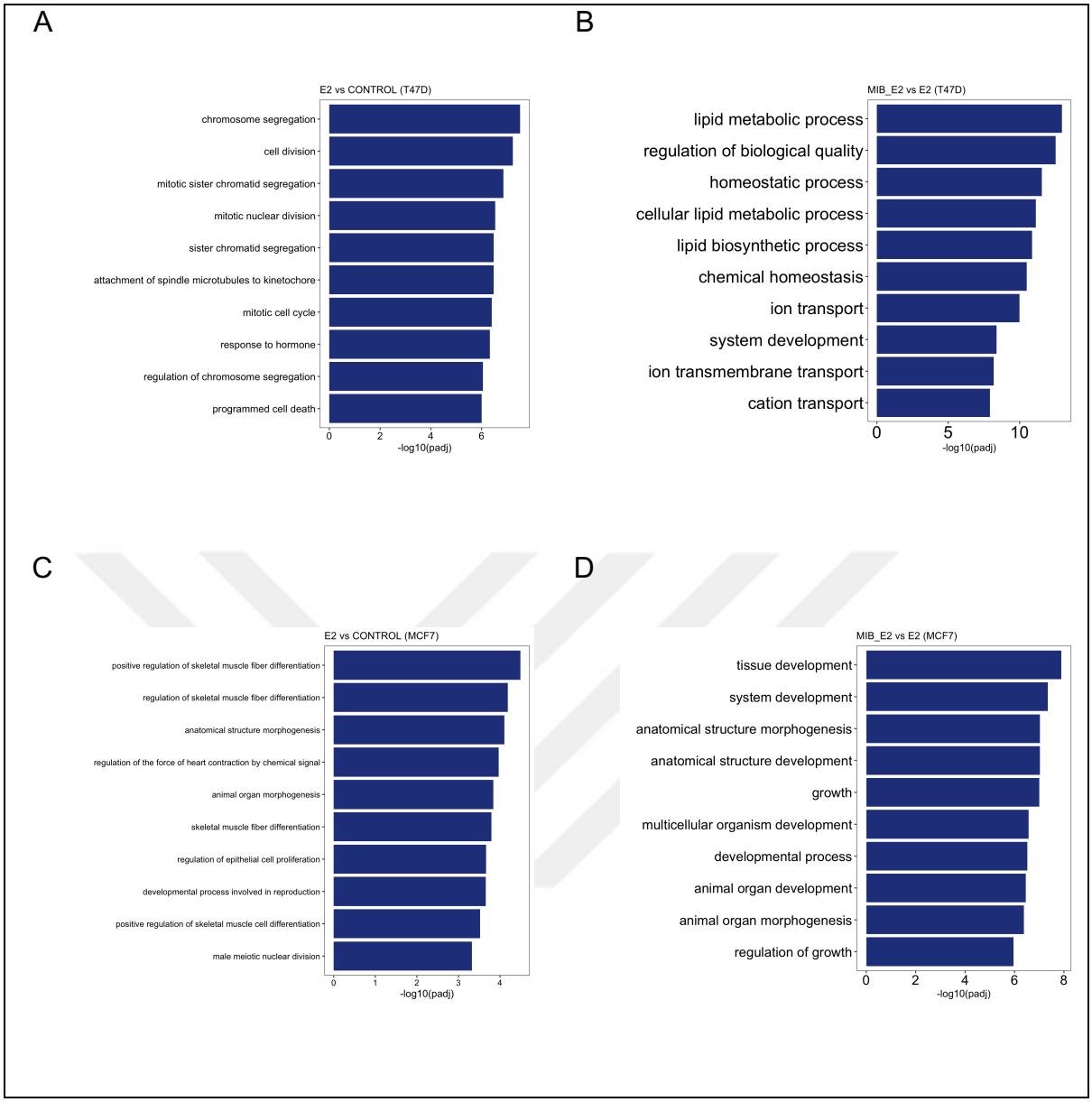

Figure 4-16 GO term enrichment analysis of E2-regulated DEGS and the effect of co-treatment with MIB in MCF7 and T47D

Gene Ontology term enrichment analysis were conducted using Go.db (Version 3.11.4), GOstats (Version 2.54.0) and org.Hs.eg.db (Version 3.11.4) packages in R (Version 4.0.3). GO terms were sorted by their p values and the top 10 terms were demonstrated for each group comparison. Bar graphs showing the top 10 GO terms that were most significantly overrepresented in a term enrichment analysis of DEGs from the comparison between E2 vs Control in (A) T47D, (C) MCF7, and MIB_E2 vs E2 in (B) T47D, (D) MCF7. MIB: Mibolerone, E2: Oestradiol, MIB_E2: Mibolerone + Oestradiol.

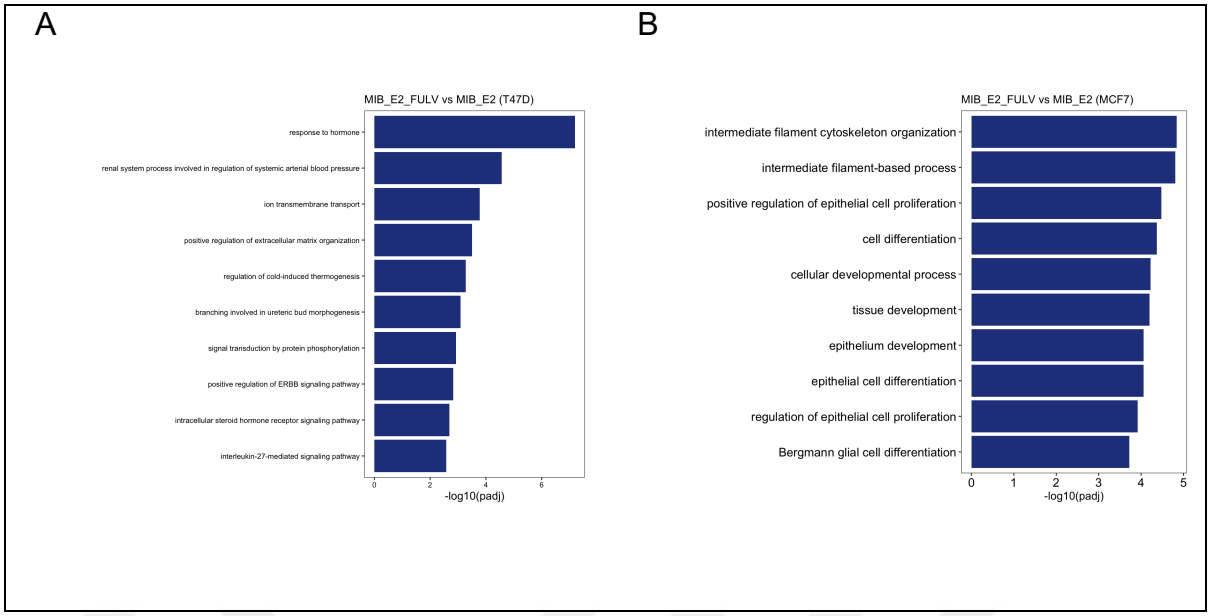

Figure 4-17 The effect of Fulvestrant on co-treatment with MIB and E2 on GO term enrichment analysis in MCF7 and T47D

Gene Ontology term enrichment analysis were conducted using Go.db (Version 3.11.4), GOstats (Version 2.54.0) and org.Hs.eg.db (Version 3.11.4) packages in R (Version 4.0.3). GO terms were sorted by their p values and the top 10 terms were demonstrated for each group comparison. Bar graphs showing the top 10 GO terms that were most significantly overrepresented in a term enrichment analysis of DEGs from the comparison between MIB_E2_FULV vs MIB_E2 in (A) T47D, (B) MCF7. MIB_E2: Mibolerone + Oestradiol, MIB_E2_FULV: Mibolerone + Oestradiol + Fulvestrant.

In conclusion, it appears that MIB regulates cell cycle related processes in T47D cells and can initiate mitosis and cell proliferation. In addition, ERα inhibition in response to FULV, induced a transcriptiome in which MIB can regulate important signalling pathways such as phosphorylation, and cellular transport. While in MCF7, activation of AR by MIB and co-treatment of MIB, E2 and FULV resulted in terms that were similar. However, this was to be expected as E2 did not have a marked impact on the MIB regulated transcriptome in MCF7 cells.

4.4 MicroRNA regulation by AR and ERα in Endocrine Sensitive Breast Cancer

Several studies have investigated miRNAs in BrCa (Miller et al., 2008; Uhlmann et al., 2010; Ward et al., 2013; Ward et al., 2014), but the association between AR, ERα and miRNAs remains unclear. For example, the receptors could execute their transcriptional regulatory mechanism on their targets via modification of miRNA expression. Therefore, small RNA-Seq was conducted to identify MIB and E2 regulated microRNAs, and to investigate the relationship between their predicted targets. MCF7 and T47D cells were incubated in hormone-depleted media for 72 hours, then treated with vehicle control (EtOH), androgen (MIB) (Mibolerone, 1 nM) or oestrogen (E2) (17-β-Oestradiol, 1 nM) for 24 hours. After RNA extraction, small RNA-Seq were performed to determine alterations in miRNA levels in response to E2 and MIB. RNA quality was checked using TBE gel electrophoresis, and after trimming the adaptors, the quality of the reads was checked (Appendix Figure 7-3).

To investigate how many miRNAs were significantly regulated by MIB and E2, 2 different cut-off for p values were compared ($p < 0.05$ and $p < 0.01$). 6 and 4 miRNAs were found to be regulated by AR, 5 and 1 miRNAs were found to be regulated by ERα, when p values < 0.05 (Appendix Figure 7-4) and < 0.01 were used, respectively. The miRNAs identified with the more stringent p value < 0.01 were chosen for further analysis.

Of the 4 miRNAs found to be regulated by MIB in T47D, miR-449c was the only one that was downregulated (Figure 4-18A, D). In E2-treated samples the only miRNA found to be significantly regulated was miR-100 (Figure 4-18B, E). When E2- and MIB-treated samples were compared, it was found that 2 out of 5 miRNAs (miR-449b, miR-449c) were found to be relatively upregulated by E2, and downregulated by MIB,

whereas miR-21, miR-129-2, and miR-584 were relatively upregulated by MIB, and downregulated by E2 (Figure 4-18C, F). Some of these have been previously established to have an important role in BrCa. For example, miR-21 is a known oncomiR, and promotes proliferation by targeting tumour suppressor genes (Kumarswamy et al., 2011; Feng and Tsao, 2016). Whereas downregulation of miR-100, which was found to be upregulated by E2 in this study, was reported to be associated with apoptosis (Gong et al., 2015; Petrelli et al., 2020). Table 4-3 summarises the known roles of these miRNAs in cancer. Surprisingly, the RNA-Seq analysis of small RNA expression, in response to E2 and MIB, found no miRNAs to be significantly regulated in MCF7 (Figure 4-19A, B, C).

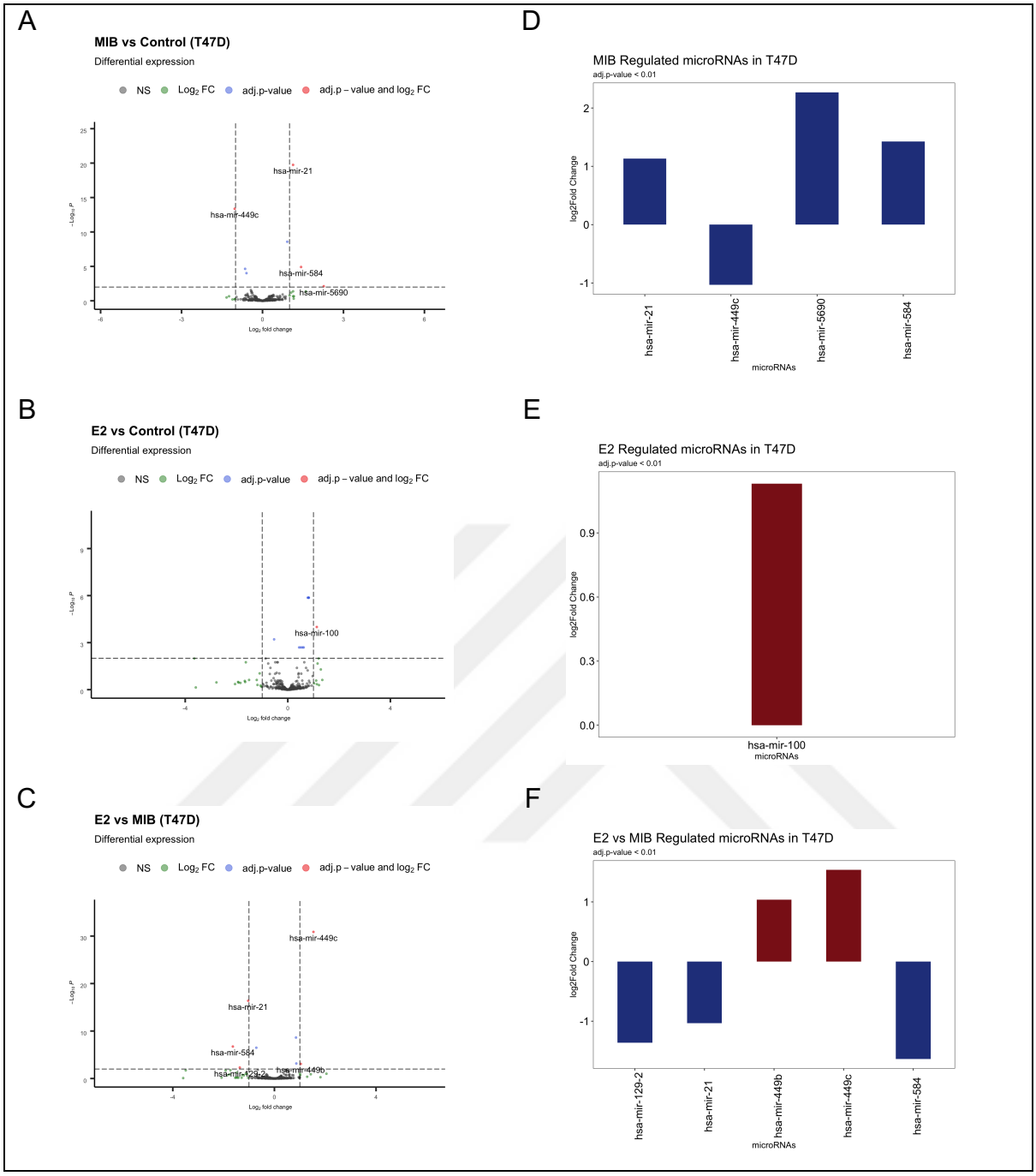

Figure 4-18 MIB- and E2-regulated miRNAs in T47D

T47D cells were incubated in hormone-depleted media for 72 hours. Cells were then treated with vehicle control (Ethanol, EtOH), MIB (Mibolerone, 1 nM), or E2 (Oestradiol, 1 nM), for 24 hours. RNA was harvested. 3 independent replicates per treatment group were conducted. The changes in miRNAs in response to different treatments were analysed by small RNA-Seq. Differentially expressed miRNAs were analysed using DESeq2 (version 1.28.1) and visualised as volcano plots using EnhancedVolcano (Version 1.6.0) and bar plots. Cut-off values are padj < 0.01 and log2FoldChange > 1. Volcano plots showing differentially expressed miRNAs, comparing (A) MIB versus control, (B) E2 versus Control, (C) E2 versus MIB. Bar plots showing differentially expressed miRNAs, comparing (D) MIB versus control, (E) E2 versus Control, (F) E2 versus MIB.

Table 4-3 Differentially expressed microRNAs in T47D, and their role in cancer

miRNA	Role in Cancer
miR-21	Upregulated in BrCa, anti-apoptotic (Kumarswamy et al., 2011; Zhang and Ma, 2012; Singh and Mo, 2013; Feng and Tsao, 2016)
miR-100	Downregulation leads to apoptosis in HER2-overexpressed BrCa, predictor in Luminal A tumours (Gong et al., 2015; Petrelli et al., 2020)
miR-449c	Overexpression sensitizes TNBC cells to chemotherapy (Tormo et al., 2019)
miR-584	Pro-apoptotic in gastric cancer (Li et al., 2017)
miR-5690	Associated with poor prognosis in head neck squamous cell carcinomas (Ma et al., 2020), decreased blood levels in BrCa patients who received radiotherapy (Marczyk et al., 2021)

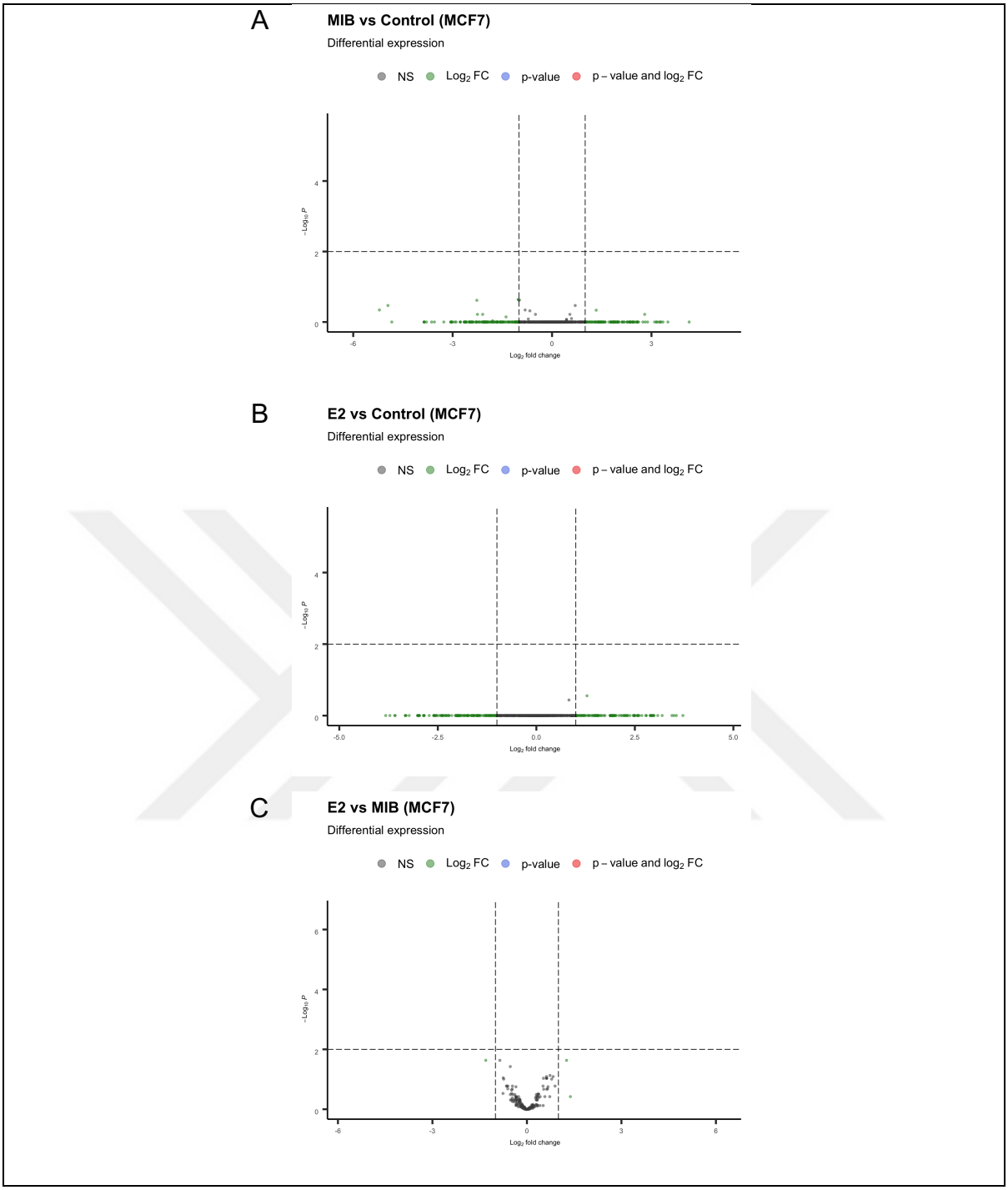

Figure 4-19 No miRNAs were found to be significantly regulated by E2 or MIB in MCF7

MCF7 cells were incubated in hormone-depleted media for 72 hours. Cells were then treated with vehicle control (Ethanol, EtOH), MIB (Mibolerone, 1 nM), or E2 (Oestradiol, 1 nM), for 24 hours. RNA was harvested. 3 independent replicates per treatment group were conducted. The changes in miRNAs in response to different treatments were analysed by small RNA-Seq. Differentially expressed miRNAs were analysed using DESeq2 (version 1.28.1) and visualised as volcano plots using EnhancedVolcano (Version 1.6.0). Cut-off values are padj < 0.01 and log2FoldChange > 1. Volcano plots showing differentially expressed miRNAs, comparing (A) MIB versus control, (B) E2 versus Control, (C) E2 versus MIB.

To investigate if there is an association between the miRNAs found to be regulated by the AR and ERα, and the DEGs previously identified in Section 4.3, potential miRNA targets were identified using TargetScan (release 7.2, March 2018). The number of targets for each miRNA varied, with miR-5690 having the most, and miR-100 having the least number of potential target genes (4580 and 25, respectfully) (Figure 4-20).

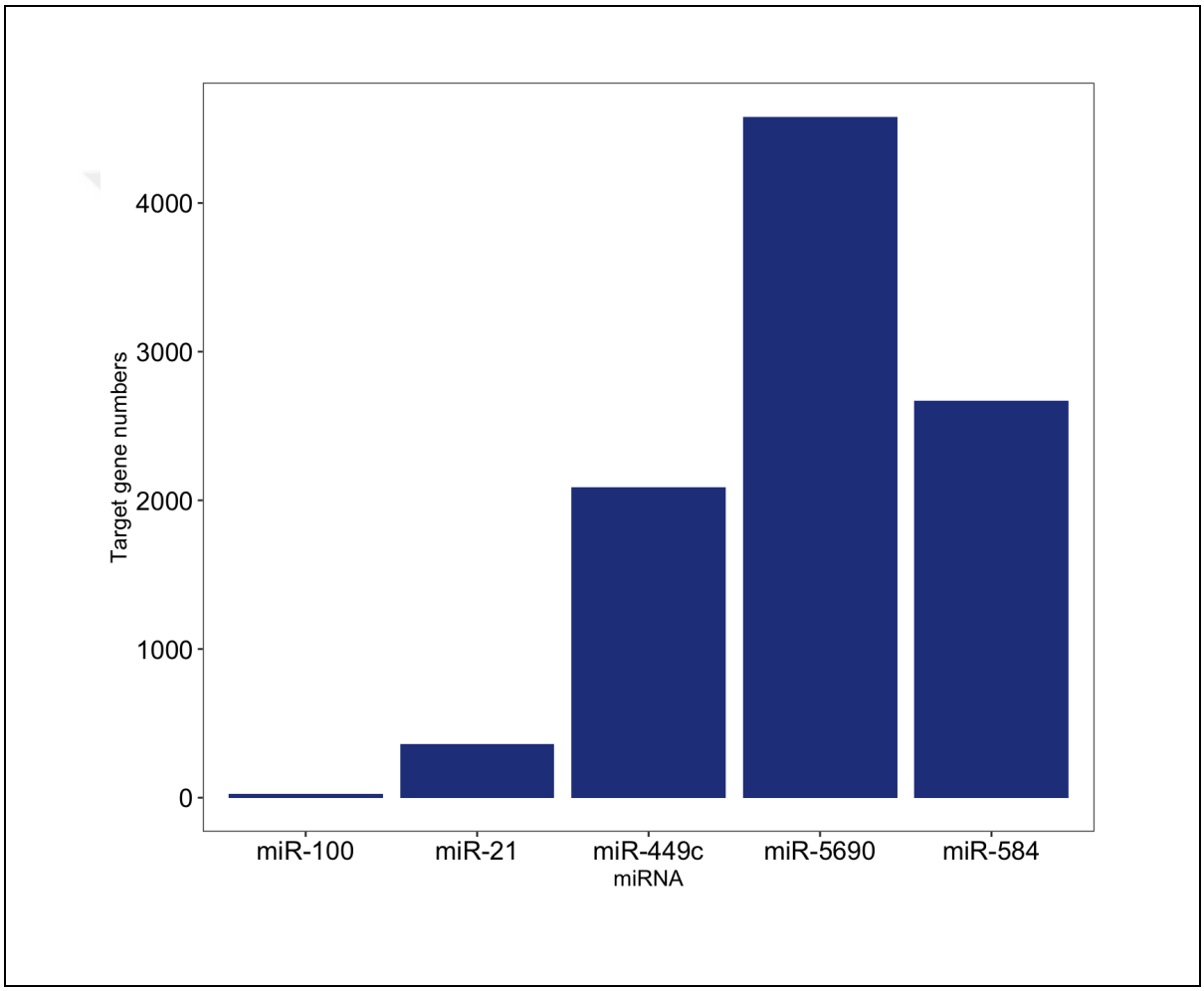

Figure 4-20 The number of potential target genes for the differentially expressed miRNAs

Target genes are obtained from TargetScan (release 7.2, March 2018) using default parameters.

The potential miRNA targets were compared to the DEGs identified in T47D cells to see if mRNA expression correlated with target expression. For example, MIB-upregulated miRNAs were compared to MIB-downregulated DEGs, to investigate the relationship between miRNAs and DEGs. The number of overlapping predicted miR-21 targets and MIB-downregulated DEGs was 14 (Figure 4-21A). This figure was 75 for miR-584, 114 for miR-5690, and 23 for miR-449c (Figure 4-21B, C, Figure 4-22A). The list of the DEGs for each miRNA is listed in Appendix Table 7-5. No DEGs in the E2-downregulated group were found to match with miR-100's predicted targets.

To investigate the role that the potential miRNA targets play in BrCa cells, GO analysis was performed on the target DEGs of each miRNA. MIB-upregulated miRNAs regulated different biological pathways; miR-21 targets were associated with tissue morphogenesis, anatomical structure and organ development, and stem cell division (Figure 4-21D); miR-584 targets were associated with regulation of developmental processes (Figure 4-21E); miR-5690 targets were not only found to regulate developmental and structural processes but also G-protein coupled receptor pathways and transmembrane transportation (Figure 4-21F). The targets of the MIB-downregulated miRNA, miR-449c found terms such as cell signalling and cellular steroid response to be enriched (Figure 4-22B).

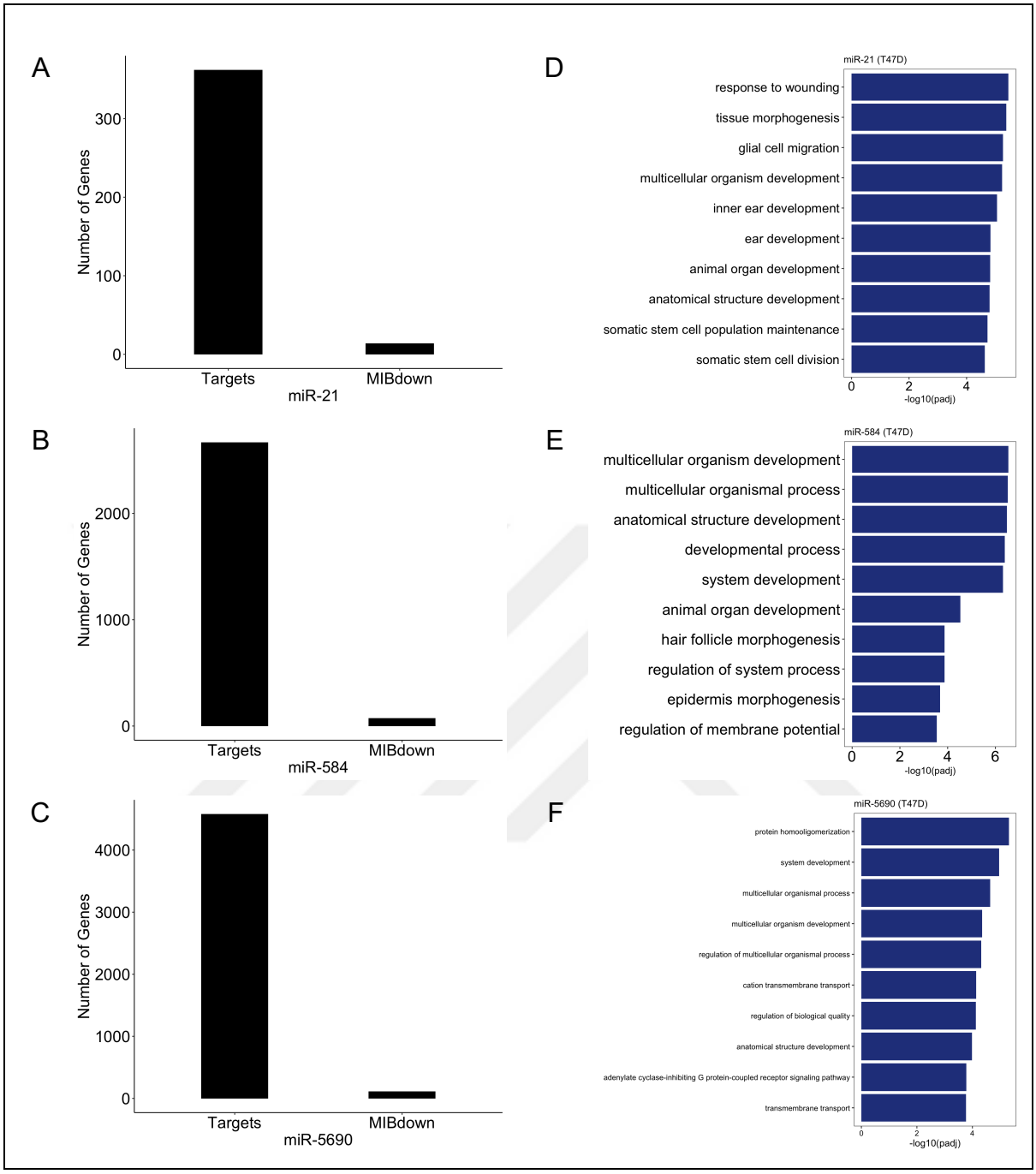

Figure 4-21 Comparison of MIB-regulated miRNAs predicted targets with MIB-regulated DEGs, and their GO analysis

T47D cells were incubated in hormone-depleted media for 72 hours. Cells were then treated with vehicle control (Ethanol, EtOH), MIB (Mibolerone, 1 nM) for 24 hours. RNA was harvested. 3 independent replicates per treatment group were conducted. The changes in miRNAs in response to different treatments were analysed by small RNA-Seq. Differentially expressed miRNAs were analysed using DESeq2 (version 1.28.1). Cut-off values are padj < 0.01 and log2FoldChange > 1. Target genes for each miRNA are obtained from TargetScan (release 7.2, March 2018) using default parameters. Bar plots comparing the predicted targets for MIB-upregulated miRNAs and MIB-downregulated DEGs for (A) miR-21, (B) miR-584, (C) miR-5690. Gene Ontology term enrichment analysis were conducted using Go.db (Version 3.11.4), GOstats (Version 2.54.0) and org.Hs.eg.db (Version 3.11.4) packages in R (Version 4.0.3). GO terms were sorted by their p values and the top 10 terms were demonstrated for each group comparison. Bar graphs showing the top 10 GO terms that were most significantly overrepresented in a term enrichment analysis of target DEGs for (D) miR-21, (E) miR-584, (F) miR-5690.

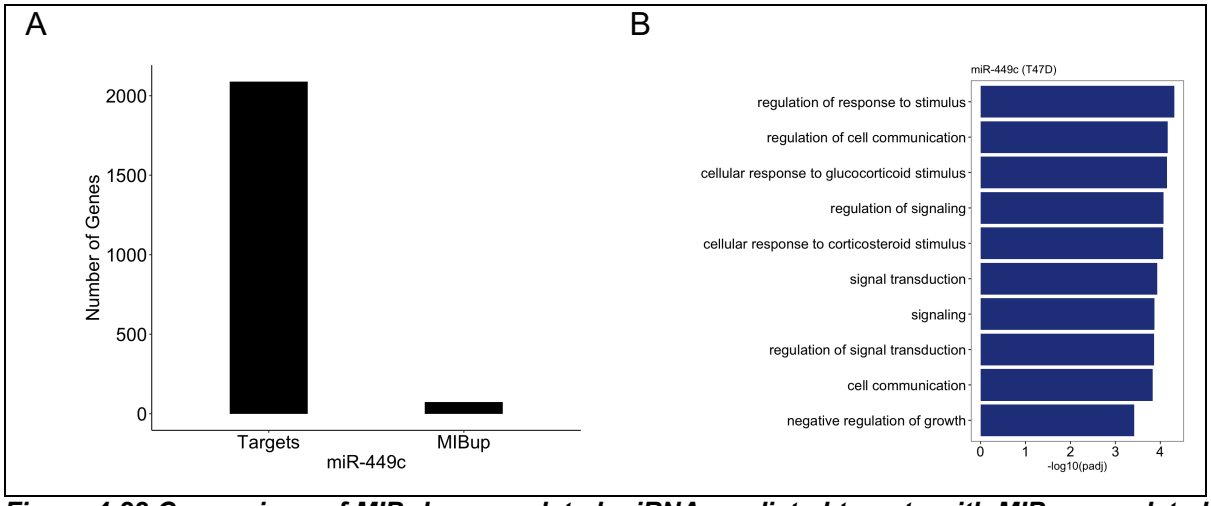

Figure 4-22 Comparison of MIB-downregulated miRNA predicted targets with MIB-upregulated DEGs, and its GO analysis

T47D cells were incubated in hormone-depleted media for 72 hours. Cells were then treated with vehicle control (Ethanol, EtOH), MIB (Mibolerone, 1 nM) for 24 hours. RNA was harvested. 3 independent replicates per treatment group were conducted. The changes in miRNAs in response to different treatments were analysed by small RNA-Seq. Differentially expressed miRNAs were analysed using DESeq2 (version 1.28.1). Cut-off values are padj < 0.01 and log2FoldChange > 1. Target genes for each miRNA are obtained from TargetScan (release 7.2, March 2018) using default parameters. Bar plots comparing the predicted targets for MIB-downregulated miRNAs and MIB-upregulated DEGs for (A) miR-449c. Gene Ontology term enrichment analysis were conducted using Go.db (Version 3.11.4), GOstats (Version 2.54.0) and org.Hs.eg.db (Version 3.11.4) packages in R (Version 4.0.3). GO terms were sorted by their p values and the top 10 terms were demonstrated for each group comparison. Bar graphs showing the top 10 GO terms that were most significantly overrepresented in a term enrichment analysis of target DEGs for (B) miR-449c.

4.5 Discussion

4.5.1 The effects of AR-ERα crosstalk on transcriptomic landscape of breast cancer cells

Development of mammary gland, and transformation of mammalian epithelial cells after pubertal hormonal changes, are mainly dependent on ERα signalling (Macias and Hinck, 2012; Arendt and Kuperwasser, 2015). Unsurprisingly, ERα signalling is also the master oncogenic driver of the majority of BrCa cases (Zwart et al., 2011; Renoir et al., 2013). It has been shown that in BrCa, ERα signalling circumvents intracellular regulatory mechanisms, facilitating oncogenic cellular processes, driving tumour development and progression (Carroll, 2016). Therefore, inhibiting ERα signalling via blocking oestradiol synthesis with AIs, or inhibition of the receptor itself with antioestrogens have improved mortality rates significantly. However, resistance to existing therapies occurs in most cases and this remains a challenge in the clinical management of BrCa (Zwart et al., 2011; Chang, 2012; Rondón-Lagos et al., 2016).

Androgen signalling has been shown to inhibit mammary gland development during puberty (Somboonporn et al., 2004). Initially it was thought that an imbalance between oestrogen and androgen could result in BrCa development (Garay and Park, 2012; Secreto et al., 2019). Hence, androgens were used as a treatment for BrCa for their inhibitory actions on breast epithelial cells (Kotsopoulos and Narod, 2012). However, because of their side effects and the risk of being converted into oestrogens via the aromatisation process, their use for BrCa was discontinued (Garay and Park, 2012). In recent years, there has been emerging evidence demonstrating the importance of AR for BrCa (Giovannelli et al., 2019; Venema et al., 2019; Michmerhuizen et al., 2020; Anestis et al., 2020; Hickey, Selth, et al., 2021). It has been shown that AR is expressed in up to 90% of BrCa tumours (Rahim and O'Regan, 2017). However, it was found that AR might have different roles in BrCa depending on the subtype. Further, overexpression of AR has also been associated with endocrine resistance (de Amicis et al., 2010; Rechoum et al., 2014; Pietri et al., 2016; Ravaioli et al., 2017; Gucalp and Traina, 2017).

In vitro experiments with ERα-positive BrCa cell lines demonstrated that treatment with androgens reduces cell proliferation (Macedo et al., 2006). However, it

was also shown that antiandrogens such as flutamide and ENZA reduce the proliferation of ERα-positive disease (Boccuzzi et al., 1995; Cochrane et al., 2014). Therefore, the role of AR in ERα-positive disease is still yet to be resolved.

IHC, genomic and gene expression analysis of BrCa has facilitated the identification of multiple BrCa subtypes (Curtis et al., 2012; Dawson et al., 2013; Giovannelli et al., 2018). Characterisation of these datasets has identified the molecular mechanisms driving tumour growth in the different subtypes. This study aimed to identify the changes in the transcriptomes of 2 ERα- and, AR-positive BrCa cell lines, MCF7 and T47D, when treated with MIB, E2 and FULV to better understand what AR regulates and how it is affected by an antioestrogen treatment.

In both cell lines, the number of DEGs increased significantly in response to the MIB, E2 and FULV treatment, compared to the other treatment arms. This again supports the idea of AR becoming more active in the absence of active ERα. Further, activation of AR when ERα is inhibited by FULV changed the gene expression profile of the cells. A ChIP-Seq study of ZR-75-1 cells showed that the AR was recruited to almost half of ERα binding sites, demonstrating the significant overlap between AR and ERα cistromes (Hickey, Selth, et al., 2021). Treatment with DHT resulted in loss of ERα occupancy and gain of AR occupancy at known E2 binding sites such as *PGR*, *MYB*, indicating the ability of the AR to interact with EREs in ZR-75-1 cells. DHT induction of AR not only resulted in redistribution of ERα binding sites, but also affected the recruitment of coactivators.

In this study, the proportion of E2-regulated genes that were disrupted by MIB was more than the proportion of MIB-regulated genes that were disrupted by E2 in T47D, whereas in MCF7, the opposite was seen. MCF7 and T47D are known to have similar ERα levels, but MCF7 cells are known to express low AR levels as compared to T47D (Birrell et al., 1995; Hickey, Selth, et al., 2021). Hence the expression levels of AR might be a contributing factor as to why these alterations in gene expression differed between the lines.

In MCF7, some gene clusters were downregulated, whereas others were upregulated in response to MIB_E2_FULV. Interestingly, the upregulated genes consisted of both oncogenic and tumour suppressor genes. For example, genes that are known to be associated with apoptosis, and tumour suppression such as *CDKN2A*, *TNFSF10*, *RPRM* (Kuribayashi et al., 2008; Carroll, 2016; Buchegger et al., 2017) were found to be upregulated in MIB_E2_FULV. Also, genes that are related to cancer

cell proliferation, invasiveness, and metastasis (*KLK14*, *FBN1*) (Fritzsche et al., 2006; Wang et al., 2015; Ren et al., 2019) were also upregulated. The outcome of this AR signalling, proliferative or antiproliferative, is likely to be decided as a result of selective pressure. However, whether these genes were upregulated because the inhibitory action of ERα was blocked by FULV, or upregulated as a result of the active AR in the presence of FULV needs further investigation as this study lacked an arm that consisted of E2 and FULV co-treatment.

This work has also identified some MIB-responsive genes, the expression of which changed from upregulatory to downregulatory, or downregulatory to upregulatory under different treatments. For example, MIB-only treatment increased the expression of *KLK10* that was shown to be pro-apoptotic in PrCa cells (Hu et al., 2015). However, its expression was found to be downregulated in MIB_E2_FULV. Further, the MIB-regulated gene *CMTM7*, which acts as a tumour suppressor (Li et al., 2014), was also found to be downregulated in MIB_E2_FULV. This therefore demonstrates that AR regulation of pro-apoptotic and tumour suppressor genes shifts to a more pro-oncogenic signature when ERα is inhibited. These changes in gene expression could be validated in samples from patients who received FULV therapy.

FOXN was found to be downregulated by MIB, and upregulated in MIB_E2_FULV. FOX family proteins are coregulators that regulate transcription and DNA binding of TFs (Hickey et al., 2012). Little is known about the function of FOXN, but it has been shown that FOXA1, another member of the FOX family, is an important mediator of steroid receptor DNA binding and transcriptional activity in BrCa and PrCa (Hurtado et al., 2011; Robinson and Carroll, 2012; Hickey et al., 2012). FOXA1 mediates the transcriptional activity of AR in ERα-negative tumours (Robinson et al., 2011; Ni et al., 2011). Also, the majority of metastases from luminal tumours have been found to have high FOXA1 expression (Hickey et al., 2012). Therefore, it is possible that in tumour cells, the AR regulates the expression of cofactors and pioneer factors to enhance signalling when ERα is no longer functional.

In BrCa, *AKAP12* has been shown to have tumour suppressor activity and is downregulated in BrCa cells compared to normal cells. However, it has been found to be upregulated in advanced stages of BrCa, and lymph node metastases of BrCa patients suggesting that its role throughout diseases progression shifts from a tumour suppressive one to an oncogenic one (Gelman, 2012; Soh et al., 2018). Further, *AKAP12* upregulation was found to inhibit angiogenesis of the tumour via the

regulation of Src (Gelman, 2012). The RNA-Seq analysis found that *AKAP12* was downregulated by E2, and upregulated by MIB_E2, and MIB_E2_FULV. It is possible that the tumour suppressive action of the AR, in ERα-positive disease, is as a result of upregulation of tumour suppressors such as *AKAP12*. However, once ERα is inhibited, it is possible that *AKAP12* activity shifts to being pro-oncogenic. Additional work will be needed to see if this hypothesis is correct.

Interestingly, comparison of DEGs that were exclusively upregulated by MIB_E2_FULV in MCF7 and T47D showed that *FBN1* was the only gene that was mutually upregulated in both cell lines. High *FBN1* expression was associated with oncogenesis and was affiliated with metastasis in ovarian cancer (Wang et al., 2015). It was also demonstrated that *FBN1* expression correlates with high expression of proteins which promote invasiveness of BrCa cells (Ren et al., 2019). Hence this could be a candidate gene to look at how or if AR facilitates BrCa invasiveness through regulation of *FBN1* expression in tumour cells that are ERα-negative or when ERα is inhibited.

The RNA-Seq data also showed that *MMPED2* was the only common DEG that was MIB_E2_FULV downregulated in MCF7 and T47D. *MPPED2* has been previously shown to be downregulated in BrCa (Pellecchia et al., 2019). Analysis of TCGA dataset demonstrated that BrCa tissue samples had lower *MMPED2* mRNA levels, especially in TNBC tumours compared to normal tissue. Further, IHC analyses also showed that MMPED2 expression is lower in BrCa tumours as compared to normal breast tissue (Pellecchia et al., 2019). Interestingly, when overexpressed, *MMPED2* reduced the migration of BrCa cells. *MMPED2* could therefore be another target of AR, that promotes tumour aggressiveness, when ERα is inhibited.

RNA-Seq of 7 patient derived xenograft models treated with E2-only or co-treatment with E2 and DHT, showed that E2 induces cell cycle related pathways such as FOXM1, G2M checkpoint. Addition of DHT downregulated these pathways, demonstrating that AR inhibits these ERα induced pro-oncogenic pathways (Hickey, Selth, et al., 2021). The data presented here demonstrates that similar to E2, MIB can induce cell cycle related pathways in ERα-positive BrCa cells. In T47D cells, GO analysis showed that FULV inhibition of ERα and activation of AR by MIB resulted with the activation of pathways that are related to phosphorylation and cellular proliferation. In response to the selective pressure resulting from antioestrogen treatment, it is

therefore possible that the AR becomes active and regulates cellular pathways that promote tumour proliferation.

4.5.2 Oestrogen and Androgen regulated microRNAs in breast cancer cells

Recent sequencing technologies have showed that the noncoding genome also plays an important role in gene regulation, tissue homeostasis, and disease progression, including cancer (Peng and Croce, 2016). Amongst noncoding RNAs, miRNAs have also emerged as important regulators of gene expression in BrCa. Some miRNAs have been associated with a certain subtype, and these have been shown to have tumour suppressor or oncogenic activity, and some have been linked to therapy resistance (Iorio et al., 2011; Wang et al., 2018; Bandini and Fanini, 2019; Loh et al., 2019). For example, the higher expression of miR-21, miR-210 and miR-211, and lower expression of miR-145, miR-205 was associated with the TNBC subtype, and miR-342 was found to be overexpressed in ERα-positive HER2-positive tumours (Singh and Mo, 2013). A study which investigated the differentially expressed miRNAs in luminal basal epithelial cells found that miR-200c and miR-429 were upregulated in luminal breast epithelial cells (Bockmeyer et al., 2011). Some miRNAs have also been associated with metastasis. For example, miR-9, miR-21, miR-155 were found to promote metastasis, while miR-20, miR-30, miR-146, miR-206 were found to suppress metastatic events in BrCa (Iorio et al., 2011; Singh and Mo, 2013; Loh et al., 2019). It has also been proposed that BrCa release miRNAs into bloodstream and that quantification of these in the form of liquid biopsies could be a way to detect BrCa (Wu et al., 2012). Coexpression analysis of miRNAs in BrCa patients' serums and tumour tissues revealed that miR-222 was significantly increased in both specimens, and could be a potential biomarker for BrCa detection (Wu et al., 2012).

As described previously, the AR plays an important role in BrCa development and progression, but the role of AR regulation of miRNAs in BrCa is unknown. It was found that miRNAs that silence AR signalling are decreased or lost in PrCa, whereas miRNAs that enhance AR signalling are highly expressed in PrCa (Fernandes et al., 2019). This study aimed to identify which miRNAs are regulated by the AR and ERα in BrCa to see if these might have an impact on the disease. The interaction between

AR and miRNAs have been mostly studied in PrCa, as AR is the main oncogenic driver in this disease. In the data presented here, 4 miRNAs were found to be regulated by MIB in T47D cells. In one study, qPCR analysis of MCF7 cells found that MIB treatment led to a reduction in miR-21 expression (Casaburi et al., 2016). However, it has also been reported that miR-21 is overexpressed in TNBC and associated with poor prognosis, metastasis and chemotherapy resistance and has therefore been classified as oncomiR in BrCa (Singh and Mo, 2013). Interestingly, miR-21 was upregulated by MIB in T47D cells, and the downstream targets of miR-21 were associated with tissue development and morphogenesis, indicating that it has a role in cell differentiation pathways in BrCa.

In PrCa, miR-21 expression is increased in response to AR signalling and this miRNA increases AR expression by a positive feedback mechanism, contributing to PrCa tumour progression (Fernandes et al., 2019). However, whether it has an enhancer effect on AR signalling, and proliferative or antiproliferative effect in BrCa cells needs further investigation. Antisense oligonucleotide experiments and miRNA mimics could be used to better understand the role of AR-regulation of miR-21 in BrCa.

qPCR analysis of miRNAs in MCF7 and T47D found that the AR upregulates the tumour suppressor miR-let-7a (Zhang et al., 2018). However, miR-let-7a was not among the miRNAs that were regulated by AR in this study. This might be because of the differences between experimental conditions. In the Zhang et al. 2018 study, the cells were incubated in hormone-depleted media for 24 hours, prior to exposure to DHT for 48 hours. Interestingly, miR-let-7a was also found to be upregulated in MDA-MB-453 cells, a cell line which AR is known to promote proliferation (Lyu et al., 2014).

The expression of miR-100 has been shown to be downregulated in MDA-MB-453 cells in response to AR signalling (Ahram et al., 2017). The level of this miRNA was found to be higher in mesenchymal cell lines (SUM159, MDA-MB-23), compared to epithelial cells (MCF7, T47D) by qPCR analysis (Chen et al., 2014). The data demonstrated here found that E2 treatment led to the upregulation of miR-100 in T47D cells, however it was not amongst the miRNAs regulated by androgen. It appears that the regulation of this miRNA is altered by different factors in different BrCa subtypes and might be context specific.

AR upregulation of miR-449c has been previously shown to sensitize TNBC cells to doxorubicin treatment, and is associated with regulation of cell cycle related genes (Tormo et al., 2019). Another AR upregulated miRNA, miR-584 was found to inhibit

cervical cancer cell proliferation, and promote apoptosis in gastric cancer (Li et al., 2017; Wang et al., 2020). It therefore appears that AR regulated miRNAs have varying roles dependent upon the cancer type. However, the AR regulated miRNAs identified in this study (miR-584, miR-5690, miR-449c) have not been previously associated with AR signalling or linked to ERα-positive BrCa before.

In conclusion, it was found that a number of genes that are related to apoptosis, proliferation, and metastasis are regulated by AR when ERα is inhibited by FULV, and MIB can induce cell cycle related pathways in endocrine sensitive BrCa cells. The analysis of miRNAs in response to MIB treatment in endocrine sensitive BrCa cells identified different miRNAs which were shown to be associated with different roles in not only BrCa but also other cancers. Therefore, their role in AR signalling in BrCa warrants further investigation.

Chapter 5
Investigation of AR Mutations Identified in Breast Cancer

Investigation of AR Mutations Identified In Breast Cancer

5.1 Introduction

The activation of the AR signalling pathway is the main cornerstone in PrCa oncogenesis. As a result, most of our knowledge about this pathway comes from PrCa research. Hormonal therapies are effective initially in PrCa, but often fail and the disease progresses to a more aggressive stage termed castrate resistant PrCa (CRPC) which is associated with poor prognosis and survival (Brooke and Bevan, 2009). One mechanism that has been proposed to explain CRPC is mutations in AR that enhance activity or reduce ligand specificity (Brooke and Bevan, 2009). More than 150 mutations of AR have been identified in PrCa, and most of the mutations are somatic and single base changes (Gottlieb et al., 2012). It has been found that these mutations that occur in PrCa patients usually cause a gain of function which leads the receptor to be active in the absence of the cognate ligand (Gottlieb et al., 2012) and are responsible for one third of the resistant cases (Rau et al., 2005). Importantly, compared to primary tumours, metastatic tissues have higher mutation rates (Rau et al., 2005) and most of the mutations are located in the AR LBD. These LBD mutations often result in the receptor being activated by alternative ligands, including other hormones and antiandrogens (Buchanan et al., 2001), thus resulting in resistance to existing therapies.

It has been shown that AR plays an important role in pathological pathways that drive BrCa development and outcome (Mehta et al., 2015; Rahim and O'Regan, 2017; Rangel et al., 2018; Venema et al., 2019). It is also well known that tumours can develop mutations and manipulate pathways to become resistant to therapies (Alluri et al., 2014), therefore it is possible that AR-positive BrCa cells could also develop AR mutations under selective pressure to become more aggressive and/or resistant to therapies.

This chapter focuses on some of the AR mutations that were found to be associated with BrCa, and aims to understand the activity and the role of these mutations in the disease.

5.2 Identification of AR Mutations in Breast Cancer

As previously mentioned, it has been found that AR is expressed in almost all cases of BrCa, occurring in up to 90% of all tumours (Rahim and O'Regan, 2017), and it has been shown that AR has an antiproliferative effect on tumour growth in the presence of ERα (Fioretti et al., 2014). To investigate the role of AR mutants in BrCa, 6328 samples from 13 studies (MSK, Cancer Cell 2018; MSK, Nature Cancer 2020; Duke-NUS, Nat Genet 2015; METABRIC, Nature 2012 & Nat Commun 2016; MSKCC, NPJ Breast Cancer 2019; British Columbia, Nature 2015; British Columbia, Nature 2012; Broad, Nature 2012; Sanger, Nature 2012; TCGA, Cell 2015; INSERM, PLoS Med 2016; The Metastatic Breast Cancer Project; MSKCC, J Pathol 2015) in the cBioPortal (https://www.cbioportal.org/) cancer database was interrogated (Cerami et al., 2012). 50 AR mutations (35 missense, 5 in frame, 8 truncating, 2 fusion) were found to be associated with the disease. 20 of the missense mutations (with single base pair changes) that have not been previously studied (Figure 5-1 and Table 5-2) were investigated. To investigate if the mutations might have an effect upon receptor function, the PROVEAN (http://provean.jcvi.org), mutation analysis tool was used, which predicts whether an amino acid substitution is likely to have an impact on the biological function of a protein. Only 6 of the mutations were predicted to have significant perturbation on the biological activity of the AR (Table 5-1).

15 mutations were found in the N-Terminal Domain (NTD), 1 in the DNA Binding Domain (DBD) and 4 in the Ligand Binding Domain (LBD) (Figure 5-1A). A crystal structure is not available for the full-length AR, but structures do exist for the DBD and LBD (PDB codes for AR DBD: 1R4I, LBD: 2AMA). To investigate these mutations further, the location of the substitutions in these domains was visualised using PyMOL (version 2.5.2) (Figure 5-1B, C). Mutations E830K and R856C are found in helices 10 and 11 of the LBD, and are not near the coactivator interaction surface or residues important in ligand binding. In contrast, H875Y does lie close to the region that helix 12 interacts with following ligand binding.

The majority (14 out of 20) of the mutations (R13W, R31H, E81Q, E187Q, S361N, R386G, G409R, A430T, Q445P, Q488*, G525A, A810V, R856C, H875Y) were found in ERα-positive, HER2-negative tumours (Table 5-2). S336P was the only AR mutation that was found in TNBC, whereas E830K was the only mutant that was

found in ERα-positive, PR-positive, HER2-positive tumour. The hormone receptor status for the other tumours, expressing L57Q, E304K, T338I and L561M was not available in the database. 10 of the tumour samples had *TP53* mutation and 2 (S336P, G525A) out of these 10 also had a *BRCA* mutation. 60% of the samples also had a mutation in *PIK3CA* (Phosphatidylinositol-4,5-Bisphosphate 3-Kinase Catalytic Subunit Alpha). Detailed characteristics of the tumour samples are listed in Table 5-2.

Using site-directed mutagenesis, the substitutions were inserted into the pSV-AR plasmid. After mutagenesis reactions were completed, successful base pair changes in the AR were confirmed by Sanger sequencing (Appendix Figure 7-5).

Table 5-1 Prediction of the impact of mutations in AR's biological function

The PROVEAN mutation prediction tool was used to assess the effects of the mutations upon AR function. Prediction cut-off value = -2.5

Variant	Provean Score	Prediction
R13W	-1.522	Neutral
R31H	-1.896	Neutral
L57Q	-0.090	Neutral
E81Q	-0.180	Neutral
E187Q	-1.026	Neutral
E304K	-1.155	Neutral
S336P	-1.018	Neutral
T338I	-1.254	Neutral
S361N	-0.463	Neutral
R386G	-3.073	Deleterious
G409R	-2.137	Neutral
A430T	0.229	Neutral
Q445P	-2.448	Neutral
Q488*	-1.592	Neutral
G525A	-2.715	Deleterious
L561M	-1.443	Neutral
A810V	-2.525	Deleterious
E830K	-3.011	Deleterious
R856C	-6.118	Deleterious
H875Y	-4.098	Deleterious

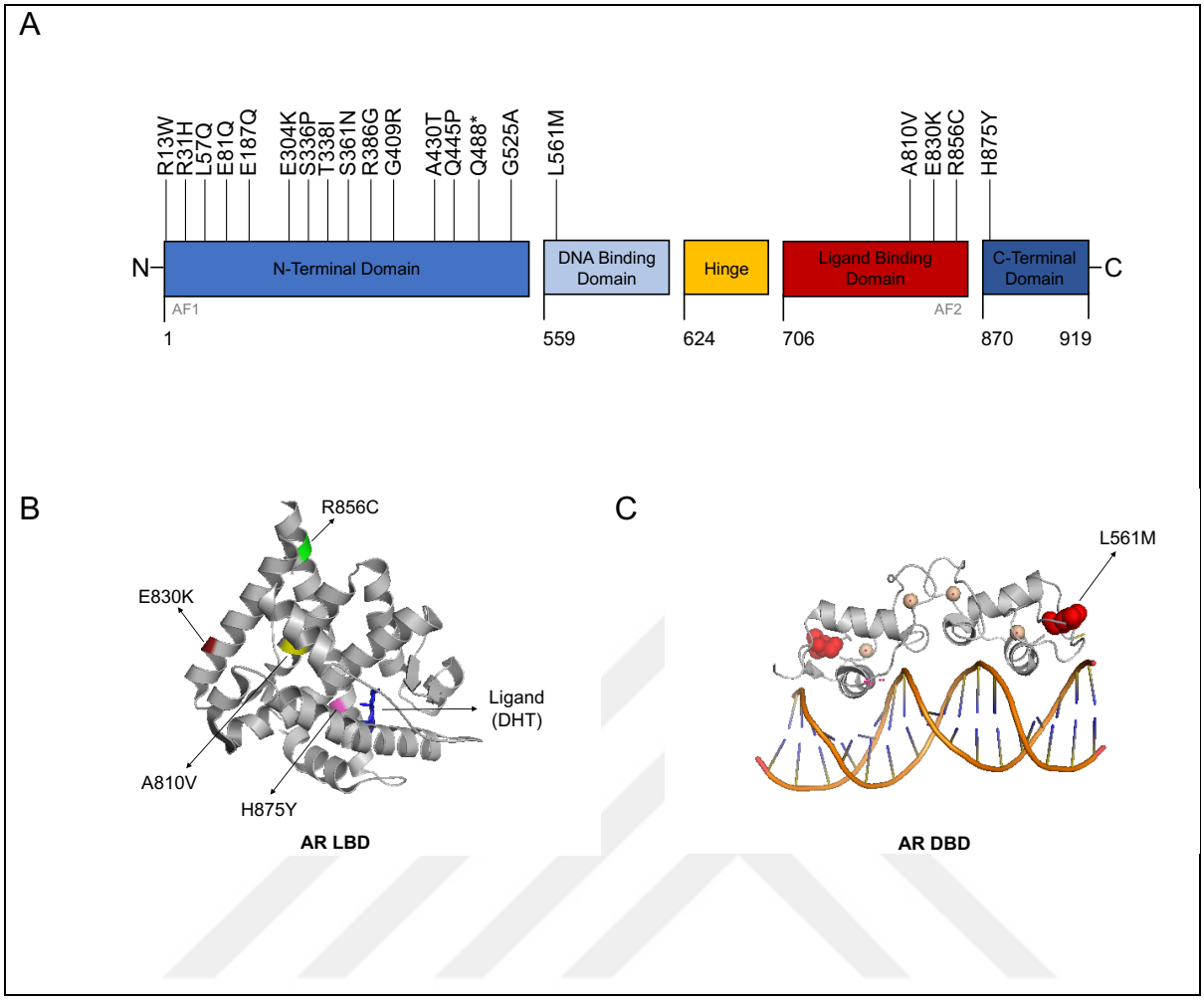

Figure 5-1 Locations of AR mutations identified in Breast Cancer

(A) The locations of the mutations on the different domains of the AR. Crystal structures of AR (B) LBD (PDB: 2AMA) and (C) DBD (PDB: 1R4I) domains highlighting the exact location of the AR mutations associated with BrCa. AF1 and 2, Activation Function 1 and 2; LBD, Ligand Binding Domain; DBD, DNA Binding Domain. Amino acids are numbered to indicate the locations of domains. AR crystal structures were visualised using PyMOL software (version 2.5.2) (https://pymol.org/). Mutations identified using cBioPortal.

Table 5-2 AR mutations found in BrCa and characteristics of tumour samples

Mutations were identified using the cBioPortal database. ND, Not Determined.

AR Mutation	BrCa Type	ER	PR	HER2	Ki67	BRCA	P53 Mutation	ER mutation	Other alterations	Variant frequency in the sample	Total number of mutations in the sample
R13W	Breast invasive ductal carcinoma	+	+	-	-	-	+	ESR1 (E380Q)	PIK3CA	0.33	6
R31H	Breast invasive lobular carcinoma	+	+	-	-	BRCA2	-	-	NOTCH3	0.21	12
L57Q	Invasive breast carcinoma	ND	ND	+	-	-	+	-	-	0.41	80
E81Q	Breast invasive ductal carcinoma	+	+	-	-	-	+	-	PIK3CA	0.42	4
E187Q	Breast invasive ductal carcinoma	+	+	-	-	-	-	-	PIK3CA, MAP3K1, FOXA1	0.14	21
E304K	Invasive breast carcinoma	+	ND	-	+	-	+	ESR2 (Q232H)	PIK3CA	0.38	773
S336P	Breast invasive ductal carcinoma	-	-	+	+	BRCA1 deletion	+	-	Myc	0.63	89
T338I	Invasive breast carcinoma	+	ND	-	-	-	+	-	PIK3CA	0.13	76
S361N	Breast invasive ductal carcinoma	+	+	-	-	-	-	-	CDK1	0.13	137
R386G	Breast invasive ductal carcinoma	+	+	-	-	-	+	-	PIK3CA, FGFR2	0.13	90
G409R	Breast invasive ductal carcinoma	+	+	-	-	-	-	ESR1 (D538G)	PIK3CA, GATA3, MAP3K1	0.18	15
A430T	Breast invasive ductal carcinoma	+	-	-	-	-	+	-	PIK3CA	0.12	5
Q445P	Breast invasive ductal carcinoma	+	+	-	-	-	-	-	mTOR, FGFR1	0.47	4
Q488*	Breast invasive ductal carcinoma	+	+	-	-	-	+	-	PTEN, MAP3K1, NOTCH2	0.22	24
G525A	Breast invasive ductal carcinoma	+	-	-	-	BRCA2	+	-	PIK3CA, MAP2K1, NOTCH1, FOXA1, mTOR, Jak1, PTEN	0.22	444
L561M	Breast invasive ductal carcinoma	ND	ND	ND	-	-	-	-	MSH2	0.04	45
A810V	Breast invasive lobular carcinoma	+	+	-	-	-	-	-	PIK3CA	0.20	29
E830K	Breast invasive lobular carcinoma	+	+	+	-	BRCA2	-	-	PIK3CA	0.13	16
R856C	Breast invasive ductal carcinoma	+	-	-	-	-	-	-	Myc, CDK6	0.31	1
H875Y	Breast invasive lobular carcinoma	+	+	-	-	-	-	-	PIK3CA	0.27	5

To confirm that the wild-type (WT) AR and mutant receptors were successfully expressed when transiently transfected into COS-1 cells and to check the expression levels, immunoblotting was performed (Figure 5-2). In the absence of hormone, AR levels were found to be low. However, in the presence of androgen AR levels were markedly higher. This was expected as it is known that AR is stabilised in the presence of androgen (Davey and Grossmann, 2016; Lakshmana and Baniahmad, 2019). The majority of the mutants had higher expression levels compared to the WT when exposed to MIB. Q488* should result in a truncated form of the AR (approximately 60 kDa). However, this was undetectable in the presence/absence of MIB, even though an N-Terminal primary antibody was used. A430T was also undetectable. Therefore, the majority of the mutants were detectable, with higher levels evident in the presence of androgen.

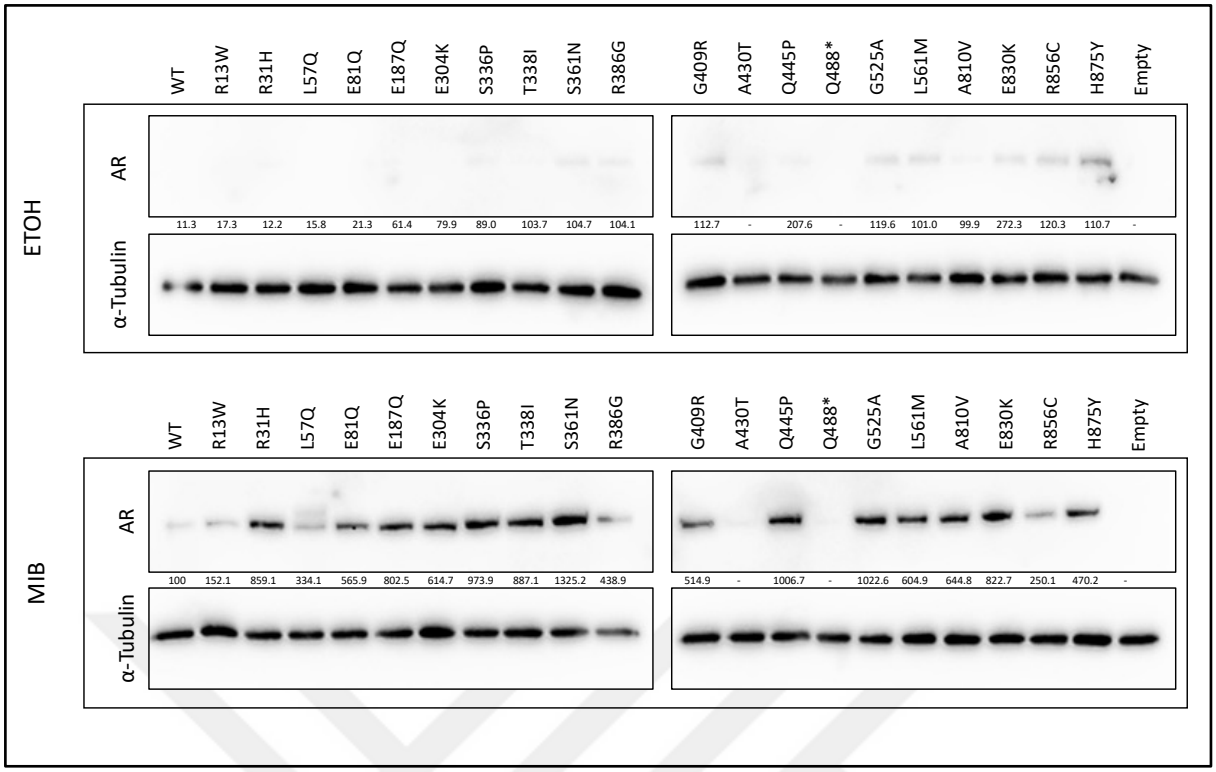

Figure 5-2 The mutant ARs are successfully expressed in COS-1 cell line

COS-1 cells were seeded in hormone-depleted media, incubated for 24 hours, and transfected with the pSV-AR expression plasmid for the wild-type (WT) and mutant ARs. Cells were incubated in hormone-depleted media for another 24 hours prior to treatment with EtOH or 1 nM MIB, and after treatment, incubated for a further 24 hours. The cells were collected, lysed and AR levels visualised using western blotting. α-Tubulin was used as a loading control. Densitometry was performed using ImageJ (version 1.53) software and results were made relative to AR WT levels in the presence of MIB (1 nM).

5.3 Some AR mutants are less active than wild-type AR

To investigate the transcriptional activity of the WT and mutant ARs, COS-1 cells were transfected with an expression plasmid for the ARs (pSV-AR) along with an ARE luciferase reporter plasmid (TAT-GRE-EIB-LUC) (Figure 5-3A). 24 hours after transfection, cells were treated with either vehicle (EtOH) or MIB (0.1, 1 and 10 nM) (Figure 5-3B). The activity of the WT AR was significantly enhanced in the presence of MIB, with maximal activity achieved in the presence of 1 nM of the hormone (ANOVA, $p \leq 0.0001$). None of the mutants were found to be more active than WT in the absence of ligand. The most active mutant compared to WT, at the lowest MIB concentration (0.1 nM) was S361N (2.26-fold increase in the activity compared to WT); however, this was not found to be statistically significant. The majority of mutants had similar activity to the WT when exposed to MIB at 1 and 10 nM, with the exception of 4 mutants (L57Q, A430T, Q488*, R856C) which were significantly less active in comparison with WT AR's activity.

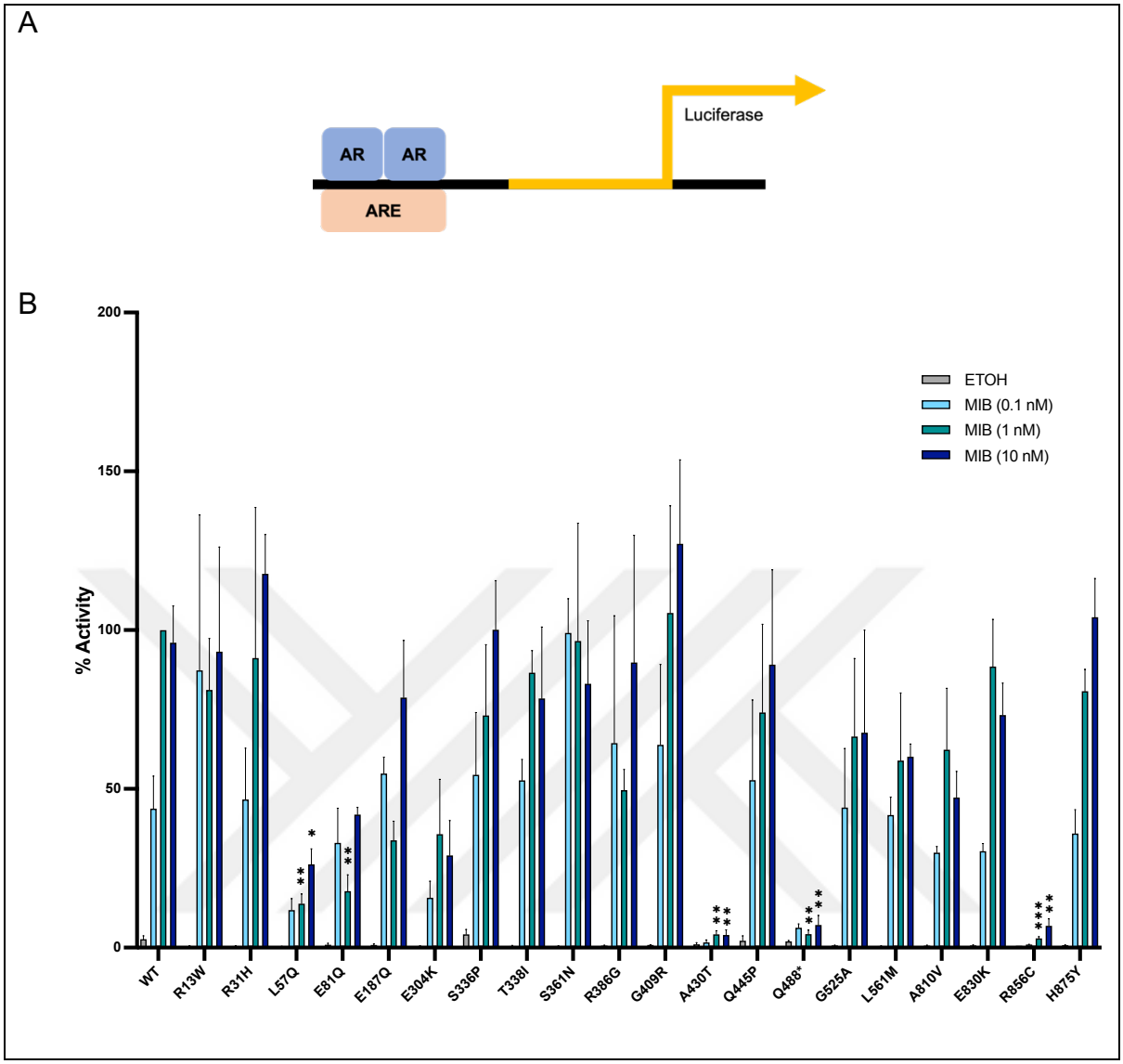

Figure 5-3 Transcriptional activity of mutant ARs in response to androgen

(A) Schematic representation of the reporter assay. COS-1 cells were seeded in hormone-depleted media, incubated for 24 hours, and transfected with the pSV-AR expression plasmid for the wild-type (WT) and mutant ARs (R13W, R31H, L57Q, E81Q, E187Q, E304K, S336P, T338I, S361N, R386G, G409R, A430T, Q445P, Q488, G525A, L561M, A810V, E830K, R856C, H875Y), TAT-GRE-EIB-LUC reporter and renilla expression plasmid. Cells were incubated in hormone-depleted media for another 24 hours prior to treatment. Cells were treated with (B) EtOH (ethanol), or MIB (Mibolerone) (0.1 nM, 1 nM, 10 nM) for 24 hours. Luciferase activity was normalised to renilla activity and results were made relative to AR WT activity in the presence of 1 nM MIB. Graphs are the average of 3 individual experiments, each with triplicate repeats and generated with GraphPad Prism 9 software. ANOVA. * p ≤ 0.05, **p ≤ 0.01, ***p ≤ 0.001. Mean ± 1SE.*

5.4 Some AR mutants are activated by alternative hormones

It has been well documented that in PrCa, mutations of the AR can change ligand specificity of the receptor, allowing the receptor to become constitutively active or be activated by other ligands (McDonald et al., 2000; Brooke and Bevan, 2009). For example, the T877A mutation of AR in PrCa was found to be responsive to oestrogens and progestins (Eisermann et al., 2013).

To investigate if AR mutations in BrCa are activated by alternative ligands, the reporter assays were performed with hormones/drugs relevant to BrCa (i.e., E2, Prog, TAM, FULV). AR and ARE luciferase reporter transfected cells were treated with either vehicle (EtOH), Prog, TAM, FULV, or varying concentrations of E2 for 24 hours. Although some mutants were found to be activated by E2 at high concentration (100 nM), most of the mutations seemed to have similar activity to that of WT AR in response to E2 at low concentrations (1 nM, 10 nM). H875Y was the only mutant that had significantly increased activity at all E2 concentrations tested (Figure 5-4A). 4 of the mutants (R31H, R386G, A810V, H875Y) were more active than WT at 100 nM E2 treatment with a nearly 6-fold increase in activity in comparison with WT. Interestingly, other than the 4 mutants that were found to be transcriptionally inactive in response to MIB (L57Q, A430T, Q488*, R856C, Figure 5-3), 3 additional mutants (E81Q, E304K, E830K) also had decreased activity, at the highest E2 concentration tested, (approximately 40%) compared to WT AR.

In response to progesterone, H875Y was also found to have significantly increased activity (9-fold increase compared to WT) (Figure 5-4B). In contrast, the activity of the other mutants, in response to progesterone was similar to the WT. Receptor activity was also investigated in response to the antioestrogens, TAM and FULV. None of the mutations were significantly activated in response to either of the antioestrogens (Figure 5-4C).

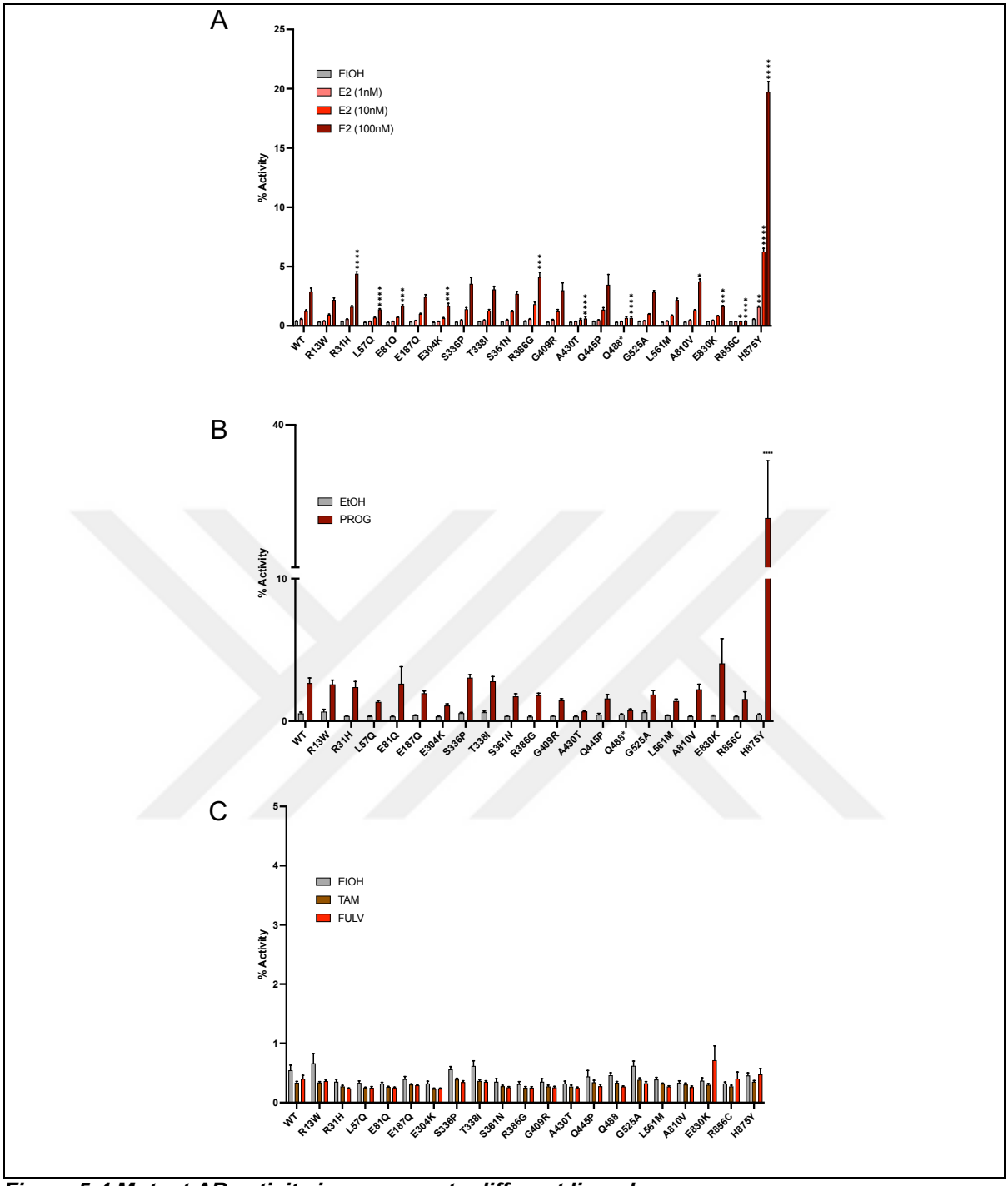

Figure 5-4 Mutant AR activity in response to different ligands

COS-1 cells were seeded in hormone-depleted media, incubated for 24 hours, and transfected with the pSV-AR expression plasmid for the wild-type and mutant ARs (R13W, R31H, L57Q, E81Q, E187Q, E304K, S336P, T338I, S361N, R386G, G409R, A430T, Q445P, Q488, G525A, L561M, A810V, E830K, R856C, H875Y), TAT-GRE-EIB-LUC reporter, and renilla expression plasmid. Cells were incubated in hormone-depleted media for another 24 hours prior to treatment. Cells were treated with (A) EtOH (ethanol), or E2 (1 nM, 10 nM, 100 nM), (B) EtOH, or Prog (progesterone) (10 nM), (C) EtOH, TAM (tamoxifen) (100 nM) or FULV (fulvestrant) (100 nM) for 24 hours to evaluate receptor activity. Luciferase activity was normalised to renilla activity and results were made relative to AR wild-type (WT) activity in the presence of 1 nM MIB. Graphs are the average of 3 individual experiments, each with triplicate repeats and generated with GraphPad Prism 9 software. ANOVA. * p ≤ 0.05, **p ≤ 0.01, ***p ≤ 0.001, ****p ≤ 0.001. Mean ± 1SE.*

5.5 Cellular localisation of some AR mutants differs than wild-type in response to androgen

It is well known that when there is no androgen present, AR's localisation is mainly cytoplasm, and upon ligand binding it translocates to the nucleus, and binds its response elements in DNA and initiates transcription (Pietri et al., 2016). To see if the localisation of AR was affected by the mutations found in BrCa, confocal microscopy was performed with GFP-AR (pSV-AR fused to Green fluorescent protein) for the WT and the mutant receptors with the exception of L57Q and Q488*, cloning of which were unsuccessful (Figure 5-5). COS-1 cells were plated at 20% confluency on cover slips in 24-well plates. Cells were transfected with plasmids encoding GFP-AR, WT or the mutants, using FuGENE HD (Promega), and incubated for 24 hours before treatment with the ligand MIB (1 nM) for 2 hours. Cells were counterstained with DAPI, nuclear staining (blue) and imaged using fluorescent microscopy. As expected, in the absence of androgen the WT AR was found to be predominantly localised in the cytoplasm and upon androgen treatment AR translocated to the nucleus (Figure 5-5).

Interestingly, S336P and A430T were predominantly localised to the nucleus in the presence and absence of ligand. Several of the mutants (E304K, T338I, G409R and Q445P) were also found to have greater nuclear localisation compared to WT, in the absence of ligand. All mutants with the exceptions of E187Q, E830K, and R856C, were predominantly localised to the nucleus upon androgen treatment. The cellular localisations of the AR mutants are summarised in Table 5-3.

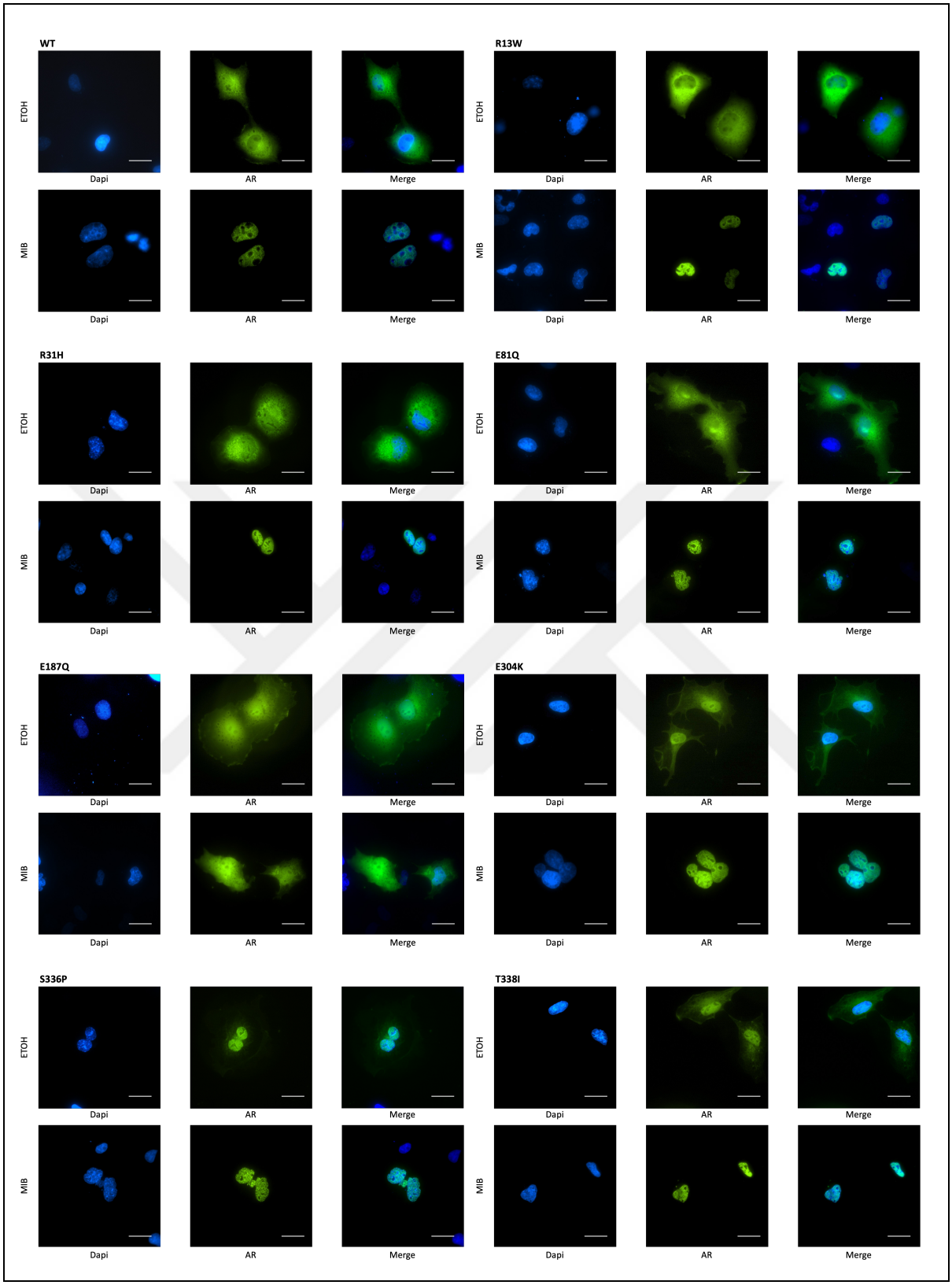
WT
R13W
R31H
E81Q
E187Q
E304K
S336P
T338I
ETOH
MIB
Dapi
AR
Merge

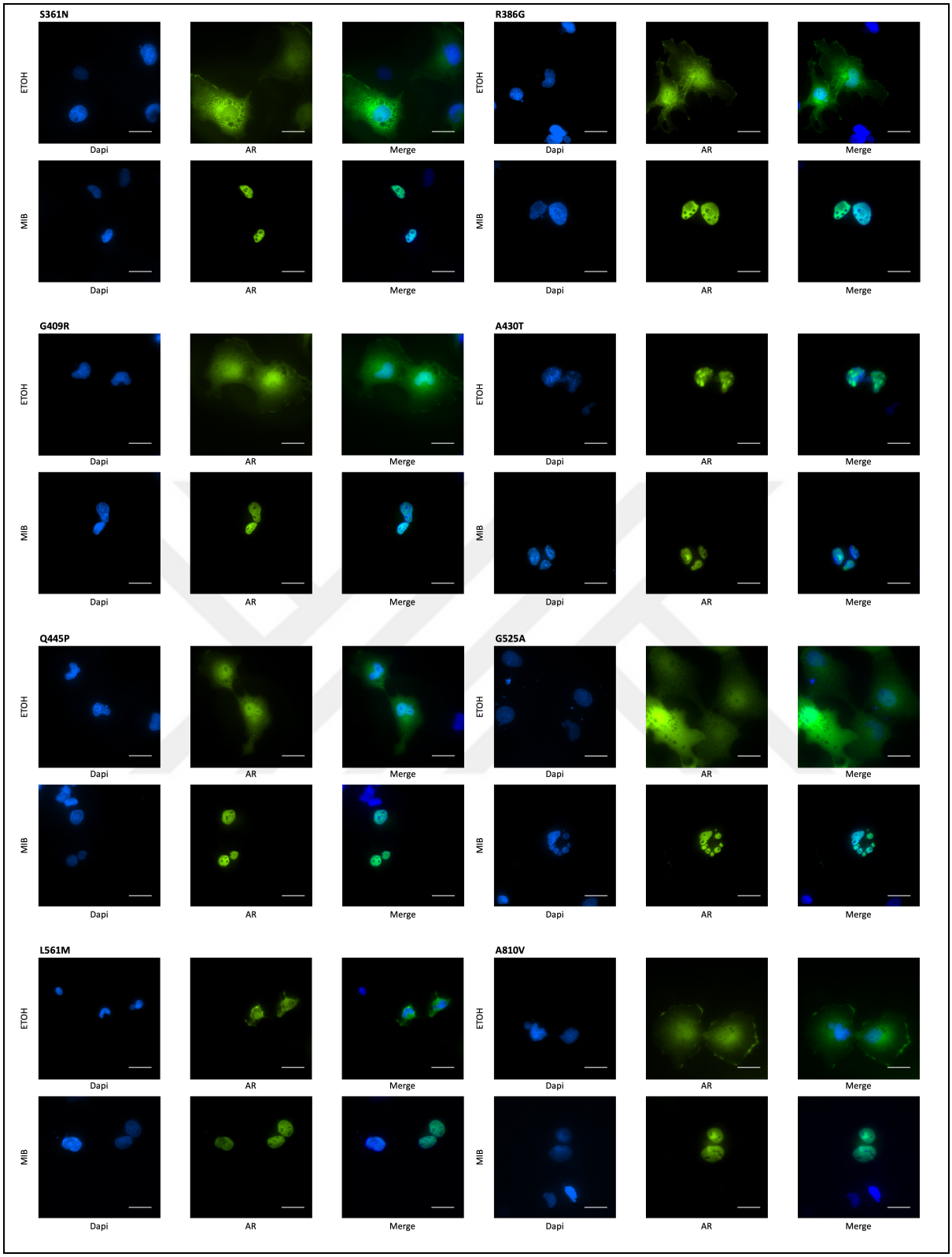
S361N
R386G
G409R
A430T
Q445P
G525A
L561M
A810V
ETOH
MIB
Dapi
AR
Merge

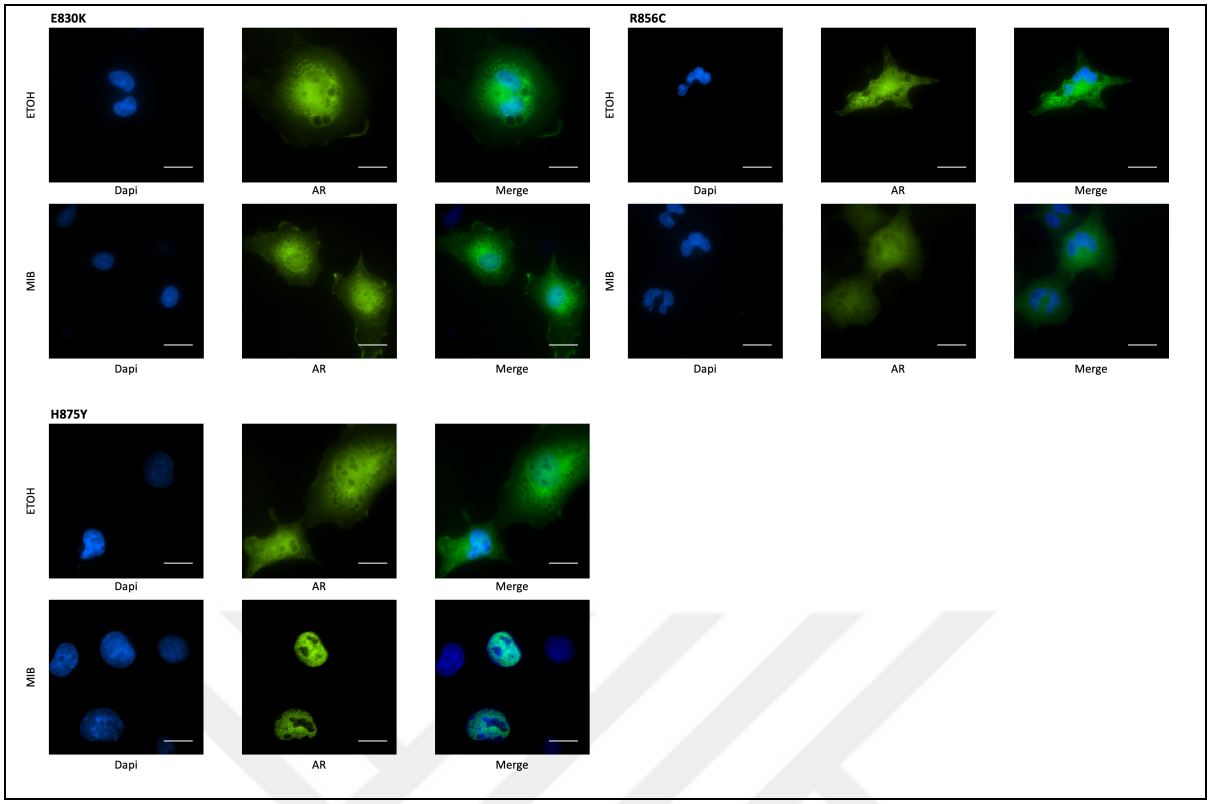

Figure 5-5 Cellular localisation of wild-type and mutant ARs in response to androgen

COS-1 cells were transiently transfected with plasmids encoding wild-type and mutant ARs (R13W, R31H, E81Q, E187Q, E304K, S336P, T338I, S361N, R386G, G409R, A430T, Q445P, G525A, L561M, A810V, E830K, R856C, H875Y), fused to Green fluorescent protein (GFP-AR). Cells were cultured in hormone-depleted media for 24 hours and fixed with 4% paraformaldehyde following 2 hours of treatment with EtOH (ethanol), and MIB (Mibolerone, 1 nM). Confocal microscopy was used to visualise the localisation of the ARs. 4',6-diamidino-2-phenylindole (Dapi) was used for nuclear staining (blue). Scale bar = 10 µm.

Table 5-3 Cellular localisation of AR mutants in response to androgen treatment

COS-1 cells were transiently transfected with plasmids encoding wild-type and mutant ARs (R13W, R31H, E81Q, E187Q, E304K, S336P, T338I, S361N, R386G, G409R, A430T, Q445P, G525A, L561M, A810V, E830K, R856C, H875Y), fused to Green fluorescent protein (GFP-AR). Confocal microscopy was used to visualise the localisation of the ARs. N, nuclear; C, cytoplasmic; EtOH, Ethanol; MIB, Mibolerone.

AR mutant	EtOH	MIB
R13W	C	N
R31H	C	N
E81Q	C	N
E187Q	C	C+N
E304K	C+N	N
S336P	N	N
T338I	C+N	N
S361N	C	N
R386G	C	N
G409R	C+N	N
A430T	N	N
Q445P	C+N	N
G525A	C	N
L561M	C	N
A810V	C	N
E830K	C	C
R856C	C	C
H875Y	C	N

5.6 Some AR mutants could inhibit the transcriptional activity of ERα

Some of the AR mutations, identified in BrCa, affect receptor specifity/activity/cellular localisation (Figure 5-3, Figure 5-4, Figure 5-5). Some were found to be transcriptionally dead, some were activated by different ligands, and some were predominantly localised in the nucleus in the absence of androgen. However, the crosstalk of these mutant receptors with ERα is also critical to analyse the effect of these variants in BrCa.

To further analyse the effects of these mutations on the transcriptional activity of ERα, their crosstalk with ERα was investigated using reporter assays. Cells were transfected with ERα, WT or mutant AR, and the ERE luciferase reporter, and then treated with vehicle (EtOH) or MIB and E2 (Figure 5-6). As expected, WT AR reduced ERα activity. Most of the mutants (R31H, E81Q, E304K, S336P, S361N, R386G, A430T, Q445P, Q488*, L561M, A810V, E830K, R856C, H875Y) inhibited ERα activity to a similar extent as WT. However, L57Q, E187Q, G409R, G525A had little effect upon ERα activity. Interestingly, R13W and T338I, enhanced the transcriptional activity of ERα.

The reporter assays demonstrated that some of the AR mutations identified in BrCa have the same effect as WT AR on ERα activity, whereas some of the substitutions had no effect upon ERα activity. More interestingly, some of the variants were found to enhance ERα activity.

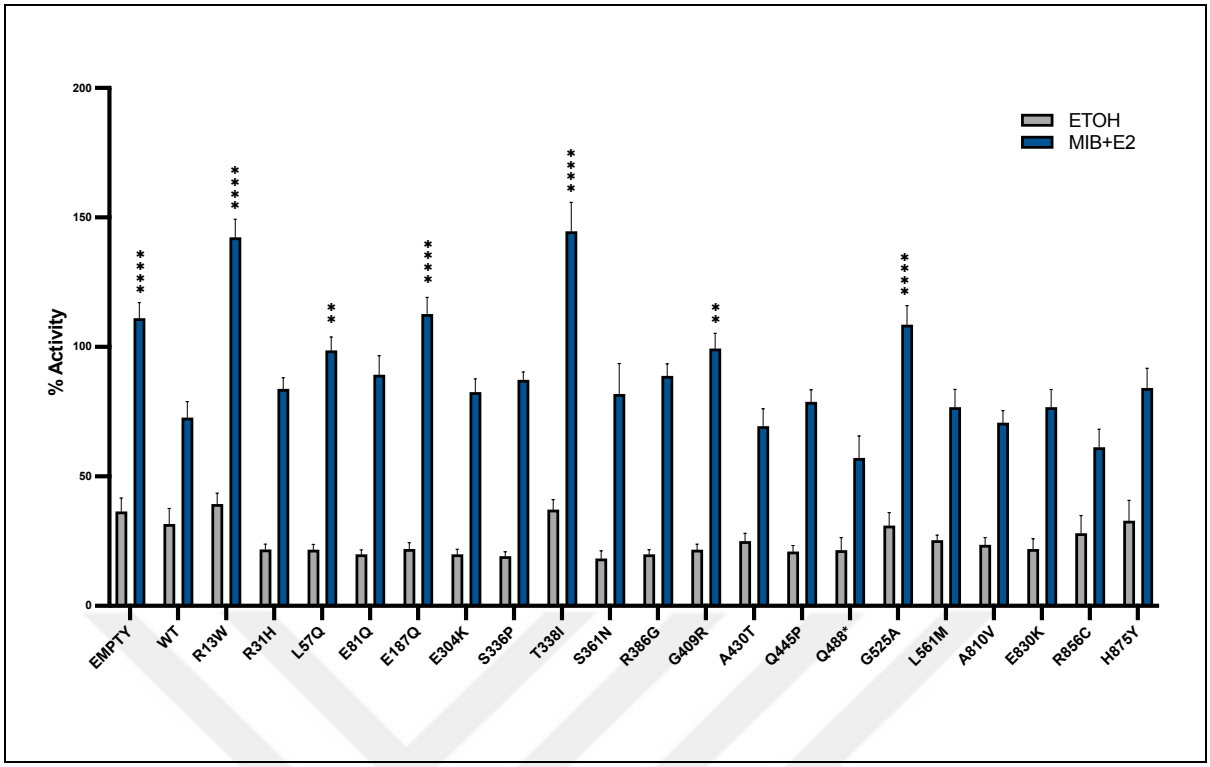

Figure 5-6 The crosstalk of WT and mutant ARs with ERα

COS-1 cells were seeded in hormone-depleted media, incubated for 24 hours, and transfected with an expression plasmid for ERα (pSG5-ERα), ERE luciferase reporter (3xERE-TATA-LUC), and renilla expression plasmid, along with either an empty plasmid, or an expression plasmid for wild-type (WT)/mutant AR (R13W, R31H, L57Q, E81Q, E187Q, E304K, S336P, T338I, S361N, R386G, G409R, A430T, Q445P, Q488, G525A, L561M, A810V, E830K, R856C, H875Y). Cells were incubated in hormone-depleted media for another 24 hours prior to treatment. Cells were treated with EtOH (ethanol), MIB (Mibolerone, 1 nM), E2 (17-β-Oestradiol, 1 nM) and in combination for 24 hours to evaluate receptor activity. Luciferase activity was normalised to renilla activity and results were made relative to ERα activity in the presence of 1 nM E2-only treatment. Graphs are the average of 3 individual experiments, each with triplicate repeats and generated with GraphPad Prism 9 software. ANOVA. **p ≤ 0.01, ****p ≤ 0.001. Mean ± 1SE.*

Table 5-4 Summary of mutant AR's biological activity in response to different treatments

Compared to WT AR: +, more active/enhances activity; -, less active/inhibits activity; C, cytoplasmic; N, nuclear; NA, data not available; ERE, ERα reporter; EtOH, Ethanol; MIB, Mibolerone.

AR Mutation	EtOH	Mibolerone			Oestradiol			Progesterone	Tamoxifen	Fulvestrant	ERE	Localisation	
		0.1 nM	1 nM	10 nM	1 nM	10 nM	100 nM					EtOH	MIB
R13W											+	C	N
R31H							+				-	C	N
L57Q			-	-			-					NA	NA
E81Q			-				-				-	C	N
E187Q												C	C+N
E304K							-				-	C+N	N
S336P											-	N	N
T338I											+	C+N	N
S361N											-	C	N
R386G							+				-	C	N
G409R												C+N	N
A430T			-	-			-				-	N	N
Q445P											-	C+N	N
Q488*			-	-			-				-	NA	NA
G525A												C	N
L561M											-	C	N
A810V							+				-	C	N
E830K							-				-	C	C
R856C			-	-		-	-				-	C	C
H875Y					+	+	+	+			-	C	N

5.7 Discussion

The expression of AR is linked to a better clinical outcome when coexpressed with ERα in BrCa (Peters et al., 2009; Castellano et al., 2010). However, in hormone receptor negative tumours the AR expression has been associated with proliferation, metastasis, lymphatic invasion, and poor survival rates (McGhan et al., 2014; Roseweir et al., 2017), suggesting that AR might be oncogenic in the absence of ERα.

More than 1000 mutations have been identified in *AR* and some of them are linked to diseases such as Androgen Insensitivity Syndrome (AIS), PrCa, Kennedy's disease (Gottlieb et al., 2012; Tan et al., 2015). Some of these AR mutations have also been found in therapy resistant PrCa tumour samples and metastasis sites, and it has been demonstrated that some of the substitutions found in the LBD region are activated by antiandrogens and other ligands (Fenton et al., 1997; Buchanan et al., 2001; Peters et al., 2009; Eisermann et al., 2013). An earlier study that was conducted with androgen independent PrCa patient samples found that tumours which were treated with androgen deprivation therapy in combination with the antiandrogen flutamide had mutant ARs that were stimulated by the drug, whereas tumours that were treated with only androgen deprivation therapy did not (Taplin et al., 1999), demonstrating that therapies provide a selective pressure upon the tumour.

The AR mutations in BrCa patients were found only in 1% of 6328 BrCa patient samples (5915 patients) investigated, and large number of alterations in the AR were gene amplifications. This low incidence of the AR mutations could be because the samples in the cBioPortal database are from early-stage tumours. In support of this, AR mutations are found to be less prevalent in early stage PrCa, and more prevalent in CRPC, and ERα mutations were found to be rare in early stage BrCa tumours. The *ESR1* mutation rate was 5% in this database cohort, however studies have shown that up to 20% of patients' ER gene (*ESR1*) is mutated in advanced or metastatic BrCa (Alluri et al., 2014). The incidence rate for AR mutations in advanced BrCa is still unknown. Larger studies involving advanced, and therapy resistant disease are therefore needed to quantify the incidence of the AR mutations in BrCa.

The majority of mutations that were identified in BrCa samples were in the NTD region of the receptor (unlike PrCa in which most mutations occur in LBD), and only a subset resulted in a change in the receptor's activity (Table 5-4 summarises the

changes in the mutant ARs), suggesting that some are passenger mutations. Although the DBD and LBD are necessary for the receptor to form a homodimer upon ligand exposure and bind to DNA, it has also been shown that NTD is critical for the transcriptional activity of AR (Callewaert et al., 2006; Dehm and Tindall, 2007). For example, the N/C (N-terminal/C-terminal) interaction has been shown to be critical for receptor's function (Wilson, 2011; Tan et al., 2015). Furthermore, the NTD harbours AF1, which constitutes two important transactivation units (TAU), TAU1 and TAU5 (Dehm and Tindall, 2007). TAU1 has been shown to have an impact upon AR transcriptional activity without coactivator recruitment (Callewaert et al., 2006). TAU5, on the other hand, acts as a coactivator recruiter (Dehm and Tindall, 2007). Thus, the change in the activity (L57Q, E81Q, A430T, Q488*) and localisation (S336P, A430T) of the receptor with the mutations in the NTD might be as a result of disruption of the TAUs. However, as the structure of the NTD has not been determined, further studies are needed to confirm these arguments.

Two of the NTD mutants, R13W and T338I, had similar activity to the WT receptor in response to the different hormones investigated (androgen, oestrogen, progesterone); however, surprisingly these variants were found to enhanced ERα's activity. This would suggest that these mutations result in receptors that activate instead of repressing ERα activity, which could promote BrCa growth.

The L57Q mutation has also been found in patient samples with hepatocellular carcinoma (Yeh et al., 2007), and in advanced PrCa (Tilley et al., 1996; Hay and McEwan, 2012). It has been reported that it has a loss of function in receptor's activity in response to DHT (0.1, 1, and 10 nM) via reporter assays using different ARE reporters (Hay and McEwan, 2012). In agreement with these reports, L57Q was also found to have reduced activity, in response to androgen, in this study.

S336P, the only mutation identified in ERα-negative, HER2-negative disease, was constitutively nuclear, and has also been identified in a patient with hormone resistant PrCa bone metastases (Hay and McEwan, 2012; Gottlieb et al., 2012). There are contradictory reports about the activity of this mutant in response to ligand. One study has shown that this substitution caused a loss of function in the receptor's activity when compared to WT, in response to DHT, using GRE_2-TAT-Luc reporter (Hay and McEwan, 2012). Another study has shown that the activity of this mutant receptor was not changed in comparison with WT when exposed to R1881, using the MMTV-Luc reporter (Li et al., 2005), in agreement with the results of this study which

showed no difference in the receptor's activity in response to different concentrations of MIB. The difference between these two studies could be explained by the different reporter elements used as it has been reported that the response element used in the latter study could be transactivated by AR without the need of androgen for N/C interaction (He et al., 2002). Further studies, comparing different luciferase reporters' response to ligand would be beneficial to determine the change of function caused by this substitution. Interestingly, the confocal microscopy showed that localisation of this mutant was constitutively nuclear. As it was shown that AR can become oncogenic and drive tumorigenesis in ERα receptor negative tumours, an ERα-negative BrCa cell line (e.g., MDA-MB-231) could be genetically engineered to express the mutant AR, facilitating further analyses to assess the effects of this mutation in BrCa.

Reporter assays also showed that Q488* was transcriptionally inactive which was expected as the mutant receptor was truncated, and did not have DBD and LBD regions. In agreement with this finding, the mutation has been associated with complete AIS (CAIS) (Boehmer et al., 2001). However, this mutant was not detectable at the protein level, despite the use of an N-Terminal AR antibody, suggesting that this variant was not expressed. Therefore, expression of the mutant receptor needs to be verified before any conclusions can be drawn. The only mutation that occurred in the DBD region (L561M) did not have a significant effect on receptor activity or translocation to the nucleus. This might be because it is not in one of the amino acids known to be important in DNA recognition/binding (Tan et al., 2015). It was also predicted by Provean that this mutant would not have an effect on the receptor function/activity.

Confocal microscopy identified that 2 of the 4 LBD mutations (E830K and R856C) were not able to translocate to the nucleus upon androgen treatment, demonstrating that trans-localisation is disrupted by these alterations. Reporter assays showed that AR transcriptional activity was disrupted by the R856C mutation, suggesting that R856C could affect the NLS. In agreement with these findings, R856C was also identified in patients with CAIS (Melo et al., 2003; Ledig et al., 2005), and is associated with a loss of function in the AR. Surprisingly, E830K had similar transcriptional activity to the WT receptor in reporter assays. In contrast, the other LBD mutations (A810V and H875Y) were able to translocate to the nucleus. This was expected for A810V, as the residue does not lie close to the ligand binding region, and reporter assays showed no change in the activity of the receptor compared to WT.

H875Y, which was close to the ligand binding pocket, did not cause a change in the receptor's activity as compared to WT upon androgen binding. However, this substitution reduced ligand specifity, increasing receptor activity in response to different ligands. H875Y mutation has been reported in metastatic androgen independent PrCa (Taplin et al., 1995), and is activated by E2, progesterone and hydroxyflutamide (Taplin et al., 1995; Taplin et al., 1999; McDonald et al., 2000). In accordance with these studies, this study has shown that the H875Y mutation, which was found in hormone receptor positive, HER2-negative tumour sample, was activated by progesterone and E2 (1, 10, and 100 nM), in addition to androgen.

It seems that some AR mutations in BrCa are activated by alternative hormones or transcriptionally dead, and that some of the mutations affect crosstalk with ERα. Interestingly, a number of mutations were found to decrease AR transcriptional activity in response to androgen, supporting the idea that ERα-positive BrCa tumours silence AR signalling pathway as this may give an advantage to the tumour for growth. However, the incidence of AR mutations in advanced and therapy resistant BrCa remains unknown. It is therefore possible that AR mutations do play a role in tumour progression and sequencing of advanced stage tumours will be needed to clarify the importance of these variants in BrCa. Although the incidence rate of AR mutations is low in BrCa, sequencing of tumours from patients with advanced disease will provide valuable information on the role of AR mutations in this stage of the disease. This knowledge could have important implications and lead to more effective and targeted treatment options for this stage of the disease.

Conclusions & Future Work

6.1 Conclusions

The majority of BrCa cases are endocrine sensitive (luminal A and luminal B) which means that the ERα, a ligand-dependent TF, is the main oncogenic driver and the tumour is dependent on oestrogens for proliferation and progression (Ali and Coombes, 2002; Renoir et al., 2013). As a result, blocking the ERα signalling pathway using antioestrogens or AIs is the cornerstone treatment for endocrine sensitive tumours (Perou et al., 2000; Ali and Coombes, 2002; Michmerhuizen et al., 2020). Antioestrogen treatments have significantly improved therapy outcomes and decreased mortality rates for early stage BrCa; however, therapy resistance is almost inevitable for the majority of patients who receive endocrine therapy (Fan et al., 2015; Murphy and Dickler, 2016; Haque and Desai, 2019; Szostakowska et al., 2019).

The AR is expressed in almost all BrCa subtypes, and several studies have shown that there is a strong association between ERα and AR expression in the disease (Castellano et al., 2010; Park et al., 2011; Rahim and O'Regan, 2017; Rangel et al., 2018; Vidula et al., 2019). AR overexpression in early BrCa is associated with better disease-free survival, and low expression of AR correlates with an increased risk of relapse, and cancer-associated deaths in ERα-positive BrCa patients (Peters et al., 2009; Vera-Badillo et al., 2014). Approximately one fifth of ERα-positive tumours, after receiving endocrine therapies, will lose ERα expression and become resistant to the existing therapies (Harrell et al., 2006). The AR is expressed in 90% of BrCa tumours, and there is a growing evidence that AR could replace ERα's activity, promoting cell division and proliferation, making the tumour ERα independent (Peters et al., 2009; Robinson et al., 2011; Carroll, 2016). The AR has been found to be expressed in almost 75% of metastasis sites in BrCa, and it is the only steroid receptor found in 25% of metastatic samples (Hickey et al., 2012). However, androgen signalling in ERα-positive BrCa has not been fully characterised.

It has been suggested that AR acts as a tumour suppressor and that activation of AR could be a treatment option for ERα-positive disease (Hickey, Dwyer, et al., 2021). Indeed, androgens were historically used as a treatment for BrCa (Garay and Park, 2012; Kotsopoulos and Narod, 2012). However, other studies have suggested that oestrogen-dependent tumours could become androgen dependent and therefore

AR activity should be blocked (Boccuzzi et al., 1995; de Amicis et al., 2010; Cochrane et al., 2014; Rechoum et al., 2014).

This study aimed to characterise AR signalling using cell line models and to elucidate the role of AR signalling when cells are treated with antioestrogens. The role of AR in TNBC has gained much attention recently, as the treatment options are limited for this subgroup of BrCa patients. TNBC tumours expressing AR are clinically defined as molecular apocrine tumours. Molecular apocrine cells are responsive to DHT for growth and androgen induces proliferative pathways. Inhibition of AR, using antiandrogens induces apoptosis and blocks androgen-induced growth, suggesting that in the absence of ERα signalling, activation of AR promotes proliferation and oncogenesis in BrCa (Doane et al., 2006; Naderi and Hughes-Davies, 2008; Chia et al., 2011; Ni et al., 2011; Ni et al., 2013). AR overexpression has also been proposed as a mechanism to explain endocrine resistance (especially for TAM and AI) (de Amicis et al., 2010; Cochrane et al., 2014; Ciupek et al., 2015; Chia et al., 2019; Michmerhuizen et al., 2020). For example, MCF7 cells were stably transfected with aromatase and/or AR (MCF7-aromatase, MCF7-aromatase-AR). Cells were then treated with androgens, an oestrogen precursor, and the aromatase inhibitor, anastrozole. It was found that anastrozole inhibited the androgen-stimulated growth of MCF7-aromotase cells but not MCF7-aromatase-AR cells. Treatment with antiandrogen blocked the proliferation of MCF7-aromatase cells and reversed the sensitivity of MCF7 cells to anastrozole (Rechoum et al., 2014).

The data presented here demonstrated that AR-ERα crosstalk is inhibitory. ERα was found to be inhibitory to AR target gene expression, DNA binding, and protein expression. Further, AR reduces ERα protein expression, and inhibits E2-induced cell proliferation. However, this inhibitory crosstalk is reversed when ERα is inhibited by antioestrogens. It was also demonstrated that AR target gene expression increases when antioestrogens block ERα, especially FULV; AR expression in MCF7 cells increases following antioestrogen treatment; MIB-induced AR activation reverses the inhibitory effect of FULV on BrCa cell proliferation. Further, the pro-oncogenic activity of MIB upon proliferation was inhibited by ENZA, demonstrating that this effect of MIB was mediated by AR. In agreement with these findings, it was demonstrated that AR expression levels are higher in metastasis sites as compared to primary tumours, and altered in patient tumour samples who received short term and long-term endocrine therapy (Schrijver et al., 2017; Aceto et al., 2018). It is known that therapy-induced

selective pressure selects for tumour cells with alterations that provides the cell with a growth advantage. It is therefore possible that AR signalling becomes active and selected for in tumours treated with antioestrogen therapies. This therapy escape mechanism could result in the cells taking on a molecular apocrine state. Inhibiting both receptors could potentially prevent tumours from the AR becoming active and therefore prevent resistance to endocrine therapies.

RNA-Seq analysis identified some candidate genes which AR activates to promote cell proliferation when ERα is inhibited by FULV. These genes might represent novel therapeutic targets and warrant further investigation. Thus, the characterisation of AR gene expression profiles on tumours from patients before and after receiving antioestrogen treatment would provide valuable information on the role of the AR, and downstream targets, in therapy response and disease progression. These genes could also be used as biomarkers and could be used to identify patients who would benefit from antiandrogen treatment.

The analysis of BrCa associated AR mutations revealed that some substitutions altered the activity of the receptor in response to its ligand. The mutants that have decreased activity in response to androgen treatment might provide an advantage to the tumours. As the crosstalk between AR and ERα was found to be inhibitory, inactivating AR might be an escape mechanism for the tumours to facilitate disease progression in ERα-positive disease. Some mutations also led to an increase in the transcriptional activity of ERα, therefore it is also possible that tumours might select for AR mutations, enhancing androgen signalling, resulting in a potential mechanism of therapy resistance. Analysis of the incidence rate of AR mutations in BrCa, particularly in advanced endocrine resistant stages of the disease would further our understanding of the role of these variants in the disease.

AR-targeted therapies, used for the treatment of PrCa, have been tested on BrCa patients in several clinical trials (Gucalp et al., 2013; Pietri et al., 2016). For example, there is an ongoing phase II study (NCT02955394) that is investigating the efficacy of the pre-operative administration of FULV and ENZA compared to FULV only treatment in ERα-positive BrCa. Another ongoing phase II study (NCT02953860) is evaluating the efficacy of ENZA and FULV combination in patients with ERα-positive advanced stage BrCa. However, the results of these studies have not been published yet. The data presented here supports the use of combined antioestrogen and antiandrogen treatment as a therapeutic option of BrCa, as this may reduce the development of

endocrine resistance. Further, antiandrogens could be an effective treatment option for endocrine resistant tumours and screening for AR expression (and AR target genes) could be used as prognostic marker(s) to identify patients who are most likely to benefit from these inhibitors.

6.2 Limitations and Future Work

Cell lines provide an insightful understanding of specific pathways by using one stimulant, as the cells can be starved from specific hormones. However, in physiological conditions tumours are exposed to different type of hormones and stimulants, which limits the findings of these experiments presented here. Although *in vitro* experiments with cell lines are good models to identify ERα-positive tumours' characteristics, *in vivo* models or patient derived *ex plants* are necessary to further identify, and confirm, the underlying mechanisms driving tumour growth. For example, the efficacy of antiandrogen treatments in patient tumour samples could also be investigated using patient derived xenograft models.

Elucidating the role of AR signalling in ERα-positive BrCa will help to selectively choose patients to receive antiandrogen therapies. Characterisation of the role of the AR in gene regulation, oncogenesis, and therapy resistance, is therefore needed. However, it is known that posttranslational modifications of steroid receptors are essential for the functioning of the receptor, and these events could be altered by other signalling pathways such as growth factors, and kinases. Although it is essential to understand the crosstalk between 2 receptors to decipher the mechanism, painting a picture of a tumour cell requires additional complexities. This study investigated the crosstalk between two receptors via the analysis of target gene expression, DNA binding, cell migration, cell proliferation and protein expression. Alterations in one component of a signalling pathway will often have an impact on a cascade of signalling events. Therefore, it is also important to investigate the effect of other factors known to be important in BrCa progression upon AR-ERα crosstalk. For example, the crosstalk of other steroid receptors, mutations in tumour suppressor and/or oncogenes would provide a better understanding of the interactions of the receptors in different backgrounds.

The RNA-Seq analysis identified interesting changes in gene expression profiles, however different treatment arms would also be informative in understanding the effect of AR-ERα crosstalk. For example, gene expression changes in response to E2 and FULV, MIB and FULV, and the addition of ENZA would have been useful additions to the study. It is also important to characterise the downstream alterations in protein expression in response to different treatment conditions. Therefore, proteomics analysis of AR signalling in cells treated with antioestrogens would be useful.

Having a high number of false positive target sites is a known issue for miRNA target gene prediction analysis. In this study, only one prediction tool has been used and it would be useful to use multiple prediction tools as this has been shown to increase the accuracy of target sites. However, using multiple tools might also result with false negatives. Another issue is that the role of miRNAs is highly dependent upon cellular context and prediction tools do not account for cell type differences when it comes to target prediction. To identify *bona fide* targets of the miRNAs, miRNA mimics or inhibitors (e.g. miRNA sponges, antagomirs) should be used.

References

Aceto, N., Bardia, A., Wittner, B.S., Donaldson, M.C., O'Keefe, R., Engstrom, A., Bersani, F., Zheng, Y., Comaills, V., Niederhoffer, K., Zhu, H., Mackenzie, O., Shioda, T., Sgroi, D., Kapur, R., Ting, D.T., Moy, B., Ramaswamy, S., Toner, M., Haber, D.A. and Maheswaran, S. 2018. AR Expression in Breast Cancer CTCs Associates with Bone Metastases. *Molecular cancer research : MCR*. **16**(4), pp.720–727.

Adly, L., Hill, D., Sherman, M.E., Sturgeon, S.R., Fears, T., Mies, C., Ziegler, R.G., Hoover, R.N. and Schairer, C. 2006. Serum concentrations of estrogens, sex hormone-binding globulin, and androgens and risk of breast cancer in postmenopausal women. *International journal of cancer*. **119**(10), pp.2402–7.

Ahram, M., Mustafa, E., Zaza, R., Abu Hammad, S., Alhudhud, M., Bawadi, R. and Zihlif, M. 2017. Differential expression and androgen regulation of microRNAs and metalloprotease 13 in breast cancer cells. *Cell biology international*. **41**(12), pp.1345–1355.

AJCC 2017. *American Joint Committee on Cancer. AJCC cancer staging manual.* 8th ed. (M. B. Amin, S. Edge, F. Greene, D. R. Byrd, R. K. Brookland, M. K. Washington, J. E. Gershenwald, C. C. Compton, K. R. Hess, D. C. Sullivan, J. M. Jessup, J. D. Brierley, L. E. Gaspar, R. L. Schilsky, & C. M. , Balch, eds.). New York: Springer International Publishing.

Ali, S. and Coombes, R.C. 2002. Endocrine-responsive breast cancer and strategies for combating resistance. *Nature reviews. Cancer*. **2**(2), pp.101–12.

Alluri, P.G., Speers, C. and Chinnaiyan, A.M. 2014. Estrogen receptor mutations and their role in breast cancer progression. *Breast cancer research : BCR*. **16**(6), p.494.

Alvarez-Baron, C.P., Jonsson, P., Thomas, C., Dryer, S.E. and Williams, C. 2011. The two-pore domain potassium channel KCNK5: induction by estrogen receptor alpha and role in proliferation of breast cancer cells. *Molecular endocrinology (Baltimore, Md.)*. **25**(8), pp.1326–36.

American Cancer Society 2019. American Cancer Society Breast Cancer Early Detection Recommendations. . (18 January 2019). [Accessed 7 January 2019]. Available from: https://www.cancer.org/cancer/breast-cancer/screening-tests-

and-early-detection/american-cancer-society-recommendations-for-the-early-detection-of-breast-cancer.html.

de Amicis, F., Thirugnansampanthan, J., Cui, Y., Selever, J., Beyer, A., Parra, I., Weigel, N.L., Herynk, M.H., Tsimelzon, A., Lewis, M.T., Chamness, G.C., Hilsenbeck, S.G., Andò, S. and Fuqua, S.A.W. 2010. Androgen receptor overexpression induces tamoxifen resistance in human breast cancer cells. *Breast cancer research and treatment*. **121**(1), pp.1–11.

Anestis, A., Karamouzis, M. v, Dalagiorgou, G. and Papavassiliou, A.G. 2015. Is androgen receptor targeting an emerging treatment strategy for triple negative breast cancer? *Cancer treatment reviews*. **41**(6), pp.547–53.

Anestis, A., Zoi, I., Papavassiliou, A.G. and Karamouzis, M. v 2020. Androgen Receptor in Breast Cancer-Clinical and Preclinical Research Insights. *Molecules (Basel, Switzerland)*. **25**(2), p.358.

Arce-Salinas, C., Riesco-Martinez, M.C., Hanna, W., Bedard, P. and Warner, E. 2016. Complete Response of Metastatic Androgen Receptor-Positive Breast Cancer to Bicalutamide: Case Report and Review of the Literature. *Journal of clinical oncology : official journal of the American Society of Clinical Oncology*. **34**(4), pp.e21-4.

Arendt, L.M. and Kuperwasser, C. 2015. Form and function: how estrogen and progesterone regulate the mammary epithelial hierarchy. *Journal of mammary gland biology and neoplasia*. **20**(1–2), pp.9–25.

Arpino, G., Laucirica, R. and Elledge, R.M. 2005. Premalignant and in situ breast disease: biology and clinical implications. *Annals of internal medicine*. **143**(6), pp.446–57.

Astvatsaturyan, K., Yue, Y., Walts, A.E. and Bose, S. 2018. Androgen receptor positive triple negative breast cancer: Clinicopathologic, prognostic, and predictive features. *PloS one*. **13**(6), p.e0197827.

Ayala, G., Thompson, T., Yang, G., Frolov, A., Li, R., Scardino, P., Ohori, M., Wheeler, T. and Harper, W. 2004. High levels of phosphorylated form of Akt-1 in prostate cancer and non-neoplastic prostate tissues are strong predictors of biochemical recurrence. *Clinical cancer research : an official journal of the American Association for Cancer Research*. **10**(19), pp.6572–8.

Bandini, E. and Fanini, F. 2019. MicroRNAs and Androgen Receptor: Emerging Players in Breast Cancer. *Frontiers in genetics*. **10**, p.203.

Bandyopadhyay, S., Pai, S.K., Hirota, S., Hosobe, S., Takano, Y., Saito, K., Piquemal, D., Commes, T., Watabe, M., Gross, S.C., Wang, Y., Ran, S. and Watabe, K. 2004. Role of the putative tumor metastasis suppressor gene Drg-1 in breast cancer progression. *Oncogene*. **23**(33), pp.5675–81.

Barnard, M.E., Boeke, C.E. and Tamimi, R.M. 2015. Established breast cancer risk factors and risk of intrinsic tumor subtypes. *Biochimica et biophysica acta*. **1856**(1), pp.73–85.

Barton, V.N., D'Amato, N.C., Gordon, M.A., Lind, H.T., Spoelstra, N.S., Babbs, B.L., Heinz, R.E., Elias, A., Jedlicka, P., Jacobsen, B.M. and Richer, J.K. 2015. Multiple molecular subtypes of triple-negative breast cancer critically rely on androgen receptor and respond to enzalutamide in vivo. *Molecular cancer therapeutics*. **14**(3), pp.769–78.

Baumgart, J., Nilsson, K., Stavreus Evers, A., Kunovac Kallak, T., Kushnir, M.M., Bergquist, J. and Sundström Poromaa, I. 2014. Androgen levels during adjuvant endocrine therapy in postmenopausal breast cancer patients. *Climacteric : the journal of the International Menopause Society*. **17**(1), pp.48–54.

Bear, H.D., Anderson, S., Brown, A., Smith, R., Mamounas, E.P., Fisher, B., Margolese, R., Theoret, H., Soran, A., Wickerham, D.L., Wolmark, N. and National Surgical Adjuvant Breast and Bowel Project Protocol B-27 2003. The effect on tumor response of adding sequential preoperative docetaxel to preoperative doxorubicin and cyclophosphamide: preliminary results from National Surgical Adjuvant Breast and Bowel Project Protocol B-27. *Journal of clinical oncology : official journal of the American Society of Clinical Oncology*. **21**(22), pp.4165–74.

Bevan, C.L., Hoare, S., Claessens, F., Heery, D.M. and Parker, M.G. 1999. The AF1 and AF2 domains of the androgen receptor interact with distinct regions of SRC1. *Molecular and cellular biology*. **19**(12), pp.8383–92.

Birrell, S.N., Bentel, J.M., Hickey, T.E., Ricciardelli, C., Weger, M.A., Horsfall, D.J. and Tilley, W.D. 1995. Androgens induce divergent proliferative responses in human breast cancer cell lines. *The Journal of steroid biochemistry and molecular biology*. **52**(5), pp.459–67.

Boccuzzi, G., Tamagno, E., Brignardello, E., di Monaco, M., Aragno, M. and Danni, O. 1995. Growth inhibition of DMBA-induced rat mammary carcinomas by the

antiandrogen flutamide. *Journal of cancer research and clinical oncology*. **121**(3), pp.150–4.

Böcker, W., Moll, R., Poremba, C., Holland, R., van Diest, P.J., Dervan, P., Bürger, H., Wai, D., Ina Diallo, R., Brandt, B., Herbst, H., Schmidt, A., Lerch, M.M. and Buchwallow, I.B. 2002. Common adult stem cells in the human breast give rise to glandular and myoepithelial cell lineages: a new cell biological concept. *Laboratory investigation; a journal of technical methods and pathology*. **82**(6), pp.737–46.

Bockmeyer, C.L., Christgen, M., Müller, M., Fischer, S., Ahrens, P., Länger, F., Kreipe, H. and Lehmann, U. 2011. MicroRNA profiles of healthy basal and luminal mammary epithelial cells are distinct and reflected in different breast cancer subtypes. *Breast cancer research and treatment*. **130**(3), pp.735–45.

Boehmer, A.L., Brinkmann, O., Brüggenwirth, H., van Assendelft, C., Otten, B.J., Verleun-Mooijman, M.C., Niermeijer, M.F., Brunner, H.G., Rouwé, C.W., Waelkens, J.J., Oostdijk, W., Kleijer, W.J., van der Kwast, T.H., de Vroede, M.A. and Drop, S.L. 2001. Genotype versus phenotype in families with androgen insensitivity syndrome. *The Journal of clinical endocrinology and metabolism*. **86**(9), pp.4151–60.

Boelens, M.C., Nethe, M., Klarenbeek, S., de Ruiter, J.R., Schut, E., Bonzanni, N., Zeeman, A.L., Wientjens, E., van der Burg, E., Wessels, L., van Amerongen, R. and Jonkers, J. 2016. PTEN Loss in E-Cadherin-Deficient Mouse Mammary Epithelial Cells Rescues Apoptosis and Results in Development of Classical Invasive Lobular Carcinoma. *Cell reports*. **16**(8), pp.2087–2101.

Boimel, P.J., Smirnova, T., Zhou, Z.N., Wyckoff, J., Park, H., Coniglio, S.J., Qian, B.-Z., Stanley, E.R., Cox, D., Pollard, J.W., Muller, W.J., Condeelis, J. and Segall, J.E. 2012. Contribution of CXCL12 secretion to invasion of breast cancer cells. *Breast cancer research : BCR*. **14**(1), p.R23.

Brooke, G.N. and Bevan, C.L. 2009. The role of androgen receptor mutations in prostate cancer progression. *Current genomics*. **10**(1), pp.18–25.

Buchanan, G., Greenberg, N.M., Scher, H.I., Harris, J.M., Marshall, V.R. and Tilley, W.D. 2001. Collocation of androgen receptor gene mutations in prostate cancer. *Clinical cancer research : an official journal of the American Association for Cancer Research*. **7**(5), pp.1273–81.

Buchegger, K., Riquelme, I., Viscarra, T., Ili, C., Brebi, P., Huang, T.H.-M. and Roa, J.C. 2017. Reprimo, a Potential p53-Dependent Tumor Suppressor Gene, Is Frequently Hypermethylated in Estrogen Receptor α-Positive Breast Cancer. *International journal of molecular sciences*. **18**(8), p.1525.

Burger, H.G. 2002. Androgen production in women. *Fertility and Sterility*. **77**(SUPPL. 4), pp.3–5.

Callewaert, L., van Tilborgh, N. and Claessens, F. 2006. Interplay between two hormone-independent activation domains in the androgen receptor. *Cancer research*. **66**(1), pp.543–53.

Cancer Genome Atlas Network 2012. Comprehensive molecular portraits of human breast tumours. *Nature*. **490**(7418), pp.61–70.

Cancer Research UK 2018a. Breast cancer incidence (invasive) statistics. [Accessed 8 November 2018]. Available from: https://www.cancerresearchuk.org/health-professional/cancer-statistics/statistics-by-cancer-type/breast-cancer.

Cancer Research UK 2016a. Breast cancer mortality by sex and UK country. [Accessed 15 December 2018]. Available from: https://www.cancerresearchuk.org/health-professional/cancer-statistics/statistics-by-cancer-type/breast-cancer/mortality.

Cancer Research UK 2016b. Breast cancer mortality trends over time. [Accessed 15 December 2018]. Available from: https://www.cancerresearchuk.org/health-professional/cancer-statistics/statistics-by-cancer-type/breast-cancer/mortality.

Cancer Research UK 2018b. Hormone therapy for breast cancer. [Accessed 8 November 2018]. Available from: https://www.cancerresearchuk.org/about-cancer/breast-cancer/treatment/hormone-therapy/about.

Cancer Research UK 2021. Prostate cancer statistics. [Accessed 12 September 2021]. Available from: https://www.cancerresearchuk.org/health-professional/cancer-statistics/statistics-by-cancer-type/prostate-cancer.

Cancer Research UK 2018c. Types of breast cancer surgery. [Accessed 20 December 2018]. Available from: https://www.cancerresearchuk.org/about-cancer/breast-cancer/treatment/surgery/types-surgery.

Cano, L.Q., Lavery, D.N. and Bevan, C.L. 2013. Mini-review: Foldosome regulation of androgen receptor action in prostate cancer. *Molecular and cellular endocrinology*. **369**(1–2), pp.52–62.

Cardoso, F., Bischoff, J., Brain, E., Zotano, Á.G., Lück, H.-J., Tjan-Heijnen, V.C., Tanner, M. and Aapro, M. 2013. A review of the treatment of endocrine responsive metastatic breast cancer in postmenopausal women. *Cancer treatment reviews*. **39**(5), pp.457–65.

Carroll, J.S. 2016. Mechanisms of oestrogen receptor (ER) gene regulation in breast cancer. *European journal of endocrinology*. **175**(1), pp.R41-9.

Casaburi, I., Cesario, M.G., Donà, A., Rizza, P., Aquila, S., Avena, P., Lanzino, M., Pellegrino, M., Vivacqua, A., Tucci, P., Morelli, C., Andò, S. and Sisci, D. 2016. Androgens downregulate miR-21 expression in breast cancer cells underlining the protective role of androgen receptor. *Oncotarget*. **7**(11), pp.12651–61.

Castellano, I., Allia, E., Accortanzo, V., Vandone, A.M., Chiusa, L., Arisio, R., Durando, A., Donadio, M., Bussolati, G., Coates, A.S., Viale, G. and Sapino, A. 2010. Androgen receptor expression is a significant prognostic factor in estrogen receptor positive breast cancers. *Breast cancer research and treatment*. **124**(3), pp.607–17.

CDC 2018. What Are the Risk Factors for Breast Cancer? [Accessed 21 December 2018]. Available from: https://www.cdc.gov/cancer/breast/basic_info/risk_factors.html.

Cerami, E., Gao, J., Dogrusoz, U., Gross, B.E., Sumer, S.O., Aksoy, B.A., Jacobsen, A., Byrne, C.J., Heuer, M.L., Larsson, E., Antipin, Y., Reva, B., Goldberg, A.P., Sander, C. and Schultz, N. 2012. The cBio cancer genomics portal: an open platform for exploring multidimensional cancer genomics data. *Cancer discovery*. **2**(5), pp.401–4.

Chang, M. 2012. Tamoxifen resistance in breast cancer. *Biomolecules & therapeutics*. **20**(3), pp.256–67.

Chen, C. and Okayama, H. 1987. High-efficiency transformation of mammalian cells by plasmid DNA. *Molecular and cellular biology*. **7**(8), pp.2745–52.

Chen, D., Sun, Y., Yuan, Y., Han, Z., Zhang, P., Zhang, J., You, M.J., Teruya-Feldstein, J., Wang, M., Gupta, S., Hung, M.-C., Liang, H. and Ma, L. 2014. miR-100 induces epithelial-mesenchymal transition but suppresses tumorigenesis, migration and invasion. *PLoS genetics*. **10**(2), p.e1004177.

Cheng, G., Li, Y., Omoto, Y., Wang, Y., Berg, T., Nord, M., Vihko, P., Warner, M., Piao, Y.-S. and Gustafsson, J.-A. 2005. Differential regulation of estrogen

receptor (ER)alpha and ERbeta in primate mammary gland. *The Journal of clinical endocrinology and metabolism*. **90**(1), pp.435–44.

Chia, K., Milioli, H., Portman, N., Laven-Law, G., Coulson, R., Yong, A., Segara, D., Parker, A., Caldon, C.E., Deng, N., Swarbrick, A., Tilley, W.D., Hickey, T.E. and Lim, E. 2019. Non-canonical AR activity facilitates endocrine resistance in breast cancer. *Endocrine-related cancer*. **26**(2), pp.251–264.

Chia, K.M., Liu, J., Francis, G.D. and Naderi, A. 2011. A feedback loop between androgen receptor and ERK signaling in estrogen receptor-negative breast cancer. *Neoplasia (New York, N.Y.)*. **13**(2), pp.154–66.

Cicirò, Y. and Sala, A. 2021. MYB oncoproteins: emerging players and potential therapeutic targets in human cancer. *Oncogenesis*. **10**(2), p.19.

Ciupek, A., Rechoum, Y., Gu, G., Gelsomino, L., Beyer, A.R., Brusco, L., Covington, K.R., Tsimelzon, A. and Fuqua, S.A.W. 2015. Androgen receptor promotes tamoxifen agonist activity by activation of EGFR in ERα-positive breast cancer. *Breast cancer research and treatment*. **154**(2), pp.225–37.

Clarke, C., Madden, S.F., Doolan, P., Aherne, S.T., Joyce, H., O'Driscoll, L., Gallagher, W.M., Hennessy, B.T., Moriarty, M., Crown, J., Kennedy, S. and Clynes, M. 2013. Correlating transcriptional networks to breast cancer survival: a large-scale coexpression analysis. *Carcinogenesis*. **34**(10), pp.2300–8.

Cochrane, D.R., Bernales, S., Jacobsen, B.M., Cittelly, D.M., Howe, E.N., D'Amato, N.C., Spoelstra, N.S., Edgerton, S.M., Jean, A., Guerrero, J., Gómez, F., Medicherla, S., Alfaro, I.E., McCullagh, E., Jedlicka, P., Torkko, K.C., Thor, A.D., Elias, A.D., Protter, A.A. and Richer, J.K. 2014. Role of the androgen receptor in breast cancer and preclinical analysis of enzalutamide. *Breast cancer research : BCR*. **16**(1), p.R7.

Coffey, K. and Robson, C.N. 2012. Regulation of the androgen receptor by post-translational modifications. *The Journal of endocrinology*. **215**(2), pp.221–37.

Costa, A. and Zanini, V. 2008. Precancerous lesions of the breast. *Nature Clinical Practice Oncology*. **5**(12), pp.700–704.

Crumbaker, M., Khoja, L. and Joshua, A.M. 2017. AR Signaling and the PI3K Pathway in Prostate Cancer. *Cancers*. **9**(4), p.34.

Cui, J., Shen, Y. and Li, R. 2013. Estrogen synthesis and signaling pathways during aging: from periphery to brain. *Trends in molecular medicine*. **19**(3), pp.197–209.

Curtis, C., Shah, S.P., Chin, S.-F., Turashvili, G., Rueda, O.M., Dunning, M.J., Speed, D., Lynch, A.G., Samarajiwa, S., Yuan, Y., Gräf, S., Ha, G., Haffari, G., Bashashati, A., Russell, R., McKinney, S., METABRIC Group, Langerød, A., Green, A., Provenzano, E., Wishart, G., Pinder, S., Watson, P., Markowetz, F., Murphy, L., Ellis, I., Purushotham, A., Børresen-Dale, A.-L., Brenton, J.D., Tavaré, S., Caldas, C. and Aparicio, S. 2012. The genomic and transcriptomic architecture of 2,000 breast tumours reveals novel subgroups. *Nature*. **486**(7403), pp.346–52.

Dąbrowska, E., Przylipiak, A., Zajkowska, M., Piskor, B.M., Sidorkiewicz, I., Szmitkowski, M. and Lawicki, S. 2020. Possible Diagnostic Application of CXCL12 and CXCR4 as Tumor Markers in Breast Cancer Patients. *Anticancer research*. **40**(6), pp.3221–3229.

Davey, R.A. and Grossmann, M. 2016. Androgen Receptor Structure, Function and Biology: From Bench to Bedside. *The Clinical biochemist. Reviews*. **37**(1), pp.3–15.

Dawson, S.-J., Rueda, O.M., Aparicio, S. and Caldas, C. 2013. A new genome-driven integrated classification of breast cancer and its implications. *The EMBO journal*. **32**(5), pp.617–28.

Dehm, S.M. and Tindall, D.J. 2007. Androgen receptor structural and functional elements: role and regulation in prostate cancer. *Molecular endocrinology (Baltimore, Md.)*. **21**(12), pp.2855–63.

Dimitrakakis, C. and Bondy, C. 2009. Androgens and the breast. *Breast cancer research : BCR*. **11**(5), p.212.

Doane, A.S., Danso, M., Lal, P., Donaton, M., Zhang, L., Hudis, C. and Gerald, W.L. 2006. An estrogen receptor-negative breast cancer subset characterized by a hormonally regulated transcriptional program and response to androgen. *Oncogene*. **25**(28), pp.3994–4008.

Dookeran, K.A. and Auer, P. 2017. The Emerging Role of Two-Pore Domain Potassium Channels in Breast Cancer. *Journal of Global Epidemiology and Environmental Health*., pp.27–36.

Drabsch, Y., Hugo, H., Zhang, R., Dowhan, D.H., Miao, Y.R., Gewirtz, A.M., Barry, S.C., Ramsay, R.G. and Gonda, T.J. 2007. Mechanism of and requirement for estrogen-regulated MYB expression in estrogen-receptor-positive breast cancer

cells. *Proceedings of the National Academy of Sciences of the United States of America*. **104**(34), pp.13762–7.

Eccles, S.A., Aboagye, E.O., Ali, S., Anderson, A.S., Armes, J., Berditchevski, F., Blaydes, J.P., Brennan, K., Brown, N.J., Bryant, H.E., Bundred, N.J., Burchell, J.M., Campbell, A.M., Carroll, J.S., Clarke, R.B., Coles, C.E., Cook, G.J.R., Cox, A., Curtin, N.J., Dekker, L. v, Silva, I. dos S., Duffy, S.W., Easton, D.F., Eccles, D.M., Edwards, D.R., Edwards, J., Evans, D., Fenlon, D.F., Flanagan, J.M., Foster, C., Gallagher, W.M., Garcia-Closas, M., Gee, J.M.W., Gescher, A.J., Goh, V., Groves, A.M., Harvey, A.J., Harvie, M., Hennessy, B.T., Hiscox, S., Holen, I., Howell, S.J., Howell, A., Hubbard, G., Hulbert-Williams, N., Hunter, M.S., Jasani, B., Jones, L.J., Key, T.J., Kirwan, C.C., Kong, A., Kunkler, I.H., Langdon, S.P., Leach, M.O., Mann, D.J., Marshall, J.F., Martin, L., Martin, S.G., Macdougall, J.E., Miles, D.W., Miller, W.R., Morris, J.R., Moss, S.M., Mullan, P., Natrajan, R., O'Connor, J.P.B., O'Connor, R., Palmieri, C., Pharoah, P.D.P., Rakha, E.A., Reed, E., Robinson, S.P., Sahai, E., Saxton, J.M., Schmid, P., Smalley, M.J., Speirs, V., Stein, R., Stingl, J., Streuli, C.H., Tutt, A.N.J., Velikova, G., Walker, R.A., Watson, C.J., Williams, K.J., Young, L.S. and Thompson, A.M. 2013. Critical research gaps and translational priorities for the successful prevention and treatment of breast cancer. *Breast cancer research : BCR*. **15**(5), p.R92.

Eisermann, K., Wang, D., Jing, Y., Pascal, L.E. and Wang, Z. 2013. Androgen receptor gene mutation, rearrangement, polymorphism. *Translational andrology and urology*. **2**(3), pp.137–147.

Elebro, K., Borgquist, S., Simonsson, M., Markkula, A., Jirström, K., Ingvar, C., Rose, C. and Jernström, H. 2015. Combined Androgen and Estrogen Receptor Status in Breast Cancer: Treatment Prediction and Prognosis in a Population-Based Prospective Cohort. *Clinical cancer research : an official journal of the American Association for Cancer Research*. **21**(16), pp.3640–50.

Ellis, M.J., Ding, L., Shen, D., Luo, J., Suman, V.J., Wallis, J.W., van Tine, B.A., Hoog, J., Goiffon, R.J., Goldstein, T.C., Ng, S., Lin, L., Crowder, R., Snider, J., Ballman, K., Weber, J., Chen, K., Koboldt, D.C., Kandoth, C., Schierding, W.S., McMichael, J.F., Miller, C.A., Lu, C., Harris, C.C., McLellan, M.D., Wendl, M.C., DeSchryver, K., Allred, D.C., Esserman, L., Unzeitig, G., Margenthaler, J., Babiera, G. v, Marcom, P.K., Guenther, J.M., Leitch, M., Hunt, K., Olson, J.,

Tao, Y., Maher, C.A., Fulton, L.L., Fulton, R.S., Harrison, M., Oberkfell, B., Du, F., Demeter, R., Vickery, T.L., Elhammali, A., Piwnica-Worms, H., McDonald, S., Watson, M., Dooling, D.J., Ota, D., Chang, L.-W., Bose, R., Ley, T.J., Piwnica-Worms, D., Stuart, J.M., Wilson, R.K. and Mardis, E.R. 2012. Whole-genome analysis informs breast cancer response to aromatase inhibition. *Nature*. **486**(7403), pp.353–60.

Endogenous Hormones and Breast Cancer Collaborative Group, Key, T.J., Appleby, P.N., Reeves, G.K., Travis, R.C., Alberg, A.J., Barricarte, A., Berrino, F., Krogh, V., Sieri, S., Brinton, L.A., Dorgan, J.F., Dossus, L., Dowsett, M., Eliassen, A.H., Fortner, R.T., Hankinson, S.E., Helzlsouer, K.J., Hoff man-Bolton, J., Comstock, G.W., Kaaks, R., Kahle, L.L., Muti, P., Overvad, K., Peeters, P.H.M., Riboli, E., Rinaldi, S., Rollison, D.E., Stanczyk, F.Z., Trichopoulos, D., Tworoger, S.S. and Vineis, P. 2013. Sex hormones and risk of breast cancer in premenopausal women: a collaborative reanalysis of individual participant data from seven prospective studies. *The Lancet. Oncology*. **14**(10), pp.1009–19.

Ewels, P., Magnusson, M., Lundin, S. and Käller, M. 2016. MultiQC: summarize analysis results for multiple tools and samples in a single report. *Bioinformatics (Oxford, England)*. **32**(19), pp.3047–8.

Fabi, A., Mottolese, M. and Segatto, O. 2014. Therapeutic targeting of ERBB2 in breast cancer: understanding resistance in the laboratory and combating it in the clinic. *Journal of molecular medicine (Berlin, Germany)*. **92**(7), pp.681–95.

Fan, P., Wang, J., Santen, R.J. and Yue, W. 2007. Long-term treatment with tamoxifen facilitates translocation of estrogen receptor alpha out of the nucleus and enhances its interaction with EGFR in MCF-7 breast cancer cells. *Cancer research*. **67**(3), pp.1352–60.

Fan, W., Chang, J. and Fu, P. 2015. Endocrine therapy resistance in breast cancer: current status, possible mechanisms and overcoming strategies. *Future medicinal chemistry*. **7**(12), pp.1511–9.

Fanning, S.W., Mayne, C.G., Dharmarajan, V., Carlson, K.E., Martin, T.A., Novick, S.J., Toy, W., Green, B., Panchamukhi, S., Katzenellenbogen, B.S., Tajkhorshid, E., Griffin, P.R., Shen, Y., Chandarlapaty, S., Katzenellenbogen, J.A. and Greene, G.L. 2016. Estrogen receptor alpha somatic mutations Y537S and D538G confer breast cancer endocrine resistance by stabilizing the activating function-2 binding conformation. *eLife*. **5**, p.e12792.

Farmer, P., Bonnefoi, H., Becette, V., Tubiana-Hulin, M., Fumoleau, P., Larsimont, D., Macgrogan, G., Bergh, J., Cameron, D., Goldstein, D., Duss, S., Nicoulaz, A.-L., Brisken, C., Fiche, M., Delorenzi, M. and Iggo, R. 2005. Identification of molecular apocrine breast tumours by microarray analysis. *Oncogene*. **24**(29), pp.4660–71.

Feng, Y., Spezia, M., Huang, S., Yuan, C., Zeng, Z., Zhang, L., Ji, X., Liu, W., Huang, B., Luo, W., Liu, B., Lei, Y., Du, S., Vuppalapati, A., Luu, H.H., Haydon, R.C., He, T.-C. and Ren, G. 2018. Breast cancer development and progression: Risk factors, cancer stem cells, signaling pathways, genomics, and molecular pathogenesis. *Genes & Diseases*. **5**(2), pp.77–106.

Feng, Y.-H. and Tsao, C.-J. 2016. Emerging role of microRNA-21 in cancer. *Biomedical reports*. **5**(4), pp.395–402.

Fenton, M.A., Shuster, T.D., Fertig, A.M., Taplin, M.E., Kolvenbag, G., Bubley, G.J. and Balk, S.P. 1997. Functional characterization of mutant androgen receptors from androgen-independent prostate cancer. *Clinical cancer research : an official journal of the American Association for Cancer Research*. **3**(8), pp.1383–8.

Fernandes, R.C., Hickey, T.E., Tilley, W.D. and Selth, L.A. 2019. Interplay between the androgen receptor signaling axis and microRNAs in prostate cancer. *Endocrine-related cancer*. **26**(5), pp.R237–R257.

Fioretti, F.M., Sita-Lumsden, A., Bevan, C.L. and Brooke, G.N. 2014. Revising the role of the androgen receptor in breast cancer. *Journal of molecular endocrinology*. **52**(3), pp.R257-65.

Foster, P.A. 2008. Steroid metabolism in breast cancer. *Minerva endocrinologica*. **33**(1), pp.27–37.

Fritzsche, F., Gansukh, T., Borgoño, C.A., Burkhardt, M., Pahl, S., Mayordomo, E., Winzer, K.-J., Weichert, W., Denkert, C., Jung, K., Stephan, C., Dietel, M., Diamandis, E.P., Dahl, E. and Kristiansen, G. 2006. Expression of human Kallikrein 14 (KLK14) in breast cancer is associated with higher tumour grades and positive nodal status. *British journal of cancer*. **94**(4), pp.540–7.

Garay, J.P. and Park, B.H. 2012. Androgen receptor as a targeted therapy for breast cancer. *American journal of cancer research*. **2**(4), pp.434–45.

Garner, C. 1994. Uses of GnRH agonists. *Journal of obstetric, gynecologic, and neonatal nursing : JOGNN*. **23**(7), pp.563–70.

Gelman, I.H. 2012. Suppression of tumor and metastasis progression through the scaffolding functions of SSeCKS/Gravin/AKAP12. *Cancer metastasis reviews*. **31**(3–4), pp.493–500.

Gelmann, E.P. 2002. Molecular biology of the androgen receptor. *Journal of clinical oncology : official journal of the American Society of Clinical Oncology*. **20**(13), pp.3001–15.

Gerratana, L., Basile, D., Buono, G., de Placido, S., Giuliano, M., Minichillo, S., Coinu, A., Martorana, F., de Santo, I., del Mastro, L., de Laurentiis, M., Puglisi, F. and Arpino, G. 2018. Androgen receptor in triple negative breast cancer: A potential target for the targetless subtype. *Cancer treatment reviews*. **68**, pp.102–110.

Giovannelli, P., di Donato, M., Auricchio, F., Castoria, G. and Migliaccio, A. 2019. Androgens Induce Invasiveness of Triple Negative Breast Cancer Cells Through AR/Src/PI3-K Complex Assembly. *Scientific reports*. **9**(1), p.4490.

Giovannelli, P., di Donato, M., Galasso, G., di Zazzo, E., Bilancio, A. and Migliaccio, A. 2018. The Androgen Receptor in Breast Cancer. *Frontiers in endocrinology*. **9**, p.492.

Goel, S., Sharma, R., Hamilton, A. and Beith, J. 2009. LHRH agonists for adjuvant therapy of early breast cancer in premenopausal women. *The Cochrane database of systematic reviews*. (4), p.CD004562.

Gong, Y., He, T., Yang, L., Yang, G., Chen, Y. and Zhang, X. 2015. The role of miR-100 in regulating apoptosis of breast cancer cells. *Scientific reports*. **5**, p.11650.

Gonzalez-Angulo, A.M., Morales-Vasquez, F. and Hortobagyi, G.N. 2007. Overview of resistance to systemic therapy in patients with breast cancer. *Advances in experimental medicine and biology*. **608**, pp.1–22.

Gottlieb, B., Beitel, L.K., Nadarajah, A., Paliouras, M. and Trifiro, M. 2012. The androgen receptor gene mutations database: 2012 update. *Human mutation*. **33**(5), pp.887–94.

Grant, C.E., Bailey, T.L. and Noble, W.S. 2011. FIMO: scanning for occurrences of a given motif. *Bioinformatics (Oxford, England)*. **27**(7), pp.1017–8.

Groner, A.C. and Brown, M. 2017. Role of steroid receptor and coregulator mutations in hormone-dependent cancers. *The Journal of clinical investigation*. **127**(4), pp.1126–1135.

Gucalp, A., Tolaney, S., Isakoff, S.J., Ingle, J.N., Liu, M.C., Carey, L.A., Blackwell, K., Rugo, H., Nabell, L., Forero, A., Stearns, V., Doane, A.S., Danso, M., Moynahan, M.E., Momen, L.F., Gonzalez, J.M., Akhtar, A., Giri, D.D., Patil, S., Feigin, K.N., Hudis, C.A., Traina, T.A. and Translational Breast Cancer Research Consortium (TBCRC 011) 2013. Phase II trial of bicalutamide in patients with androgen receptor-positive, estrogen receptor-negative metastatic Breast Cancer. *Clinical cancer research : an official journal of the American Association for Cancer Research*. **19**(19), pp.5505–12.

Gucalp, A. and Traina, T.A. 2017. The Androgen Receptor: Is It a Promising Target? *Annals of surgical oncology*. **24**(10), pp.2876–2880.

Hall, J.E. 2011a. Endocrinology and Reproduction *In*: *Guyton and Hall Textbook of Medical Physiology*. Philadelphia: Elsevier, pp.881–1027.

Hall, J.E. 2011b. Female Physiology Before Pregnancy and Female Hormones *In*: *Guyton and Hall Textbook of Medical Physiology*. Philadelphia: Elsevier, pp.987–1000.

Hanker, A.B., Sudhan, D.R. and Arteaga, C.L. 2020. Overcoming Endocrine Resistance in Breast Cancer. *Cancer Cell*. **37**(4), pp.496–513.

Hapangama, D.K., Kamal, A.M. and Bulmer, J.N. 2015. Estrogen receptor β: the guardian of the endometrium. *Human reproduction update*. **21**(2), pp.174–93.

Haque, M.M. and Desai, K. v 2019. Pathways to Endocrine Therapy Resistance in Breast Cancer. *Frontiers in endocrinology*. **10**, p.573.

Harrell, J.C., Dye, W.W., Allred, D.C., Jedlicka, P., Spoelstra, N.S., Sartorius, C.A. and Horwitz, K.B. 2006. Estrogen receptor positive breast cancer metastasis: altered hormonal sensitivity and tumor aggressiveness in lymphatic vessels and lymph nodes. *Cancer research*. **66**(18), pp.9308–15.

Hay, C.W. and McEwan, I.J. 2012. The impact of point mutations in the human androgen receptor: classification of mutations on the basis of transcriptional activity. *PloS one*. **7**(3), p.e32514.

He, B., Lee, L.W., Minges, J.T. and Wilson, E.M. 2002. Dependence of selective gene activation on the androgen receptor NH2- and COOH-terminal interaction. *The Journal of biological chemistry*. **277**(28), pp.25631–9.

He, J., Wu, M., Xiong, L., Gong, Y., Yu, R., Peng, W., Li, Lili, Li, Li, Tian, S., Wang, Y., Tao, Q. and Xiang, T. 2020. BTB/POZ zinc finger protein ZBTB16 inhibits

breast cancer proliferation and metastasis through upregulating ZBTB28 and antagonizing BCL6/ZBTB27. *Clinical epigenetics*. **12**(1), p.82.

Heery, D.M., Kalkhoven, E., Hoare, S. and Parker, M.G. 1997. A signature motif in transcriptional co-activators mediates binding to nuclear receptors. *Nature*. **387**(6634), pp.733–6.

Heinlein, C.A. and Chang, C. 2002. The roles of androgen receptors and androgen-binding proteins in nongenomic androgen actions. *Molecular endocrinology (Baltimore, Md.)*. **16**(10), pp.2181–7.

Hickey, T.E., Dwyer, A.R. and Tilley, W.D. 2021. Arming androgen receptors to oppose oncogenic estrogen receptor activity in breast cancer. *British journal of cancer*. **125**(12), pp.1599–1601.

Hickey, T.E., Irvine, C.M., Dvinge, H., Tarulli, G.A., Hanson, A.R., Ryan, N.K., Pickering, M.A., Birrell, S.N., Hu, D.G., Mackenzie, P.I., Russell, R., Caldas, C., Raj, G. v, Dehm, S.M., Plymate, S.R., Bradley, R.K., Tilley, W.D. and Selth, L.A. 2015. Expression of androgen receptor splice variants in clinical breast cancers. *Oncotarget*. **6**(42), pp.44728–44.

Hickey, T.E., Robinson, J.L.L., Carroll, J.S. and Tilley, W.D. 2012. Minireview: The androgen receptor in breast tissues: growth inhibitor, tumor suppressor, oncogene? *Molecular endocrinology (Baltimore, Md.)*. **26**(8), pp.1252–67.

Hickey, T.E., Selth, L.A., Chia, K.M., Laven-Law, G., Milioli, H.H., Roden, D., Jindal, S., Hui, M., Finlay-Schultz, J., Ebrahimie, E., Birrell, S.N., Stelloo, S., Iggo, R., Alexandrou, S., Caldon, C.E., Abdel-Fatah, T.M., Ellis, I.O., Zwart, W., Palmieri, C., Sartorius, C.A., Swarbrick, A., Lim, E., Carroll, J.S. and Tilley, W.D. 2021. The androgen receptor is a tumor suppressor in estrogen receptor-positive breast cancer. *Nature medicine*. **27**(2), pp.310–320.

Higa, G.M. and Fell, R.G. 2013. Sex hormone receptor repertoire in breast cancer. *International journal of breast cancer*. **2013**, p.284036.

Hon, J.D.C., Singh, B., Sahin, A., Du, G., Wang, J., Wang, V.Y., Deng, F.-M., Zhang, D.Y., Monaco, M.E. and Lee, P. 2016. Breast cancer molecular subtypes: from TNBC to QNBC. *American journal of cancer research*. **6**(9), pp.1864–1872.

Hu, J., Lei, H., Fei, X., Liang, S., Xu, H., Qin, D., Wang, Y., Wu, Y. and Li, B. 2015. NES1/KLK10 gene represses proliferation, enhances apoptosis and down-regulates glucose metabolism of PC3 prostate cancer cells. *Scientific reports*. **5**, p.17426.

Hu, X., Huang, W. and Fan, M. 2017. Emerging therapies for breast cancer. *Journal of hematology & oncology*. **10**(1), p.98.

Huang, P., Chandra, V. and Rastinejad, F. 2010. Structural overview of the nuclear receptor superfamily: insights into physiology and therapeutics. *Annual review of physiology*. **72**, pp.247–72.

Hurtado, A., Holmes, K.A., Ross-Innes, C.S., Schmidt, D. and Carroll, J.S. 2011. FOXA1 is a key determinant of estrogen receptor function and endocrine response. *Nature genetics*. **43**(1), pp.27–33.

Iorio, M. v, Casalini, P., Piovan, C., Braccioli, L. and Tagliabue, E. 2011. Breast cancer and microRNAs: therapeutic impact. *Breast (Edinburgh, Scotland)*. **20 Suppl 3**, pp.S63-70.

Jain, A., Lam, A., Vivanco, I., Carey, M.F. and Reiter, R.E. 2002. Identification of an androgen-dependent enhancer within the prostate stem cell antigen gene. *Molecular endocrinology (Baltimore, Md.)*. **16**(10), pp.2323–37.

Jenster, G., van der Korput, H.A., Trapman, J. and Brinkmann, A.O. 1995. Identification of two transcription activation units in the N-terminal domain of the human androgen receptor. *The Journal of biological chemistry*. **270**(13), pp.7341–6.

Johns Hopkins Pathology 2021. Staging & Grade - Breast Pathology. [Accessed 21 December 2021]. Available from: https://pathology.jhu.edu/breast/staging-grade/.

Jordan, V.C. 2007. SERMs: meeting the promise of multifunctional medicines. *Journal of the National Cancer Institute*. **99**(5), pp.350–6.

Kakugawa, Y., Tada, H., Kawai, M., Suzuki, T., Nishino, Y., Kanemura, S., Ishida, T., Ohuchi, N. and Minami, Y. 2017. Associations of obesity and physical activity with serum and intratumoral sex steroid hormone levels among postmenopausal women with breast cancer: analysis of paired serum and tumor tissue samples. *Breast cancer research and treatment*. **162**(1), pp.115–125.

Kato, S., Endoh, H., Masuhiro, Y., Kitamoto, T., Uchiyama, S., Sasaki, H., Masushige, S., Gotoh, Y., Nishida, E., Kawashima, H., Metzger, D. and Chambon, P. 1995. Activation of the estrogen receptor through phosphorylation by mitogen-activated protein kinase. *Science (New York, N.Y.)*. **270**(5241), pp.1491–4.

Kato, S., Masuhiro, Y., Watanabe, M., Kobayashi, Y., Takeyama, K.I., Endoh, H. and Yanagisawa, J. 2000. Molecular mechanism of a cross-talk between oestrogen and growth factor signalling pathways. *Genes to cells : devoted to molecular & cellular mechanisms*. **5**(8), pp.593–601.

Kensler, K.H., Regan, M.M., Heng, Y.J., Baker, G.M., Pyle, M.E., Schnitt, S.J., Hazra, A., Kammler, R., Thürlimann, B., Colleoni, M., Viale, G., Brown, M. and Tamimi, R.M. 2019. Prognostic and predictive value of androgen receptor expression in postmenopausal women with estrogen receptor-positive breast cancer: results from the Breast International Group Trial 1-98. *Breast cancer research : BCR*. **21**(1), p.30.

Kotsopoulos, J. and Narod, S.A. 2012. Androgens and breast cancer. *Steroids*. **77**(1–2), pp.1–9.

Kumar, V., Abbas, A.K. and Aster, J.C. 2013. Breast *In*: *Robbins Basic Pathology*. Philadelphia: Elsevier, pp.704–714.

Kumarswamy, R., Volkmann, I. and Thum, T. 2011. Regulation and function of miRNA-21 in health and disease. *RNA biology*. **8**(5), pp.706–13.

Kuribayashi, K., Krigsfeld, G., Wang, W., Xu, J., Mayes, P.A., Dicker, D.T., Wu, G.S. and El-Deiry, W.S. 2008. TNFSF10 (TRAIL), a p53 target gene that mediates p53-dependent cell death. *Cancer biology & therapy*. **7**(12), pp.2034–8.

Lakshmana, G. and Baniahmad, A. 2019. Interference with the androgen receptor protein stability in therapy-resistant prostate cancer. *International journal of cancer*. **144**(8), pp.1775–1779.

Lanzino, M., de Amicis, F., McPhaul, M.J., Marsico, S., Panno, M.L. and Andò, S. 2005. Endogenous coactivator ARA70 interacts with estrogen receptor alpha (ERalpha) and modulates the functional ERalpha/androgen receptor interplay in MCF-7 cells. *The Journal of biological chemistry*. **280**(21), pp.20421–30.

Lasko, L.M., Jakob, C.G., Edalji, R.P., Qiu, W., Montgomery, D., Digiammarino, E.L., Hansen, T.M., Risi, R.M., Frey, R., Manaves, V., Shaw, B., Algire, M., Hessler, P., Lam, L.T., Uziel, T., Faivre, E., Ferguson, D., Buchanan, F.G., Martin, R.L., Torrent, M., Chiang, G.G., Karukurichi, K., Langston, J.W., Weinert, B.T., Choudhary, C., de Vries, P., van Drie, J.H., McElligott, D., Kesicki, E., Marmorstein, R., Sun, C., Cole, P.A., Rosenberg, S.H., Michaelides, M.R., Lai, A. and Bromberg, K.D. 2017. Discovery of a selective catalytic p300/CBP inhibitor that targets lineage-specific tumours. *Nature*. **550**(7674), pp.128–132.

de Laurentiis, M., Cancello, G., D'Agostino, D., Giuliano, M., Giordano, A., Montagna, E., Lauria, R., Forestieri, V., Esposito, A., Silvestro, L., Pennacchio, R., Criscitiello, C., Montanino, A., Limite, G., Bianco, A.R. and de Placido, S. 2008. Taxane-based combinations as adjuvant chemotherapy of early breast cancer: a meta-analysis of randomized trials. *Journal of clinical oncology : official journal of the American Society of Clinical Oncology*. **26**(1), pp.44–53.

Lavinsky, R.M., Jepsen, K., Heinzel, T., Torchia, J., Mullen, T.M., Schiff, R., Del-Rio, A.L., Ricote, M., Ngo, S., Gemsch, J., Hilsenbeck, S.G., Osborne, C.K., Glass, C.K., Rosenfeld, M.G. and Rose, D.W. 1998. Diverse signaling pathways modulate nuclear receptor recruitment of N-CoR and SMRT complexes. *Proceedings of the National Academy of Sciences of the United States of America*. **95**(6), pp.2920–5.

Lebeau, A. 2010. Precancerous Lesions of the Breast. *Breast care (Basel, Switzerland)*. **5**(4), pp.204–206.

Ledig, S., Jakubiczka, S., Neulen, J., Aulepp, U., Burck-Lehmann, U., Mohnike, K., Thiele, H., Zierler, H., Brewer, C. and Wieacker, P. 2005. Novel and recurrent mutations in patients with androgen insensitivity syndromes. *Hormone research*. **63**(6), pp.263–9.

Lee, P.M.Y., Chan, W.C., Kwok, C.C.-H., Wu, C., Law, S.-H., Tsang, K.-H., Yu, W.-C., Yeung, Y.-C., Chang, L.D.J., Wong, C.K.M., Wang, F. and Tse, L.A. 2019. Associations between Coffee Products and Breast Cancer Risk: a Case-Control study in Hong Kong Chinese Women. *Scientific reports*. **9**(1), p.12684.

Lehmann, B.D., Bauer, J.A., Chen, X., Sanders, M.E., Chakravarthy, A.B., Shyr, Y. and Pietenpol, J.A. 2011. Identification of human triple-negative breast cancer subtypes and preclinical models for selection of targeted therapies. *The Journal of clinical investigation*. **121**(7), pp.2750–67.

Lei, J.T., Anurag, M., Haricharan, S., Gou, X. and Ellis, M.J. 2019. Endocrine therapy resistance: new insights. *Breast (Edinburgh, Scotland)*. **48 Suppl 1**, pp.S26–S30.

Li, H., Li, J., Su, Y., Fan, Y., Guo, X., Li, L., Su, X., Rong, R., Ying, J., Mo, X., Liu, K., Zhang, Z., Yang, F., Jiang, G., Wang, J., Zhang, Y., Ma, D., Tao, Q. and Han, W. 2014. A novel 3p22.3 gene CMTM7 represses oncogenic EGFR signaling and inhibits cancer cell growth. *Oncogene*. **33**(24), pp.3109–18.

Li, Qing, Li, Z., Wei, S., Wang, W., Chen, Z., Zhang, L., Chen, L., Li, B., Sun, G., Xu, J., Li, Qiang, Wang, L., Xu, Zhipeng, Xia, Y., Zhang, D., Xu, H. and Xu, Zekuan 2017. Overexpression of miR-584-5p inhibits proliferation and induces apoptosis by targeting WW domain-containing E3 ubiquitin protein ligase 1 in gastric cancer. *Journal of experimental & clinical cancer research : CR*. **36**(1), p.59.

Li, Sijie, Han, B., Liu, G., Li, Songyun, Ouellet, J., Labrie, F. and Pelletier, G. 2010. Immunocytochemical localization of sex steroid hormone receptors in normal human mammary gland. *The journal of histochemistry and cytochemistry : official journal of the Histochemistry Society*. **58**(6), pp.509–15.

Li, W., Cavasotto, C.N., Cardozo, T., Ha, S., Dang, T., Taneja, S.S., Logan, S.K. and Garabedian, M.J. 2005. Androgen receptor mutations identified in prostate cancer and androgen insensitivity syndrome display aberrant ART-27 coactivator function. *Molecular endocrinology (Baltimore, Md.)*. **19**(9), pp.2273–82.

Lin, H.K., Yeh, S., Kang, H.Y. and Chang, C. 2001. Akt suppresses androgen-induced apoptosis by phosphorylating and inhibiting androgen receptor. *Proceedings of the National Academy of Sciences of the United States of America*. **98**(13), pp.7200–5.

Link, T., Kuithan, F., Ehninger, A., Kuhlmann, J.D., Kramer, M., Werner, A., Gatzweiler, A., Richter, B., Ehninger, G., Baretton, G., Bachmann, M., Wimberger, P. and Friedrich, K. 2017. Exploratory investigation of PSCA-protein expression in primary breast cancer patients reveals a link to HER2/neu overexpression. *Oncotarget*. **8**(33), pp.54592–54603.

Loh, H.-Y., Norman, B.P., Lai, K.-S., Rahman, N.M.A.N.A., Alitheen, N.B.M. and Osman, M.A. 2019. The Regulatory Role of MicroRNAs in Breast Cancer. *International journal of molecular sciences*. **20**(19), p.4940.

Lumachi, F., Santeufemia, D.A. and Basso, S.M. 2015. Current medical treatment of estrogen receptor-positive breast cancer. *World journal of biological chemistry*. **6**(3), pp.231–9.

Lyu, S., Yu, Q., Ying, G., Wang, S., Wang, Y., Zhang, J. and Niu, Y. 2014. Androgen receptor decreases CMYC and KRAS expression by upregulating let-7a expression in ER-, PR-, AR+ breast cancer. *International journal of oncology*. **44**(1), pp.229–37.

Ma, B., Li, H., Qiao, J., Meng, T. and Yu, R. 2020. Immune-related miRNA signature identifies prognosis and immune landscape in head and neck squamous cell carcinomas. *Bioscience reports*. **40**(11), p.BSR20201820.

Macedo, L.F., Guo, Z., Tilghman, S.L., Sabnis, G.J., Qiu, Y. and Brodie, A. 2006. Role of androgens on MCF-7 breast cancer cell growth and on the inhibitory effect of letrozole. *Cancer research*. **66**(15), pp.7775–82.

Macias, H. and Hinck, L. 2012. Mammary gland development. *Wiley interdisciplinary reviews. Developmental biology*. **1**(4), pp.533–57.

Magnani, L., Stoeck, A., Zhang, X., Lánczky, A., Mirabella, A.C., Wang, T.-L., Gyorffy, B. and Lupien, M. 2013. Genome-wide reprogramming of the chromatin landscape underlies endocrine therapy resistance in breast cancer. *Proceedings of the National Academy of Sciences of the United States of America*. **110**(16), pp.E1490-9.

le Maire, A., Bourguet, W. and Balaguer, P. 2010. A structural view of nuclear hormone receptor: endocrine disruptor interactions. *Cellular and Molecular Life Sciences*. **67**(8), pp.1219–1237.

Mangelsdorf, D.J., Thummel, C., Beato, M., Herrlich, P., Schütz, G., Umesono, K., Blumberg, B., Kastner, P., Mark, M., Chambon, P. and Evans, R.M. 1995. The nuclear receptor superfamily: the second decade. *Cell*. **83**(6), pp.835–9.

Marczyk, M., Polańska, J., Wojcik, A. and Lundholm, L. 2021. Analysis of the Applicability of microRNAs in Peripheral Blood Leukocytes as Biomarkers of Sensitivity and Exposure to Fractionated Radiotherapy towards Breast Cancer. *International journal of molecular sciences*. **22**(16), p.8705.

Marotti, J.D., Collins, L.C., Hu, R. and Tamimi, R.M. 2010. Estrogen receptor-beta expression in invasive breast cancer in relation to molecular phenotype: results from the Nurses' Health Study. *Modern pathology : an official journal of the United States and Canadian Academy of Pathology, Inc*. **23**(2), pp.197–204.

Martinkovich, S., Shah, D., Planey, S.L. and Arnott, J.A. 2014. Selective estrogen receptor modulators: tissue specificity and clinical utility. *Clinical interventions in aging*. **9**, pp.1437–52.

Masuda, H., Baggerly, K.A., Wang, Y., Zhang, Y., Gonzalez-Angulo, A.M., Meric-Bernstam, F., Valero, V., Lehmann, B.D., Pietenpol, J.A., Hortobagyi, G.N., Symmans, W.F. and Ueno, N.T. 2013. Differential response to neoadjuvant chemotherapy among 7 triple-negative breast cancer molecular subtypes.

Clinical cancer research : an official journal of the American Association for Cancer Research. **19**(19), pp.5533–40.

McDonald, S., Brive, L., Agus, D.B., Scher, H.I. and Ely, K.R. 2000. Ligand responsiveness in human prostate cancer: structural analysis of mutant androgen receptors from LNCaP and CWR22 tumors. *Cancer research*. **60**(9), pp.2317–22.

McGhan, L.J., McCullough, A.E., Protheroe, C.A., Dueck, A.C., Lee, J.J., Nunez-Nateras, R., Castle, E.P., Gray, R.J., Wasif, N., Goetz, M.P., Hawse, J.R., Henry, T.J., Barrett, M.T., Cunliffe, H.E. and Pockaj, B.A. 2014. Androgen receptor-positive triple negative breast cancer: a unique breast cancer subtype. *Annals of surgical oncology*. **21**(2), pp.361–7.

McPherson, K., Steel, C.M. and Dixon, J.M. 2000. ABC of breast diseases. Breast cancer-epidemiology, risk factors, and genetics. *BMJ (Clinical research ed.)*. **321**(7261), pp.624–8.

Mehta, J., Asthana, S., Mandal, C.C. and Saxena, S. 2015. A molecular analysis provides novel insights into androgen receptor signalling in breast cancer. *PloS one*. **10**(3), p.e0120622.

Melo, K.F.S., Mendonca, B.B., Billerbeck, A.E.C., Costa, E.M.F., Inácio, M., Silva, F.A.Q., Leal, A.M.O., Latronico, A.C. and Arnhold, I.J.P. 2003. Clinical, hormonal, behavioral, and genetic characteristics of androgen insensitivity syndrome in a Brazilian cohort: five novel mutations in the androgen receptor gene. *The Journal of clinical endocrinology and metabolism*. **88**(7), pp.3241–50.

Merenbakh-Lamin, K., Ben-Baruch, N., Yeheskel, A., Dvir, A., Soussan-Gutman, L., Jeselsohn, R., Yelensky, R., Brown, M., Miller, V.A., Sarid, D., Rizel, S., Klein, B., Rubinek, T. and Wolf, I. 2013. D538G mutation in estrogen receptor-α: A novel mechanism for acquired endocrine resistance in breast cancer. *Cancer research*. **73**(23), pp.6856–64.

Michmerhuizen, A.R., Spratt, D.E., Pierce, L.J. and Speers, C.W. 2020. ARe we there yet? Understanding androgen receptor signaling in breast cancer. *NPJ breast cancer*. **6**, p.47.

Miller, T.E., Ghoshal, K., Ramaswamy, B., Roy, S., Datta, J., Shapiro, C.L., Jacob, S. and Majumder, S. 2008. MicroRNA-221/222 confers tamoxifen resistance in breast cancer by targeting p27Kip1. *The Journal of biological chemistry*. **283**(44), pp.29897–903.

Millikan, R.C., Newman, B., Tse, C.-K., Moorman, P.G., Conway, K., Dressler, L.G., Smith, L. v, Labbok, M.H., Geradts, J., Bensen, J.T., Jackson, S., Nyante, S., Livasy, C., Carey, L., Earp, H.S. and Perou, C.M. 2008. Epidemiology of basal-like breast cancer. *Breast cancer research and treatment*. **109**(1), pp.123–39.

Moerkens, M., Zhang, Y., Wester, L., van de Water, B. and Meerman, J.H.N. 2014. Epidermal growth factor receptor signalling in human breast cancer cells operates parallel to estrogen receptor α signalling and results in tamoxifen insensitive proliferation. *BMC cancer*. **14**, p.283.

Moore, N.L., Buchanan, G., Harris, J.M., Selth, L.A., Bianco-Miotto, T., Hanson, A.R., Birrell, S.N., Butler, L.M., Hickey, T.E. and Tilley, W.D. 2012. An androgen receptor mutation in the MDA-MB-453 cell line model of molecular apocrine breast cancer compromises receptor activity. *Endocrine-related cancer*. **19**(4), pp.599–613.

Muluhngwi, P. and Klinge, C.M. 2015. Roles for miRNAs in endocrine resistance in breast cancer. *Endocrine-related cancer*. **22**(5), pp.R279-300.

Murakami, S., Nagari, A. and Kraus, W.L. 2017. Dynamic assembly and activation of estrogen receptor α enhancers through coregulator switching. *Genes & development*. **31**(15), pp.1535–1548.

Murphy, C.G. and Dickler, M.N. 2016. Endocrine resistance in hormone-responsive breast cancer: mechanisms and therapeutic strategies. *Endocrine-related cancer*. **23**(8), pp.R337-52.

Naderi, A. and Hughes-Davies, L. 2008. A functionally significant cross-talk between androgen receptor and ErbB2 pathways in estrogen receptor negative breast cancer. *Neoplasia (New York, N.Y.)*. **10**(6), pp.542–8.

National Cancer Institute (US) 2018. Breast Cancer Treatment (PDQ®)–Health Professional Version. [Accessed 10 January 2019]. Available from: https://www.cancer.gov/types/breast/hp/breast-treatment-pdq#link/.

Need, E.F., Selth, L.A., Harris, T.J., Birrell, S.N., Tilley, W.D. and Buchanan, G. 2012. Interplay between the genomic and transcriptional networks of androgen receptor and estrogen receptor α in luminal breast cancer cells. *Molecular endocrinology (Baltimore, Md.)*. **26**(11), pp.1941–52.

Ni, M., Chen, Y., Fei, T., Li, D., Lim, E., Liu, X.S. and Brown, M. 2013. Amplitude modulation of androgen signaling by c-MYC. *Genes & development*. **27**(7), pp.734–48.

Ni, M., Chen, Y., Lim, E., Wimberly, H., Bailey, S.T., Imai, Y., Rimm, D.L., Liu, X.S. and Brown, M. 2011. Targeting androgen receptor in estrogen receptor-negative breast cancer. *Cancer cell*. **20**(1), pp.119–31.

Nicholson, R.I., Hutcheson, I.R., Jones, H.E., Hiscox, S.E., Giles, M., Taylor, K.M. and Gee, J.M.W. 2007. Growth factor signalling in endocrine and anti-growth factor resistant breast cancer. *Reviews in endocrine & metabolic disorders*. **8**(3), pp.241–53.

Notas, G., Pelekanou, V., Kampa, M., Alexakis, K., Sfakianakis, S., Laliotis, A., Askoxilakis, J., Tsentelierou, E., Tzardi, M., Tsapis, A. and Castanas, E. 2015. Tamoxifen induces a pluripotency signature in breast cancer cells and human tumors. *Molecular oncology*. **9**(9), pp.1744–59.

Nourmoussavi, M., Pansegrau, G., Popesku, J., Hammond, G.L., Kwon, J.S. and Carey, M.S. 2017. Ovarian ablation for premenopausal breast cancer: A review of treatment considerations and the impact of premature menopause. *Cancer treatment reviews*. **55**, pp.26–35.

Oeffinger, K.C., Fontham, E.T.H., Etzioni, R., Herzig, A., Michaelson, J.S., Shih, Y.-C.T., Walter, L.C., Church, T.R., Flowers, C.R., LaMonte, S.J., Wolf, A.M.D., DeSantis, C., Lortet-Tieulent, J., Andrews, K., Manassaram-Baptiste, D., Saslow, D., Smith, R.A., Brawley, O.W., Wender, R. and American Cancer Society 2015. Breast Cancer Screening for Women at Average Risk: 2015 Guideline Update From the American Cancer Society. *JAMA*. **314**(15), pp.1599–614.

Panet-Raymond, V., Gottlieb, B., Beitel, L.K., Pinsky, L. and Trifiro, M.A. 2000. Interactions between androgen and estrogen receptors and the effects on their transactivational properties. *Molecular and cellular endocrinology*. **167**(1–2), pp.139–50.

Park, S., Koo, J., Park, H.S., Kim, J.-H., Choi, S.-Y., Lee, J.H., Park, B.-W. and Lee, K.S. 2010. Expression of androgen receptors in primary breast cancer. *Annals of oncology : official journal of the European Society for Medical Oncology*. **21**(3), pp.488–492.

Park, S., Koo, J.S., Kim, M.S., Park, H.S., Lee, J.S., Lee, J.S., Kim, S.I., Park, B.W. and Lee, K.S. 2011. Androgen receptor expression is significantly associated with better outcomes in estrogen receptor-positive breast cancers. *Annals of*

oncology : official journal of the European Society for Medical Oncology. **22**(8), pp.1755–62.

Parsana, P., Amend, S.R., Hernandez, J., Pienta, K.J. and Battle, A. 2017. Identifying global expression patterns and key regulators in epithelial to mesenchymal transition through multi-study integration. *BMC cancer*. **17**(1), p.447.

Patel, H.K. and Bihani, T. 2018. Selective estrogen receptor modulators (SERMs) and selective estrogen receptor degraders (SERDs) in cancer treatment. *Pharmacology & therapeutics*. **186**, pp.1–24.

Pećina-Slaus, N. 2003. Tumor suppressor gene E-cadherin and its role in normal and malignant cells. *Cancer cell international*. **3**(1), p.17.

Pelden, S., Insawang, T., Thuwajit, C. and Thuwajit, P. 2013. The trefoil factor 1 (TFF1) protein involved in doxorubicin-induced apoptosis resistance is upregulated by estrogen in breast cancer cells. *Oncology reports*. **30**(3), pp.1518–26.

Pellecchia, S., Sepe, R., Federico, A., Cuomo, M., Credendino, S.C., Pisapia, P., Bellevicine, C., Nicolau-Neto, P., Severo Ramundo, M., Crescenzi, E., de Vita, G., Terracciano, L.M., Chiariotti, L., Fusco, A. and Pallante, P. 2019. The Metallophosphoesterase-Domain-Containing Protein 2 (MPPED2) Gene Acts as Tumor Suppressor in Breast Cancer. *Cancers*. **11**(6), p.797.

Peng, Y. and Croce, C.M. 2016. The role of MicroRNAs in human cancer. *Signal transduction and targeted therapy*. **1**, p.15004.

Perou, C.M., Sørlie, T., Eisen, M.B., van de Rijn, M., Jeffrey, S.S., Rees, C.A., Pollack, J.R., Ross, D.T., Johnsen, H., Akslen, L.A., Fluge, O., Pergamenschikov, A., Williams, C., Zhu, S.X., Lønning, P.E., Børresen-Dale, A.L., Brown, P.O. and Botstein, D. 2000. Molecular portraits of human breast tumours. *Nature*. **406**(6797), pp.747–52.

Peters, A.A., Buchanan, G., Ricciardelli, C., Bianco-Miotto, T., Centenera, M.M., Harris, J.M., Jindal, S., Segara, D., Jia, L., Moore, N.L., Henshall, S.M., Birrell, S.N., Coetzee, G.A., Sutherland, R.L., Butler, L.M. and Tilley, W.D. 2009. Androgen receptor inhibits estrogen receptor-alpha activity and is prognostic in breast cancer. *Cancer research*. **69**(15), pp.6131–40.

Peters, A.A., Ingman, W. v, Tilley, W.D. and Butler, L.M. 2011. Differential effects of exogenous androgen and an androgen receptor antagonist in the peri- and postpubertal murine mammary gland. *Endocrinology*. **152**(10), pp.3728–37.

Petrelli, A., Bellomo, S.E., Sarotto, I., Kubatzki, F., Sgandurra, P., Maggiorotto, F., di Virgilio, M.R., Ponzone, R., Geuna, E., Galizia, D., Nuzzo, A.M., Medico, E., Miglio, U., Berrino, E., Venesio, T., Ribisi, S., Provero, P., Sapino, A., Giordano, S. and Montemurro, F. 2020. MiR-100 is a predictor of endocrine responsiveness and prognosis in patients with operable luminal breast cancer. *ESMO open*. **5**(5), p.e000937.

Pietri, E., Conteduca, V., Andreis, D., Massa, I., Melegari, E., Sarti, S., Cecconetto, L., Schirone, A., Bravaccini, S., Serra, P., Fedeli, A., Maltoni, R., Amadori, D., de Giorgi, U. and Rocca, A. 2016. Androgen receptor signaling pathways as a target for breast cancer treatment. *Endocrine-related cancer*. **23**(10), pp.R485-98.

Pomerantz, M.M., Li, F., Takeda, D.Y., Lenci, R., Chonkar, A., Chabot, M., Cejas, P., Vazquez, F., Cook, J., Shivdasani, R.A., Bowden, M., Lis, R., Hahn, W.C., Kantoff, P.W., Brown, M., Loda, M., Long, H.W. and Freedman, M.L. 2015. The androgen receptor cistrome is extensively reprogrammed in human prostate tumorigenesis. *Nature genetics*. **47**(11), pp.1346–51.

Poulin, R., Baker, D. and Labrie, F. 1988. Androgens inhibit basal and estrogen-induced cell proliferation in the ZR-75-1 human breast cancer cell line. *Breast cancer research and treatment*. **12**(2), pp.213–25.

Prat, A., Pineda, E., Adamo, B., Galván, P., Fernández, A., Gaba, L., Díez, M., Viladot, M., Arance, A. and Muñoz, M. 2015. Clinical implications of the intrinsic molecular subtypes of breast cancer. *Breast (Edinburgh, Scotland)*. **24 Suppl 2**, pp.S26-35.

Qu, Q., Mao, Y., Fei, X. and Shen, K. 2013. The impact of androgen receptor expression on breast cancer survival: a retrospective study and meta-analysis. *PloS one*. **8**(12), p.e82650.

Rahim, B. and O'Regan, R. 2017. AR Signaling in Breast Cancer. *Cancers*. **9**(3), p.21.

Rakha, E.A. and Green, A.R. 2017. Molecular classification of breast cancer: what the pathologist needs to know. *Pathology*. **49**(2), pp.111–119.

Rakha, E.A., Reis-Filho, J.S., Baehner, F., Dabbs, D.J., Decker, T., Eusebi, V., Fox, S.B., Ichihara, S., Jacquemier, J., Lakhani, S.R., Palacios, J., Richardson, A.L., Schnitt, S.J., Schmitt, F.C., Tan, P.-H., Tse, G.M., Badve, S. and Ellis, I.O. 2010. Breast cancer prognostic classification in the molecular era: the role of histological grade. *Breast Cancer Research*. **12**(4), p.207.

Ramakrishnan, R., Khan, S.A. and Badve, S. 2002. Morphological changes in breast tissue with menstrual cycle. *Modern pathology : an official journal of the United States and Canadian Academy of Pathology, Inc*. **15**(12), pp.1348–56.

Rangel, N., Rondon-Lagos, M., Annaratone, L., Aristizábal-Pachon, A.F., Cassoni, P., Sapino, A. and Castellano, I. 2020. AR/ER Ratio Correlates with Expression of Proliferation Markers and with Distinct Subset of Breast Tumors. *Cells*. **9**(4), p.1064.

Rangel, N., Rondon-Lagos, M., Annaratone, L., Osella-Abate, S., Metovic, J., Mano, M.P., Bertero, L., Cassoni, P., Sapino, A. and Castellano, I. 2018. The role of the AR/ER ratio in ER-positive breast cancer patients. *Endocrine-related cancer*. **25**(3), pp.163–172.

Rau, K.-M., Kang, H.-Y., Cha, T.-L., Miller, S.A. and Hung, M.-C. 2005. The mechanisms and managements of hormone-therapy resistance in breast and prostate cancers. *Endocrine-related cancer*. **12**(3), pp.511–32.

Ravaioli, S., Tumedei, M.M., Foca, F., Maltoni, R., Rocca, A., Massa, I., Pietri, E. and Bravaccini, S. 2017. Androgen and oestrogen receptors as potential prognostic markers for patients with ductal carcinoma in situ treated with surgery and radiotherapy. *International journal of experimental pathology*. **98**(5), pp.289–295.

Rechoum, Y., Rovito, D., Iacopetta, D., Barone, I., Andò, S., Weigel, N.L., O'Malley, B.W., Brown, P.H. and Fuqua, S.A.W. 2014. AR collaborates with ERα in aromatase inhibitor-resistant breast cancer. *Breast cancer research and treatment*. **147**(3), pp.473–85.

Ren, J., Smid, M., Iaria, J., Salvatori, D.C.F., van Dam, H., Zhu, H.J., Martens, J.W.M. and ten Dijke, P. 2019. Cancer-associated fibroblast-derived Gremlin 1 promotes breast cancer progression. *Breast cancer research : BCR*. **21**(1), p.109.

Renoir, J.-M., Marsaud, V. and Lazennec, G. 2013. Estrogen receptor signaling as a target for novel breast cancer therapeutics. *Biochemical pharmacology*. **85**(4), pp.449–65.

Rezaei, R., Wu, Z., Hou, Y., Bazer, F.W. and Wu, G. 2016. Amino acids and mammary gland development: nutritional implications for milk production and neonatal growth. *Journal of animal science and biotechnology*. **7**, p.20.

Robinson, D.R., Wu, Y.-M., Vats, P., Su, F., Lonigro, R.J., Cao, X., Kalyana-Sundaram, S., Wang, R., Ning, Y., Hodges, L., Gursky, A., Siddiqui, J., Tomlins, S.A., Roychowdhury, S., Pienta, K.J., Kim, S.Y., Roberts, J.S., Rae, J.M., van Poznak, C.H., Hayes, D.F., Chugh, R., Kunju, L.P., Talpaz, M., Schott, A.F. and Chinnaiyan, A.M. 2013. Activating ESR1 mutations in hormone-resistant metastatic breast cancer. *Nature genetics*. **45**(12), pp.1446–51.

Robinson, J.L.L. and Carroll, J.S. 2012. FoxA1 is a key mediator of hormonal response in breast and prostate cancer. *Frontiers in endocrinology*. **3**, p.68.

Robinson, J.L.L., Macarthur, S., Ross-Innes, C.S., Tilley, W.D., Neal, D.E., Mills, I.G. and Carroll, J.S. 2011. Androgen receptor driven transcription in molecular apocrine breast cancer is mediated by FoxA1. *The EMBO journal*. **30**(15), pp.3019–27.

Robinson-Rechavi, M., Escriva Garcia, H. and Laudet, V. 2003. The nuclear receptor superfamily. *Journal of cell science*. **116**(Pt 4), pp.585–6.

Rondón-Lagos, M., Villegas, V.E., Rangel, N., Sánchez, M.C. and Zaphiropoulos, P.G. 2016. Tamoxifen Resistance: Emerging Molecular Targets. *International journal of molecular sciences*. **17**(8), p.1357.

Roseweir, A.K., McCall, P., Scott, A., Liew, B., Lim, Z., Mallon, E.A. and Edwards, J. 2017. Phosphorylation of androgen receptors at serine 515 is a potential prognostic marker for triple negative breast cancer. *Oncotarget*. **8**(23), pp.37172–37185.

Sanga, S., Broom, B.M., Cristini, V. and Edgerton, M.E. 2009. Gene expression meta-analysis supports existence of molecular apocrine breast cancer with a role for androgen receptor and implies interactions with ErbB family. *BMC medical genomics*. **2**, p.59.

Sarker, D., Reid, A.H.M., Yap, T.A. and de Bono, J.S. 2009. Targeting the PI3K/AKT pathway for the treatment of prostate cancer. *Clinical cancer research : an*

official journal of the American Association for Cancer Research. **15**(15), pp.4799–805.

Schrijver, W.A.M.E., Schuurman, K., van Rossum, A., Dutch Distant Breast Cancer Metastases Consortium, Peeters, T., ter Hoeve, N., Zwart, W., van Diest, P.J. and Moelans, C.B. 2017. Loss of steroid hormone receptors is common in malignant pleural and peritoneal effusions of breast cancer patients treated with endocrine therapy. *Oncotarget*. **8**(33), pp.55550–55561.

Secreto, G., Girombelli, A. and Krogh, V. 2019. Androgen excess in breast cancer development: implications for prevention and treatment. *Endocrine-related cancer*. **26**(2), pp.R81–R94.

Secreto, G., Meneghini, E., Venturelli, E., Cogliati, P., Agresti, R., Ferraris, C., Gion, M., Zancan, M., Fabricio, A.S.C., Berrino, F., Cavalleri, A. and Micheli, A. 2011. Circulating sex hormones and tumor characteristics in postmenopausal breast cancer patients. A cross-sectional study. *The International journal of biological markers*. **26**(4), pp.241–6.

Sever, R. and Glass, C.K. 2013. Signaling by nuclear receptors. *Cold Spring Harbor perspectives in biology*. **5**(3), p.a016709.

Shaffer, P.L., Jivan, A., Dollins, D.E., Claessens, F. and Gewirth, D.T. 2004. Structural basis of androgen receptor binding to selective androgen response elements. *Proceedings of the National Academy of Sciences of the United States of America*. **101**(14), pp.4758–63.

Shah, K. and Bradbury, N.A. 2015. Kinase modulation of androgen receptor signaling: implications for prostate cancer. *Cancer cell & microenvironment*. **2**(4), p.e123.

Shang, Y., Myers, M. and Brown, M. 2002. Formation of the androgen receptor transcription complex. *Molecular cell*. **9**(3), pp.601–10.

Sharifi, N., McPhaul, M.J. and Auchus, R.J. 2010. “Getting from here to there”--mechanisms and limitations to the activation of the androgen receptor in castration-resistant prostate cancer. *Journal of investigative medicine : the official publication of the American Federation for Clinical Research*. **58**(8), pp.938–44.

Siciliano, T., Simons, I.H., Beier, A.-M.K., Ebersbach, C., Aksoy, C., Seed, R.I., Stope, M.B., Thomas, C. and Erb, H.H.H. 2021. A Systematic Comparison of

Antiandrogens Identifies Androgen Receptor Protein Stability as an Indicator for Treatment Response. *Life (Basel, Switzerland)*. **11**(9), p.874.

Singh, R. and Mo, Y.-Y. 2013. Role of microRNAs in breast cancer. *Cancer biology & therapy*. **14**(3), pp.201–12.

Soh, R.Y.Z., Lim, J.P., Samy, R.P., Chua, P.J. and Bay, B.H. 2018. A-kinase anchor protein 12 (AKAP12) inhibits cell migration in breast cancer. *Experimental and molecular pathology*. **105**(3), pp.364–370.

Somboonporn, W., Davis, S.R. and National Health and Medical Research Council 2004. Testosterone effects on the breast: implications for testosterone therapy for women. *Endocrine reviews*. **25**(3), pp.374–88.

Sørlie, T., Perou, C.M., Tibshirani, R., Aas, T., Geisler, S., Johnsen, H., Hastie, T., Eisen, M.B., van de Rijn, M., Jeffrey, S.S., Thorsen, T., Quist, H., Matese, J.C., Brown, P.O., Botstein, D., Lønning, P.E. and Børresen-Dale, A.L. 2001. Gene expression patterns of breast carcinomas distinguish tumor subclasses with clinical implications. *Proceedings of the National Academy of Sciences of the United States of America*. **98**(19), pp.10869–74.

Sorlie, T., Tibshirani, R., Parker, J., Hastie, T., Marron, J.S., Nobel, A., Deng, S., Johnsen, H., Pesich, R., Geisler, S., Demeter, J., Perou, C.M., Lønning, P.E., Brown, P.O., Børresen-Dale, A.-L. and Botstein, D. 2003. Repeated observation of breast tumor subtypes in independent gene expression data sets. *Proceedings of the National Academy of Sciences of the United States of America*. **100**(14), pp.8418–23.

Speirs, V., Malone, C., Walton, D.S., Kerin, M.J. and Atkin, S.L. 1999. Increased expression of estrogen receptor beta mRNA in tamoxifen-resistant breast cancer patients. *Cancer research*. **59**(21), pp.5421–4.

van der Steen, T., Tindall, D.J. and Huang, H. 2013. Posttranslational modification of the androgen receptor in prostate cancer. *International journal of molecular sciences*. **14**(7), pp.14833–59.

Suzuki, T., Miki, Y., Akahira, J.-I., Moriya, T., Ohuchi, N. and Sasano, H. 2008. Aromatase in human breast carcinoma as a key regulator of intratumoral sex steroid concentrations. *Endocrine journal*. **55**(3), pp.455–63.

Suzuki, T., Miki, Y., Moriya, T., Akahira, J., Ishida, T., Hirakawa, H., Yamaguchi, Y., Hayashi, S. and Sasano, H. 2007. 5Alpha-reductase type 1 and aromatase in

breast carcinoma as regulators of in situ androgen production. *International journal of cancer*. **120**(2), pp.285–91.

Szelei, J., Jimenez, J., Soto, A.M., Luizzi, M.F. and Sonnenschein, C. 1997. Androgen-induced inhibition of proliferation in human breast cancer MCF7 cells transfected with androgen receptor. *Endocrinology*. **138**(4), pp.1406–12.

Szostakowska, M., Trębińska-Stryjewska, A., Grzybowska, E.A. and Fabisiewicz, A. 2019. Resistance to endocrine therapy in breast cancer: molecular mechanisms and future goals. *Breast cancer research and treatment*. **173**(3), pp.489–497.

Tan, M.H.E., Li, J., Xu, H.E., Melcher, K. and Yong, E. 2015. Androgen receptor: structure, role in prostate cancer and drug discovery. *Acta pharmacologica Sinica*. **36**(1), pp.3–23.

Taplin, M.E., Bubley, G.J., Ko, Y.J., Small, E.J., Upton, M., Rajeshkumar, B. and Balk, S.P. 1999. Selection for androgen receptor mutations in prostate cancers treated with androgen antagonist. *Cancer research*. **59**(11), pp.2511–5.

Taplin, M.E., Bubley, G.J., Shuster, T.D., Frantz, M.E., Spooner, A.E., Ogata, G.K., Keer, H.N. and Balk, S.P. 1995. Mutation of the androgen-receptor gene in metastatic androgen-independent prostate cancer. *The New England journal of medicine*. **332**(21), pp.1393–8.

Taylor, S.E., Martin-Hirsch, P.L. and Martin, F.L. 2010. Oestrogen receptor splice variants in the pathogenesis of disease. *Cancer letters*. **288**(2), pp.133–48.

Thike, A.A., Yong-Zheng Chong, L., Cheok, P.Y., Li, H.H., Wai-Cheong Yip, G., Huat Bay, B., Tse, G.M.-K., Iqbal, J. and Tan, P.H. 2014. Loss of androgen receptor expression predicts early recurrence in triple-negative and basal-like breast cancer. *Modern pathology : an official journal of the United States and Canadian Academy of Pathology, Inc*. **27**(3), pp.352–60.

Tian, J.-H., Liu, S.-H., Yu, C.-Y., Wu, L.-G. and Wang, L.-B. 2021. The Role of Non-Coding RNAs in Breast Cancer Drug Resistance. *Frontiers in oncology*. **11**, p.702082.

Tiefenbacher, K. and Daxenbichler, G. 2008. The Role of Androgens in Normal and Malignant Breast Tissue. *Breast care (Basel, Switzerland)*. **3**(5), pp.325–331.

Tilley, W.D., Buchanan, G., Hickey, T.E. and Bentel, J.M. 1996. Mutations in the androgen receptor gene are associated with progression of human prostate cancer to androgen independence. *Clinical cancer research : an official journal of the American Association for Cancer Research*. **2**(2), pp.277–85.

Tormo, E., Ballester, S., Adam-Artigues, A., Burgués, O., Alonso, E., Bermejo, B., Menéndez, S., Zazo, S., Madoz-Gúrpide, J., Rovira, A., Albanell, J., Rojo, F., Lluch, A. and Eroles, P. 2019. The miRNA-449 family mediates doxorubicin resistance in triple-negative breast cancer by regulating cell cycle factors. *Scientific reports*. **9**(1), p.5316.

Toy, W., Shen, Y., Won, H., Green, B., Sakr, R.A., Will, M., Li, Z., Gala, K., Fanning, S., King, T.A., Hudis, C., Chen, D., Taran, T., Hortobagyi, G., Greene, G., Berger, M., Baselga, J. and Chandarlapaty, S. 2013. ESR1 ligand-binding domain mutations in hormone-resistant breast cancer. *Nature genetics*. **45**(12), pp.1439–45.

Traina, T.A., Miller, K., Yardley, D.A., Eakle, J., Schwartzberg, L.S., O'Shaughnessy, J., Gradishar, W., Schmid, P., Winer, E., Kelly, C., Nanda, R., Gucalp, A., Awada, A., Garcia-Estevez, L., Trudeau, M.E., Steinberg, J., Uppal, H., Tudor, I.C., Peterson, A. and Cortes, J. 2018. Enzalutamide for the Treatment of Androgen Receptor-Expressing Triple-Negative Breast Cancer. *Journal of clinical oncology : official journal of the American Society of Clinical Oncology*. **36**(9), pp.884–890.

Uhlmann, S., Zhang, J.D., Schwäger, A., Mannsperger, H., Riazalhosseini, Y., Burmester, S., Ward, A., Korf, U., Wiemann, S. and Sahin, O. 2010. miR-200bc/429 cluster targets PLCgamma1 and differentially regulates proliferation and EGF-driven invasion than miR-200a/141 in breast cancer. *Oncogene*. **29**(30), pp.4297–306.

Usselman, C.W., Stachenfeld, N.S. and Bender, J.R. 2016. The molecular actions of oestrogen in the regulation of vascular health. *Experimental physiology*. **101**(3), pp.356–61.

Venema, C.M., Bense, R.D., Steenbruggen, T.G., Nienhuis, H.H., Qiu, S.-Q., van Kruchten, M., Brown, M., Tamimi, R.M., Hospers, G.A.P., Schröder, C.P., Fehrmann, R.S.N. and de Vries, E.G.E. 2019. Consideration of breast cancer subtype in targeting the androgen receptor. *Pharmacology & therapeutics*. **200**, pp.135–147.

Vera-Badillo, F.E., Templeton, A.J., de Gouveia, P., Diaz-Padilla, I., Bedard, P.L., Al-Mubarak, M., Seruga, B., Tannock, I.F., Ocana, A. and Amir, E. 2014. Androgen receptor expression and outcomes in early breast cancer: a systematic review and meta-analysis. *Journal of the National Cancer Institute*. **106**(1), p.djt319.

Vidula, N., Yau, C., Wolf, D. and Rugo, H.S. 2019. Androgen receptor gene expression in primary breast cancer. *NPJ breast cancer*. **5**, p.47.

Vorobiof, D.A. 2016. Recent advances in the medical treatment of breast cancer. *F1000Research*. **5**, p.2786.

Walters, K.A., Simanainen, U. and Handelsman, D.J. 2010. Molecular insights into androgen actions in male and female reproductive function from androgen receptor knockout models. *Human reproduction update*. **16**(5), pp.543–58.

Wang, L., Hsu, C.-L. and Chang, C. 2005. Androgen receptor corepressors: an overview. *The Prostate*. **63**(2), pp.117–30.

Wang, T., Feng, J. and Zhang, A. 2020. miR-584 inhibits cell proliferation, migration and invasion in vitro and enhances the sensitivity to cisplatin in human cervical cancer by negatively targeting GLI1. *Experimental and therapeutic medicine*. **19**(3), pp.2059–2066.

Wang, Y.-W., Zhang, W. and Ma, R. 2018. Bioinformatic identification of chemoresistance-associated microRNAs in breast cancer based on microarray data. *Oncology reports*. **39**(3), pp.1003–1010.

Wang, Z., Liu, Y., Lu, L., Yang, L., Yin, S., Wang, Y., Qi, Z., Meng, J., Zang, R. and Yang, G. 2015. Fibrillin-1, induced by Aurora-A but inhibited by BRCA2, promotes ovarian cancer metastasis. *Oncotarget*. **6**(9), pp.6670–83.

Ward, A., Balwierz, A., Zhang, J.D., Küblbeck, M., Pawitan, Y., Hielscher, T., Wiemann, S. and Sahin, Ö. 2013. Re-expression of microRNA-375 reverses both tamoxifen resistance and accompanying EMT-like properties in breast cancer. *Oncogene*. **32**(9), pp.1173–82.

Ward, A., Shukla, K., Balwierz, A., Soons, Z., König, R., Sahin, O. and Wiemann, S. 2014. MicroRNA-519a is a novel oncomir conferring tamoxifen resistance by targeting a network of tumour-suppressor genes in ER+ breast cancer. *The Journal of pathology*. **233**(4), pp.368–79.

Ward, E.M., DeSantis, C.E., Lin, C.C., Kramer, J.L., Jemal, A., Kohler, B., Brawley, O.W. and Gansler, T. 2015. Cancer statistics: Breast cancer in situ. *CA: a cancer journal for clinicians*. **65**(6), pp.481–95.

Watanabe, T., Oba, T., Tanimoto, K., Shibata, T., Kamijo, S. and Ito, K.-I. 2021. Tamoxifen resistance alters sensitivity to 5-fluorouracil in a subset of estrogen receptor-positive breast cancer. *PloS one*. **16**(6), p.e0252822.

Weiner, M., Skoog, L., Fornander, T., Nordenskjöld, B., Sgroi, D.C. and Stål, O. 2013. Oestrogen receptor co-activator AIB1 is a marker of tamoxifen benefit in postmenopausal breast cancer. *Annals of oncology : official journal of the European Society for Medical Oncology*. **24**(8), pp.1994–9.

WHO 2018. Cancer. [Accessed 14 December 2018]. Available from: https://www.who.int/news-room/fact-sheets/detail/cancer.

van de Wijngaart, D.J., Dubbink, H.J., Molier, M., de Vos, C., Trapman, J. and Jenster, G. 2009. Functional screening of FxxLF-like peptide motifs identifies SMARCD1/BAF60a as an androgen receptor cofactor that modulates TMPRSS2 expression. *Molecular endocrinology (Baltimore, Md.)*. **23**(11), pp.1776–86.

Wilson, E.M. 2011. Analysis of interdomain interactions of the androgen receptor. *Methods in molecular biology (Clifton, N.J.)*. **776**, pp.113–29.

Wolmark, N., Wang, J., Mamounas, E., Bryant, J. and Fisher, B. 2001. Preoperative chemotherapy in patients with operable breast cancer: nine-year results from National Surgical Adjuvant Breast and Bowel Project B-18. *Journal of the National Cancer Institute. Monographs*. (30), pp.96–102.

Wu, Q., Wang, C., Lu, Z., Guo, L. and Ge, Q. 2012. Analysis of serum genome-wide microRNAs for breast cancer detection. *Clinica chimica acta; international journal of clinical chemistry*. **413**(13–14), pp.1058–65.

Wu, W., Qian, L., Chen, X. and Ding, B. 2015. Prognostic significance of CXCL12, CXCR4, and CXCR7 in patients with breast cancer. *International journal of clinical and experimental pathology*. **8**(10), pp.13217–24.

Wu, Y. and Vadgama, J. v 2017. Androgen Receptor as a Potential Target for Treatment of Breast Cancer. *International journal of cancer research and molecular mechanisms*. **3**(1), 10.16966/2381-3318.129.

Xu, J. and Li, Q. 2003. Review of the in vivo functions of the p160 steroid receptor coactivator family. *Molecular endocrinology (Baltimore, Md.)*. **17**(9), pp.1681–92.

Xu, K., Shimelis, H., Linn, D.E., Jiang, R., Yang, X., Sun, F., Guo, Z., Chen, Hege, Li, W., Chen, Hegang, Kong, X., Melamed, J., Fang, S., Xiao, Z., Veenstra, T.D. and Qiu, Y. 2009. Regulation of androgen receptor transcriptional activity and specificity by RNF6-induced ubiquitination. *Cancer cell*. **15**(4), pp.270–82.

Yang, X., Wang, H. and Jiao, B. 2017. Mammary gland stem cells and their application in breast cancer. *Oncotarget*. **8**(6), pp.10675–10691.

Yeh, S., Hu, Y.-C., Wang, P.-H., Xie, C., Xu, Q., Tsai, M.-Y., Dong, Z., Wang, R.-S., Lee, T.-H. and Chang, C. 2003. Abnormal mammary gland development and growth retardation in female mice and MCF7 breast cancer cells lacking androgen receptor. *The Journal of experimental medicine*. **198**(12), pp.1899–908.

Yeh, S.-H., Chiu, C.-M., Chen, C.-L., Lu, S.-F., Hsu, H.-C., Chen, D.-S. and Chen, P.-J. 2007. Somatic mutations at the trinucleotide repeats of androgen receptor gene in male hepatocellular carcinoma. *International journal of cancer*. **120**(8), pp.1610–7.

Yu, X., Yi, P., Hamilton, R.A., Shen, H., Chen, M., Foulds, C.E., Mancini, M.A., Ludtke, S.J., Wang, Z. and O'Malley, B.W. 2020. Structural Insights of Transcriptionally Active, Full-Length Androgen Receptor Coactivator Complexes. *Molecular cell*. **79**(5), pp.812-823.e4.

Zhang, J., Lu, C.-Y., Chen, H.-M. and Wu, S.-Y. 2021. Neoadjuvant Chemotherapy or Endocrine Therapy for Invasive Ductal Carcinoma of the Breast With High Hormone Receptor Positivity and Human Epidermal Growth Factor Receptor 2 Negativity. *JAMA network open*. **4**(3), p.e211785.

Zhang, T., Hu, H., Yan, G., Wu, T., Liu, S., Chen, W., Ning, Y. and Lu, Z. 2019. Long Non-Coding RNA and Breast Cancer. *Technology in cancer research & treatment*. **18**, p.1533033819843889.

Zhang, W., Liu, X., Liu, S., Qin, Y., Tian, X., Niu, F., Liu, H., Liu, N. and Niu, Y. 2018. Androgen receptor/let-7a signaling regulates breast tumor-initiating cells. *Oncotarget*. **9**(3), pp.3690–3703.

Zhang, Z.J. and Ma, S.L. 2012. miRNAs in breast cancer tumorigenesis (Review). *Oncology reports*. **27**(4), pp.903–10.

Zhao, S., Chang, S.L., Linderman, J.J., Feng, F.Y. and Luker, G.D. 2014. A Comprehensive Analysis of CXCL12 Isoforms in Breast Cancer. *Translational oncology*. **7**(3), pp.429–438.

Zhigang, Z. and Wenlv, S. 2004. Prostate stem cell antigen (PSCA) expression in human prostate cancer tissues and its potential role in prostate carcinogenesis and progression of prostate cancer. *World journal of surgical oncology*. **2**, p.13.

Zhou, Y. and Liu, X. 2020. The role of estrogen receptor beta in breast cancer. *Biomarker research*. **8**, p.39.

Zwart, W., Theodorou, V. and Carroll, J.S. 2011. Estrogen receptor-positive breast cancer: a multidisciplinary challenge. *Wiley interdisciplinary reviews. Systems biology and medicine*. **3**(2), pp.216–30.

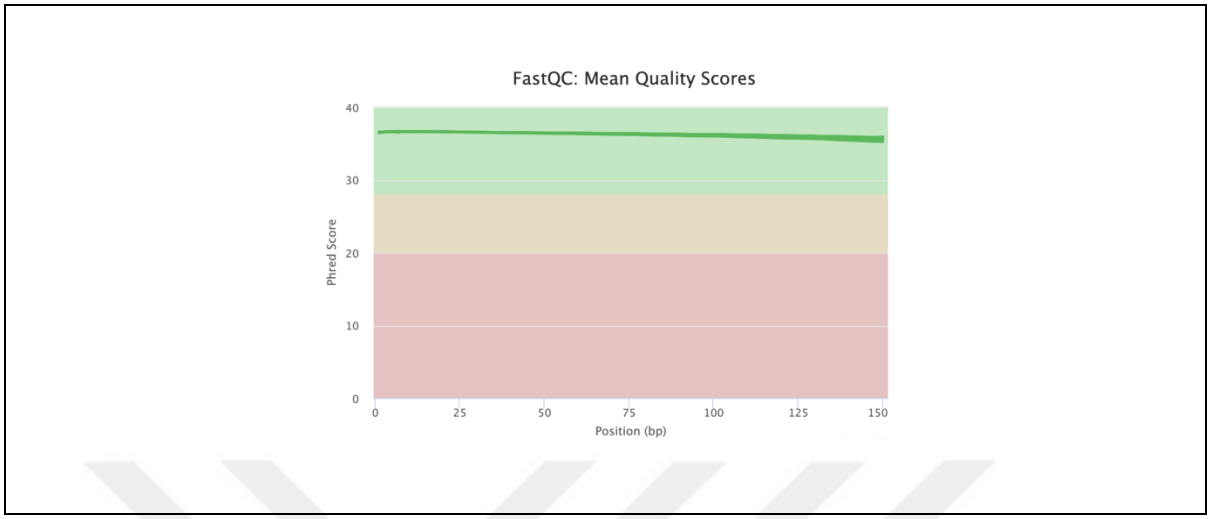

Figure 7-1 The quality of the reads of RNA-Seq samples

The quality of the reads for each sample was checked with fastQC version (0.11.7), and a summary graph visualising all sample reads (total n = 60) was created using MultiQC .

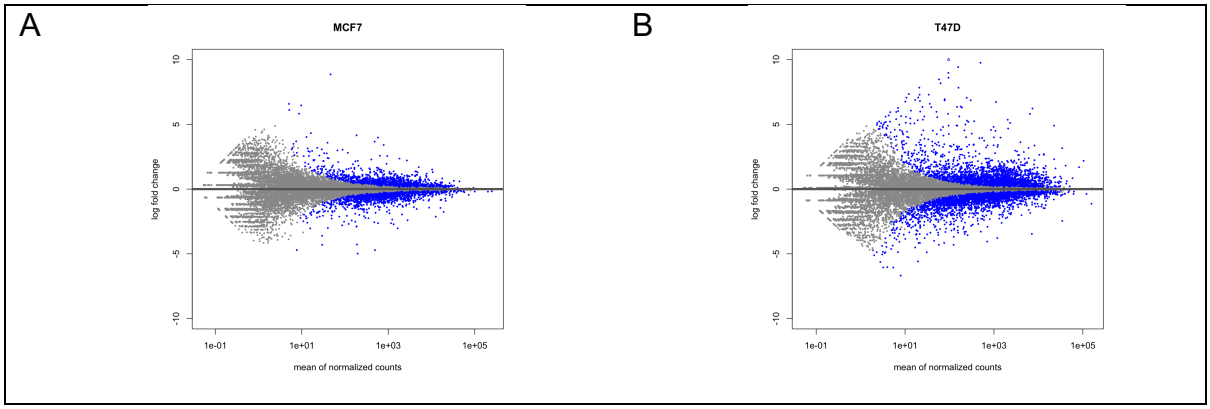

Figure 7-2 MA plots of MCF7 and T47D samples

Representative MA plots for group comparisons in (A) MCF7 and (B) T47D cells. MA plots were created after comparing MIB and control samples. Blue dots represent DEGs with a padj < 0.01.

Table 7-1 List of DEGs commonly regulated by MIB, and additional treatment combinations, in T47D

T47D						
MIBup	MIBdown	MIB_E2up	MIB_E2down	MIB_E2_FULVup	MIB_E2_FULVdown	Gene Symbols
+						MXRA8, CHD5, GPR153, SRM, LOC101929181, DRAXIN, FAM131C, PADI4, ALPL, EPHA8, STMN1, TRNP1, FAM46B, IFI6, LCK, CDCA8, EDN2, CDC20, KIF2C, PLK3, CCDC163P, DMBX1, CYP4Z1, CDKN2C, RAB3B, TTC22, C1orf168, FOXD3-AS1, AK4, DEPDC1, ACADM, CCDC18, F3, AKNAD1, GPSM2, PSRC1, EPS8L3, CSF1, KCNC4, LOC440600, ATP1A1, FAM46C, SPAG17, FAM72B, SRGAP2C, FAM72C, SRGAP2D, SRGAP2B, FAM72D, ANKRD35, ITGA10, NOTCH2NL, FMO5, ANP32E, S100A9, S100A8, S100A14, GBA, IQGAP3, HAPLN2, BCAN, LINC01133, ATP1A2, ATP1A4, CASQ1, PEA15, FCGR3A, NUF2, ATP1B1, QSOX1, FLJ23867, GLUL, C1orf21, KIF14, KIF21B, MYBPH, CHI3L1, ETNK2, FAM72A, SRGAP2, C1orf116, MIR29C, NEK2, CENPF, C1orf95, RHOU, KCNK1, GNG4, ZBTB18, AKR1C2, AKR1C3, ACBD7, NEBL, NEBL-AS1, RET, LINC00844, FAM13C, CDK1, SRGN, UNC5B, MYOZ1, KCNMA1, DLG5, KIF20B, PPP1R3C, KIF11, CEP55, GOLGA7B, ELOVL3, ADD3, NRAP, MKI67, BNIP3, C10orf91, SCART1, CDKN1C, TRIM6, TRIM22, SCUBE2, KCNJ11, ABCC8, TMEM86A, IGSF22, KIF18A, CD59, LMO2, EHF, GYLTL1B, SLC43A1, DTX4, ZP1, FADS1, INCENP, ASRGL1, AHNAK, HRASLS5, HRASLS2, RASGRP2, NEAT1, PC, GAL, ANO1, ARRB1, THRSP, ANGPTL5, BIRC3, CRYAB, ZBTB16, TAGLN, ST3GAL4-AS1, ST3GAL4, ADAMTS8, FOXM1, CD9, CDCA3, C1R, SLC2A14, A2ML1, DDX12P, STYK1, APOLD1, GPRC5A, MIR614, EMP1, DERA, CAPRIN2, DENND5B, NELL2, TUBA1B, TUBA1C, TROAP, RACGAP1, NR4A1, OR7E47P, KRT6A, KRT4, IGFBP6, ESPL1, HSD17B6, RDH16, MYO1A, NDUFA4L2, CPM, PHLDA1, TMTC2, SOCS2, CEP83-AS1, TMCC3, RMST, TMPO-AS1, GAS2L3, MYBPC1, CHPT1, SYCP3, GNPTAB, PARPBP, IGF1, MYO1H, DTX1, RASAL1, TESC, CIT, MPHOSPH9, SKA3, FLT1, N4BP2L1, TSC22D1, DLEU2, CKAP2, BORA, TGM1, NFKBIA, MIS18BP1, ATL1, CDKN3, GCH1, DLGAP5, HSPA2, PLEKHD1, CCDC177, PAPLN, RPS6KL1, TMEM63C, RPS6KA5, SERPINA5, SERPINA3, CLMN, C14orf180, ATP10A, OCA2,

						ARHGAP11B, LOC100288637, ARHGAP11A, BUB1B, PHGR1, KNSTRN, CASC5, OIP5, NUSAP1, PLA2G4E, NEDD4, CCNB2, PIF1, KIF23, GRAMD2, CTSH, FAH, HOMER2, ISG20, PRC1, ADAMTS17, RGS11, MEIOB, HS3ST6, NPW, ABCA17P, CCNF, PRSS27, ARL6IP1, TMC5, ACSM3, LOC81691, PLK1, LOC554206, LCMT1-AS1, LCMT1, LCMT1-AS2, NUPR1, SULT1A2, KIF22, GDPD3, SHCBP1, NETO2, MT2A, MT1X, PLLP, MMP15, NDRG4, CES4A, PLEKHG4, LINC01572, ZFHX3, CENPN, HSD17B2, ATP2C2, SLC22A31, RPH3AL, CAMKK1, ATP2A3, FAM64A, YBX2, GUCY2D, ALOX15B, PER1, AURKB, HS3ST3B1, ULK2, SPAG5, RHOT1, LRRC37A8P, RDM1, PPP1R1B, TCAP, PNMT, TOP2A, KRT16, STAT5A, ITGA2B, DBF4B, KIF18B, SP6, PRR15L, PHOSPHO1, LOC102724596, NGFR, LPO, SEPT4, PPM1E, PRR11, KPNA2, SLC16A6, LLGL2, UBALD2, BIRC5, LINC00482, RAC3, DCXR, FASN, CCDC57, TYMSOS, NDC80, DLGAP1-AS1, LINC00667, EPB41L3, NDUFV2-AS1, LDLRAD4-AS1, ABHD3, ANKRD29, LAMA3, ZBTB7C, SKA1, NEDD4L, ATP8B3, NFIC, PLIN5, LRG1, TNFAIP8L1, KDM4B, FUT3, C3, ZNF812, CDKN2D, C19orf38, SPC24, JUNB, SYCE2, RASAL3, PGLYRP2, CYP4F22, CYP4F8, CRLF1, TMEM59L, FXYD3, ARHGAP33, WDR62, TMEM91, LIPE, KCNN4, CEACAM19, ZNF541, KLK13, VSIG10L, ZNF331, UBE2S, ZNF582-AS1, MBOAT2, ATP6V1C2, FKBP1B, TP53I3, CENPA, PLB1, CDC42EP3, KCNG3, HAAO, BUB1, CKAP2L, DBI, ARHGAP15, SPC25, DLX1, FRZB, STK17B, SGOL2, CFLAR, ICA1L, CYP27A1, SGPP2, SERPINE2, NPPC, EFHD1, INPP5D, HJURP, RAMP1, SIRPA, TGM3, ADAM33, CDC25B, LINC00654, JAG1, ABHD12, TPX2, PXMP4, FAM83D, WISP2, SLPI, UBE2C, ZMYND8, KCNB1, KCNG1, AURKA, STMN3, SIK1, MGC39584, CLDN8, IL10RB-AS1, LINC00160, SLC25A18, LOC101929372, PRODH, YPEL1, LOC100128531, RASL10A, THOC5, PISD, HMOX1, RASD2, MB, MAFF, SUN2, APOBEC3B, LOC100130899, MCHR1, CHADL, SERHL2, SCUBE1, FBLN1, LOC730668, GTSE1, PIM3, SGOL1, VIPR1, VIPR1-AS1, KIF15, PHF7, ALCAM, KIAA1524, HGD, EAF2, SLC15A2, RBP2, RBP1, GPR87, LINC00886, BCL6, TPRG1-AS1, ATP13A4, MFSD7, TACC3, MRFAP1, LOC93622, S100P, PSAPL1, NCAPG, LIMCH1, NMU, TMPRSS11E, UGT2B11, EPGN, GPAT3, MANBA, CENPE, EGF, NDNF, CCNA2, SCLT1, CLGN, MND1, HMGB2, SAP30, SCRG1, NEIL3, ACSL1, LINC01093, LINC01018, SRD5A1, DNAH5, FAM105A, MYO10, RANBP3L, LIFR, DEPDC1B, HTR1A, CCNB1, SMA4, ARHGEF28, RHOBTB3, ELL2, LOX, LMNB1, P4HA2-AS1, P4HA2, KIF20A, CDC25C, ARHGAP26, ADRB2, SH3TC2, ABLIM3, ARHGEF37, FAXDC2, PTTG1, HMMR, CTB-178M22.2, SH3PXD2B, NEURL1B, CREBRF, MXD3, COL23A1, ADAMTS2, SLC22A23, RBM24, HIST1H3B, HIST1H1D, HIST1H3F, HIST1H2AK, ZNF165, ZSCAN12P1, CDSN, SLC44A4, C2, KIFC1, IP6K3, FKBP5, LOC285847, ARMC12, CLPSL2, CLPSL1, LHFPL5, TDRG1, LRFN2, PGC, GNMT, GTPBP2,

						VEGFA, ADGRF1, CRISP2, ELOVL5, KLHL31, TTK, FRK, CENPW, ENPP3, ENPP1, EYA4, SGK1, MTFR2, SASH1, RAET1E, AKAP12, LOC100507642, GPR146, SNX8, CYTH3, CHN2, LOC102724484, ANLN, EGFR, LAT2, DTX2, DTX2P1-UPK3BP1-PMS2P11, STEAP1, STEAP2, PDK4, GJC3, AZGP1, AZGP1P1, KMT2E-AS1, NAMPT, PRKAR2B, CBLL1, SLC26A3, AASS, HILPDA, LINC-PINT, AKR1D1, EPHB6, KEL, PIP, CNTNAP2, NCAPG2, MTMR9, CDCA2, CHRNA2, PBK, LINC01605, CEBPD, CA8, FBXO43, SYBU, FAM83A, ATAD2, WDYHV1, FBXO32, NDRG1, PSCA, AQP3, ARHGEF39, CNTNAP3, KLF9, ANXA1, FRMD3, GAS1, CKS2, GADD45G, UNQ6494, TBC1D2, KLF4, TXN, SLC31A2, ORM2, ASTN2, PHF19, C5, CNTRL, STOM, PTGS1, CRAT, LOC100272217, FIBCD1, ARRDC1, ARRDC1-AS1, ARSF, PIR, ACE2, RBBP7, SH3KBP1, MAP7D2, PHEX, MAOA, EDA2R, STARD8, KIF4A, HMGN5, DRP2, FRMPD3, TSC22D3, TMEM164, TRPC5OS, GPC4, HMGB3, GABRQ, IRAK1
	+					LOC100130417, TP73, PLEKHG5, PER3, TMEM51, ARHGEF19, AKR7A3, UBXN10, GRHL3, NCMAP, MAN1C1, TMEM200B, SYNC, TEKT2, KCNQ4, ARTN, FAAHP1, PTGER3, ADGRL2, LMO4, GBP1, SLC16A4, CASQ2, IGSF3, CERS2, S100A4, ATP8B2, CFAP45, SLAMF9, PCP4L1, SOAT1, TDRD5, LAMC2, NMNAT2, NCF2, APOBEC4, HMCN1, LINC01351, CSRP1, GPR37L1, GOLT1A, LRRN2, SLC45A3, RAB7B, LAMB3, TGFB2, DUSP10, TMEM63A, WNT3A, C1orf145, PGBD5, GREM2, OPN3, TRIM58, CAMK1D, HACD1, ARMC3, ENKUR, GPR158, LINC00836, RAB18, MKX, MKX-AS1, ARMC4, OGDHL, DKK1, PLAU, PAPSS2, LGI1, SLC35G1, PLCE1, SH3PXD2A, ITPRIP, VWA2, C10orf82, CPXM2, NKX1-2, TUB, SBF2-AS1, ADM, GALNT18, ANO5, SLC1A2, PAMR1, PRDM11, GLYATL1, SIPA1, SHANK2, SYTL2, AMOTL1, MAML2, TRPC6, C11orf88, CADM1, MCAM, OAF, SC5D, CLMP, B4GALNT3, CACNA1C, FKBP4, TSPAN9, ARHGDIB, PIK3C2G, ST8SIA1, LMNTD1, PTHLH, AMIGO2, KCNH3, GLIPR1, KITLG, LUM, CFAP54, UNG, FAM222A, LINC01405, OAS2, WDR66, GJB2, UBL3, LINC00365, FREM2, ENOX1, LCP1, SPRY2, SLITRK5, HS6ST3, SALL2, MMP14, PTGER2, FUT8, PLEK2, VASH1, STON2, SERPINA10, GSC, TCL1B, C14orf132, LPCAT4, PAK6, GATM, CGNL1, IGDCC3, SEMA7A, LINGO1, RASGRF1, PAQR4, TNFRSF12A, SEC14L5, ABAT, SHISA9, XYLT1, ABCC6P1, HSD3B7, PYCARD, CX3CL1, HYDIN, MLKL, MAF, CDH13, LOC102724163, SERPINF1, TEKT1, EFNB3, ALOXE3, RNF222, EVPLL, RHBDL3, CCL2, TMEM132E, SLFN11, LHX1, RARA, KRT17, PTRF, CNTNAP1, CNTD1, NXPH3, HLF, MRC2, PRR29, RGS9, SOX9, SMIM5, FOXJ1, RNF157-AS1, SOCS3, LOC101928674, AATK, NOL4, RAB27B, TCF4, BCL2, CDH7, CYB5A, MISP, ADAMTSL5, PLK5, CELF5, CNN1, TPM4, TMEM221, LPAR2, CCNE1, DPF1, AXL, ATP1A3, RELB, SIGLEC6, ID2, CYS1, MATN3, CAPN14, EHD3, LTBP1, PLEKHH2, MSH6, LOC100129434,

						CCDC85A, BOLA3-AS1, DNAH6, TCF7L1, TEKT4, MGAT4A, CHST10, NPAS2, LIMS2, GRB14, MYO3B, GPR155, PLCL1, FN1, IGFBP5, EPHA4, DOCK10, PP14571, MIR149, C2orf54, SNPH, SPEF1, LRRN4, FERMT1, ISM1, GGTLC1, VSX1, PROCR, MYL9, JPH2, PREX1, FAM65C, BCAS1, BMP7, RBM11, NCAM2, GRIK1, GRIK1-AS2, PCP4, DSCAM-AS1, UMODL1, RSPH1, GNAZ, ZDHHC8P1, EMID1, LIF, C1QTNF6, RAC2, MGAT3, TEF, A4GALT, KIAA1644, IL5RA, LRRN1, UBP1, ENTPD3, TNNC1, CACNA1D, CHDH, FOXP1, ROBO2, BOC, FSTL1, MYLK, SLCO2A1, C3orf80, B3GALNT1, SPTSSB, BCHE, ZBBX, WDR49, SERPINI1, MECOM, LINC01208, SOX2, LINC00888, MAP6D1, C3orf70, LIPH, ADIPOQ, TP63, CLDN1, CLDN16, MB21D2, FAM43A, FGFR3, EVC, AFAP1, CPZ, LINC00504, FGFBP1, PROM1, ATP8A1, NIPAL1, ERVMER34-1, RASL11B, KIAA1211, ANXA3, CCSER1, BMPR1B, TSPAN5, ARHGEF38, ARSJ, PCDH18, INPP4B, DCLK2, GRIA2, NPY5R, LRP2BP, PDLIM3, FAM149A, FAT1, C5orf49, ROPN1L, CDH10, NPR3, RAI14, CDC20B, MCIDAS, CCNO, IL31RA, FAM169A, F2RL1, VCAN, NR2F1-AS1, NR2F1, SEMA6A, LINC00992, PRDM6, TCF7, NME5, EGR1, NDST1, SYNPO, ANXA6, GALNT10, NIPAL4, CCNJL, KCNMB1, GPRIN1, SNCB, CD83, ID4, IER3, MICB, LINC01016, GRM4, PAQR8, LINC00472, COL12A1, ELOVL4, FUT9, CD24, SOBP, LAMA4, DSE, RSPH4A, L3MBTL3, CTGF, MYB, ESR1, TIAM2, ZDHHC14, DLL1, GPER1, GLCCI1, THSD7A, SCIN, TWIST1, MACC1, DFNA5, JAZF1, CREB5, AMPH, GLI3, STK17A, RASA4CP, PKD1L1, SEMA3C, RUNDC3B, NPTX2, ORAI2, NRCAM, SMKR1, ATP6V0A4, KRBA1, CLDN23, LOC100506990, NKX3-1, CLU, DUSP26, TACC1, JPH1, CRISPLD1, TMEM64, PDP1, GEM, SDC2, MATN2, ARC, CDKN2B, MOB3B, ARID3C, GLIPR2, S1PR3, WNK2, FBP1, CDC14B, GALNT12, KIF12, LHX2, WDR38, FAM78A, SLC2A6, COL5A1, STS, CFAP47, NDP, EFHC2, SLC9A7, TIMP1, SHROOM4, XAGE2, AR, SLC16A2, MAGEE1, ITM2A, TBX22, MUM1L1, KLHL13, DOCK11, L1CAM
			+			EXTL1, PALMD, CD101, NUAK2, IFIT2, LINC00865, DNMBP, HPX, CHST1, PTPRCAP, LOC101928100, PCED1B, RND1, HCAR1, SHISA2, REM2, RIPK3, EGLN3, DAPK2, SMAD6, RAB26, CCL22, ADAD2, MAP2K6, ANGPTL4, SYDE1, CEACAM6, KIF5C, ARL4C, VSTM2L, MX2, MN1, UBA7, TM4SF1, AGXT2, CCL28, ATXN1, HCP5, GLYATL3, WBSCR28, MMP16, LPAR1, LOC101929331
		+				RNF223, LAPTM5, GRIK3, SLC22A15, DDR2, KCNH1, CAPN8, ADRB1, FIBIN, MYEOV, TSKU, SLC6A12, FMN1, FSIP1, BMF, TNFAIP8L3, NOG, RBBP8, FGF21, GREB1, FAM49A, TGFA, MPHOSPH10, TFCP2L1, TUBA3D, PNPLA3, NEK10, MRAS, TIPARP, LRRC31, TPRG1, ANK2, DUSP1, PRDM1, FYN, ZNF703, RCL1, AKNA, OPHN1

		+			+	HES2, CITED4, PFKFB3, ST8SIA6, ADRA2A, IFITM10, CHRM4, GRIK4, LINC00565, LINC01588, ACOT6, GPR132, RASGRP1, LOC102723344, C15orf59, TPSG1, SLC47A1, RAPGEFL1, MAPT, WFIKKN2, ANKFN1, KCNF1, YBEY, SEC14L6, HDAC11, SEMA3G, IL6ST, CCDC69, NEDD9, GATA4, STC1, MYBL1, PTGES, RAI2
	+	+			+	NKAIN1, CXCL12, PGR, SERPINA6, CACNA1H, NOD2, KRT13, EGLN2, CYP2B7P, CYP2S1, PSG9, C5AR2, MREG, KCNK15, RIMS4, CISH, PXK, KCTD6, BFSP2, DOK7, KCNK5, AMZ1, C8orf46, SPINK4, FGD3, SUSD3, OLFM1, GRPR
+		+				AGT, SYT8, MS4A15, BEST1, SLC37A2, INHBE, CORO2B, SCNN1G, HSD11B2, TAT, CA4, ST6GALNAC1, GREB1L, KCNE4, MAFB, PHACTR3, CLIC6, RUNX1, KLHDC7B, CSTA, KLF15, LAMP3, FGF18, SEPT14, PEBP4, JAK2, LCN2
	+		+			RASSF5, BAMBI, CHRM1, CAPN5, SLITRK6, EFNB2, CCDC154, KCNS3, ZFP36L2, IL1R1, ITGB6, C2orf72, FGD5, NAALADL2, FGF12, NDST4, RIMS1, LOC100132735, AGPAT4, HDAC9, RGAG4, RNF128
					+	PADI3, NR5A2, LINC00173, HEATR4, NECAB2, IGFBP4, RAB37, SPEG, FAM86HP, CCDC110, TPBG, HOXA11, SGK3, UBR5-AS1, NXNL2
+		+			+	PTCHD2, ACOT11, TNNI2, RLTPR, KLK10, TUBA3E, DEFB132, MAP1B, MAN1A1, GJA1, ADGRA2
	+	+				PDZK1, RGCC, FAM184B, NPY1R, KCNQ5, MET, ZFPM2, SYN1, CITED1
	+				+	TMEM229B, SULF2, ABCC13, ACOX2, SCGB3A1, PHACTR1, GNG11, OLFML2A
+					+	KRT5, TGM2, COL6A2, ASPHD2, SEC14L2, CMTM7
				+		MALAT1, B4GALNT2, LINC01004
			+	+		KIF26A, C16orf45, TRPM8
	+		+	+		C1orf64, KCNC1, FOXN
+			+			SORBS1, TSPEAR, PRICKLE4
+			+	+		CPNE7, FLRT3, TM4SF18
	+			+		MS4A7, KRT81

Table 7-2 List of DEGs commonly regulated by E2, and additional treatment combinations, in T47D

T47D						
E2up	E2down	MIB_E2up	MIB_E2down	MIB_E2_FULVup	MIB_E2_FULVdown	Gene Symbols
		+				MXRA8, CHD5, GPR153, ERRFI1, CASZ1, LOC101929181, MIR3972, PADI4, PINK1-AS, ALPL, WNT4, ZNF436, ASAP3, TRNP1, FAM46B, MAP3K6, IFI6, SMPDL3B, LCK, ZC3H12A, FHL3, SLC2A1, LOC101929626, DMBX1, CYP4B1, CYP4X1, CYP4Z1, RAB3B, TTC22, C1orf168, AK4, ACADM, F3, SLC44A3, TMEM56, AKNAD1, GPSM2, EPS8L3, KCNC4, LOC440600, ATP1A1, FAM46C, NOTCH2, SRGAP2C, SRGAP2B, ANKRD35, ITGA10, NBPF10, NOTCH2NL, PRKAB2, FMO5, NBPF14, CTSS, PBXIP1, ZBTB7B, DCST2, DCST1, MUC1, THBS3, GBA, HCN3, HAPLN2, BCAN, LINC01133, ATP1A2, ATP1A4, CASQ1, FCGR3A, CREG1, ADCY10, ATP1B1, TOR1AIP2, QSOX1, FLJ23867, GLUL, C1orf21, MYBPH, CHI3L1, ETNK2, PLEKHA6, SRGAP2, C1orf116, CAPN8, C1orf95, ITPKB, RHOU, AGT, KCNK1, AKR1C2, AKR1C3, NET1, SFMBT2, FAM107B, NEBL, NRP1, FZD8, LINC00839, RASGEF1A, FAM13C, SRGN, DDIT4, USP54, MYOZ1, ZNF503, DLG5, DLG5-AS1, PPP1R3C, CYP26A1, SORBS1, GOLGA7B, SCD, ELOVL3, ADD3, NRAP, BNIP3, PNPLA2, CRACR2B, MUC5AC, CDKN1C, TRIM22, SCUBE2, PARVA, KCNJ11, ABCC8, TMEM86A, IGSF22, CD59, LMO2, EHF, LDLRAD3, TP53I11, DTX4, ZP1, FADS1, FADS2, ASRGL1, AHNAK, HRASLS2, NEAT1, SLC29A2, PC, CHKA, ANO1, CHRDL2, ARRB1, THRSP, ANGPTL5, BIRC3, CRYAB, ZBTB16, THY1, SLC37A2, ST3GAL4-AS1, ST3GAL4, KIRREL3, B3GAT1, CD9, SCNN1A, TAPBPL, LPCAT3, C1S, SLC2A14, A2ML1, STYK1, GPRC5A, MIR614, CAPRIN2, DENND5B, FGD4, NELL2, VDR, GPD1, GALNT6, NR4A1, OR7E47P, KRT6A, KRT4, KRT79, HSD17B6, RDH16, MYO1A, CPM, LINC01481, PHLDA1, TMCC3, MYBPC1, CHPT1, SYCP3, GNPTAB, CHST11, SLC41A2, MYO1H, DTX1, RASAL1, TESC, CCDC64, FLT1, N4BP2L1, NBEA, FOXO1, DGKH, TSC22D1, PCDH17, KLF5, LMO7-AS1, LMO7, DNAJC3-AS1, LOC101928841, AKAP6, NFKBIA, GCH1, HSPA2, PAPLN, PGF, FOS, TMEM63C, RPS6KA5, CLMN, CCDC85C, C14orf180, ATP10A, PHGR1, PPP1R14D, EHD4-AS1, PLA2G4E, CAPN3, TNFAIP8L3, NEDD4,

						CORO2B, PCAT29, GRAMD2, NEO1, CTSH, FAH, HOMER2, AKAP13, AP3S2, ARPIN, ZNF710, IDH2, SEMA4B, FURIN, ADAMTS17, PRSS27, VASN, PPL, EMP2, PLA2G10, TMC5, ACSM1, LCMT1-AS1, LCMT1, CLN3, IL27, NUPR1, GDPD3, BCL7C, NETO2, MT2A, PLLP, CNGB1, MMP15, NOL3, FHOD1, SLC9A5, HSD11B2, TAT, ZFHX3, LDHD, HSD17B2, LINC00304, SLC22A31, RPH3AL, ATP2A3, GUCY2D, PER1, SREBF1, ULK2, TRAF4, CPD, RHOT1, PPP1R1B, TCAP, PNMT, GRB7, KRT24, KCNH4, STAT5B, STAT5A, G6PC, SP6, PRR15L, PHOSPHO1, ZNF652, LOC102724596, NGFR, DLX3, ACSF2, NOG, SEPT4, CA4, SMARCD2, FADS6, KIAA0195, LLGL2, ACOX1, ST6GALNAC1, GAA, LINC00482, TMEM105, RAC3, DCXR, CCDC57, DLGAP1-AS1, MTCL1, GREB1L, ABHD3, NPC1, ANKRD29, LAMA3, AQP4-AS1, ZBTB7C, NEDD4L, TSHZ1, ATP8B3, NFIC, LRG1, KDM4B, TNFSF9, C3, CAMSAP3, CDKN2D, JUNB, SYCE2, RASAL3, CYP4F8, CRLF1, PLEKHF1, FXYD3, ZFP36, TMEM91, KCNN4, NKPD1, SLC8A2, ZNF541, LIN7B, VSIG10L, ZNF582-AS1, MBOAT2, C2orf48, HPCAL1, ATP6V1C2, FAM49A, FKBP1B, MAPRE3, PLB1, CDC42EP3, KCNG3, HAAO, NAGK, MPHOSPH10, DQX1, CNGA3, MERTK, C2orf76, ARHGEF4, TUBA3D, ARHGAP15, DLX1, DLX2, FRZB, GULP1, CFLAR, ICA1L, CYP27A1, SGPP2, EFHD1, INPP5D, JAG1, ABHD12, NECAB3, TP53INP2, FER1L4, MAFB, ZMYND8, KCNB1, BCAS4, PHACTR3, STMN3, SIK1, MGC39584, CLDN8, IL10RB-AS1, LINC00160, LOC100133286, CBR3-AS1, DOPEY2, RIPK4, COL6A1, LOC101929372, PRODH, YPEL1, LOC100128531, RASL10A, THOC5, NIPSNAP1, GATSL3, SELM, INPP5J, PLA2G3, PISD, HMOX1, RASD2, MB, SUN2, GRAP2, SERHL2, PNPLA3, FBLN1, PIM3, PLXNB2, NEK10, TTC21A, CSRNP1, VIPR1, VIPR1-AS1, ARIH2OS, ABHD6, ALCAM, ZBED2, HGD, EAF2, SLC15A2, PDIA5, KLF15, MRAS, RBP2, RBP1, CP, GPR87, ARHGEF26-AS1, MME, TIPARP, LINC00886, LINC00880, GPR160, KLHL24, FETUB, BCL6, TPRG1-AS1, ATP13A4, LOC100505920, MFSD7, MAN2B2, MRFAP1, LOC93622, LOC100129931, PSAPL1, CWH43, TMPRSS11E, UGT2B11, EPGN, SHROOM3, LINC01094, HERC3, MANBA, EGF, NDNF, PGRMC2, SCRG1, HPGD, ACSL1, LINC01093, LINC01018, SRD5A1, DNAH5, FAM105A, MYO10, LIFR, SEPP1, HTR1A, GCNT4, SERINC5, SSBP2, RHOBTB3, LOX, P4HA2-AS1, P4HA2, PCDHGB6, PCDH1, ARHGAP26, ADRB2, ABLIM3, FAXDC2, ADRA1B, CTB-178M22.2, WWC1, FGF18, DUSP1, ATP6V0E1, CREBRF, CPEB4, COL23A1, ADAMTS2, CDSN, HSPA1B, SLC44A4, C2, HLA-DMA, B3GALT4, IP6K3, PACSIN1, FKBP5, LOC285847, ARMC12, LRFN2, PGC, PRPH2, CRISP2, CRISP3, ELOVL5, PRDM1, FRK, ENPP3, ENPP1, EYA4, SGK1, IL20RA, ABRACL, SASH1, PPP1R14C, SOD2, FAM20C, GPR146, SNX8, GNA12, LOC221946, CCDC126, CHN2, LOC102724484, PRR15, GGCT, EGFR, SEPT14, DTX2, DTX2P1-UPK3BP1-PMS2P11, KIAA1324L, STEAP1, STEAP2, PDK4, GJC3, AZGP1, AZGP1P1, COL26A1,

						KMT2E-AS1, CBLL1, SLC26A3, AASS, IMPDH1, HILPDA, TSPAN33, CALD1, CREB3L2, AKR1D1, EPHB6, KEL, CNTNAP2, MTMR9, PEBP4, BNIP3L, DPYSL2, CHRNA2, RNF122, LINC01605, CEBPD, XKR9, TPD52, SYBU, FAM83A-AS1, ATAD2, WDYHV1, KLHL38, SPATC1, KANK1, JAK2, PLIN2, FRMPD1, KLF9, FRMD3, CORO2A, TBC1D2, KLF4, C9orf152, TXN, C9orf84, SLC31A2, ASTN2, BRINP1, STOM, LHX6, PTGS1, CCBL1, CRAT, LINC00963, FIBCD1, GRIN1, LRRC26, CYSRT1, ARRDC1, ARRDC1-AS1, PIR, ACE2, RBBP7, MAP7D2, PHEX, ARX, MAOA, TSPYL2, FOXO4, CYSLTR1, HMGN5, TSC22D3, TMEM164, CAPN6, TRPC5OS, APLN, GPC4, CD99L2, HMGB3, GABRQ, IRAK1
			+			TP73, PLEKHG5, PIK3CD, KAZN, AKR7A3, UBXN10, GRHL3, LOC100506985, NCMAP, PTAFR, TMEM200B, GJB5, TEKT2, FAM183A, ARTN, GNG12, PTGER3, MCOLN2, MCOLN3, GBP1, ARHGAP29, SLC16A4, PIFO, CASQ2, ATP1A1-AS1, ATP8B2, CFAP45, RGS16, LAMC2, NMNAT2, NCF2, APOBEC4, HMCN1, CFHR3, CSRP1, GPR37L1, LGR6, ATP2B4, LRRN2, SLC45A3, RAB7B, CD34, LAMB3, TGFB2, TMEM63A, ACTA1, PGBD5, FMN2, GREM2, OPN3, CHML, CAMK1D, HACD1, ARMC3, ENKUR, GPR158, RAB18, MKX, MKX-AS1, ARMC4, SVIL, ZNF239, GPRIN2, ZNF488, DKK1, STOX1, SFTPA2, PAPSS2, ACTA2, IFIT2, IFIT1, FFAR4, LGI1, PLCE1, DNMBP, WNT8B, ITPRIP, VWA2, PNLIPRP2, C10orf82, CPXM2, NKX1-2, TUB, LOC440028, SBF2-AS1, ADM, MPPED2, SLC1A2, PRDM11, CDC42EP2, WNT11, MYO7A, RAB38, TRPC6, GUCY1A2, C11orf88, CADM1, OAF, UBASH3B, LOC100128239, B4GALNT3, ANO2, TMEM52B, SSPN, ARNTL2, LRRK2, AMIGO2, PCED1B, WNT10B, KCNH3, AQP5, KRT75, HOXC12, ITGA5, METTL7B, ARHGEF25, GRIP1, GLIPR1, KITLG, LUM, CFAP54, C12orf75, CCDC42B, SDSL, LRRC43, GJB2, SHISA2, UBL3, LINC00365, FREM2, LHFP, ENOX1, LCP1, MLNR, SPRY2, SLITRK6, SLITRK5, GPC6, SALL2, REM2, FRMD6, PTGER2, FUT8, PLEK2, GALNT16, VASH1, SERPINA10, GSC, C14orf132, TNFAIP2, JAG2, TMEM121, PAK6, GATM, SLC27A2, LYSMD2, CGNL1, DAPK2, IGDCC3, SMAD3, LARP6, HCN4, LOXL1-AS1, LOXL1, CSPG4, LINGO1, RASGRF1, ARNT2, NHLRC4, ABCA3, KREMEN2, PAQR4, TNFRSF12A, ABAT, XYLT1, ITGAL, PYCARD, CCL22, CX3CL1, CCDC102A, MLKL, TMEM231, LOC102724163, ADAD2, FAM92B, VPS9D1-AS1, SCARF1, SERPINF2, SERPINF1, LOC728392, TEKT1, EFNB3, ALOXE3, RNF222, MEIS3P1, CCL2, RAD51D, SLFN11, GAS2L2, LHX1, C17orf96, RARA, PTRF, CNTNAP1, RND2, HLF, C17orf67, BZRAP1, TBX2-AS1, MRC2, PRR29, LOC100507002, RGS9, LINC00673, SSTR2, TTYH2, USH1G, FOXJ1, RNF157-AS1, SOCS3, LOC101928674, AATK, RAB31, NOL4, TCF4, PMAIP1, BCL2, CDH7, CELF5, TMEM221, DPF1, RYR1, AXL, TGFB1, ATP1A3, RELB, FPR3, CMPK2, ID2, CYS1, KCNS3, MATN3, LTBP1, ZFP36L2, STON1, C2orf73, LOC100129434, CCDC85A, WDR54, LOXL3, DOK1, TCF7L1,

						ARID5A, MGAT4A, LIMS2, CCDC74B, NCKAP5, ITGB6, LINC01116, DNAH7, PLCL1, FN1, TNS1, SLC4A3, EPHA4, DOCK10, ARL4C, PP14571, MIR149, SNPH, LRRN4, FERMT1, ISM1, CFAP61, GGTLC1, TTLL9, PROCR, TGIF2, JPH2, PREX1, FAM65C, NFATC2, BMP7, GATA5, SOX18, CYP4F29P, RBM11, NCAM2, GRIK1, GRIK1-AS2, IGSF5, DSCAM, DSCAM-AS1, MX1, TFF3, RSPH1, GNAZ, RAB36, GGT5, MN1, LIF, LARGE, KCTD17, MGAT3, SHISA8, A4GALT, KIAA1644, SRGAP3, PRRT3, CAND2, FGD5, TRANK1, CCDC13, CCR1, SLC38A3, SEMA3B, PPM1M, TNNC1, CACNA1D, DNAH12, FOXP1, ROBO2, ROBO1, GPR156, FSTL1, MYLK, KALRN, CDV3, SLCO2A1, ESYT3, SPSB4, TRPC1, PLSCR1, C3orf80, B3GALNT1, SPTSSB, BCHE, ZBBX, SERPINI1, EIF5A2, NAALADL2, LINC01208, LINC00888, MAP6D1, ADIPOQ, TP63, CLDN1, FAM43A, FGFR3, CFAP99, AFAP1, FGFBP1, PROM1, PPARGC1A, RELL1, RHOH, SGCB, KIAA1211, ANXA3, TIGD2, BMPR1B, ARHGEF38, NPNT, ARSJ, INPP4B, NPY5R, PALLD, TENM3, TLR3, FAT1, C5orf49, ROPN1L, FAM134B, NPR3, RAI14, SPEF2, CCL28, PARP8, CDC20B, MCIDAS, CCNO, FAM169A, VCAN, NREP, SEMA6A, LINC00992, TNFAIP8, ZNF474, PRDM6, TCF7, EGR1, PCDHAC2, SPRY4, SLC26A2, SYNPO, ANXA6, GALNT10, SAP30L-AS1, CCNJL, KCNMB1, SNCB, PRR7, FLT4, MAK, CD83, STMND1, DCDC2, ZNF311, HCP5, MICB, TNF, CFB, SCUBE3, SLC29A1, RUNX2, GLYATL3, RIMS1, COL12A1, ELOVL4, GPR63, DDO, RSPH4A, PKIB, L3MBTL3, CTGF, MYB, LOC100132735, RAB32, TIAM2, DLL1, LFNG, GLCCI1, SCIN, AHR, TWIST1, DFNA5, CREB5, DPY19L1, AMPH, GLI3, STK17A, IGFBP3, PKD1L1, SEMA3C, CALCR, NRCAM, LRRN3, FLNC, SMKR1, ATP6V0A4, CLDN23, FAM167A, HR, CLU, SCARA3, DUSP26, TACC1, LYN, LINC01301, LOC102724623, CYP7B1, JPH1, GEM, SDC2, MATN2, AARD, ENPP2, LY6E, MAFA, RLN2, TYRP1, ELAVL2, MOB3B, ARID3C, GLIPR2, ALDH1B1, S1PR3, WNK2, GALNT12, KIF12, TNFSF15, LHX2, WDR38, C9orf171, COL5A1, CACNA1B, TMEM47, EFHC2, SYN1, TIMP1, SHROOM4, XAGE2, MAGEE1, P2RY10, ITM2A, SYTL4, RNF128, KLHL13, DOCK11, PLAC1, SLITRK4, FLNA
+						TNFRSF18, EPHA2, EPHA8, SNHG12, LAPTM5, COL16A1, GRIK3, CDC20, KIF2C, FOXD3-AS1, JAK1, GADD45A, DEPDC1, SARS, SLC22A15, FAM72D, ARHGEF2, IQGAP3, NUF2, GAS5, FAM129A, KCNT2, KIF21B, FAM72A, KCNH1, RET, UNC5B, CEP55, PIPSL, ATRNL1, FAM24B, MKI67, SYT8, FIBIN, KIF18A, SLC43A1, BEST1, SNHG1, RASGRP2, PDE2A, ROBO3, ADAMTS15, RAD51AP1, CDCA3, RACGAP1, ESPL1, SHMT2, NDUFA4L2, XPOT, ALDH1L2, HRK, GJB6, SKA3, F7, GAS6-AS2, PCK2, TGM1, CDKN3, LINC00341, SYNE3, WARS, ARHGAP11B, FMN1, THBS1, FSIP1, KNSTRN, NUSAP1, PRTG, CCNB2, PIF1, NR2E3, CPLX3, PLK1, ATP2C2, LOC102724467, FAM64A,

						AURKB, HS3ST3B1, TOP2A, HOXB9, LPO, TEX14, PPM1E, SCN4A, SDK2, MGAT5B, NDC80, DLGAP1-AS2, EPB41L3, TAF4B, SKA1, DIRAS1, PLIN5, LONP1, PGLYRP2, GDF15, LINC00662, CD22, PAPL, FGF21, KLK13, FLJ33534, GREB1, ADCY3, CENPA, ATP6V1E2, CCDC88A, FOXI3, BUB1, TFCP2L1, ERICH2, NABP1, GPR1, KCNE4, SERPINE2, HJURP, SMOX, LINC00654, INSM1, TPX2, CCM2L, SNHG17, FAM83D, ADA, WISP2, PABPC1L, UBE2C, CEBPB-AS1, EVA1C, LINC01426, RUNX1, SH3BGR, TSPEAR-AS2, TUBA8, CLDN5, MAFF, MOV10L1, KLHDC7B, KIF15, CMSS1, CSTA, SIAH2, RPL22L1, LAMP3, GPAT3, HERC5, ANK2, CLGN, HMGB2, EPB41L4A-AS1, SNX24, CDC25C, HSPA9, ARAP3, SH3PXD2B, STC2, RBM24, ZSCAN12P1, CLPSL2, GTPBP2, FYN, RAET1E, MTHFD1L, RPS6KA2, BMPER, LAT2, SAMD9L, ASNS, BHLHA15, EZH2, FAM86B3P, EGR3, TNFRSF10B, CDCA2, PBK, ZNF703, EIF4EBP1, CA8, C8orf34, SULF1, SNTB1, MYC, VLDLR, B4GALT1, PSAT1, NFIL3, LCN2, SH3KBP1, EDA2R, STARD8, KIF4A, CITED1, RAB33A, DUSP9
	+					PERM1, LOC102724312, VWA1, KLHDC7A, EXTL1, FOXO6, RIMKLA, OVGP1, CD101, ANKRD34A, LOC653513, CTSK, SELENBP1, IVL, CREB3L4, IGSF9, SLAMF9, PVRL4, PCP4L1, HSD17B7, PLA2G4A, VASH2, KMO, LINC00836, BAMBI, SYT15, BLNK, OLMALINC, KAZALD1, HPX, TRIM3, CHST1, GLYATL1, TMEM132A, SYT7, RPLP0P2, SIPA1, CORO1B, P2RY2, P2RY6, DLG2, UPK2, POU2F3, TSPAN9, ARHGDIB, PLEKHG7, MVK, HCAR1, CAB39L, KCTD12, SLC39A2, RIPK3, EGLN3, LPCAT4, DISP2, RHOV, PLA2G4F, NOX5, NR2F2-AS1, RAB26, SEC14L5, CRYM, LOC388282, CLEC3A, MAF, MVD, SNAI3, SLC25A35, NEK8, TMEM132E, ERBB2, KRT222, KRTAP3-1, ARL4D, MAP2K6, SOX9, HID1, SMIM5, ACER1, CERS4, RAB3D, LPPR2, TPM4, UPK1A, CEACAM6, LYPD3, FOSB, ZNF350-AS1, ERVV-2, RNF225, EHD3, EPAS1, OR7E91P, VAMP5, PROM2, KIF5C, FSIP2, C2orf72, C2orf54, ACSS1, ZNF341-AS1, VSTM2L, BCAS1, RBBP8NL, KCNE2, TMPRSS2, ABCG1, LOC101928233, COMT, ZDHHC8P1, PIK3IP1, CSF2RB, CYP8B1, SPINK8, UBA7, PDZRN3, CNTN3, STX19, TM4SF1, PLCH1, HTR3E, LIPH, CLDN16, FGF12, ATP8A1, RASL11B, ODAM, ANTXR2, NDST4, SPRY1, NR3C2, CTSO, FAM198B, MSMO1, LPCAT1, AMACR, AGXT2, NR2F1-AS1, NR2F1, MEGF10, ACSL6, CCNI2, PCDHA4, PCDHGC3, UNC5A, FGFR4, CD24, AGPAT4, TTYH3, RASA4CP, UPK3B, SSPO, INSIG1, MMP16, ST3GAL1, ACER2, CDKN2B, SLC2A6, SARDH, NDP, FAM155B
+			+			TGFBR3, PPM1J, PDZK1, KIRREL, ADAMTS4, DDR2, ADORA1, FCMR, SIPA1L2, RBP4, ANKRD2, SFXN2, NAV2, WT1, RAB3IL1, MCAM, CLMP, RERG, INHBE, ESR2, GPR68, ITPK1, C15orf48, IL32, LOC105447648, SLFN5, KRT17, NXPH3, RBBP8, ADAMTSL5, CNN1, CHST8, IGFL1, KLK5, PLEKHH2, FHL2, LYPD1, NPPC, PRSS56, FOXA2, OLIG1,

						PCP4, TFF1, TMPRSS3, TIMP3, TRH, FGFBP2, AREG, NPY1R, LOC90768, PDLIM3, TUBB2B, ELOVL2, MBOAT1, IER3, LINC01016, MDGA1, PAQR8, KCNQ5, HEY2, SNX10, MET, KCP, SGK223, NEIL2, ZFPM2, ARC, COL27A1, AKNA, PIP5KL1, BGN, RAB39B
	+	+				EDN2, CYP4Z2P, DHCR24, HMGCS2, NBPF13P, S100A9, S100A8, PKP1, ELF3, KCNMA1, LINC01519, ELF5, ALDH3B2, GDPD5, EMP1, ST8SIA1, LINC00936, TRPV4, SLC7A8, ARHGAP5-AS1, PLEKHD1, CCDC177, BMF, SQRDL, APOBR, LINC00324, ACACA, FASN, ZNF750, TBXA2R, ZNF812, ZSCAN5A, DBI, ACKR3, PXMP4, SLC25A18, LRRC31, SOD3, PCDH7, CNGA1, RANBP3L, GLRX, SOWAHA, SH3TC2, ARHGEF37, SLC22A23, GNMT, ADGRF1, STEAP4, PIP, TCAF2, FAM83A, FBXO32, NDRG1, PSCA, AQP3, PTCH1, ABCA1, CDKL5, SYP, VGLL1
					+	CITED4, NR5A2, LINC00173, HEATR4, GPR132, CACNA1H, NOD2, WFIKKN2, RAB37, EGLN2, C5AR2, KCNF1, MREG, SPEG, YBEY, HDAC11, CISH, FAM86HP, SCGB3A1, NEDD9, TPBG, AMZ1, STC1, C8orf46, UBR5-AS1, PTGES
	+		+			IGSF3, RASSF5, CHRM1, CAPN5, OAS2, HS6ST3, EFNB2, TCL1B, SEMA7A, CCDC154, CDH13, RAB27B, IL1R1, MYO3B, ENTPD3, MECOM, SOX2, PCDH18, GRM4, LINC00472, HDAC9, RGAG4, SLC16A2
+			+		+	NKAIN1, CXCL12, ADRA2A, SERPINA6, C15orf59, NECAB2, IGFBP4, KRT13, PSG9, KCNK15, RIMS4, SULF2, SEMA3G, PXK, KCTD6, ACOX2, BFSP2, DOK7, KCNK5, GATA4, SPINK4, OLFM1
+					+	PFKFB3, ST8SIA6, IFITM10, GRIK4, LINC00565, ACOT6, RASGRP1, LOC102723344, TPSG1, SLC47A1, RAPGEFL1, MAPT, CYP2B7P, SEC14L6, IL6ST, MAP1B, HOXA11, MYBL1, SGK3, NXNL2, RAI2
+		+				FAM131C, S100A14, MS4A15, GAL, ADAMTS8, IGFBP6, RMST, SERPINA5, SERPINA3, SCNN1G, MT1X, KRT16, FUT3, CYP4F22, SLPI, KCNG1, CLIC6, MCHR1, S100P, NEURL1B
		+			+	HES2, PADI3, ACOT11, CHRM4, KRT5, LINC01588, TUBA3E, DEFB132, COL6A2, SEC14L2, CMTM7, CCDC69, MAN1A1, GJA1
			+		+	PGR, TMEM229B, CYP2S1, ABCC13, CCDC110, PHACTR1, GNG11, FGD3, SUSD3, OLFML2A, GRPR
+		+			+	PTCHD2, TNNI2, RLTPR, ANKFN1, KLK10, TGM2, ASPHD2, ADGRA2
				+		MALAT1, C16orf45, CPNE7, B4GALNT2, FLRT3, LINC01004
			+	+		KRT81, FOXN4, KIF26A

	+		+	+		C1orf64, KCNC1, MS4A7
	+	+		+		TRPM8, TM4SF18

Table 7-3 List of DEGs commonly regulated by MIB, and additional treatment combinations, in MCF7

MCF7						
MIBup	MIBdown	MIB_E2up	MIB_E2down	MIB_E2_FULVup	MIB_E2_FULVdown	Gene Symbols
					+	TP73, RBP7, E2F2, NKAIN1, CDCA8, CDC20, RAD54L, CDKN2C, ORC1, ITGB3BP, CELSR2, PPM1J, OLFML3, FAM72D, CKS1B, IQGAP3, NOS1AP, C1orf226, UBE2T, DTL, EXO1, MCM10, PDSS1, RET, CDK1, PPIF, FAM25A, ANKRD2, ATRNL1, GFRA1, ADAM12, CTSD, TRPM5, CD44, SLC1A2, FAM111B, FEN1, CDCA5, SPDYC, GAL, DDIAS, PRSS23, LOC101054525, CHEK1, FKBP4, RAD51AP1, CDCA3, SLC2A14, H2AFJ, C12orf60, SMCO3, ART4, RERG, SYT10, TUBA1B, TUBA1A, SLC5A8, FAM216A, HSPB8, P2RX7, KNTC1, BRCA2, CCNA1, KIAA0226L, MYO16, LOC101928841, DHRS2, POLE2, LINC01588, GALNT16, ZDHHC22, VRK1, DIO3, KIF26A, GPR132, RASGRP1, RAD51, WDR76, C2CD4A, CA12, ABHD2, FANCI, TICRR, BLM, PKMYT1, RMI2, LOC105447648, SHCBP1, ABCC11, MT2A, MT1X, LDHD, OSGIN1, DNAAF1, GINS2, SLC7A5, CDT1, SERPINF1, GSG2, SMTNL2, AURKB, NTN1, HS3ST3A1, SLC47A1, RAPGEFL1, CDC6, RARA, PSMC3IP, BRCA1, ITGA2B, C17orf104, KIF18B, MAPT-AS1, MAPT, EME1, BRIP1, SNORA76C, LOC440461, TK1, BIRC5, TYMS, NDC80, RAB31, LINC00669, SLC14A1, SKA1, KISS1R, UHRF1, SPC24, ZNF833P, C19orf57, PODNL1, ASF1B, EPS15L1, CHST8, WDR62, KLK12, RRM2, KCNF1, GREB1, OTOF, TTC7A, CHAC2, CCDC85A, MCEE, LINC01291, REEP1, ASTL, FAM178B, CKAP2L, SPC25, CDCA7, PPP1R1C, PLCL1, MREG, FAM132B, CCM2L, E2F1, MYBL2, RIMS4, UBE2C, LINC01522, CDH26, ABCC13, TIAM1, CLIC6, CHAF1B, PCP4, TFF3, TFF1, TMPRSS3, CDC45, SEPT5-GP1BB, GGT5, MCM5, DMC1, CENPM, PNPLA3, RIBC2, FBLN2, SCN5A, KIF15, PTH1R, SEMA3B, CISH, ADAMTS9, HEG1, MCM2, VEPH1, GNB4, TPRG1, ZNF732, DOK7, NCAPG, KLB, KIT, EREG, BTC, ARSJ, MAD2L1, CCNA2, PLK4, MND1, NPY1R, NPY5R, HMGB2, NEIL3, LOC90768, CENPU, CCDC110, TRIP13, PRLR, C5orf34, CENPK, LOC101928858, CENPH, DHFR, ISOC1, SOWAHA, LOC101927934, CXCL14, ANXA6, HMMR, STC2, FGFR4, ELOVL2, ELOVL2-AS1, RBM24, TUBB, TCF19, KIFC1, C6orf141, COL12A1,

						GJA1, PKIB, TPD52L1, CENPW, MYB, ADAT2, RAET1E, LINC01558, MLLT4-AS1, RADIL, AGR2, AGR3, ANLN, ADCY1, CALCR, STRIP2, PRKAG2-AS1, XRCC2, DLC1, STC1, ESCO2, PBK, GINS4, PLAT, TMEM64, DSCC1, MYC, SLC1A1, RLN2, KIF24, ARHGEF39, MELK, FAM189A2, CENPP, SUSD3, ZNF367, PTRH1, SH2D3C, PIP5KL1, PRRX2, FANCB, AP1S2, XK, SYTL5, ERCC6L, CITED1, CENPI, GLA, TMEM164, IGSF1, MIR503HG, MAMLD1
				+		TMEM51-AS1, KLHDC7A, RAP1GAP, HTR1D, EXTL1, TSPAN1, CTSS, SELENBP1, RGS16, RGL1, EDARADD, RASSF4, CTNNA3, C10orf54, KCNMA1, SLIT1, LINC01164, SCART1, SLC15A3, P2RY6, CAPN5, LOC101928944, CCDC83, TMPRSS4, ROBO3, CACNA1C, A2M, CLEC7A, LMO3, ABCC9, RND1, KRT81, KRT3, LIN7A, PPFIA2, NTN4, DRAM1, TCP11L2, TBX3, HCAR3, TMEM132B, P2RX2, TNFRSF19, FLT1, PCDH8, PCDH17, ANG, RNASE4, LINC01269, CLMN, BMF, SEMA6D, SLC12A1, FBN1, IGDCC3, STRA6, CYP1A1, FAM174B, ALDH1A3, RAB26, PLA2G10, TMC5, GDPD3, ZNF423, CCL22, CDH5, ADAMTS18, PKD1L2, SPIRE2, ALDH3A1, GSDMB, CCR7, ABCC3, RNF43, SLC16A5, LOC101928766, PTPRM, RAB27B, TLE6, PALM3, MIR3189, CILP2, UPK1A, CEACAM5, CEACAM6, CEACAM1, SRRM5, LOC284379, CACNG6, TTYH1, FAM179A, CAPN13, EPAS1, ATOH8, FAHD2CP, IL1R1, SLC9A4, ACOXL, KYNU, TFPI, PID1, FER1L4, SALL4, BCAS1, B3GALT5, PLAC4, TMPRSS2, IL17REL, LMCD1, VILL, VIPR1, ERC2, UPK1B, ACAD11, TM4SF1, LXN, TNFSF10, KCCAT211, CHRD, LIPH, ATP13A4, APOD, SLC51A, HS3ST1, SLIT2, LGI2, ATP8A1, AMTN, FAM13A-AS1, FAM13A, SPRY1, AHRR, SEMA5A, SNHG18, NIM1K, PLK2, ENC1, IQGAP2, SLC12A2, FSTL4, DRD1, RNF144B, LTB, LRFN2, GSTA1, FUT9, GRIK2, TSPAN12, ATP6V0A4, LINC00689, PSD3, HEY1, ST3GAL1, CDKN2A, GNE, DAPK1, C9orf47, S1PR3, GABBR2, ABCA1, C8G, RNF224, SLC34A3, CA5B, CDKL5, NHSL2, KIAA2022, RNF128, MBNL3, VGLL1, FGF13
+						HES2, ERRFI1, SLC45A1, MEAF6, RAB3B, C1orf168, AKNAD1, CD53, ITGA10, NBPF13P, KIAA0040, RGS2, LINC00704, NEBL, COL13A1, MICAL2, ABCC8, CEP126, DRD2, ZBTB16, SLC37A2, LINC00940, IGF1, RASL11A, RGCC, SLITRK6, BATF, KIAA0125, SORD, RORA, ACSBG1, GP2, SCNN1G, MYLK3, PLLP, RLTPR, PYY, MIR21, LAMA3, KLK6, KLK8, KLK10, KLK11, KLK14, CDC42EP3, AFF3, ZNF385B, MAP2, IGFBP2, TGM2, ADAMTS1, SEC14L2, SERHL2, LOC730668, MIRLET7BHG, WNT5A, ZPLD1, ALCAM, CD86, DZIP1L, LINC01213, B3GNT5, FAM43A, S100P, UGT2B11, UGT2B28, EPGN, SHROOM3, HERC3, TSPAN5, PPP3CA, FLJ20021, LEF1, FAM105A, SEPP1, MCCC2, MAP1B, ARHGEF37, PDE6A, SH3PXD2B, F13A1, FKBP5, LOC285847, ARMC12, CD109, AIM1,

						ENPP3, SLC2A12, AKAP12, PDE10A, TP53TG1, CROT, PDK4, CYP3A43, AZGP1, AZGP1P1, DOCK4, CAV1, SNAI2, TPD52, PAG1, CA2, SYBU, TG, CNTNAP3, KLF9, DIRAS2, CRAT, WWC3, MAOB, NUDT10, SEPT6, SRPK3
		+			+	GRIK3, CITED4, PDZK1, S100A7, PRG4, NR5A2, VIM-AS1, CXCL12, MAT1A, LOXL4, SFXN2, PGR, GRIK4, MGP, KRT6A, KRT5, GPR68, FMN1, CT62, ST3GAL2, SERPINF2, NXPH3, S1PR5, C5AR2, SYNDIG1, HCK, WISP2, CECR6, SUSD2, C1QTNF6, MGAT3, BFSP2, AREG, TUBB2B, BMP6, LINC01016, COL21A1, HEY2, HMGA1P7, AMZ1, EGR3, C8orf46, RGS22, DEPTOR, NXNL2, ARHGAP6, GRPR, XKRX, ARHGAP36, SOX3
	+					ST6GALNAC5, SPRR3, MKX, JMJD1C-AS1, ACACB, ADGRD1, SGCG, SCG5, LOXL1, HAS3, COLEC12, FAM84A, GRB14, ZNF804A, ITPR1, LINC00504, PTGER4, ST8SIA4, CMAHP, RUNDC3B, NR4A3
			+	+		RNF207, GRHL3, VTCN1, SEC31B, KCNC1, KCNJ8, KRT4, EGLN3, GLP2R, CCDC68, CLIP4, KCNJ3, STAT4, ZBTB20, ADCY5, ST6GAL1, PPP2R2B, PDE7B, AKR1B10, FER1L6
+					+	MYPN, SYNPO2L, SYT8, TRPC6, NAGS, SLC16A6, UGT2B17, UGT2B15, SLC26A2, FGF18, BMPER, EBF2, SGK3, SYTL4
+			+	+		C10orf10, ADRA2A, EMP1, ST6GALNAC1, NRP2, ALPP, MME, FYB, PSCA, IGFBPL1
	+			+		WNT11, AQP2, LOC101927318, VAT1L, RPRM, DAB2, ASB9
+				+		DNASE2B, C1orf116, SMPD3, TBC1D8, TRPM8, HSD17B11, ADH1C
	+				+	ASCL1, BCL2, SLC4A10, CSPG5, RAMP3, NECAB1
		+				LOC143666, KRT6C, RN7SL1, GSG1L
	+	+			+	VIM, VCAN, SHH, PLAC1
+		+			+	ADRB1, VWA2, SGK1, MYBL1
			+			PLA2G2F, CORO2B
	+		+	+		CP

Table 7-4 List of DEGs commonly regulated by E2, and additional treatment combinations, in MCF7

MCF7						
E2up	E2down	MIB_E2up	MIB_E2down	MIB_E2_FULVup	MIB_E2_FULVdown	Gene Symbols
					+	TP73, RBP7, E2F2, GRIK3, CDCA8, CDC20, RAD54L, CDKN2C, ORC1, ITGB3BP, CELSR2, PPM1J, FAM72D, PDZK1, S100A7, CKS1B, IQGAP3, NOS1AP, C1orf226, NR5A2, UBE2T, DTL, EXO1, MCM10, VIM, PDSS1, RET, CDK1, PPIF, ANKRD2, ATRNL1, GFRA1, ADAM12, CTSD, SYT8, TRPM5, CD44, SLC1A2, FAM111B, FEN1, CDCA5, SPDYC, GAL, DDIAS, LOC101054525, CHEK1, FKBP4, RAD51AP1, CDCA3, H2AFJ, SMCO3, RERG, SYT10, TUBA1B, TUBA1A, KRT6A, KRT5, SLC5A8, FAM216A, HSPB8, P2RX7, KNTC1, BRCA2, KIAA0226L, MYO16, DHRS2, POLE2, LINC01588, GALNT16, ZDHHC22, VRK1, DIO3, KIF26A, GPR132, FMN1, RASGRP1, RAD51, WDR76, C2CD4A, CA12, CT62, ABHD2, FANCI, TICRR, BLM, PKMYT1, RMI2, LOC105447648, SHCBP1, ABCC11, MT1X, ST3GAL2, LDHD, OSGIN1, DNAAF1, GINS2, SLC7A5, CDT1, SERPINF2, SERPINF1, GSG2, SMTNL2, AURKB, NTN1, HS3ST3A1, SLC47A1, RAPGEFL1, CDC6, RARA, PSMC3IP, BRCA1, ITGA2B, C17orf104, KIF18B, MAPT-AS1, MAPT, EME1, BRIP1, SNORA76C, LOC440461, TK1, BIRC5, TYMS, NDC80, RAB31, LINC00669, SLC14A1, SKA1, KISS1R, UHRF1, S1PR5, SPC24, ZNF833P, C19orf57, PODNL1, ASF1B, EPS15L1, CHST8, WDR62, C5AR2, KLK12, RRM2, KCNF1, TTC7A, CHAC2, CCDC85A, MCEE, LINC01291, REEP1, ASTL, FAM178B, CKAP2L, SLC4A10, SPC25, CDCA7, PPP1R1C, MREG, FAM132B, CCM2L, E2F1, MYBL2, WISP2, RIMS4, UBE2C, LINC01522, ABCC13, TIAM1, CLIC6, CHAF1B, PCP4, TFF3, TFF1, TMPRSS3, CDC45, SEPT5-GP1BB, GGT5, MCM5, C1QTNF6, DMC1, CENPM, PNPLA3, RIBC2, FBLN2, KIF15, PTH1R, CSPG5, SEMA3B, CISH, ADAMTS9, MCM2, GNB4, TPRG1, ZNF732, DOK7, NCAPG, KLB, KIT, EREG, BTC, ARSJ, MAD2L1, CCNA2, PLK4, MND1, NPY5R, HMGB2, NEIL3, LOC90768, CENPU, CCDC110, TRIP13, PRLR, C5orf34, CENPK, LOC101928858, CENPH, DHFR, VCAN, ISOC1, SOWAHA, CXCL14, SLC26A2, ANXA6, HMMR, STC2, FGFR4, TUBB2B, ELOVL2, ELOVL2-AS1, TUBB, TCF19, KIFC1, C6orf141, COL12A1, TPD52L1,

						CENPW, MYB, ADAT2, LINC01558, MLLT4-AS1, AMZ1, RADIL, AGR2, AGR3, ANLN, RAMP3, ADCY1, CALCR, STRIP2, PRKAG2-AS1, XRCC2, DLC1, STC1, ESCO2, PBK, GINS4, PLAT, TMEM64, NECAB1, RGS22, DSCC1, MYC, SLC1A1, RLN2, KIF24, ARHGEF39, MELK, FAM189A2, NXNL2, CENPP, SUSD3, ZNF367, PTRH1, SH2D3C, PIP5KL1, ARHGAP6, FANCB, AP1S2, XK, SYTL5, ERCC6L, XKRX, CENPI, GLA, TMEM164, IGSF1, MIR503HG, MAMLD1
				+		RNF207, TMEM51-AS1, KLHDC7A, RAP1GAP, HTR1D, GRHL3, EXTL1, TSPAN1, DNASE2B, CTSS, SELENBP1, RGS16, RGL1, RASSF4, CTNNA3, C10orf54, KCNMA1, SEC31B, SCART1, KCNC1, SLC15A3, P2RY6, CAPN5, TMPRSS4, ROBO3, CACNA1C, LMO3, KCNJ8, ABCC9, RND1, AQP2, KRT81, KRT3, LIN7A, PPFIA2, NTN4, DRAM1, TCP11L2, TBX3, HCAR3, TMEM132B, P2RX2, TNFRSF19, FLT1, PCDH8, PCDH17, ANG, EGLN3, LINC01269, CLMN, BMF, SEMA6D, SLC12A1, FBN1, IGDCC3, STRA6, CYP1A1, FAM174B, RAB26, PLA2G10, TMC5, GDPD3, ZNF423, CCL22, CDH5, ADAMTS18, PKD1L2, SPIRE2, GLP2R, ALDH3A1, GSDMB, CCR7, ABCC3, RNF43, ST6GALNAC1, LOC101928766, PTPRM, RAB27B, CCDC68, TLE6, PALM3, MIR3189, CILP2, UPK1A, CEACAM5, CEACAM6, CEACAM1, SRRM5, LOC284379, CACNG6, TTYH1, FAM179A, CLIP4, CAPN13, EPAS1, ATOH8, FAHD2CP, TBC1D8, IL1R1, SLC9A4, ACOXL, KYNU, TFPI, STAT4, NRP2, PID1, ALPP, TRPM8, FER1L4, SALL4, BCAS1, B3GALT5, PLAC4, TMPRSS2, IL17REL, LMCD1, VILL, VIPR1, ERC2, ZBTB20, ACAD11, TM4SF1, LXN, TNFSF10, KCCAT211, CHRD, LIPH, ST6GAL1, ATP13A4, APOD, SLC51A, HS3ST1, SLIT2, ATP8A1, AMTN, HSD17B11, FAM13A-AS1, FAM13A, ADH1C, SEMA5A, SNHG18, FYB, NIM1K, PLK2, ENC1, IQGAP2, SLC12A2, FSTL4, PPP2R2B, DRD1, RNF144B, LTB, LRFN2, GSTA1, FUT9, GRIK2, TSPAN12, ATP6V0A4, LINC00689, PSD3, HEY1, ST3GAL1, CDKN2A, GNE, DAPK1, C9orf47, S1PR3, ABCA1, C8G, RNF224, SLC34A3, CA5B, CDKL5, NHSL2, KIAA2022, RNF128, MBNL3, VGLL1, FGF13
		+				ERRFI1, SLC45A1, MEAF6, RAB3B, PALMD, AKNAD1, NBPF13P, RGS2, LINC00704, NEBL, PRKG1, HMX3, MICAL2, ABCC8, SMCO4, DRD2, ZBTB16, SLC37A2, C1R, RGCC, SLITRK6, TMEM63C, KIAA0125, ACSBG1, GP2, MYLK3, PLLP, RLTPR, ANKRD29, LAMA3, DSG4, SULT2B1, KLK4, KLK6, KLK8, KLK10, KLK11, KLK13, CDC42EP3, ZNF385B, MAP2, DNER, C2orf72, B3GNT7, TGM2, KCNG1, PHACTR3, SLC25A18, SEC14L2, LOC730668, WNT5A, ZPLD1, CD86, B3GNT5, UGT2B11, HERC3, LEF1, FAM105A, MAP1B, DPYSL3, ARHGEF37, SH3PXD2B, SLC44A4, FKBP5, GNMT, CD109, AIM1, SLC2A12, IGFBP3, CROT, AZGP1P1, DOCK4, CNTNAP2, SNAI2, TPD52, CA2, SYBU, TG, NDRG1, CNTNAP3, PTCH1, CRAT, WWC3, MAOB, NUDT10

+					+	CITED4, OLFML3, PRG4, VIM-AS1, CXCL12, MAT1A, FAM25A, LOXL4, SFXN2, PRSS23, PGR, SLC2A14, C12orf60, ART4, MGP, CCNA1, LOC101928841, GPR68, NXPH3, GREB1, OTOF, PLCL1, SYNDIG1, HCK, CDH26, SUSD2, MGAT3, BFSP2, VEPH1, UGT2B17, UGT2B15, AREG, NPY1R, LOC101927934, BMP6, RBM24, LINC01016, COL21A1, PKIB, HEY2, HMGA1P7, SGK1, RAET1E, EGR3, C8orf46, MYBL1, DEPTOR, GRPR, CITED1, SYTL4, PLAC1, SOX3
	+			+		VTCN1, EDARADD, WNT11, LOC101927318, KRT4, RNASE4, ALDH1A3, VAT1L, SLC16A5, UPK1B, ADCY5, CP, LGI2, SPRY1, AHRR, PDE7B, FER1L6, GABBR2, ASB9
			+			ANKRD1, ACACB, ADGRD1, C14orf132, COLEC12, FAM84A, GRB14, LINC00504, ANK2, PTGER4, ST8SIA4, CMAHP, SCIN, DPY19L2P1, COL14A1, NR4A3
		+			+	NKAIN1, SYNPO2L, GRIK4, MT2A, NAGS, SLC16A6, CECR6, SCN5A, HEG1, FGF18, GJA1, BMPER, EBF2, PRRX2
			+	+		SLIT1, LINC01164, LOC101928944, CCDC83, A2M, CLEC7A, RPRM, KCNJ3, DAB2, AKR1B10
+						CALHM3, KRT6B, ISG20, TFCP2L1, MIR4442, EPGN, CAV1, LY6H
		+		+		C1orf116, C10orf10, ADRA2A, EMP1, SMPD3, IGFBPL1
+		+			+	MYPN, ADRB1, VWA2, TRPC6, SGK3
			+		+	ASCL1, BCL2, SHH
	+					ITGB7, LAT
	+	+		+		MME, PSCA
	+	+				AKAP12
+			+			CYP26B1
+			+		+	ARHGAP36
+		+				F13A1

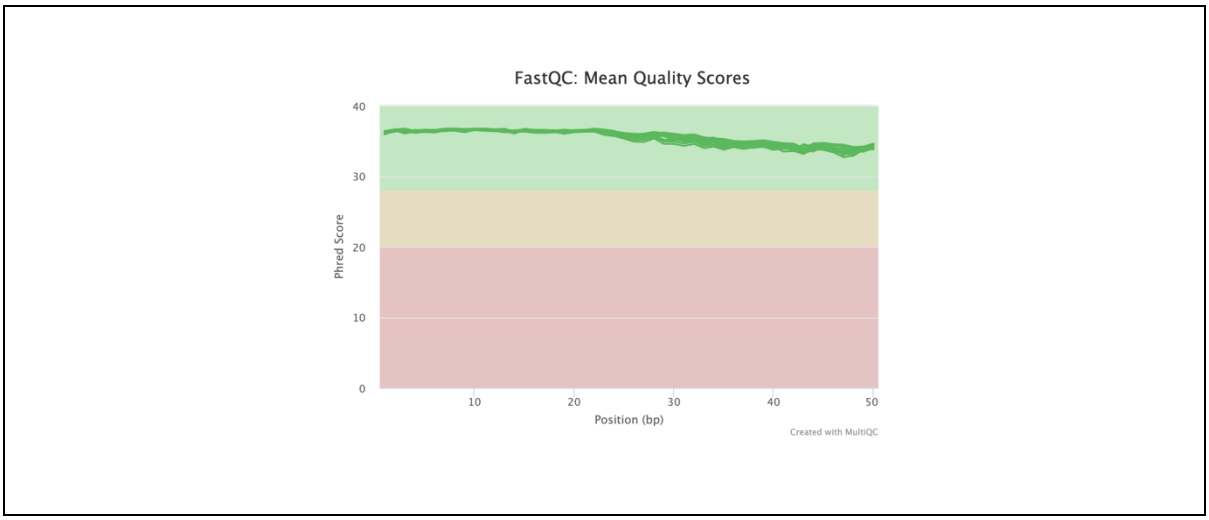

Figure 7-3 The quality of the reads of small RNA-Seq samples

The quality of the reads for each sample was checked with fastQC version (0.11.7), and a summary graph visualising all sample reads (total n = 18) was created using MultiQC.

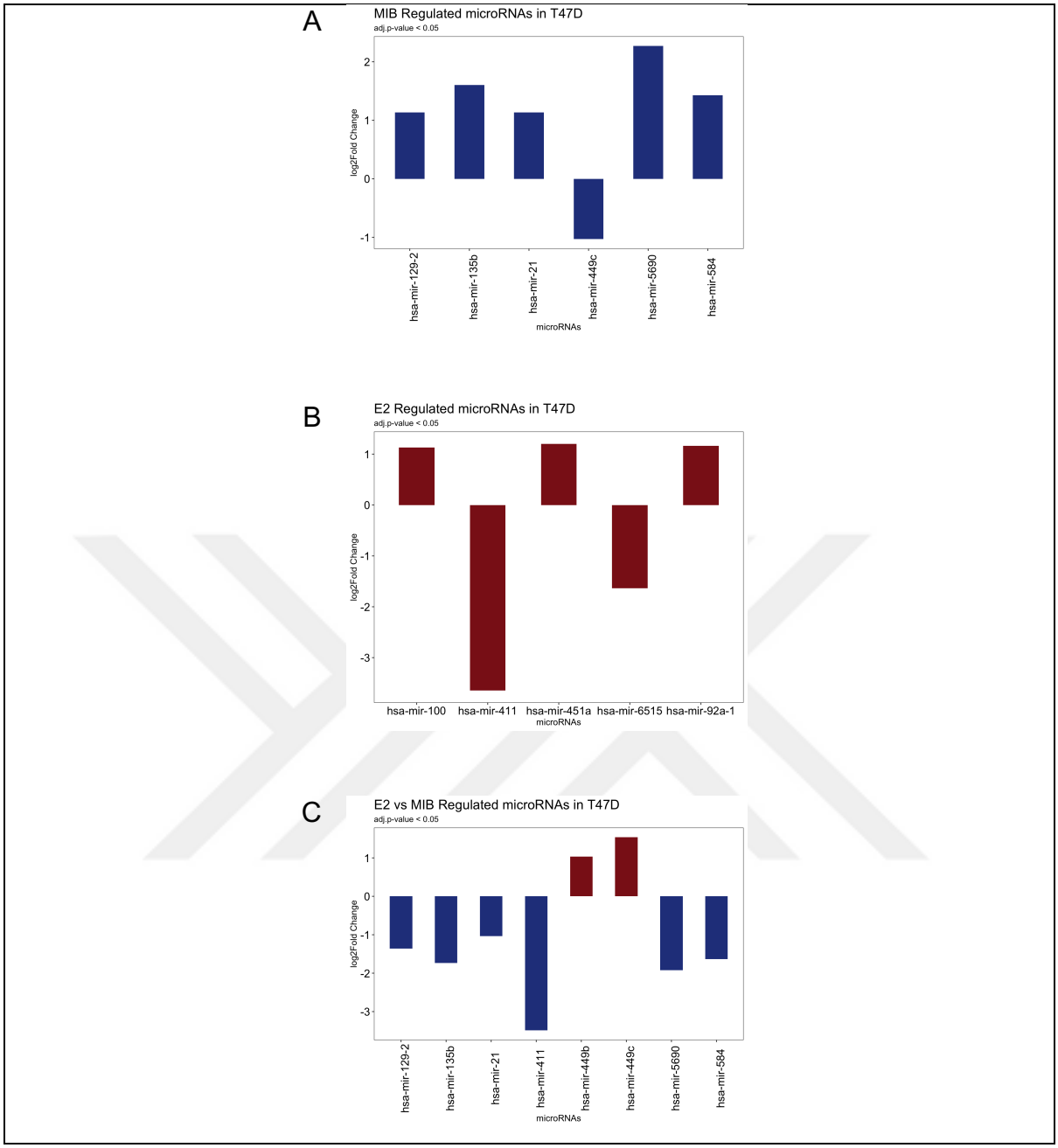

Figure 7-4 MIB and E2 regulated miRNAs (p value <0.05) in T47D

T47D cells were incubated in hormone-depleted media for 72 hours. Cells were then treated with vehicle control (Ethanol, EtOH), MIB (Mibolerone, 1 nM), or E2 (Oestradiol, 1 nM), for 24 hours. RNA was harvested. 3 independent replicates per treatment group were conducted. The changes in miRNAs in response to different treatments were analysed by small RNA-Seq. Differentially expressed miRNAs were analysed using DESeq2 (version 1.28.1) and visualised as bar plots. Cut-off values are padj < 0.05 and log2FoldChange > 1. Bar plots showing differentially expressed miRNAs, comparing (A) MIB versus control, (B) E2 versus Control, (C) E2 versus MIB.

Table 7-5 miRNA target genes in T47D

miRNA	Target Genes	Gene Symbols
miR-21	MIB-downregulated	CADM1, EPHA4, FOXP1, GLCCI1, JPH1, MATN2, MCAM, MKX, NIPAL1, ROBO2, SOX2, SPRY2, TGFB2, ZFP36L2
miR-449c	MIB-upregulated	ADAMTS8, AKR1C2, ALOX15B, ANKRD29, ANP32E, ANXA1, APOBEC3B, APOLD1, ASPHD2, ASTN2, AURKA, BUB1, C1orf95, CA8, CAPRIN2, CDC42EP3, CLGN, CLIC6, CLMN, CREBRF, DEFB132, DRAXIN, EDA2R, EGF, EMP1, ENPP1, FAM13C, FBXO32, FRZB, GABRQ, GLUL, GNG4, GPC4, GPR146, GPRC5A, HAAO, HS3ST3B1, IRAK1, ISG20, ITGA10, KCNK1, KIF18B, KIF21B, KLF9, KLHL31, LIFR, LMNB1, MAP7D2, MTMR9, MYBPC1, NCAPG2, NETO2, NUPR1, OIP5, P4HA2, PBK, PGLYRP2, RAB3B, RASD2, RPS6KA5, SAP30, SASH1, SCRG1, SH3TC2, SKA3, SLC15A2, SRGAP2, THOC5, TMCC3, TMTC2, TRIM22, VIPR1, WISP2
miR-584	MIB-downregulated	ABAT, ARHGEF19, ARHGEF38, BCAS1, C2orf72, CDH13, CLDN1, CLMP, CLU, CRISPLD1, DOCK11, EHD3, ERVMER34-1, ESR1, EVC, FGF12, FREM2, FSTL1, FUT9, GLIPR1, GNG11, GPR158, GRB14, GRM4, HS6ST3, IGDCC3, IGFBP5, IGSF3, INPP4B, ITPRIP, KCNC1, KCNK15, KCNK5, KITLG, KLHL13, LAMA4, LAMC2, LRP2BP, MAML2, MATN3, MCIDAS, MGAT4A, MYL9, MYLK, NCAM2, NOL4, ORAI2, PAQR8, PCDH18, PCP4L1, PDLIM3, PRDM6, PTGER3, PTHLH, RAB18, RASGRF1, RIMS1, RNF128, SC5D, SERPINA10, SH3PXD2A, SHANK2, SLC16A4, SLC35G1, SLITRK6, SOAT1, SOBP, STON2, TGFB2, THSD7A, TP63, TPM4, TWIST1, ZDHHC14, ZFP36L2
miR-5690	MIB-downregulated	ADIPOQ, AGPAT4, AMZ1, ANXA6, ATP8A1, ATP8B2, AXL, BCHE, BOC, C11orf88, C1orf64, C2orf72, C3orf70, C5AR2, C8orf46, CACNA1C, CACNA1H, CASQ2, CDC14B, CDH7, CGNL1, CHDH, CLDN1, CLU, CREB5, CTGF, CYB5A, DCLK2, DOCK11, EFNB3, EGR1, EHD3, ENOX1, ENTPD3, EPHA4, ERVMER34-1, EVC, FAM169A, FERMT1, FOXJ1, FREM2, GALNT10, GLI3, GNAZ, GPR158, GPR37L1, GRM4, HLF, HS6ST3, IGDCC3, IL1R1, IL5RA, INPP4B, ITPRIP, KCNC1, KCNK5, KCNQ4, KCNQ5, KITLG, LAMA4, LIPH, LPAR2, LRP2BP, MACC1, MAML2, MLKL, MOB3B, MREG, MYO3B, NCMAP, NDST1, NMNAT2, NPR3, OLFML2A, ORAI2, PCP4L1, PGR, PLCE1, PLEKHG5, PRDM6, PTGER2, PTGER3, PYCARD, RAB18, RIMS4, RNF128, RNF222, S1PR3, SC5D, SDC2, SEC14L5, SEMA6A, SH3PXD2A, SHANK2, SHROOM4, SIGLEC6, SLC16A4, SLC1A2, SLC45A3, SLC9A7, SOAT1, SOBP, ST8SIA1, STON2, TCF4, TCF7L1, THSD7A, TP63, TUB, UBL3, UBP1, VCAN, VWA2, ZFPM2

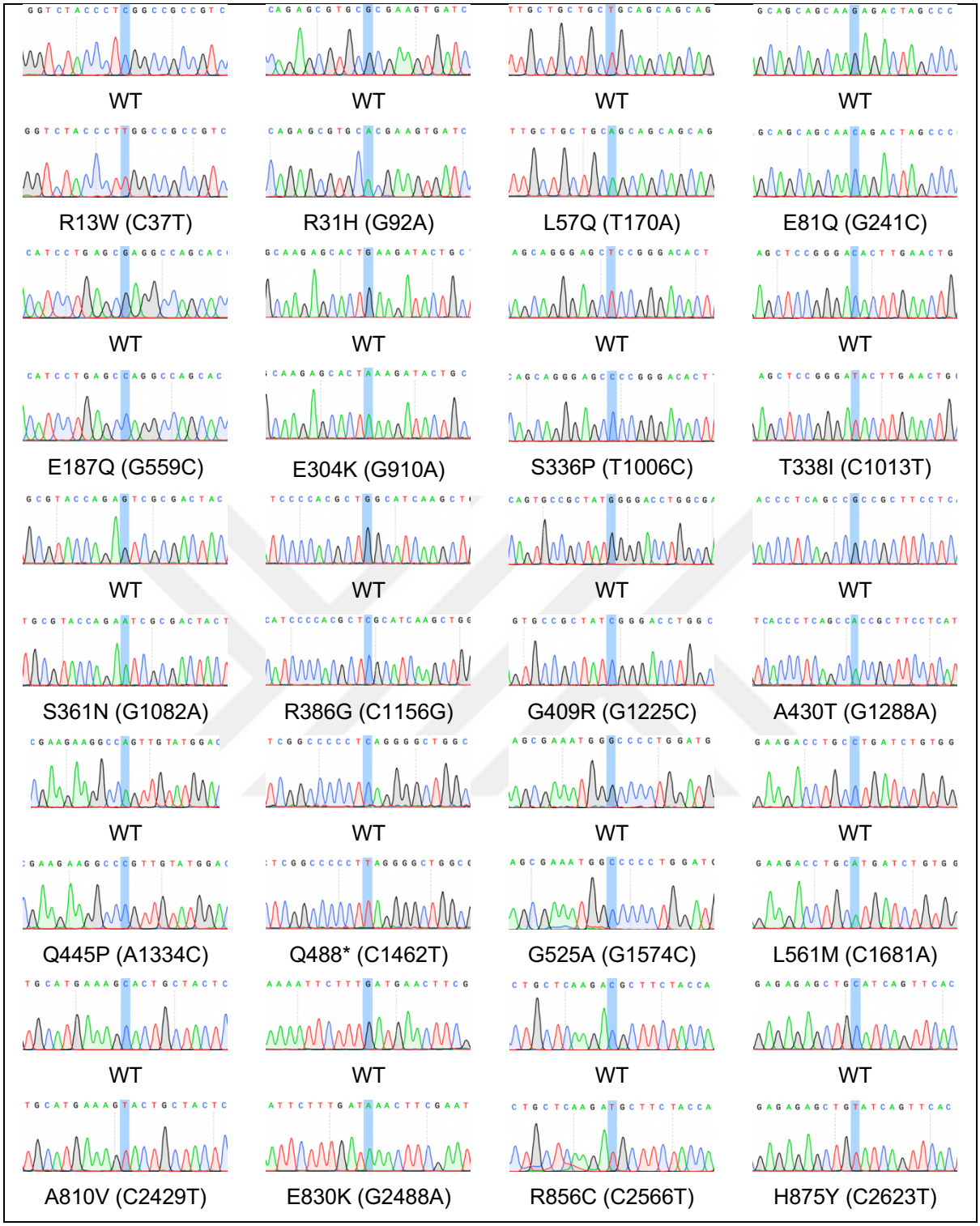

Figure 7-5 Chromatographs of the wild-type and mutant Androgen Receptors

Chromatographs showing the AR mutants: R13W, R31H, L57Q, E81Q , E187Q, E304K, S336P, T338I, S361N, R386G, G409R, A430T, Q445P, Q488, G525A, L561M, A810V, E830K, R856C, H875Y. Mutations were introduced into the AR expression plasmid (pSV-AR) using site-directed mutagenesis and plasmids were transformed into E. coli. Plasmids were harvested and mutations verified by Sanger sequencing (Eurofins). Changes in single base pair that results in the desired amino acid substitution are highlighted. Chromatograms generated using SnapGene Viewer (Version 4.2.11).*